University of Alberta

Enantioselective Formation of Propargylic Alcohols

by

Erin Rae Sullivan

A thesis submitted to the Faculty of Graduate Studies and Research
in partial fulfillment of the requirements for the degree of

Doctor of Philosophy

Chemistry

©Erin Sullivan
Fall 2011
Edmonton, Alberta

Dedication

To my parents, Cathy & Chris Graham

Abstract

Propargylic alcohol natural products are found in many species of terrestrial plants and marine organisms. Because these compounds are usually isolated from the natural source in only small amounts, few studies of propargylic alcohol natural products have been conducted to date. Nevertheless, these studies show compounds with this backbone have diverse biological activities and potential for pharmaceutical applications. Recently, routes have been developed for the asymmetric addition of monoynes to aldehydes, forming propargylic alcohols in high enantioselectivities. At the commencement of this thesis research, however, little work had been reported toward the asymmetric addition of polyynes to aldehydes. As outlined in Chapter 1, the polyynol functionality is quite prevalent in nature, and therefore efficient synthetic routes to this framework could provide compounds to help improve our understanding of the origin of their diverse biological activities. Chapter 2 addresses the asymmetric addition of terminal di- and triynes to aldehydes along, with a one-pot Fritsch-Buttenberg-Wiechell rearrangement-asymmetric addition reaction. The asymmetric addition of terminal diynes and triynes would be a more direct route to polyynol natural products, avoiding the use of tedious cross-coupling reactions. The one-pot protocol would again be a more expedient route and would circumvent the isolation of an unstable terminal polyyne.

A second functional group that has shown wide application in natural product synthesis is the homoallylic propargylic alcohol moiety, as it contains three distinct synthetic handles: the alkyne, alkene and alcohol. The most direct

route to a homoallylic propargylic alcohol is to perform an allylation reaction on a propargylic aldehyde. The most frequent allyl transfer method applied in natural product synthesis is an allylation with an allylboron reagent known as an allylboration reaction. Despite the popularity of this framework, no catalytic asymmetric allylboration reaction currently exists for propargylic aldehydes. Current methodologies to homoallylic propargylic alcohols either apply a stoichiometric amount of a chiral allylborane or the use of harsh allyl metal species. Chapter 3 describes the catalytic asymmetric allylboration of propargylic aldehydes.

Acknowledgements

Table of Contents

List of Tables

List of Figures

List of Schemes

List of Symbols and Abbreviations

Symbol/Abbreviation	Definition
Ac	acetyl
allylBpin	4,4,5,5-tetramethyl-2-(prop-2-en-1-yl)-1,3,2-dioxaborolane
aq	aqueous
ar	aromatic
b	broad
BINOL	1,1'-binaphthalene-2,2'-diol
BOM	benzyloxylmethoxy
n-Bu	*n*-butyl
t-Bu	*t*-butyl
°C	degrees Celcius
calcd	calculated
CAN	ceric ammonium nitrate
CD	circular dichroism
cm	centimeter(s)
d	doublet
dd	doublet of doublets
ddd	doublet of doublets of doublets
DHQD	dihydroquinidine
DIBAL-H	diisobutylaluminum hydride
DMAP	dimethylaminopyridine
DMF	*N,N*-dimethylformamide
dt	doublet of triplets
ED_{50}	effective dosage required for the desired result within 50% of the population
ee	enantiomeric excess
EI	electron impact
equiv	equivalents
ESI	electrospray ionization
Et	ethyl
g	gram(s)
h	hour(s)
HPLC	high performance liquid chromatography
HRMS	high resolution mass spectrometry
Hünig's Base	diisopropylethylamine
Hz	Hertz
i	iso
IC_{50}	drug concentration required to decrease cell growth by 50%
IPC	isopinocamphenyl
IR	infrared spectroscopy
J	coupling constant (in NMR spectroscopy)
L.A. or LA	Lewis Acid

LBA	Lewis assisted Brønsted Acid
LD_{50}	compound concentration required to cause death to 50% of the population
m	multiplet or medium
Me	methyl
mg	milligram
mmol	millimole(s)
mol	mole(s)
MS	mass spectrometry or molecular sieves
m/z	mass to charge ratio
NMR	nuclear magnetic resonance
OMe	methoxy
ORTEP	Oak Ridge thermal ellipsoid plot
OTf	trifluoromethanesulfonate
Ph	phenyl
pin	pinacol
Pr	propyl
ProPhenol	(*R,R*)-(−)-2,6-bis[2-hydroxydiphenyl-methyl)-1-pyrrolidinyl-methyl]-4-methylphenol
i-Pr	isopropyl
q	quartet
qt	quartet of triplets
R	generic alkyl group
R_f	retention factor
rt	room temperature
s	singlet or strong
satd	saturated
t	triplet
t	tertiary
TBAF	tetra-*n*-butylammonium fluoride
TBDPS	*tert*-butyldiphenylsilyl
TBS	*tert*-butyldimethylsilyl
THF	tetrahydrofuran
THP	2-hydropyranyl
TIPS	triisopropylsilyl
TLC	thin layer chromatography
TMEDA	*N,N,N',N'*-tetramethylethylenediamine
TMS	trimethylsilyl
TRIP-PA	(*R*)-3,3'-bis(2,4,6-triisopropylphenyl)-1,1'-binaphthyl-2,2'-diyl hydrogenphosphate
Ts	toluenesulfonic acid
w	weak
λ	wavelength
μ	micro
δ	Delta

Chapter 1- Propargylic Polyyne Alcohols – A Class of Natural products and potential drug targets.

1.1 Polyyne Natural Products

Natural product studies continue to be a major source of inspiration for drug discovery and design. Currently, about half of all prescribed medicines are extracted or derived from terrestrial plants and microorganisms. Most of the synthetic drugs, it should be noted, were originally inspired by novel compounds discovered in terrestrial organisms.[1,2] Polyynes are a class of natural products, where a polyyne is defined as a compound that contains two or more conjugated C≡C units. Isolated polyyne natural products have a wide range of biological activities, including but not limited to: antifungal, antibacterial, antimicrobial, anti-inflammatory, anti-HIV, anti-tumor, anticancer, and pesticidal.[3-6] They are found within a vast range of natural sources, including for example: terrestrial plants, fungi, bacteria, marine sponges, and marine corals.[3,7,8] Despite being found in a wide variety of organisms, many of these highly unsaturated polyyne compounds are unstable due to polymerization as well as photolytic, oxidative, and pH–dependent decomposition both in solution and the solid state.[9,10]

According to Bohlmann, the first isolated polyyne natural product was dehydromatricaria ester (**1.1**, Figure 1.1), isolated from an *Artemisia* species in 1826.[10] In 2008 it is recorded that more than 2,000 acetylenic natural products

have been isolated,[3] while in 2006, Shi Shun and Tykwinski documented that over 1,000 compounds containing two or more conjugated C≡C bonds had been isolated from natural sources.[7] Minto suggests that the recent growth in the number of isolated polyyne natural products is likely the result of new methods that allow for improved isolation and structure elucidation of these unstable compounds.[3]

H₃C—≡—≡—≡—

1.1 H₃CO₂C
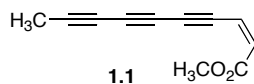
Figure 1.1. Chemical structure of dehydromatricaria ester (**1.1**).

A subdivision of polyyne natural products that shows promising biological activity are those containing a propargylic alcohol. The propargylic alcohol polyyne backbone has been found in numerous compounds from terrestrial and marine organisms.[2,3,7,11] The polyyne backbone of these isolated natural products contains a diyne, triyne, tetrayne, or a pentayne with five repeating C≡C.[12,13]

There are many reviews on the synthesis of propargylic alcohols for the formation of natural products (Figure 1.2),[14-18] and there are numerous reviews on isolated acetylenic natural products.[3,7,8,13,19] There has yet to be an article that focuses on the existence of propargylic alcohol natural products. Here we present a summary of the propargylic alcohol polyynes that have been isolated from natural sources. Synthetic strategies to access the propargylic backbone are then critically discussed.

1.2 Propargylic alcohol polyynes from plants

Falcarinol (**1.2**) and falcarindiol (**1.3**) are two of the most widely studied naturally occurring polyynes.[7,8,13] Falcarinol and falcarindiol have been isolated from a wide range of plants within the Araliaceae and Apiaceae (Umbelliferae) families, including: carrots, fennel, celery, ginseng, parsley and parsnips.[8] Falcarinol (**1.2**) has been initially isolated by Takahashi *et al.* in 1964 and given the name panaxynol.[20,21] After synthesis in 1966, the structure of panaxynol has been established as the same structure as falcarinol (**1.2**) and the two names, panaxynol and falcarinol are used interchangeably.[21-23] Both falcarinol (**1.2**) and falcarindiol (**1.3**) show anti-inflammatory and anti-platelet-aggregatory effects, antifungal activity, as well as cytotoxicity against human tumor cells, with falcarinol being slightly more active.[8,24,25] Interestingly, the concentration of falcarindiol is found to play a key role in the bitter taste sometimes found in carrots.[24]

1.2 R^1 = R^3 = H, R^2 = OH
1.3 R^1 = R^2 = OH, R^3 = H
1.4 R^1 = H, R^2, R^3 = O

1.5 R^1 = H, R^2 = OH
1.6 R^1 = H, R^2 = OAc
1.7 R^1 = OMe, R^2 = OH

1.8 R^1 = Cl, R^2 = OH, 1-*ene*
1.11 R^1 = OH, R^2 = OH, 1-*ene*
1.12 R^1 = OAc, R^2 = OH, 1-*ene*
1.13 R^1 = R^2 = OH

1.9

1.10
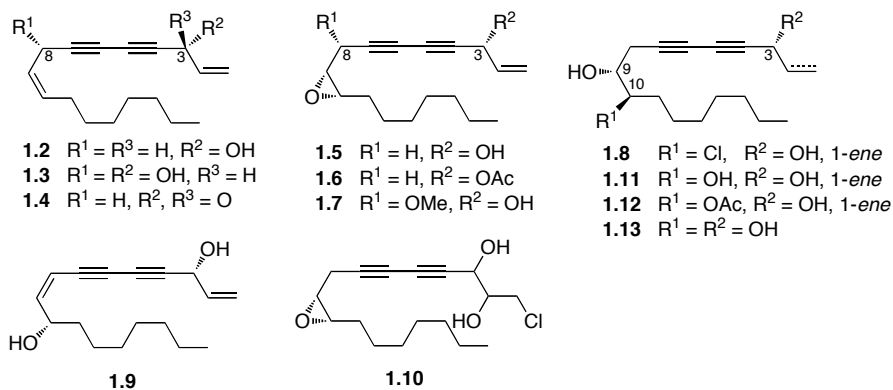
Figure 1.2. Structures of the C$_{17}$ natural products **1.2–1.13**.

The propargylic alcohol at the C3 position of both falcarinol (**1.2**) and falcarindiol (**1.3**) is important for the bioactivity of these compounds. It has been proposed that bioactivity is associated with the hydrophobicity of the compounds and their ability to form a stabilized carbocation with the loss of water. This allows such compounds to act as reactive alkylating agents towards various biomolecules.[26] To support this theory Purup *et al.* have demonstrated that when falcarinol (**1.2**) is oxidized at the 3-hydroxy position to falcarinon (**1.4**), potency towards cell proliferation of human intestinal cancer cells (Caco-2 cells) decreases significantly, by an order of magnitude.[26] The reduction in reactivity of falcarindiol (**1.3**) versus falcarinol (**1.2**) has been attributed to the ability of **1.3** to generate two active centers and therefore giving reduced lipophilic character. However, falcarinol and falcarindiol have a synergistic relationship in their ability to inhibit proliferation of intestinal cancer cells,[26-28] suggesting that other polyynes might also show increased potency against cancer cells when working in a synergistic fashion.

Falcarinol and falcarindiol are only a small fraction of a wide variety of C17 propargylic alcohol diynes found within plants. Panaxydol (**1.5**) is one of the most studied compounds found within the genus *Panax*. Panaxydol shows a strong ED_{50} value of 0.016 µg/mL against human gastric adenocarcinoma (MK-1) cells, while the ED_{50} for normal fibroblasts cells is approximately 700 times higher.[29] Related to panaxydol (**1.5**) are 3-acetylpanaxydol (**1.6**), 8-methoxy-panaxydol (**1.7**) and panaxydol chlorohydrine (**1.8**). Another highly studied

compound within the genus *Panax* is panaxydiol (**1.9**), which has a related chlorinated compound called 1-chloropanaxydiol (**1.10**). The natural product from the genus *Panax* that has been the most studied is panaxytriol (**1.11**). For a long time there existed a dispute over the stereochemistry of **1.11**; the stereochemistry has been set as (3*R*,9*R*,10*R*)-panaxytriol in 2002 after multiple syntheses.[30] Related compounds to panaxytriol (**1.11**) are 10-acetylpanaxytriol (**1.12**) and dihydropanaxacol (**1.13**). There also exists a list of compounds related to falcarinol (**1.2**) and falcarindiol (**1.3**) shown in Figure 1.3 (compounds **1.14**– **1.27**).[27,31] Recently Schmiech *et al.* isolated falcarindiolone-8-acetate (**1.24**), falcarindiolone-9-acetate (**1.25**), (*E*)-1-methoxy-falcarindiolone-8-acetate (**1.26**) and (*E*)-1-methoxy-falcarindiolone-9-acetate (**1.27**), however no biological testing has been performed.[27]
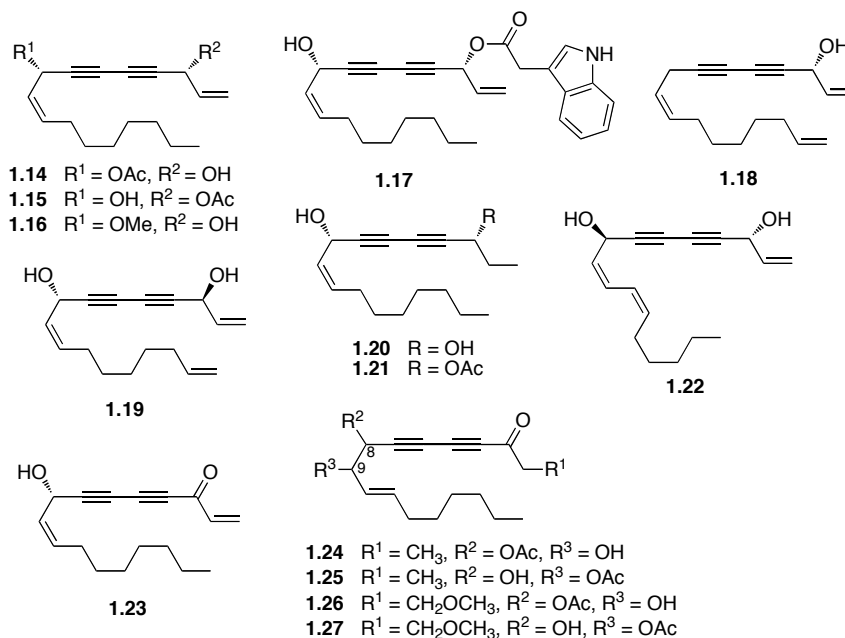
Figure 1.3. Diynols from the genus *Panax* (**1.14**–**1.27**).

5

A group of C_{17}–propargylic alcohol diynes isolated from the roots of *Panax ginseng* (Araliaceae) are the ginsenoynes A, C, D, H & K (**1.28–1.32**, Figure 1.4).[32] Ginsenoynes A (**1.28**) and C (**1.29**) have been tested against four cancer cell lines in vitro and ginsenoyne A (**1.28**) shows promising activity against human lung (A549), ovarian (SK-OV-3), melanoma (SK-MEL-2), and colon (HCT-15) cancer.[33] Falcarindiol (**1.3**), panaxytriol (**1.11**), panaxydol chlorohydrine (**1.8**), and most of the ginsenoynes (**1.28–1.32**) exert greater cytotoxicity than 5-fluorouracil or cisplatin. It is panaxydol (**1.5**), however, that is the most potent with an IC_{50} of 0.19 µM for leukemia L-1210 cells.[34] Compound **1.33** from *P. ginseng* also inhibits growth of L-1210 cells with an IC_{50} of 14 µg/mL.[32]
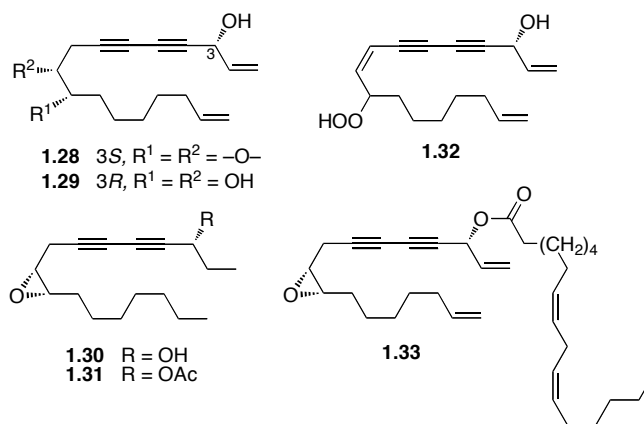
Figure 1.4. Ginsenoynes A, C, D, H & K (**1.28–1.32**) and **1.33**.

Another plant within the Araliaceae family, *Dendropanax arboreus*, contains the diynols dendroarboreol A (**1.34**) and B (**1.35**), 1,2-dihydrodendroarboreol B (**1.36**), *trans*-1,9,16-hepta-decatriene-4,6-diyne-3,8-diol

(**1.37**) and **1.38** (Figure 1.5).[35,36] Dendroarboreol B (**1.35**) and **1.38** show higher in vitro cytotoxicity towards LOX melanoma in mice than the other compounds (**1.34**, **1.36** and **1.37**).[2] Compound *trans*-1,9,16-hepta-decatriene-4,6-diyne-3,8-diol (**1.37**) shows cytotoxicities below 15 μg/mL for five out of the six tumor cell lines tested: human colon cancer (LS174T, SKCO1 & COLO32ODM), colorectal adenocarcinoma (WIDR) and breast cancer cells (MCF7); while activity towards breast cancer cells MDA231 is significantly less (IC$_{50}$ of 37.6 μg/mL).[2]
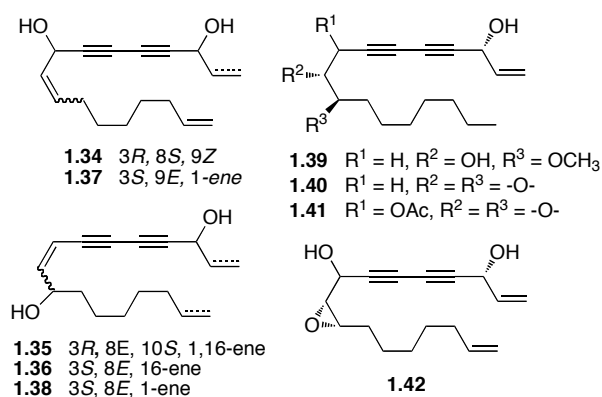
Figure 1.5. Dendroarboreol A (**1.34**) and B (**1.35**), 1,2-dihydrodendroarboreol B (**1.36**), *trans*-1,9,16-hepta-decatriene-4,6-diyne-3,8-diol (**1.37**), **1.38**, PQ-1 (**1.39**), PQ-2 (**1.40**), PQ-6 (**1.41**), and **1.42**.

Several compounds isolated from *Panax quinquefolium* (Araliaceae) have shown activity against leukemia (Figure 1.5). Panaquinquecol-1 and -2 (PQ-1 and PQ-2, **1.39** and **1.40**, respectively) completely inhibit leukemia cells (L-1210) in tissue cultures at a concentration of 0.5 μg/mL,[37] while **1.41** (PQ-6) and **1.42** show IC$_{50}$ values of 0.5 and 0.3 μg/mL respectively.[2,38] Compound **1.42** also

inhibits Ehrlich and HeLa cell lines with IC_{50} values of 1.3 and 2.1 μg/mL, respectively.[39]
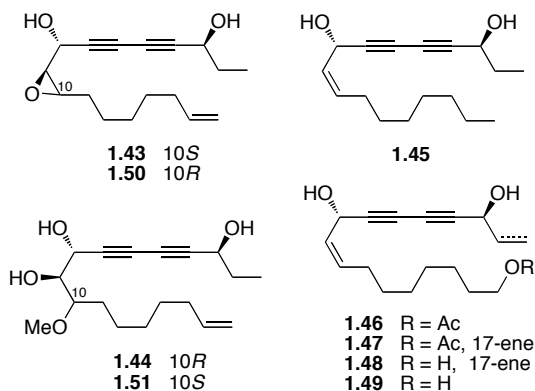
Figure 1.6. Oploxynes A (**1.43**), B (**1.44**), and their C10 epimers (**1.50–1.51**), oplopandiol (**1.45**), oplopandiol acetate (**1.46**), and **1.47–1.49**.

The stems of *Oplopanax elatus* have been traditionally used in Chinese and Korean medicine to treat inflammation.[5] From these stems the propargylic alcohol diynes oploxynes A (**1.43**) and B (**1.44**) were isolated in 2010 and are related to oplopandiol (**1.45**), oplopandiol acetate (**1.46**), and **1.47–1.49** (Figure 1.6).[5,6,40-42] Diynol oploxyne A (**1.43**) shows a nitric oxide inhibition IC_{50} of 1.98 μM and IC_{50} of 3.08 μM towards prostaglandin E_2 in murine machrophage RAW264.7 cells, while oploxyne B (**1.44**) shows no cytotoxicity against them. Nitric oxide and prostaglandin E_2 inhibition in murine macrophage RAW264.7 cells suggest the possible application of these compounds towards the treatment of inflammation.[5]

Recently, Yadav *et al.* synthesized oploxynes A and B (**1.43**–**1.44**) along with their C10 epimers and revised the oploxyne B structure from the (3*S*,8*R*,9*R*,10*R*)-**1.44** isomer to the enantiomer (3*R*,8*S*,9*S*,10*S*)-**1.44**. At the same time they have tested these compounds against four different cancer cell lines and determined that oploxyne A (**1.43**) and the corresponding C10 epimer (**1.50**) have high potency against neuroblastoma (SK-N-SH); the results being similar or improved to what has been shown for doxorubicin. Interestingly (−)–oploxyne B (**1.44**) shows significant activity against human prostate cancer cell lines (DU-145), while the potency of the C10 epimer (**1.51**) decreases by ca. one order of magnitude.[43] These particular compounds demonstrate the importance of stereochemistry and shows how minor changes can alter potency towards specific biological targets.
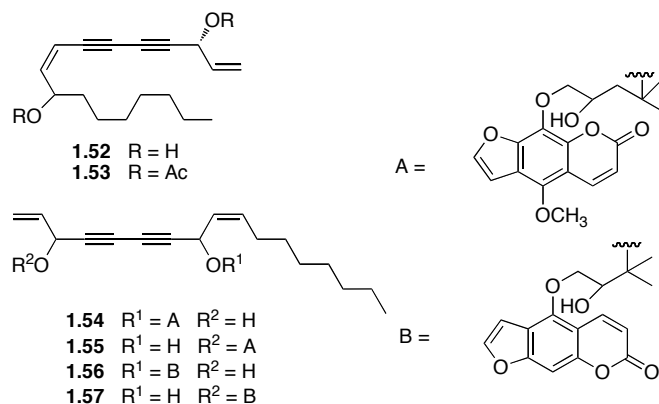
Figure 1.7. Seselidiol (**1.52**), seselidiol acetate (**1.53**) and the japoangelols A–D (**1.54**–**1.57**).

Although numerous diynols are found in plants of both the Araliaceae and Apiaceae families, some are so far unique to the Apiaceae family. The ethanol extract of the roots of *Seseli mairei* shows significant cytotoxicity (ED_{50} values less than 20 µg/mL) in nasopharyngeal carcinoma cells (KB), and lymphocytic leukemia in mice (P-388 and L1210). From this extract, Lee and coworkers have been able to isolate seselidiol (**1.52**, Figure 1.7) and the corresponding acetate (**1.53**).[44] Both **1.52** and **1.53** show moderate cytotoxicity against the above mentioned tumor cell lines (ED_{50} values less than 10 µg/mL).[2,44,45]

The japoangelols A–D (**1.54**–**1.57**, isolated from the roots of *Angelica japonica*) show high inhibitory activity on human gastric adenocarcenoma MK-1 cell growth along with heptadeca-1,8-diene-4,6-diyne-3,10-diol (**1.58**, Figure 1.8),[46] 9,10-epoxy-16-hydroxy-octadeca-17-ene-12,14-diyne-1-al (**1.59**),[47] falcarinol (**1.2**), falcarindiol (**1.3**), panaxytriol (**1.11**) and panaxydol (**1.5**).[2,47-49] Japoangelols A–D (**1.54**–**1.57**) also show moderate activity against HeLa and B16F10 (murine melanoma) cells.[50]
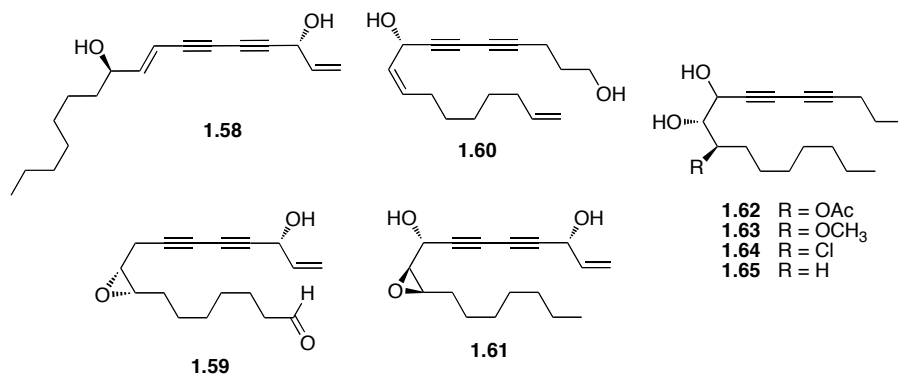
Figure 1.8. Propargylic diynols from the Apiaceae family **1.58**–**1.65**.

Both water hemlock and water dropwort are highly toxic plants in the Apiaceae family, whose cytotoxicity is due, at least in part, to the polyynes found within.[51,52] Most polyynes in these plants have low lethal dosages (LD_{50} values of 0.76–10 mg/kg in mice). At slightly lower concentrations they are found to bind to specific locations in the GABA–gated Cl^- channels of $GABA_A$ receptors in the brain cortex of rats ($IC_{50} = 0.3$–10 μM).[53,54] This shows that compounds similar to these C_{17} natural products might have application in the design of anticonvulsant drugs. The least deadly of these compounds is virol B (**1.60**; Figure 1.8; $LD_{50} \geq$ 393 mg/kg in mice) with an IC_{50} of 6 μM. Even though virol B (**1.60**) has desirable properties as a possible drug (high lethal dose and lower IC_{50} values), it is the least studied. The lone synthesis of virol B (**1.60**) tentatively determined absolute configuration, while multiple synthetic pathways have been reported for analogs virols A and C, which do not contain a propargylic alcohol group.[51,53,55,56]

Compound **1.61** (Figure 1.8) has been isolated from the seeds of tubular water dropwort (*Oenanthe fistulosa*).[57] The *Oenanthe* species are proposed to be the famous sardonic herbs used in pre-Roman Sardinia. The toxic herb was fed to elderly people who were no longer able to support themselves. The herb's effects include intoxication and muscular contractions of the face (sardonic smile). Once intoxicated, victims were dropped from a height or beaten to death. Interestingly, it is not the propargylic alcohol polyynes found in water dropwort **1.61** and falcarindiol (**1.3**) that are highly toxic and lead to convulsions, but rather, the other non-propargylic polyynes with similar structures.[57]
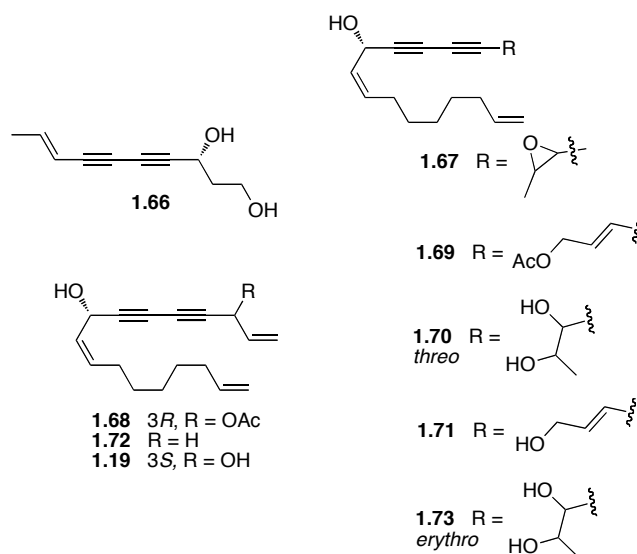
Figure 1.9. Compounds isolated from *Gymnaster koraiensis*.

A group of compounds that are structurally related to falcarinol (**1.2**) and falcarindiol (**1.3**) are the ciryneols A–C (**1.62**–**1.64**, Figure 1.8), which are isolated from *Cirsium japonicum* (Compositae) along with **1.65**. Compounds **1.62**–**1.65** inhibit the growth of nasopharyngeal carcinoma cells (KB cells) *in vitro*.[58] The gymnasterkoreaynes have been isolated from another plant found within the Compositae family (*Gymnaster koraiensis*) by Bae and coworkers.[59] Gymnasterkoreaynes A–F (**1.66**–**1.71**, Figure 1.9) have been isolated at the same time as two other related compounds 1,9,16-heptadecatrien-4,6-diyn-8-ol (**1.72**) and (3*S*,8*S*)-dehydrofalcarindiol (**1.19**). All eight compounds have been evaluated against the L-1210 tumor cell line, which shows that gymnasterkoreaynes B (**1.67**), C (**1.68**), F (**1.70**) and (3*S*,8*S*)-dehydrofalcarindiol (**1.19**) exert significant cytotoxicities with ED$_{50}$ values ranging from 0.12–3.3 μg/mL.[59-62] Later, Dat *et*

al. have isolated gymnasterkoreayne G (**1.73**) and found that it inhibits NFAT transcription factor (NFAT is a cytoplasmic protein whose excessive activation provokes immunopathological reactions, including inflammation and transplant rejection).[63] This modulation of immune response could be useful in the therapy of immune diseases.[63] Gymnasterkoreayne B (**1.67**) and **1.72** show the greatest inhibitory activity (IC_{50} values of 1.44 µM and 4.95 µM, respectively).[63]
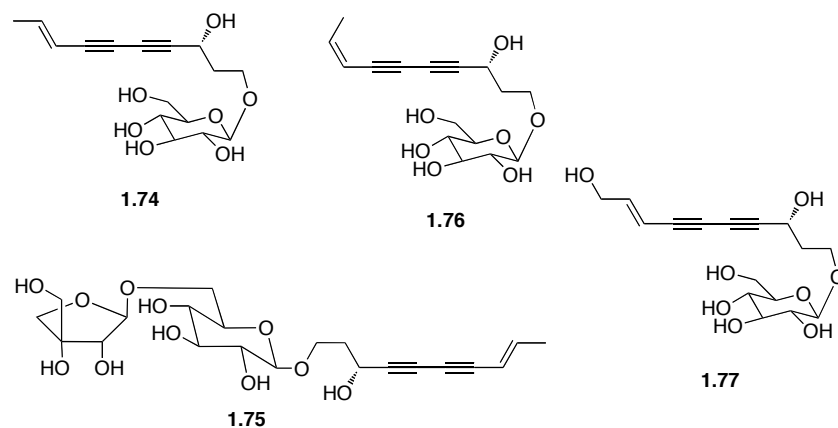
Figure 1.10. Gymnasterkoreasides A (**1.74**, also known as bidensyneoside A_1), B (**1.75**) along with bidensyneosides A_2 (**1.76**), and C (**1.77**).

Gymnasterkoreasides A (**1.74**) and B (**1.75**) are propargylic alcohol diynes which have also been isolated from *Gymnaster koraiensis* and are only a small fraction of examples of polyyne glycosides (Figure 1.10).[13] Bidensyneoside A_2 (**1.76**) is found in the methanolic extract of hairy beggarticks (*Bidens parviflora*) along with propargylic alcohol diyne glycoside bidensyneoside C (**1.77**).[64] All of

the bidensyneosides have been found to inhibit both histamine release and nitric oxide production.[64]
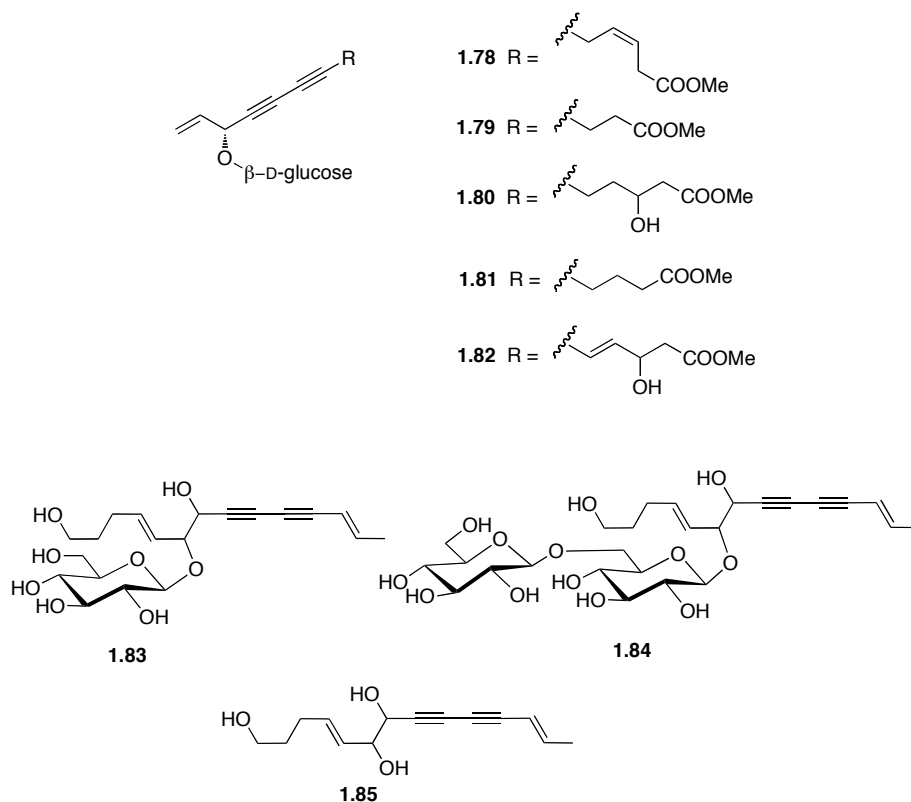
Figure 1.11. Helianthenates A–E (**1.78–1.82**), lobetyolin (**1.83**), lobetyolinin (**1.84**) and lobetyol (**1.85**).

Other examples of propargylic alcohol diyne glycosides are the methyl β-D-glucopyranosyl helianthenates A–E (**1.78–1.82**) isolated from a species of sunflower (*Helianthus tuberosus*) and lobetyolin (**1.83**), lobetyolinin (**1.84**) and the corresponding aglycone lobetyol (**1.85**) from the hairy root culture of *Lobelia inflata* (Figure 1.11). Although there has been much work towards the isolation of

1.83–1.85 there has been little reported on biological activities.[65] Likewise no biological testing has been performed to date on the other known propargylic alcohol diyne glycosides pratialin-A (**1.86**), pratialin-B (**1.87**),[66] panaxfurayne A (**1.88**), panaxfurayne B (**1.89**)[67,68] and compound **1.90** (Figure 1.12).[69]

Figure 1.12. Pratialin-A (**1.86**), pratialin-B (**1.87**), panaxfuraynes A (**1.88**) and B (**1.89**), and **1.90**.

Cordifolioidyne A (**1.91**, Figure 1.13) has been proven to be ineffective as an antibacterial agent at concentrations up to 100 µg/mL.[65,70] Both **1.92**[71] and the corresponding aglycone (1,3*R*,8*R*-trihyroxydec-9-en-4,6-yne, **1.93**)[72] exhibit moderate activity against the enzyme 12-lipoxygenase with an IC_{50} of 30 µg/mL.[71] The polyacetyleneginsenoside-Ro structure (**1.94**) is made up of the two thoroughly studied compounds ginsenoside-Ro and panaxytriol (**1.11**). Although **1.94** has been isolated back in 2002, the only biological testing performed to date

shows that it exhibits inhibition of replication of HIV-1 in vitro with a modest

IC$_{50}$ value of 11.1 μM.[73]
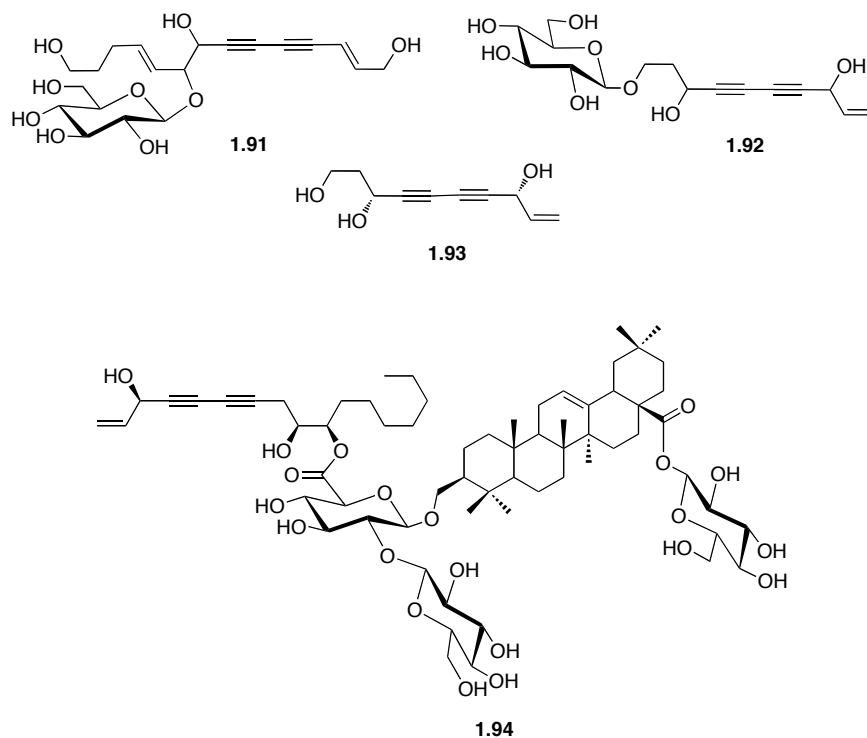
Figure 1.13. Cordifolioidyne A (**1.91**), **1.92**, aglycone **1.93**, and polyacetyleneginsenoside-Ro (**1.94**).

Finally, the diynols **1.95** and **1.96** (Figure 1.14) have been isolated by Bauer and co-workers from the rhizomes of *Atractylodes lancea*.[74,75] Although the *n*-hexanes extract of the rhizomes shows inhibitory activity against 5-LOX and COX-1, the isolated diynols show no significant inhibitory effects or any other anti-inflammatory activity.[72]

Figure 1.14. Diynols **1.95** and **1.96** isolated from the rhizomes of *Atractylodes lancea.*

Besides propargylic alcohol diynes, propargylic alcohols with longer acetylenic chains are also found in plants. For example minquartynoic acid (**1.97**, Figure 1.15) shows high activity against human lymphocytic leukemia with an ED_{50} value of 0.18 µg/mL, and it is also reported by both Boyd [76] and Fort[77-79] to have anti-HIV-1 activity. Minquartynoic acid also has ED_{50} values of less than 6 µg/mL for human breast, lung, oral epidermoid carcinoma, colon cancer, prostate cancer, ovarian cancer, and neuroblastoma cancer.[80] Altering the structure of **1.97** at C18 through addition of a hydroxy group, gives 18-hydroxyminquartynoic acid (**1.98**) which shows activity for human oral epidermoid carcinoma with an ED_{50} value of less than 6 µg/mL.[80]

Figure 1.15. Minquartynoic acid (**1.97**), 18-hydroxyminquartynoic acid (**1.98**), bidensyneoside B (**1.99**), tetrayne glycosides **1.100–1.101**, and pentayne glycoside **1.102**.

Bidensyneoside B (**1.99**), is an example of a propargylic alcohol triyne glycoside.[64] Polyyne glycoside tetraynes **1.100** and **1.101** have also been identified, however, no biological testing is reported to date.[81-83] Finally, a single propargylic alcohol pentayne glycoside **1.102** has been isolated and shows activity against *Pseudomonas aeruginosa* and *Staphylococcus aureus*.[12,84]

1.3   Propargylic Alcohol Polyynes from Marine sources

Although plants are the most abundant source of propargylic alcohol diynes to date, many are also found in marine organisms. One such class of propargylic alcohol diynes that has received a lot of attention is that of the

strongylodiols. Strongylodiols A–C (**1.103**–**1.105**, Figure 1.16), isolated from the Okinawan marine sponge of the genus *Strongylophora* by Watanabe *et al.* in 2000, show potent cytotoxicity towards human T–lymphocyte leukemia (MOLT–4) cells with IC_{50} values ranging from 0.35–0.85 μg/mL.[85] Strongylodiols A–C are intriguing because instead of being isolated as a racemic mixture or an enantiomerically pure propargylic alcohol, they are found as enantioenriched mixtures ranging from 84:16 for strongylodiol C, to 91:9 for strongylodiol A, to 97:3 for strongylodiol B. Later, Watanabe *et al.* isolated Strongylodiols D–J (**1.106**–**1.112**), which are also found as enantioenriched mixtures.[86] Many synthetic strategies have been explored in order to access strongylodiols A (**1.103**) and B (**1.104**), however, there has not been a reported synthesis of other strongylodiols. As well, no further biological testing has been reported.
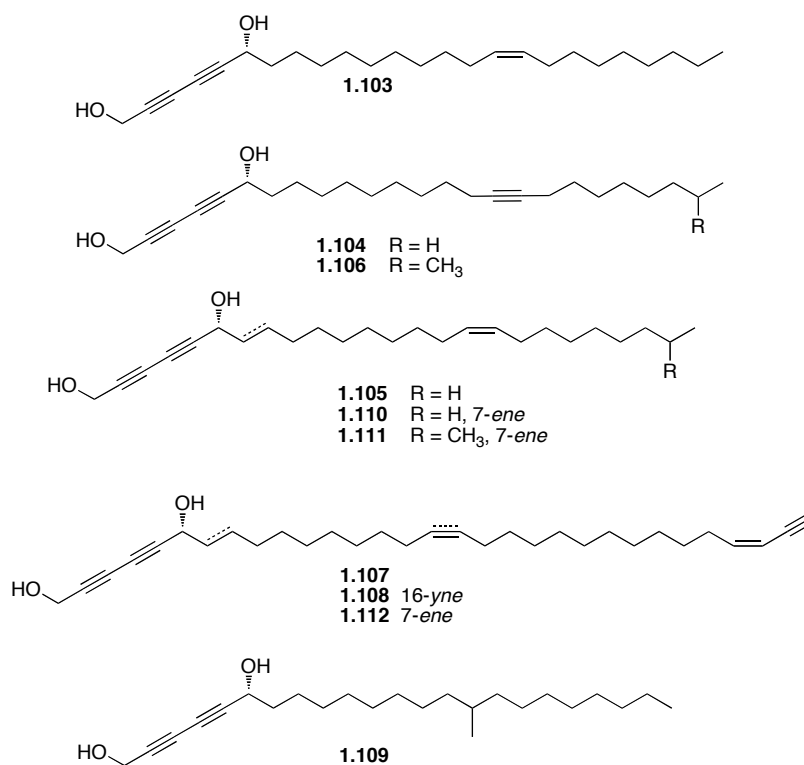
Figure 1.16. Strongylodiols A–J (**1.103**–**1.112**).
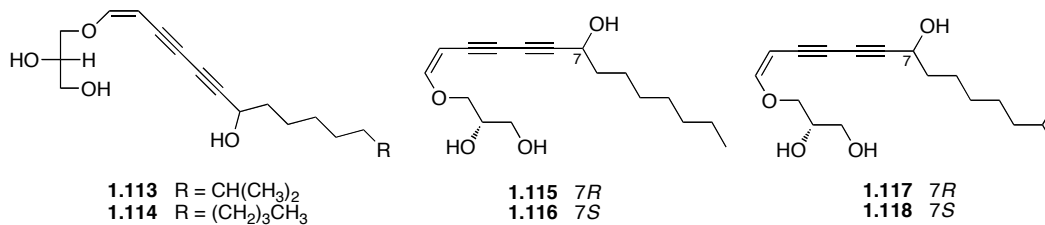
Figure 1.17. Compounds **1.113**, **1.114**, and the petrosynes (**1.115**–**1.118**).

A second class of polyyne marine natural products are vinyl ethers **1.113**–**1.118** (Figure 1.17). Compounds **1.113** and **1.114** are isolated from a sponge in the Petrosiidae family and were found to make up approximately 7% of the

20

membrane lipids in the sponge.[87] The petrosynes (**1.115–1.118**) have also been isolated from the Okinawan sponges and petrosyne Ia (**1.115**) shows moderate antifungal and antibacterial activity towards *Trichophyton mentagrophytes* and *Staphylococcus aureus*.[88] Iguchi *et al.* assigned stereochemistry for **1.115** by synthesizing all possible isomers by starting with either D-mannitol or L-ascorbic acid.[88]

1.119 R^1 = H, R^2 = Br, R^3 = H	**1.121** R = H
1.120 R^1 = Br, R^2 = H, R^3 = H	**1.125** R = SO_3H
1.124 R^1 = H, R^2 = Br, R^3 = SO_3H	
1.122 R^1 = OH, R^2 = H	**1.123**
1.126 R^1 = H, R^2 = SO_3H	
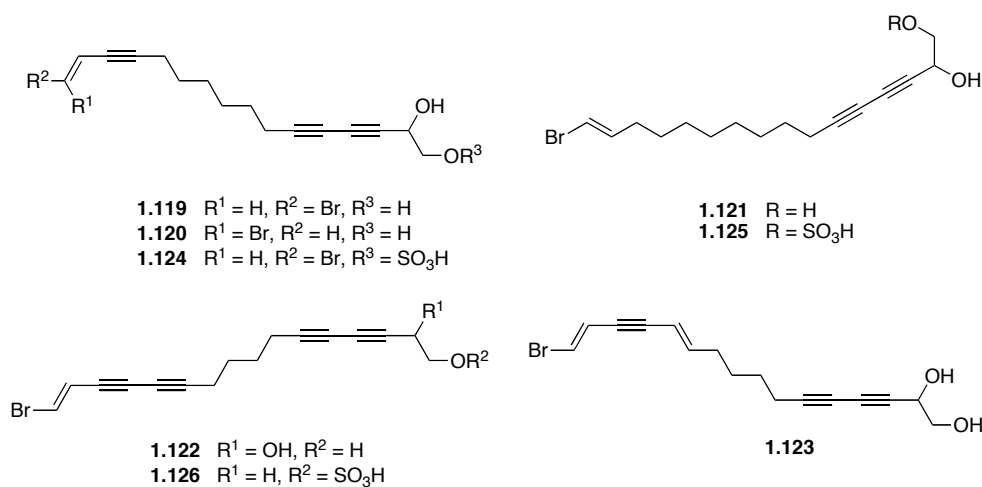
Figure 1.18. Diplynes A–E (**1.119–1.123**), diplyne A 1-sulfate (**1.124**), diplyne C 1-sulfate (**1.125**), and 2-deoxydiplyne D sulfate (**1.126**).

D-Mannitol has also been used as a starting point for Gung and coworkers in the syntheses of the (+)-diplynes (**1.119–1.123**) in order to confirm absolute stereochemistry (Figure 1.18).[89,90] Diplynes A–E (**1.119–1.123**) are examples of brominated polyynes which are isolated from the Philippine sponge *Diplastrella sp.* along with the sulfate derivatives diplyne A 1-sulfate (**1.124**), diplyne C 1-

sulfate (**1.125**) and 2-deoxydiplyne D sulfate (**1.126**). Only the sulfate derivatives show activity towards HIV-1 integrase.[91]
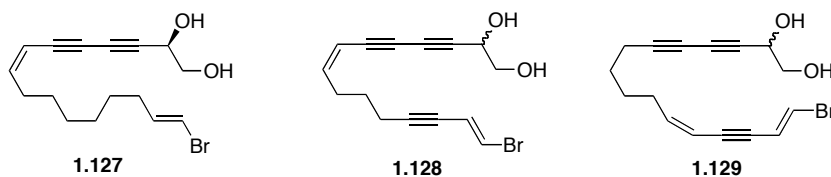
Figure 1.19. Faulknerynes A–C (**1.127–1.129**).

Recently Ko *et al.* isolated (+)-dipyne C (**1.121**) from the Bahamian sponge *Diplastrella sp.* along with faulknerynes A–C (**1.127–1.129**, Figure 1.19).[92] Diplyne C (**1.121**) is an example of a compound being isolated from both a sponge native to the Pacific ocean and one native to the Atlantic ocean. Insufficient amounts of faulknerynes A–C (**1.127–1.129**) have been isolated to compare optical rotations to known compounds or to synthesize Mosher ester derivatives toward determining absolute configuration. Using CD, however, Ko *et al.* suggest that both diplyne C (**1.121**) and faulkneryne A (**1.127**) exist as the (*R*)-enantiomer. While a lack of material has prevented biological testing on the faulknerynes B and C,[92] diplyne C (**1.121**) is cytotoxic against cultured human colon tumor cells (HTC-116) with an ED_{50} of 3.5 μg/mL.

22
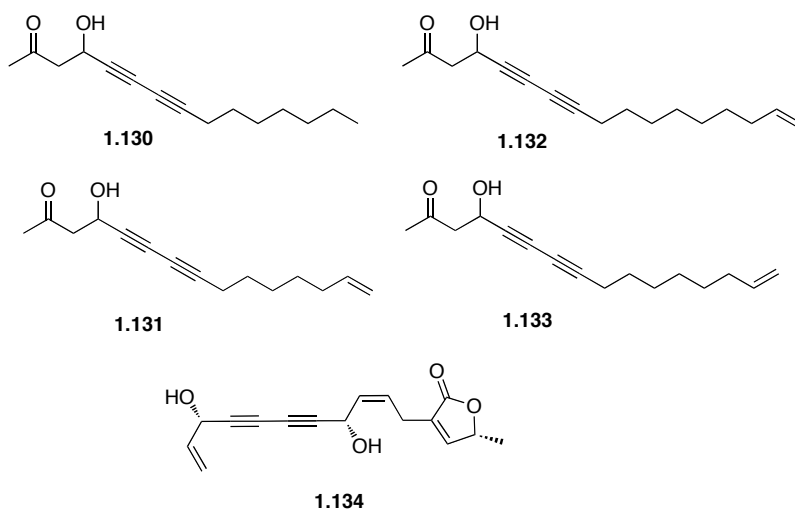
Figure 1.20. Montiporynes I–K (**1.130**–**1.132**), homomontiporyne J (**1.133**) and γ–lactone **1.134**.

Montiporynes I–K (**1.130**–**1.132**) and homomontiporyne J (**1.133**) are found in the *Monitpora sp.* coral (Figure 1.20).[93,94] From 2.5 kg of wet coral only 5.7, 15, 14, and 0.8 mg have been isolated of **1.130**–**1.133**, respectively. The absolute configuration of these compounds has not been determined due to the fact that they eliminate to the corresponding α,β-unsaturated ketone when derivatization is attempted to form the Mosher ester. It is interesting to note that diynes found within stony corals are usually 2,4-diynes, which raises a question on the origin of the 5,7-diynes **1.130**–**1.133**. Alam *et al.* proposed that the aldehyde form of other 2,4-diynes found within Montipora could undergo a crossed-aldol condensation with acetone to give the montiporynes, however, none of the corresponding aldehydes have been observed.

Montiporyne I (**1.130**) has similar or better potency than cisplatin when tested against human skin and ovarian cancer cell lines (ED$_{50}$ values of 1.40 and 1.81 µg/mL, respectively, cisplatin ED$_{50}$ values of 2.18, and 1.09 µg/mL). Finally, the γ–lactone **1.134** is also isolated from a soft coral, called *Sarcophyton trocheliophorum*, and gives positive results in a brine shrimp toxicity assay.[95]
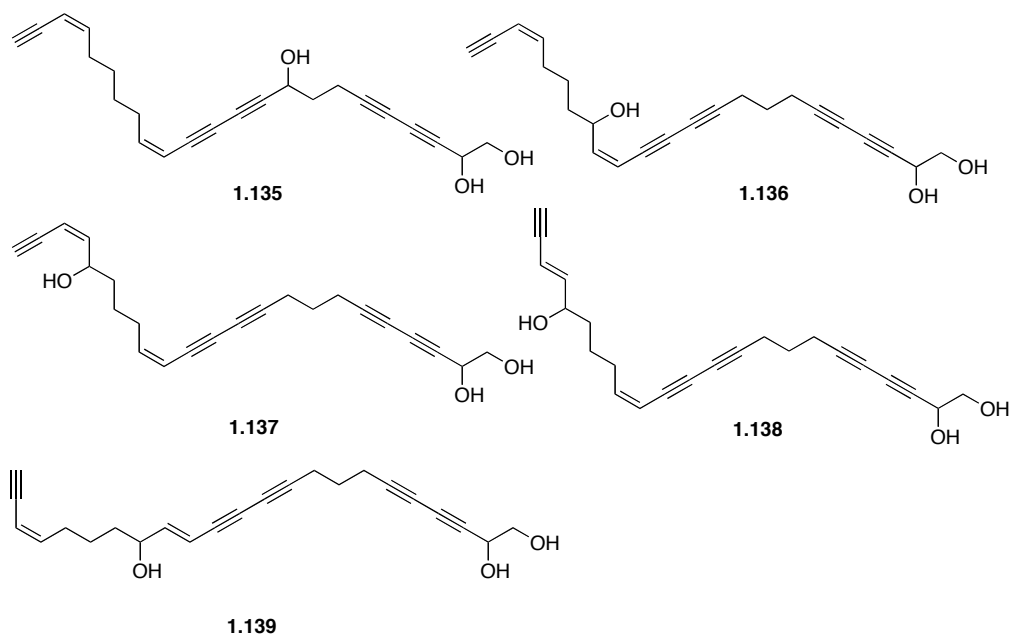
Figure 1.21. Callytriols A–E (**1.135–1.139**).

Callytriols A–E (**1.135–1.139**, Figure 1.21) have been isolated from the sponge family Callyspongiidae,[96] and callytriols A–E are the first examples of acetylenic derivatives that influence larval settlement and metamorphosis of sessile (anchored) marine animals. Also isolated from Callyspongiidae are the related compounds (–)-siphonodiol (**1.140**, Figure 1.22), (–)-tetrasiphonodiol

24

(**1.141**), 14,15-dihydrosiphonodiol (**1.142**), as well as **1.143** and the sulfated versions of (−)-siphonodiol called callyspongins A (**1.144**) and B (**1.145**).[97-99] Compounds **1.140**–**1.142** are H,K-ATPase inhibitors and (−)-siphonodiol (**1.140**) also shows modest activity against *Staphylococcus aureus* and *Streptococcus pyogenes* C-203.[98] Compounds **1.140**, **1.142**, and **1.143** show antiproliferative activity against human promyelocytic leukemia cells (HL-60).[100] (−)-Siphonodiol (**1.140**) is closely related to the diplynes (**1.119**–**1.123**), though it lacks the bromine end group. Callyspongins A (**1.144**) and B (**1.145**) inhibit fertilization of starfish gametes at low concentrations.[99]
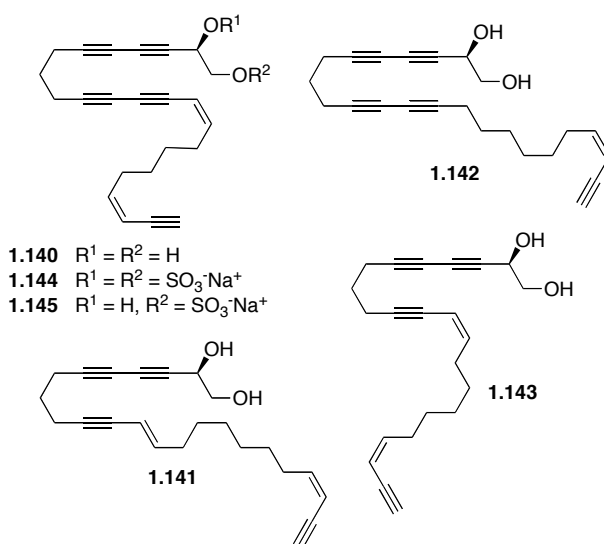
Figure 1.22. Propargylic alcohol polyynes (**1.140**–**1.145**) from the family Callyspongiidae.

The pellynols (**1.146**–**1.154**) and pellynone (**1.155**) are the first acetylenic natural products to be isolated from the genus *Pellina* (Figure 1.23).[101,102]

Pellynols A–H (**1.146**–**1.153**) and pellynone (**1.155**) have been first isolated by Fu *et al.* and are structurally quite similar to the previously isolated melynes A–C (**1.156**–**1.158**), 18-hydroxyrenierin-1 (**1.159**) and -2 (**1.160**).[101-104] Later, when Boyd and co-workers first isolated pellynol I (**1.154**), they demonstrated that pellynol I (**1.155**) along with pellynols A–D (**1.146**–**1.149**) and F (**1.151**) show activity against human melanoma and ovarian tumor cell lines in vitro.[105] Zhou and Molinski have also determined that pellynol A (**1.146**) and I (**1.154**) show high in vitro activities against human colon cancer (IC_{50} values of 0.026 μg/mL and less than 0.008 μg/mL, respectively).[106]
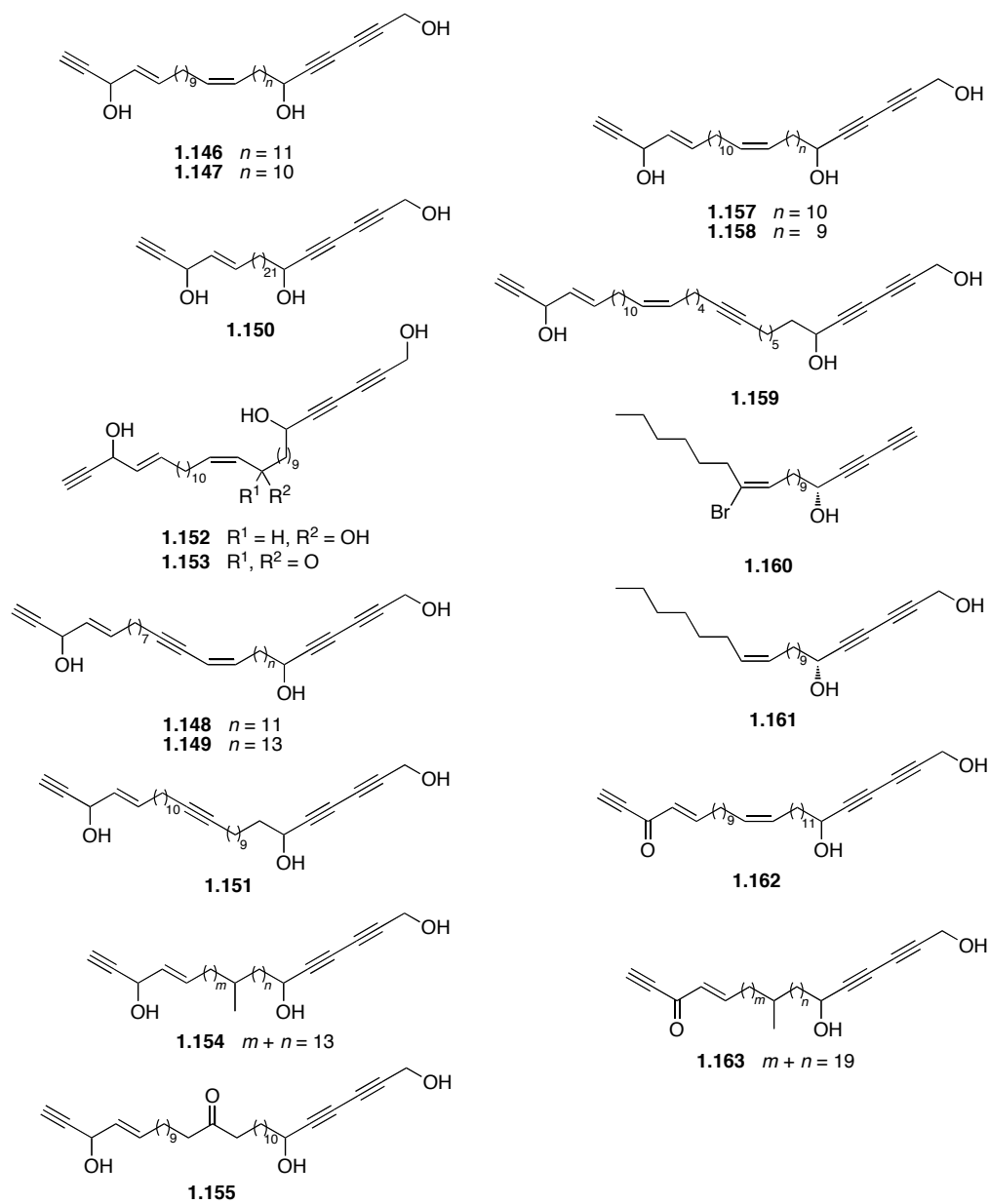
Figure 1.23. Pellynols A–I **1.146**–**1.154**, pellynone **1.155**, Melynes A–C (**1.156**–**1.158**), 18-hydroxyrenierin-1 (**1.159**) and -2 (**1.160**) and halicynones A (**1.161**) and B (**1.162**).

27

At the same time, Zhou *et al.* have isolated halicynone A (**1.161**) and B (**1.162**) from the marine sponge *Haliclona sp.*[106] Notably, without a terminal 1-yn-3-ol functionality, **1.161**–**1.162** show significantly less potency than the pellynols (**1.146**–**1.154**), with IC$_{50}$ values greater than 78 µg/mL against human colon cancer (in vitro).[106]

Related to the pellynols (**1.146**–**1.154**) and halicynones (**1.161**–**1.162**) are the triangulynes A–F and H (**1.163**–**1.169**) which contain a terminal propargylic alcohol moiety.[107] Dai *et al.* have tested the triangulynes against the NCI human tumor cell line panels and report potent cytotoxicities for these compounds against leukemia, colon, and melanoma tumor cells.[107] The related compound triangulynic acid (not shown), which does not contain a propargylic triynol unit, shows reduced non-differential cytotoxicity.[107]
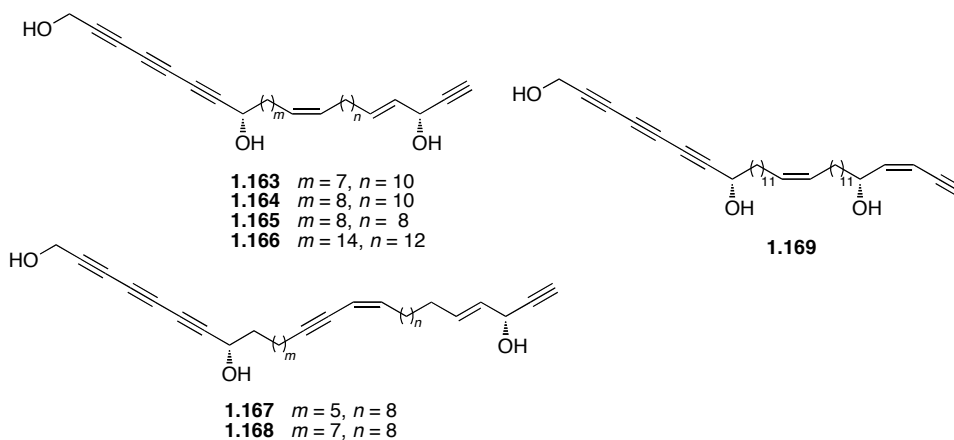
Figure 1.24. Triangulynes A–F and H **1.163**–**1.169**.

28

1.4 Propargylic alcohol polyynes from other sources

Propargylic alcohol triynes are also found in bacteria such as L-660,631 (**1.170**, Figure 1.25) which has been originally isolated from *Actinomecetes* fermentation.[108] Later, Patel *et al.* have isolated **1.170** from *Microbisporia sp.*, where it is called Sch 31828 acid.[109] The acid (**1.170**) and the corresponding methyl ester (**1.171**) show a broad spectrum of in vitro antifungal activity.[7,110]

1.170 R = H
1.171 R = CH₃
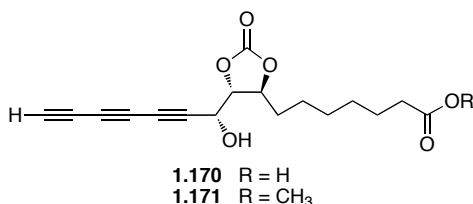
Figure 1.25. L-660,631 (**1.170)** and methyl ester **1.171**.

Thaller and co-workers have isolated the propargylic alcohol diyne (+)-**1.172** from cultures of the fungus *Fayodia bisphareigera* and later synthesized the compound to prove absolute configuration (Figure 1.26).[111] Thaller's group has also isolated a C7 diynol, C9 diynetriol, and a C9 dihydroxy-diynone (**1.173–1.175**) from the fungal cultures *Gymnopilus spectabilis* and *Clitoc rhizophora*.[112] The diynol scobinynediol-I (**1.176**) has been isolated from the fungal culture *Psathyrella scobinacea* by Taha[113] while the propargylic alcohol triyne **1.177** has been isolated from cultures of the Fungus *Collybia peronata* by Jones and co-workers.[114] For the propargylic alcohol polyynes **1.172–1.177**, no biological testing has been published to date.
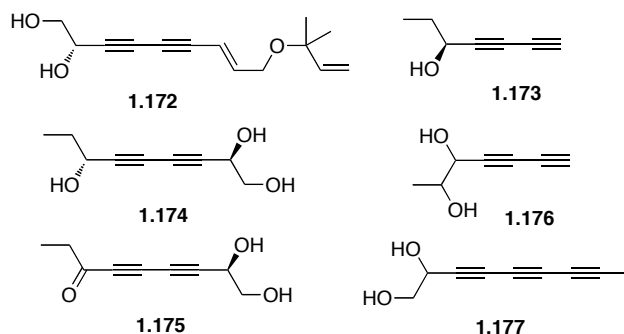
Figure 1.26. Compounds **1.172**–**1.177** from fungal cultures.

The only propargylic diynol from a fungal species that has been evaluated for biological activity is Phomallenic acid A (**1.178**).[115] Phomallenic acid A is an allenic propargylic alcohol diyne isolated from the fungal family Ascomycota, and the stereospecific formation of the (*R*)-allene is expected to be enzymatic. Phomallenic acid A shows antibacterial activity and it is also an inhibitor of the condensation step in fatty acid biosynthesis.[116]
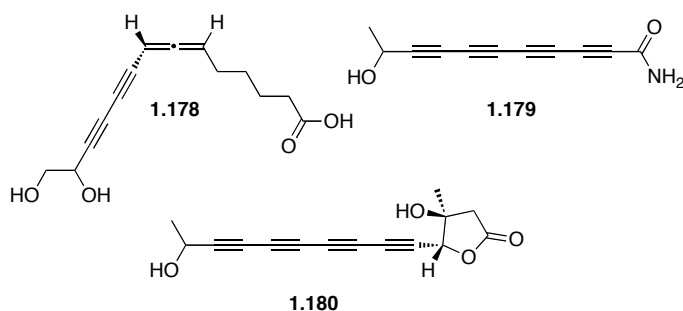
Figure 1.27. Phomallenic acid A (**1.178**), tetraynamide **1.179**, and tetraynoic acid–γ–lactone **1.180**.

Two propargylic alcohol tetraynes have been isolated from the fungus *Mycena virdimarginata* by Bäuerle *et al* (Figure 1.27).[117] The tetrayne tetraynamide **1.179** is active against both Gram-positive and Gram-negative bacteria, yeasts, filamentous fungi, and Ehrlich ascites tumor cells.[118] The tetraynoic acid-γ-lactone **1.180** has similar activities, however, less pronounced.[7,118]

1.5 Origins of biological activity

As described in the previous sections, propargylic alcohol polyynes show a vast array of cytotoxic and inhibitory effects. To render compounds from this class viable as drugs, however, more studies are needed to better outline the basis of biological activity.[3] In particular, structure–activity relationships would provide a better understanding of how slight variations in structure can cause vast differences in cytotoxicity. For example, as shown earlier the presence of the additional hydroxy group at C18 of 18-hydroxyminquartynoic acid results in substantially reduced activity in comparison to minquartynoic acid (**1.98** and **1.97**, see Figure 1.15). Likewise, the presence of the C3 hydroxyl group in C_{17} polyynes such as falcarinol (**1.2**) and panaxydol (**1.5**) is known to enhance biological activity, in comparison to compounds such as falcarindiol (**1.3**) which contain a second hydroxy group at C8.[26] Purup *et al.* propose that the difference in activity is related to the hydrophobicity of each compound, as well as the ability of each to form a stable carbocation.[26] Thus, in both cases (i.e., 18-hydroxyminquartynoic

acid **1.98** and falcarindiol **1.3**), the presence of a second hydroxy group results in decreased biological activity in comparison to the more lipophilic analog (falcarinol **1.2** and minquartynoic acid **1.97**, respectively).
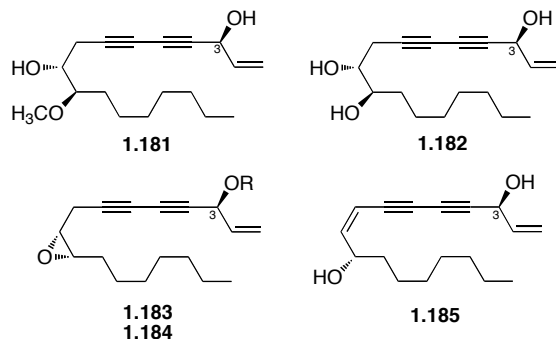
Figure 1.28. Unnatural polyynes **1.181**, **1.182**, **1.183**, **1.184**, and **1.185** with 3*S* configuration.

Satoh *et al.* have illustrated that the C3 epimers of PQ-1 (**1.181**), panaxytriol (**1.182**), panaxydol (**1.183**), acetylpanaxydol (**1.184**), and panaxydiol (**1.185**) having the (3*S*)-configurations (IC$_{50}$ values of 0.01–0.1 µg/mL) are approximately ten times more potent against leukemia cells (L-1210) than the naturally occurring (3*R*)-epimer (IC$_{50}$ values of 0.1–1.0 µg/mL).[119] The stereochemistry at C9 and C10 have no effect on potency for these compounds; however this is not always the case, as mentioned, the C10 epimers of oploxyne B (**1.44** and **1.51**, Figure 1.6) show significantly different potencies.[43]

Recently, Zloh *et al.* have studied the relationship between the electronic properties and biological activities of polyyne natural products; with this they have qualitatively postulated that antimicrobial activity correlates with the

presence of a hydrophobic group on the polyyne.[120] It has also been determined that antiproliferative activity increases with increasing lipole and a correlation is observed between LUMO energies and activity, suggesting that a charge transfer might be involved in the mechanism of action. Although many things have been postulated to account for the activity of propargylic polyynes within the body,[121] there is no direct proof on the mechanism of action.

From the above discussion, several general trends become clear for polyyne natural products containing a propargylic alcohol group. 1) In spite of selected studies that show great promise, the biological activity of many derivatives remains unstudied due to the minimal amount of the material isolated from the natural sources. 2) Only the most basic aspects surrounding the mode of action for this class of polyynol natural products, as well as structure property relationships, have so far been elucidated. 3) In many cases, it is only possible to establish absolute stereochemistry for the natural product through synthetic methods. Thus, the development of improved methods of enantioselective synthesis of polyyne propargylic alcohols is most definitely warranted.

1.6   Synthesis of Polyyne Natural Products with a propargylic alcohol

Typically, methods toward the synthesis of asymmetric propargylic alcohols generate the stereogenic center of the propargylic alcohol early in the synthetic route. The chiral building block is then subjected to a generally

cumbersome and often low yielding process of cross-coupling reactions to eventually extend the acetylenic backbone. Several examples will be used to illustrate this approach.

1.6.1 Enzymatic Reactions

A common route to obtain propargylic alcohols in an enantioselective fashion is through the use of enzymes. Faber and coworkers have shown that both falcarinol and panaxytriol can be synthesized in this fashion.[30] Starting from 1,4-dichloro-2-butyne the racemic propargylic alcohol **1.186** was obtained in two steps and a 29% yield (Scheme 1.1). *Candida antarcitica* lipase B selectively acylates (*R*)-**1.186** to (*R*)-**1.187**, and an *in situ* Mitsunobu reaction then converts the remaining enantiomer (*S*)-**1.186** to (*R*)-**1.186**. This gives an overall yield of 82% and 99% *ee* for (*R*)-**1.186** after removal of the acyl group from (*R*)-**1.187**. The cross-coupling reaction between **1.186** and **1.188** gave falcarinol (**1.2**) in a 69% yield.[30]
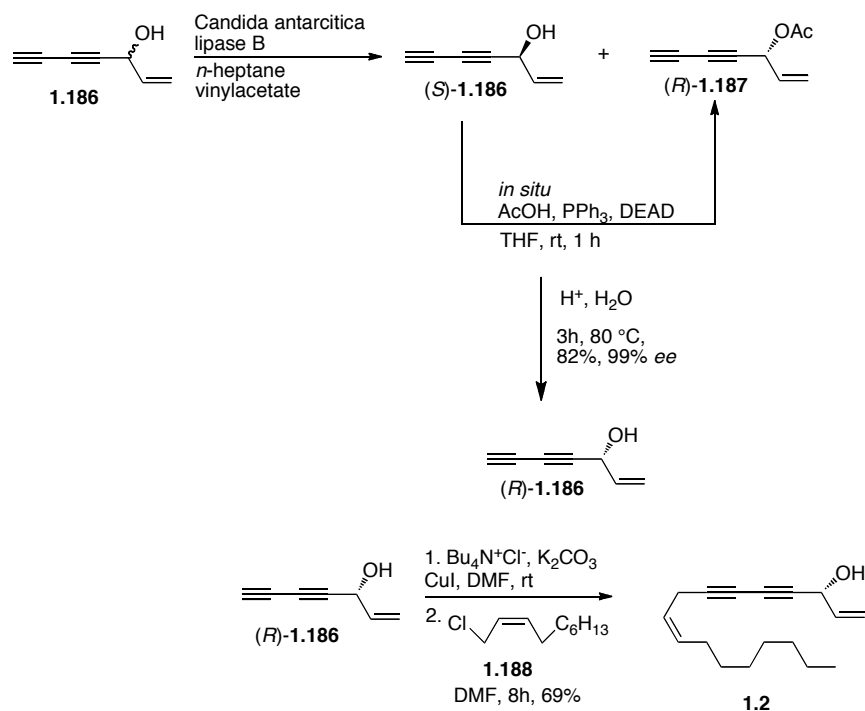
Scheme 1.1. Faber's enzymatic synthesis of (3*R*)-falcarinol (**1.2**).[30]

A drawback to this reaction sequence is the fact that three steps are needed to convert the racemic propargylic alcohol diyne to the enantioenriched product. Although the enantioselectivity in this particular example is quite high, this is not always the case. Enzymes tend to be substrate dependent and even slight changes to the backbone can result in drastic changes in enantioselectivity. Because of this uncertainty, most research groups have avoided the use of enzymes in natural product polyyne synthesis.

1.6.2   Chiral Pool

The chiral pool often provides the building blocks needed to access the desired polyynol natural products. Examples of this approach are shown with the syntheses of the diplynes by Gung and coworkers starting from D-mannitol (Scheme 1.2).[89,90] The bromoacetylene **1.189** is prepared from D-mannitol in four steps and a 17% overall yield and then cross-coupled with either **1.190** or **1.192** to give **1.191** or **1.193** in 45 or 63% yield, respectively. After removal of the acetonide protecting group from **1.191**, diplyne C (**1.121**) was obtained in a 7% overall yield from D-mannitol. Toward diplyne E, cross-coupling of **1.189** with **1.192** gave compound **1.193**, which was taken on through six synthetic steps to give the desired product **1.123** in a 2% overall yield from D-mannitol. Thus, while the chiral pool offers readily available chiral building blocks to polyyne products, one would need to start with, for example 50 g of D-mannitol to obtain 1.6 g of diplyne E (**1.123**), highlighting one of the drawbacks in introducing chirality in the first stages of the synthetic scheme. A second point that can be made here is the inefficiency that is often encountered in oxidative acetylenic coupling reactions (as in the formation of **1.191** and **1.193**). The yield of these reactions is often ca. 50%, and when this step occurs after chirality is incorporated, it is often the major reason for a low overall yield, demonstrating an inefficient use of chiral starting material.
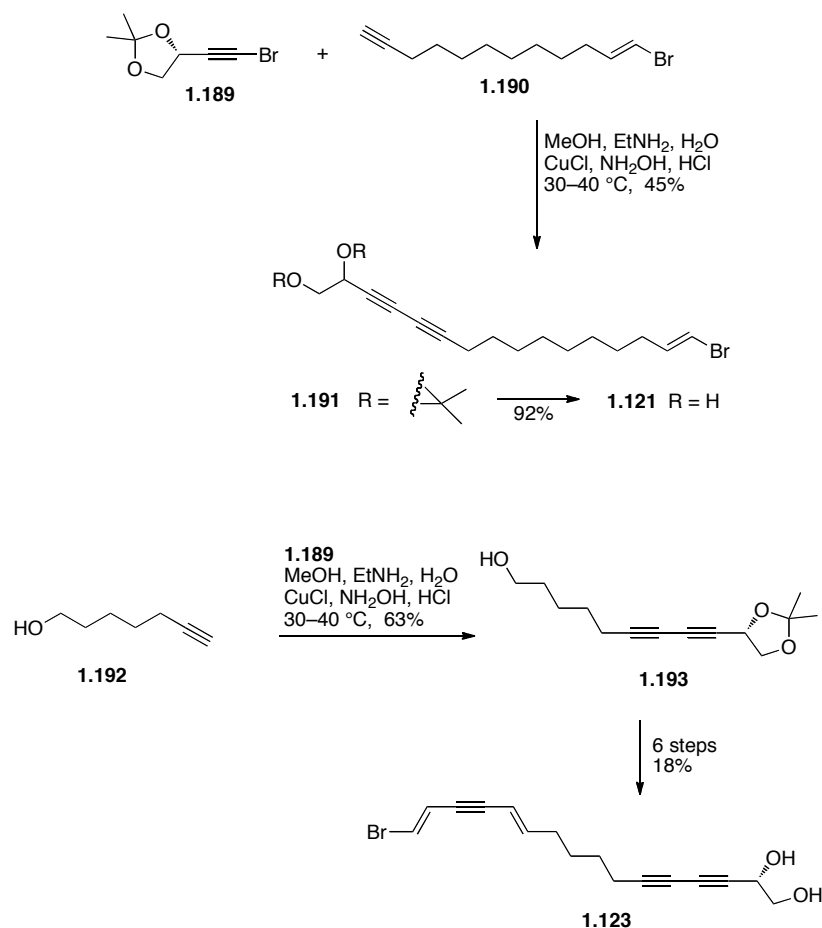
Scheme 1.2. Gung's synthesis of (+)–diplyne C (**1.121**) and E (**1.123**).

1.6.3 Asymmetric Epoxidation

Asymmetric epoxidation and double elimination can also be used to give a propargylic alcohol. This is demonstrated in Yadav and coworkers' synthesis of (R)-strongylodiol A (**1.103**, Scheme 1.3). Starting from 1,10-decanediol, nine steps gave the allylic alcohol **1.194**, which underwent a Sharpless asymmetric epoxidation and subsequent conversion of the alcohol to the epoxy-chloride **1.195**

in 76% yield over the two steps. In the presence of strong base they obtained the optically active propargylic alcohol **1.196**, which still needed to undergo the copper catalyzed cross-coupling reaction to give strongylodiol A (**1.103**).
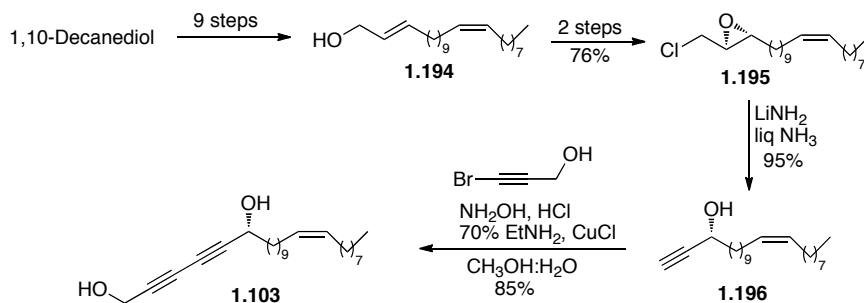
Scheme 1.3. Yadav's synthesis of (*R*)-strongylodiol A (**1.103**).[122]

1.6.4   Enantioselective Ketone Reduction

A common way to obtain an optically active propargylic alcohol is the stereoselective reduction of a ketone. An example of this approach is demonstrated in Scheme 1.4 with Baldwin's synthesis of (*R*)-strongylodiol B. Starting from 9-dodecyn-1-ol, Baldwin's group obtained the corresponding aldehyde **1.197** in three steps and a 43% yield, which was reacted with the TMS-lithium acetylide to give the racemic alcohol **1.198**. Alcohol **1.198** was oxidized to ketone **1.199** with IBX and then selectively reduced in the presence of Noyori's Ru–catalyst (catalyst 1) to give the alcohol **1.200** in a 95% *ee*. After removal of the silyl protecting group, a copper catalyzed cross-coupling reaction with 1-bromo-2-propyn-3-al gave strongylodiol B (**1.104**) in eight steps and a 22% yield. A downside to this reaction sequence is that two steps are needed to convert

racemic **1.198** to the enantioenriched alcohol **1.200**, with two further steps required to give the product.
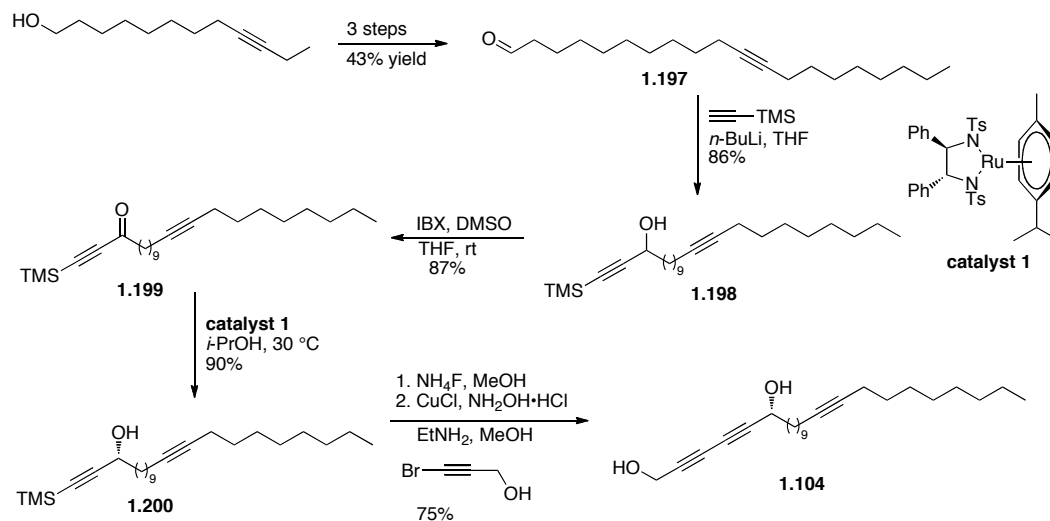
Scheme 1.4. Baldwin's synthesis of strongylodiol B (1.104).[123]

1.6.5   Asymmetric Addition to an Alkyne

Asymmetric addition of an acetylide to an aldehyde is the most expedient route to optically active propargylic alcohols. The first example of an asymmetric addition of an alkyne into an aldehyde has been reported by Mukiayama *et al.* in 1979, using chiral ligand **1.201** (Scheme 1.5).[124] Although this route gives respectable yields and enantioselectivities, it requires the use of a lithium acetylide and temperatures below –123 °C.
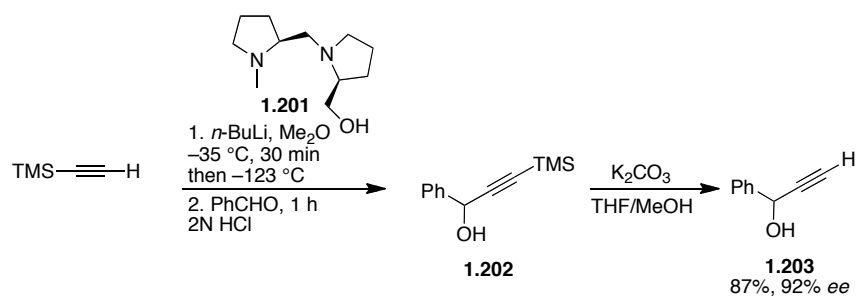
Scheme 1.5. Mukaiyama's route to propargylic alcohols.

Zinc acetylides have been known to function well as nucleophiles in addition reactions to carbonyl compounds.[125,126] It was not until 2000, however, that a mild and highly enantioselective protocol for this process was reported.[16] Carreira and co-workers found that when zinc triflate was combined with triethylamine and a terminal acetylene in the presence of (*R,S*)- or (*S,R*)-*N*-methylephedrine, the resulting acetylide would react with an aldehyde to give a propargylic alcohol product with high enantioselectivities (>90% *ee*, in most cases).[127-131] This method works quite well for many aldehydes and demonstrates a drastic improvement on previous methods for obtaining chiral propargylic alcohols.
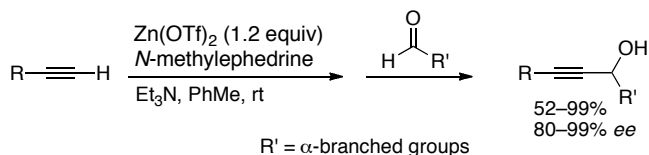
Scheme 1.6. Carreira's route to the asymmetric synthesis of propargylic alcohols.

Carreira and coworkers have quite thoroughly studied the scope of the reaction described in Scheme 1.6 using monoyne precursors, while only one example of a diyne addition has been described, toward the syntheses of strongylodiols A and B (Scheme 1.7).[132] The synthesis of both strongylodiols derives from diyne **1.204**, via an enantioselective addition to either aldehyde **1.205** or **1.206** to give **1.207** and **1.208** with enantioselectivities of 82 and 80%, respectively. Removal of the silyl protecting group from **1.207** and **1.208** then gave either strongylodiol A or B in either five or six longest linear steps.
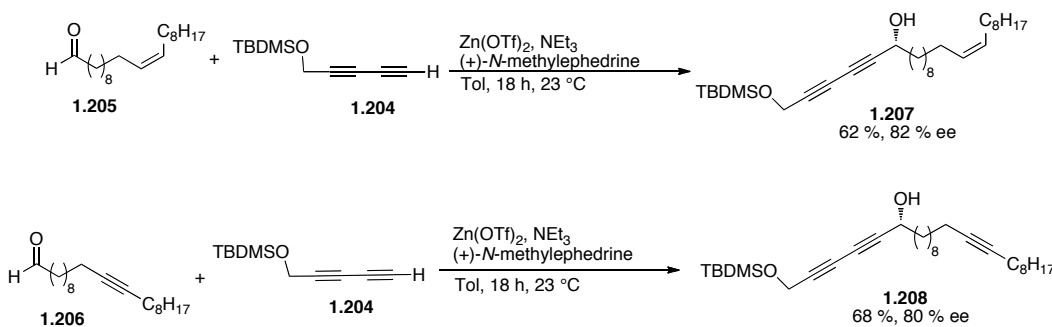
Scheme 1.7. Carreira's synthesis of strongylodiols A and B.

Since Carreira's synthesis of the strongylodiols, the only other example of an asymmetric addition of a polyyne into an aldehyde has been reported by Trost and coworkers.[133] In the Trost protocol, dimethylzinc is used in the presence of the catalyst (*S,S*)-ProPhenol, to give the propargylic alcohols in good to excellent yields and enantioselectivities. The substrates that work best with the Trost protocol are α,β-unsaturated and non α-branched aldehydes, which is the

opposite trend to that observed using the Carreira method which gave the best enantioselectivities with α-branched aldehydes.

$$R-\!\!\equiv\!\!\equiv\!\!-H \xrightarrow[\substack{Ph_3PO, ZnMe_2 \text{ (3 equiv)}\\ PhMe, 4\ ^\circ C}]{(S,S)\text{-ProPhenol (10 mol\%)}} \xrightarrow[]{\underset{H}{\overset{O}{\parallel}}\!\!\diagup\!\!R'} R-\!\!\equiv\!\!\equiv\!\!\underset{\underset{R'}{|}}{\overset{OH}{|}}$$
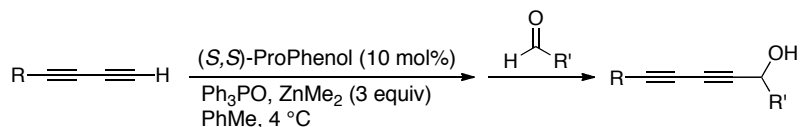
Scheme 1.8. The Trost protocol.

1.7   Homoallylic Propargylic Alcohols

Another prevalent class of propargylic alcohols found in nature are the homoallylic propargylic alcohols (**1.209**). This backbone is a starting point in accessing a wide range of synthetically important building blocks, as both the alkyne and alkene can be used as synthetic handles to obtain more complex structures (please see more of a focus on this topic in Chapter 3). Because of its significant synthetic viability, this backbone is also often exploited in natural product syntheses. The most direct way to access this backbone is to perform an allylation reaction on a propargylic aldehyde. Common allylation methods to date require a stoichiometric chiral reagent and usually the use of harsh metals (Ti, Sn, Cr, Zr, Ag, Rh).[134-143] An example of a reaction that does not use harsh or toxic metals is in an allylboration reaction, however, the only reported allylborations of propargylic aldehydes to date require the use of stoichiometric chiral allylboranes[144-147] or allylboronates.[148-152] Recently, catalytic asymmetric allylboration methods for saturated[153-155] (Equation 1.1) and α,β-unsaturated

(Equation 1.2) aldehydes have been developed,[156] however any attempts to use these protocols with propargylic aldehydes has resulted in a decrease of enantioselectivity to nearly racemic.[155] Due to space constraints, more information on the allylboration reaction and developments towards the catalytic asymmetric allylboration reaction will be postponed until Chapter 3.

1.209
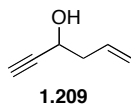
Figure 1.29. An example of a homoallylic propargylic alcohol **1.204**.
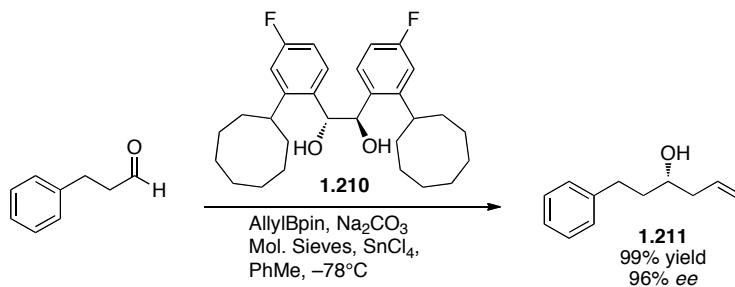
Equation 1.1. A catalytic asymmetric allylboration method that works well on aliphatic aldehydes by Hall and coworkers.
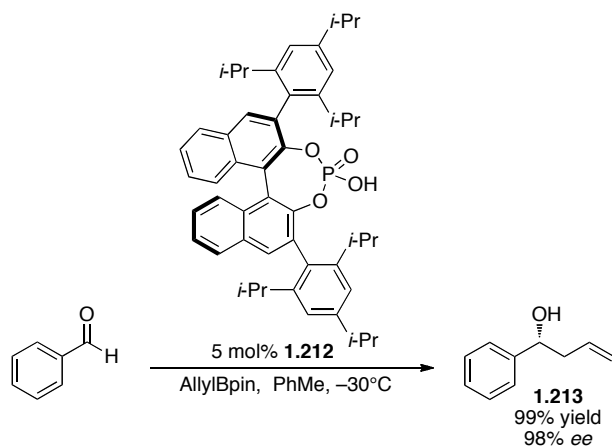
Equation 1.2. A catalytic asymmetric allylboration method that works well on α,β-aldehydes by Antilla and coworkers.

1.8   Goals of this Research

Our approach was two fold. First by applying a method similar to that used by Carreira and coworkers, we would optimize conditions for the asymmetric addition of diynes into α-branched aldehydes. With a protocol previously used in the Tykwinski group[9,157] we could access polyynes in an expedient fashion and then explore the scope of the asymmetric alkynylation of diynes into aldehydes. This protocol would also allow us to develop the asymmetric addition of triynes to aldehydes, which has not yet been reported. Another process that will be discussed is the *in situ* formation of the asymmetric propargylic diyne or triyne framework from the corresponding dibromoolefin precursor, through the use of a one–pot protocol.[158]

The second focus of this research will be to look at developing a catalytic asymmetric allylation of propargylic aldehydes. Starting with methods applied by Rauniyar *et al.*[153-155] we will look at the development of a method for the catalytic asymmetric allylboration of propargylic aldehydes.

1.9   References

(1)   Newman, D. J.; Cragg, G. M. *J. Nat. Prod.* **2007**, *70*, 461-477.

(2)   Dembitsky, V. *Lipids* **2006**, *41*, 883-924.

(3)   Minto, R.; Blacklock, B. *Prog. Lipid Res.* **2008**, *47*, 233-306.

(4)   Zidorn, C.; Johrer, K.; Ganzera, M.; Schubert, B.; Sigmund, E.; Mader, J.; Greil, R.; Ellmerer, E.; Stuppner, H. *J. Agric. Food Chem.* **2005**, *53*, 2518-2523.

(5)   Yang, M.; Kwon, H.; Kim, Y.; Lee, K.; Yang, H. *J. Nat. Prod.* **2010**, *73*, 801-805.

(6)   Kobaisy, M.; Abramowski, Z.; Lermer, L.; Saxena, G.; Hancock, R. E.; Towers, G. H.; Doxsee, D.; Stokes, R. W. *J. Nat. Prod.* **1997**, *60*, 1210-1213.

(7)   Shi Shun, A. L. K.; Tykwinski, R. R. *Angew. Chem. Int. Ed.* **2006**, *45*, 1034-1057.

(8)   Christensen, L.; Brandt, K. *J. Pharm. Biomed. Anal.* **2006**, *41*, 683-693.

(9)   Chalifoux, W. A.; Tykwinski, R. R. *C. R. Chim.* **2009**, *12*, 341-358.

(10)   Bohlmann, F.; Burkhardt, T.; Zdero, C. *Naturally Occurring Acetylenes*; Academic Press: New York, 1973.

(11)   Siddiq, A.; Dembitsky, V. *Anti-Cancer Agents Med. Chem.* **2008**, *8*, 132-170.

(12)   Rucker, G.; Kehrbaum, S.; Sakulas, H.; Lawong, B.; Goeltenboth, F. *Planta Med.* **1992**, *58*, 266-269.

(13)   Pan, Y.; Lowary, T. L.; Tykwinski, R. R. *Can. J. Chem.* **2009**, *87*, 1565-1582.

(14)   Pu, L. *Tetrahedron* **2003**, *59*, 9873-9886.

(15)   Trost, B. M.; Weiss, A. H. *Adv. Synth. Catal.* **2009**, *351*, 963-983.

(16)   Ashwanden, P.; Carreira, E. M. *Acetylene Chemistry: Chemistry, Biology and Material Science* **2005**, 101–138.

(17)   Cozzi, P. G.; Hilgraf, R.; Zimmermann, N. *Eur. J. Org. Chem.* **2004**, 4095-4105.

(18)   Lu, G.; Li, Y. M.; Li, X. S.; Chan, A. S. C. *Coord. Chem. Rev.* **2005**, *249*, 1736-1744.

(19)   Gung, B. W. *C. R. Chim.* **2009**, *12*, 489-505.

(20)   Takahashi, M.; Isoi, K.; Kimura, Y.; Yoshikura, M. *Yakugaku Zasshi.* **1964**, *84*, 752-756.

(21)   Hansen, L.; Boll, P. M. *Phytochemistry* **1986**, *25*, 285-293.

(22)   Takahashi, M.; Yoshikura, M. *Yakugaku Zasshi.* **1966**, *86*, 1051-1053.

(23)   Bohlmann, F.; Niedballa, U.; Rode, K. M. *Chem. Ber.* **1966**, *99*, 3552-3558.

(24)   Baranska, M.; Schulz, H.; Baranski, R.; Nothnagel, T.; Christensen, L. *J. Agric. Food Chem.* **2005**, *53*, 6565-6571.

(25)   Matsuura, H.; Saxena, G.; Farmer, S. W.; Hancock, R. E. W.; Towers, G. H. N. *Planta Med.* **1996**, *62*, 256-259.

(26)   Purup, S.; Larsen, E.; Christensen, L. P. *J. Agric. Food Chem.* **2009**, *57*, 8290-8296.

(27)   Schmiech, L.; Alayrac, C.; Witulski, B.; Hofmann, T. *J. Agric. Food Chem.* **2009**, *57*, 11030-11040.

(28)   Metzger, B.; Barnes, D.; Reed, J. *J. Agric. Food Chem.* **2008**, *56*, 3554-3560.

(29)   Matsunaga, H.; Katano, M.; Yamamoto, H.; Fujito, H.; Mori, M.; Takata, K. *Chem. Pharm. Bull.* **1990**, *38*, 3480.

(30)   Mayer, S.; Steinreiber, A.; Orru, R.; Faber, K. *J. Org. Chem.* **2002**, *67*, 9115-9121.

(31)   Yamazoe, S.; Hasegawa, K.; Shigemori, H. *Phytochemistry* **2007**, *68*, 1706-1711.

(32)   Hirakura, K.; Fushimi, K.; Chin, M.; Japan Kokai Tokkyo Koho: Japanese Patent: JP 06025088 A2 19940201 Heisei., 1994, p 6.

(33)   Yang, M. C.; Seo, D. S.; Choi, S. U.; Park, Y. H.; Lee, K. R. *Arch. Pharmacal Res.* **2008**, *31*, 154-159.

(34)   Kazuhiro, F. F., K.; Chin, M.; KoKai Tokkyo Koho: Japanese Patent: JP 06025088 A2 19940201, 1994, p 6.

47

(35)   Chen, W.-H.; Ma, X.-M.; Wu, Q.-X.; Shi, Y.-P. *Can. J. Chem.* **2008**, *86*, 892-898.

(36)   Bernart, M. W.; Cardellina, J. H.; Balaschak, M. S.; Alexander, M. R.; Shoemaker, R. H.; Boyd, M. R. *J. Nat. Prod.* **1996**, *59*, 748-753.

(37)   Fujimoto, Y.; Satoh, M.; Takeuchi, N.; Kirisawa, M. *Chem. Pharm. Bull.* **1991**, *39*, 521-523.

(38)   Fujimoto, Y.; Hongcheng, W.; Kirisawa, M.; Satoh, M.; Takeuchi, N. *Phytochemistry* **1992**, *31*, 3499-3501.

(39)   Fujihashi, T.; Okuma, T.; Hirakura, K.; Mihashi, H. **1991**, 14.

(40)   Huang, W.; Yang, J.; Zhao, J.; Wang, C.-Z.; Yuan, C.-S.; Li, S.-p. *J. Pharm. Biomed. Anal.* **2010**, *53*, 906-910.

(41)   Huang, W. H.; Zhang, Q. W.; Wang, C. Z.; Yuan, C. S.; Li, S. P. *Molecules (Basel, Switzerland)* **2010**, *15*, 1089-1096.

(42)   Xu, L.; Wu, X. H.; Zheng, G. R.; Cai, J. C. *Chin. Chem. Lett.* **2000**, *11*, 213-216.

(43)   Yadav, J.; Boyapelly, K.; Alugubelli, S.; Pabbaraja, S.; Vangala, J.; Kalivendi, S. *J. Org. Chem.* **2011**, *76*, 2568–2576.

(44)   Hu, C. Q.; Chang, J. J.; Lee, K. H. *J. Nat. Prod.* **1990**, *53*, 932-935.

(45)   Oliveira, J. M.; Palmeira, D. J.; Comassetob, J. V.; Menezes, P. H. *J. Braz. Chem. Soc.* **2010**, *21*, 362-366.

(46)   Shim, S. C.; Chang, S. K.; Hur, C. W.; Kim, C. K. *Phytochemistry* **1987**, *26*, 2849-2850.

(47)   Saita, T.; Katano, M.; Matsunaga, H.; Kouno, I.; Fujito, H.; Mori, M. *Biol. Pharm. Bull.* **1995**, *18*, 933-937.

(48)   Furumi, K.; Fujioka, T.; Fujii, H.; Okabe, H.; Nakano, Y.; Matsunaga, H.; Katano, M.; Mori, M.; Mihashi, K. *Bioorg. Med. Chem. Lett.* **1998**, *8*, 93-96.

(49)   Kim, J. Y.; Lee, K. W.; Kim, S. H.; Wee, J. J.; Kim, Y. S.; Lee, H. J. *Planta Med.* **2002**, *68*, 119-122.

(50)   Fujioka, T.; Furumi, K.; Fujii, H.; Okabe, H.; Mihashi, K.; Nakano, Y.; Matsunaga, H.; Katano, M.; Mori, M. *Chem. Pharm. Bull.* **1999**, *47*, 96-100.

(51)   Ohta, T.; Uwai, K.; Kikuchi, R.; Nozoe, S.; Oshima, Y.; Sasaki, K.; Yoshizaki, F. *Tetrahedron* **1999**, *55*, 12087-12098.

(52)   Wittstock, U.; Hadacek, F.; Wurz, G.; Teuscher, E.; Greger, H. *Planta Med.* **1995**, *61*, 439-445.

(53)   Uwai, K.; Ohashi, K.; Takaya, Y.; Ohta, T.; Tadano, T.; Kisara, K.; Shibusawa, K.; Sakakibara, R.; Oshima, Y. *J. Med. Chem.* **2000**, *43*, 4508-4515.

(54)   Uwai, K.; Ohashi, K.; Takaya, Y.; Oshima, Y.; Furukawa, K.; Yamagata, K.; Omura, T.; Okuyama, S. *Brain Res.* **2001**, *889*, 174-180.

(55)   Fiandanese, V.; Bottalico, D.; Cardellicchio, C.; Marchese, G.; Punzi, A. *Tetrahedron* **2005**, *61*, 4551-4556.

(56)   Gung, B. W.; Omollo, A. O. *Eur. J. Org. Chem.* **2009**, 1136-1138.

(57)   Appendino, G.; Pollastro, F.; Verotta, L.; Ballero, M.; Romano, A.; Wyrembek, P.; Szczuraszek, K.; Mozrzymas, J.; Taglialatela-Scafati, O. *J. Nat. Prod.* **2009**, *72*, 962-965.

(58)   Takaishi, Y.; Okuyama, T.; Masuda, A.; Nakano, K.; Murakami, K.; Tomimatsu, T. *Phytochemistry* **1990**, *29*, 3849-3852.

(59)   Jung, H.; Min, B.; Park, J.; Kim, Y.; Lee, H.; Bae, K. *J. Nat. Prod.* **2002**, *65*, 897-901.

(60)   Jung, H.; Hung, T.; Minkyun, N.; Byung Sun, M.; Byoung Mog, K.; Kihwan, B. *Nat. Prod. Sci.* **2009**, *15*, 110-113.

(61)   Setzer, W. N.; Green, T. J.; Whitaker, K. W.; Moriarty, D. *Planta Med.* **1995**, *61*, 470-471.

(62)   Moriarty, D. M.; Huang, J.; Yancey, C. A.; Zhang, P.; Setzer, W. N.; Lawton, R. O.; Bates, R. B.; Caldera, S. *Planta Med.* **1998**, *64*, 370-372.

(63)   Dat, N. T.; Cai, X. F.; Shen, Q.; Lee, I. S.; Lee, E. J.; Park, Y. K.; Bae, K. H.; Kim, Y. H. *Chem. Pharm. Bull.* **2005**, *53*, 1194-1196.

(64)   Wang, N.; Yao, X.; Ishii, R.; Kitanaka, S. *Chem. Pharm. Bull.* **2001**, *49*, 938-942.

(65)   Jang, D. S.; Lee, Y. M.; Jeong, I. H.; Kim, J. S. *Arch. Pharm. Res.* **2010**, *33*, 875-880.

(66)   Ishimaru, K.; Osabe, M.; Yan, L.; Fujioka, T.; Mihashi, K.; Tanaka, N. *Phytochemistry* **2003**, *62*, 643-646.

(67)   Lee, S. M.; Bae, K. H.; Sohn, H. J. *Tetrahedron Lett.* **2009**, *50*, 416-418.

(68)   Lee, S. M.; Lee, H. B.; Lee, C. G. *Food Chem.* **2010**, *123*, 955-958.

(69)   Kitajima, J.; Kamoshita, A.; Ishikawa, T.; Takano, A.; Fukuda, T.; Isoda, S.; Ida, Y. *Chem. Pharm. Bull.* **2003**, *51*, 1106-1108.

(70)   Mei, R. Q.; Lu, Q.; Hu, Y. F.; Liu, H. Y.; Bao, F. K.; Zhang, Y.; Cheng, Y. X. *Helv. Chim. Acta* **2008**, *91*, 90-96.

(71)   Stavri, M.; Ford, C. H. J.; Bucar, F.; Streit, B.; Hall, M. L.; Williamson, R. T.; Mathew, K.; Gibbons, S. *Phytochemistry* **2005**, *66*, 233-239.

(72)   Stavri, M.; Mathew, K. T.; Gibson, T.; Williamson, R. T.; Gibbons, S. *J. Nat. Prod.* **2004**, *67*, 892-894.

(73)   Zhang, H.; Lu, Z.; Tan, G. T.; Qiu, S.; Farnsworth, N. R.; Pezzuto, J. M.; Fong, H. H. S. *Tetrahedron Lett.* **2002**, *43*, 973-977.

(74)   Lehner, M. S.; Steigel, A.; Bauer, R. *Phytochemistry* **1997**, *46*, 1023-1028.

(75)   Resch, M.; Heilmann, J.; Steigel, A.; Bauer, R. *Planta Med.* **2001**, *67*, 437-442.

(76)   Rashid, M.; Gustafson, K.; Cardellina, J.; Boyd, M. *Nat. Prod. Res.* **2001**, *15*, 21-26.

(77)   Fort, D.; King, S.; Carlson, T.; Nelson, S. *Biochem. Syst. Ecol.* **2000**, *28*, 489-490.

(78)   Marles, R.; Farnsworth, N.; Neill, D. *J. Nat. Prod.* **1989**, *52*, 261-266.

(79)   Rasmussen, H.; Christensen, S.; Kvist, L.; Kharazmi, A.; Huansi, A. *J. Nat. Prod.* **2000**, *63*, 1295-1296.

(80)   Ito, A.; Cui, B.; Chávez, D.; Chai, H. B.; Shin, Y. G.; Kawanishi, K.; Kardono, L. B. S.; Riswan, S.; Farnsworth, N. R.; Cordell, G. A. *J. Nat. Prod.* **2001**, *64*, 246-248.

(81)   Pagani, F.; Romussi, G. *Phytochemistry* **1971**, *10*, 2233-2233.

(82)   Pagani, F.; Romussi, G.; Bohlmann, F. *Chem. Ber.* **1972**, *105*, 3126-3127.

(83)   Bauer, R.; Redl, K.; Davis, B. *Phytochemistry* **1992**, *31*, 2035-2037.

(84)   Tobinaga, S.; Sharma, M. K.; Aalbersberg, W. G. L.; Watanabe, K.; Iguchi, K.; Narui, K.; Sasatsu, M.; Waki, S. *Planta Med.* **2009**, *75*, 624-628.

(85)   Watanabe, K.; Tsuda, Y.; Yamane, Y.; Takahashi, H.; Iguchi, K.; Naoki, H.; Fujita, T.; Van Soest, R. W. M. *Tetrahedron Lett.* **2000**, *41*, 9271-9276.

(86)   Watanabe, K.; Tsuda, Y.; Hamada, M.; Omori, M.; Mori, G.; Iguchi, K.; Naoki, H.; Fujita, T.; Van Soest, R. W. M. *J. Nat. Prod.* **2005**, *68*, 1001-1005.

(87)   Perry, N. B.; Becker, E. G.; Blunt, J. W.; Lake, R. J.; Munro, M. H. G. *J. Nat. Prod.* **1990**, *53*, 732-734.

(88)   Iguchi, K.; Kitade, M.; Kashiwagi, T.; Yamada, Y. *J. Org. Chem.* **1993**, *58*, 5690-5698.

(89)   Gung, B.; Gibeau, C.; Jones, A. *Tetrahedron: Asymmetry* **2004**, *15*, 3973-3977.

(90)   Gung, B.; Gibeau, C.; Jones, A. *Tetrahedron: Asymmetry* **2005**, *16*, 3107-3114.

(91)   Lerch, M.; Harper, M.; Faulkner, D. *J. Nat. Prod.* **2003**, *66*, 667-670.

(92)   Ko, J.; Morinaka, B. I.; Molinski, T. F. *J. Org. Chem.* **2011**, *76*, 667-670.

(93)   Alam, N.; Bae, B. H.; Hong, J.; Lee, C. O.; Im, K. S.; Jung, J. H. *J. Nat. Prod.* **2001**, *64*, 1059-1063.

(94)   Alam, N.; Hong, J.; Lee, C.; Choi, J.; Im, K.; Jung, J. *Chem. Pharm. Bull.* **2002**, *50*, 661-662.

(95) Řezanka, T.; Dembitsky, V. M. *Tetrahedron* **2001**, *57*, 8743-8749.

(96) Tsukamoto, S.; Kato, H.; Hirota, H.; Fusetani, N. *J. Nat. Prod.* **1997**, *60*, 126-130.

(97) Tada, H.; Yasuda, F. *Chem. Lett.* **1984**, 779-780.

(98) Fusetani, N.; Sugano, M.; Matsunaga, S.; Hashimoto, K. *Tetrahedron Lett.* **1987**, *28*, 4311-4312.

(99) Uno, M.; Ohta, S.; Ohta, E.; Ikegami, S. *J. Nat. Prod.* **1996**, *59*, 1146-1148.

(100) Umeyama, A.; Matsuoka, N.; Mine, R.; Nakata, A.; Arimoto, E.; Matsui, M.; Shoji, N.; Arihara, S.; Takei, M.; Hashimoto, T. *J. Nat. Med.* **2010**, *64*, 93-97.

(101) Fu, X.; Abbas, S. A.; Schmitz, F. J.; Vidavsky, I.; Gross, M. L.; Laney, M.; Schatzman, R. C.; Cabuslay, R. D. *Tetrahedron* **1997**, *53*, 799-814.

(102) Fu, X.; Schmitz, F. J.; Kelly, M. *J. Nat. Prod.* **1999**, *62*, 1336-1338.

(103) Cimino, G.; De Stefano, S. *Tetrahedron Lett.* **1977**, *18*, 1325–1328.

(104) Quiñoà, E.; Crews, P. *Tetrahedron Lett.* **1988**, *29*, 2037-2040.

(105) Rashid, M. A.; Gustafson, K. R.; Boyd, M. R. *Nat. Prod. Res.* **2000**, *14*, 387-392.

(106) Zhou, G. X.; Molinski, T. F. *Mar. Drugs* **2003**, *1*, 46-53.

(107) Dai, J. R.; Hallock, Y. F.; Cardellina II, J. H.; Gray, G. N.; Boyd, M. R. *J. Nat. Prod.* **1996**, *59*, 860-865.

(108) Lewis, M.; Menes, R. *Tetrahedron Lett.* **1987**, *28*, 5129-5132.

(109) Patel, M.; Conover, M.; Horan, A.; Loebenberg, D.; Marquez, J.; Mierzwa, R.; Puar, M.; Yarborough, R.; Waitz, J. *J. Antibiot.* **1988**, *41*, 794-797.

(110) El-Tarabily, K. A.; Sivasithamparam, K. *Soil Biol. Biochem.* **2006**, *38*, 1505-1520.

(111) Ahmed, M.; Broad, G. J.; Jones, E. R. H.; Taha, A. A.; Thaller, V. *J. Chem. Res., Synop.* **1982**, 199-199.

(112) Ord, M. R.; Piggin, C. M.; Thaller, V. *J. Chem. Soc., Perkin Trans. 1* **1975**, 687-689.

(113) Taha, A. A. *Phytochemistry* **2000**, *55*, 921-926.

(114) Higham, C. A.; Jones, E. R. H.; Keeping, J. W.; Thaller, V. *J. Chem. Soc., Perkin Trans. 1* **1974**, 1991-1994.

(115) Young, K.; Jayasuriya, H.; Ondeyka, J. G.; Herath, K.; Zhang, C.; Kodali, S.; Galgoci, A.; Painter, R.; Brown-Driver, V.; Yamamoto, R. *Antimicrob. Agents Chemother.* **2006**, *50*, 519-526.

(116) Wright, H. T.; Reynolds, K. A. *Curr. Opin. Microbiol.* **2007**, *10*, 447-453.

(117) Bäuerle, J.; Anke, T.; Jente, R.; Bosold, F. *Arch. Microbiol.* **1982**, *132*, 194-196.

(118) Jente, R.; Bosold, F.; Bauerle, J.; Anke, T. *Phytochemistry* **1985**, *24*, 553-559.

(119) Satoh, Y.; Satoh, M.; Isobe, K.; Mohri, K.; Yoshida, Y.; Fujimoto, Y. *Chem. Pharm. Bull.* **2007**, *55*, 561-564.

(120) Zloh, M.; Bucar, F.; Gibbons, S. *Theor. Chem. Acc.* **2007**, *117*, 247-252.

(121) Peng, W.; Sun, J.; Lin, F.; Han, X.; Yu, B. *Synlett* **2004**, 259-262.

(122) Yadav, J.; Kumar Mishra, R. *Tetrahedron Lett.* **2002**, *43*, 1739-1741.

(123) Kirkham, J.; Courtney, T.; Lee, V.; Baldwin, J. *Tetrahedron Lett.* **2004**, *45*, 5645-5647.

(124) Mukaiyama, T.; Suzuki, K.; Soai, K.; Sato, T. *Chem. Lett.* **1979**, 447-448.

(125) Soai, K.; Niwa, S. *Chem. Rev.* **1992**, *92*, 833-856.

(126) Tombo, R. G. M.; Didier, E.; Loubinoux, B. *Synlett* **1990**, 547–548.

(127) Frantz, D. E.; Fässler, R.; Tomooka, C. S.; Carreira, E. M. *Acc. Chem. Res.* **2000**, *33*, 373-381.

(128) Frantz, D. E.; Fässler, R.; Carreira, E. M. *J. Am. Chem. Soc.* **2000**, *122*, 1806-1807.

(129) Anand, N.; Carreira, E. *J. Am. Chem. Soc.* **2001**, *123*, 9687-9688.

(130) Sasaki, H.; Boyall, D.; Carreira, E. M. *Helv. Chim. Acta* **2001**, *84*, 964-971.

(131) Boyall, D.; Frantz, D. E.; Carreira, E. M. *Org. Lett* **2002**, *4*, 2605-2606.

(132) Reber, S.; Knoepfel, T.; Carreira, E. *Tetrahedron* **2003**, *59*, 6813-6817.

(133) Trost, B.; Chan, V.; Yamamoto, D. *J. Am. Chem. Soc.* **2010**, *132*, 5186-5192.

(134) de Fatima, A.; Kohn, L. K.; Antonio, M. A.; de Carvalho, J. E.; Pilli, R. A. *Biorg. Med. Chem.* **2004**, *12*, 5437-5442.

(135) Bhunia, S.; Sohel, S. M. A.; Yang, C.-C.; Lush, S.-F.; Shen, F.-M.; Liu, R.-S. *J. Organomet. Chem.* **2009**, *694*, 566-570.

(136) Fürstner, A.; Schlecker, A. *Chem. Eur. J.* **2008**, *14*, 9181-9191.

(137) Madec, D.; Férézou, J.-P. *Eur. J. Org. Chem.* **2006**, 92-104.

(138) Razon, P.; N'zoutani, M.-A.; Dhulut, S.; Bezzenine-Lafollée, S.; Pancrazi, A.; Ardisson, J. *Synthesis* **2005**, 109-121.

(139) Reddy, L. R.; Gais, H. J.; Woo, C. W.; Raabe, G. *J. Am. Chem. Soc.* **2002**, *124*, 10427-10434.

(140) Denmark, S. E.; Wynn, T. *J. Am. Chem. Soc.* **2001**, *123*, 6199-6200.

(141) Marshall, J. A.; Palovich, M. R. *J. Org. Chem.* **1998**, *63*, 4381-4384.

(142) Nowotny, S.; Tucker, C. E.; Jubert, C.; Knochel, P. *J. Org. Chem.* **1995**, *60*, 2762-2772.

(143) Jubert, C.; Nowotny, S.; Kornemann, D.; Antes, I.; Tucker, C. E.; Knochel, P. *J. Org. Chem.* **1992**, *57*, 6384-6386.

(144) Sonawane, R.; Joolakanti, S.; Arseniyadis, S.; Cossy, J. *Synlett* **2009**, 213-216.

(145) Smith III, A. B.; Ott, G. R. *J. Am. Chem. Soc.* **1998**, *120*, 3935-3948.

(146) Nicolaou, K.; Murphy, F.; Barluenga, S.; Ohshima, T.; Wei, H.; Xu, J.; Gray, D.; Baudoin, O. *J. Am. Chem. Soc.* **2000**, *122*, 3830-3838.

(147) Dineen, T. A.; Roush, W. R. *Org. Lett.* **2004**, *6*, 2043-2046.

(148) Peng, F.; Hall, D. G. *J. Am. Chem. Soc.* **2007**, *129*, 3070-3071.

(149) Chandra, J.; Reddy, M. *ARKIVOC* **2007**, *2*, 121-144.

(150) Roush, W. R.; Wada, C. K. *J. Am. Chem. Soc.* **1994**, *116*, 2151-2152.

(151) Roush, W. R.; Park, J. C. *Tetrahedron Lett.* **1991**, *32*, 6285-6288.

(152)   Roush, W. R.; Park, J. C. *J. Org. Chem.* **1990**, *55*, 1143-1144.

(153)   Rauniyar, V.; Hall, D. G. *J. Org. Chem.* **2009**, *74*, 4236-4241.

(154)   Rauniyar, V.; Zhai, H.; Hall, D. G. *J. Am. Chem. Soc.* **2008**, *130*, 8481-8490.

(155)   Rauniyar, V.; Hall, D. G. *Angew. Chem. Int. Ed.* **2006**, *45*, 2426-2428.

(156)   Jain, P.; Antilla, J. *J. Am. Chem. Soc.* **2010**, *132*, 11884-11886.

(157)   Jahnke, E.; Tykwinski, R. R. *Chem. Commun.* **2010**, *46*, 3235-3249.

(158)   Luu, T.; Morisaki, Y.; Cunningham, N.; Tykwinski, R. R. *J. Org. Chem.* **2007**, *72*, 9622-9629.

Chapter 2- Enantioselective Addition of Terminal Di– and Triynes to Aldehydes[†]

2.1 Introduction

As the previous chapter demonstrates, over one hundred acetylenic natural products have been isolated that contain a propargylic alcohol moiety.[1-5] The diversity of natural sources that produce such polyynols is impressive, and equally remarkable is the structural variation of the polyynol framework. Also, from this class of natural products, many members have been shown to be biologically active.[6] Since these compounds are typically isolated in small quantities, synthetic routes are needed in order to further study this interesting class of compounds.

Traditional methods for incorporating an optically active propargylic alcohol moiety into a polyyne framework start with the formation of a propargylic alcohol with the desired stereochemistry.[7-9] Then through the generally cumbersome and often low yielding process of cross–coupling reactions, extension of the acetylenic backbone is achieved.[4] Because the chiral building block is incorporated early in the synthesis, this route is often less efficient than a protocol in which the propargylic stereocenter is created late in the synthesis through the asymmetric addition of an oligoyne to an aldehyde.

[†] Portions of this chapter have been published. (a) Graham, E. R.; Tykwinski, R. R. *J. Org. Chem.* **2011**, *76*, 6574-6583.
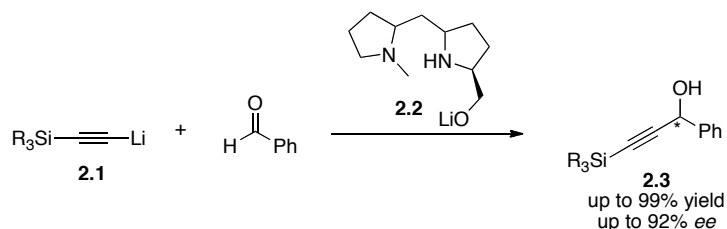
Equation 2.1. Mukaiyama's asymmetric addition of a lithium acetylide to an aldehyde.[10]

The first asymmetric addition of an acetylide to an aldehyde was reported by Mukaiyama *et al.* in 1979, with the asymmetric addition of a lithium acetylide **2.1** to benzaldehyde in the presence of the diamino alkoxide **2.2** (Equation 2.1).[10] Removal of the silyl protecting group in **2.3** would then allow for extension of the acetylenic backbone through cross–coupling reactions. Besides the challenge of extending the polyyne backbone after forming the stereocenter, other drawbacks to using a lithium acetylide is that it does not tolerate many functional groups, as well as the necessity of reaction temperatures of –123 °C in order to obtain respectable enantioselectivities.
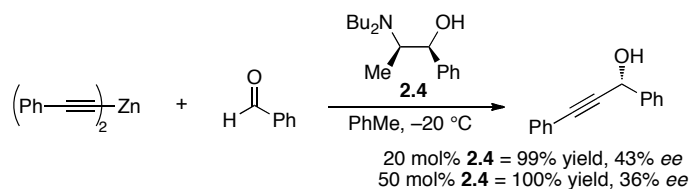
Equation 2.2. Niwa and Soai's asymmetric addition of a zinc acetylides to an aldehyde.[11]

Later, in 1990 Niwa and Soai have shown the first examples of zinc acetylide additions with enantioselectivities of 43% *ee* with 20 mol% loading of ligand **2.4**, while increasing the amount of ligand further resulted in decreased enantioselectivities (Equation 2.2).[11] That same year, Tombo and coworkers have shown that a stoichiometric amount of the lithiated amino alcohol **2.5** in the presence of a zinc acetylide gives propargylic alcohols with enantioselectivities up to 88% *ee*.[12] A few years later, Corey and Cimprich have prepared borylacetylides that give good yields and enantioselectivities in the presence of oxazaborolidine **2.6** (Scheme 2.1).[13]
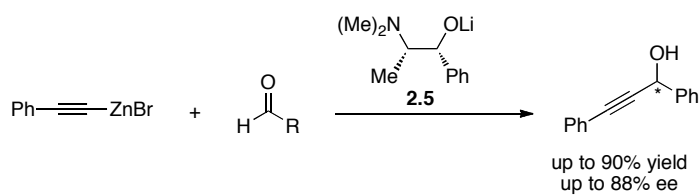
Equation 2.3. Tombo's asymmetric addition of a zinc acetylide to an aldehyde.[12]
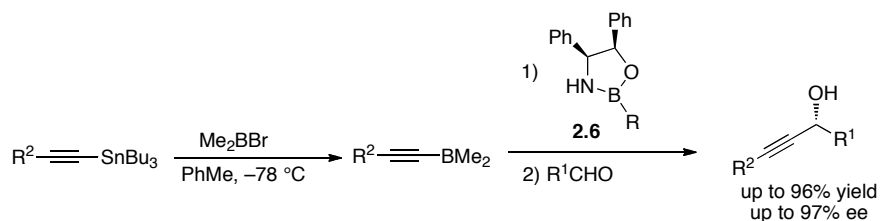
Scheme 2.1. Corey and Cimprich addition of a borylacetylide to an aldehyde.[13]

While many others have used different variations of the chiral amino alcohol as a catalyst or ligand, these protocols still require harsh conditions to generate the zinc acetylide. Carreira and coworkers have found that zinc acetylides could be created under mild conditions in the presence of $Zn(OTf)_2$ and a mild amine base.[14,15] Conversely, when the terminal acetylene is subjected to either $Zn(OTf)_2$ or Et_3N no reaction occurred. Two possibilities have been suggested to account for these observations. In the first, π-complexation of the $Zn(OTf)_2$ to the alkyne makes the proton on the terminal acetylene more acidic so it can be removed by Et_3N. Alternatively, a hydrogen bond formed between nitrogen of the amine base and the proton of the acetylene makes the alkyne more activated towards complexation with $Zn(OTf)_2$ (Figure 2.1).
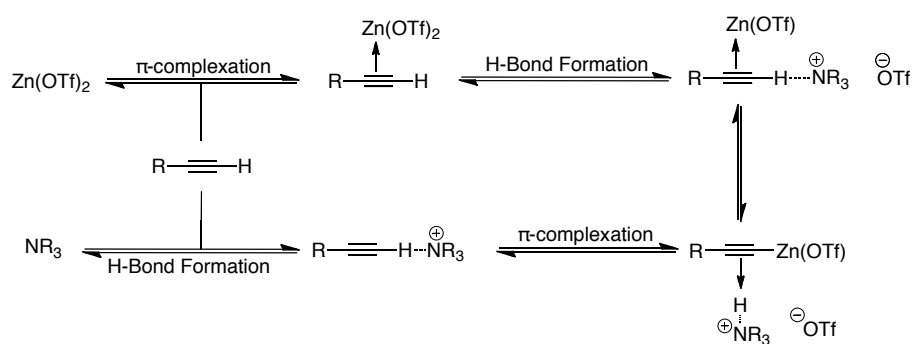
Figure 2.1. Reactions of terminal acetylenes with $Zn(OTf)_2$ and Et_3N.

Carreira and coworkers have developed a mild asymmetric alkynylation reaction (Scheme 2.2) using $Zn(OTf)_2$ and the amino alcohol *N*-methylephedrine. Carreira's alkynylation reaction works well with α-branched aldehydes,[14-17]

although it is less efficient with unsaturated aldehydes and those that lack α-branching.[18] Since the initial report by Carreira, others have expanded on this process using variations of the *N*-methylephedrine ligand,[19-23] although little work has been directed towards developing conditions directly applicable to di- or triynes.[24,16]
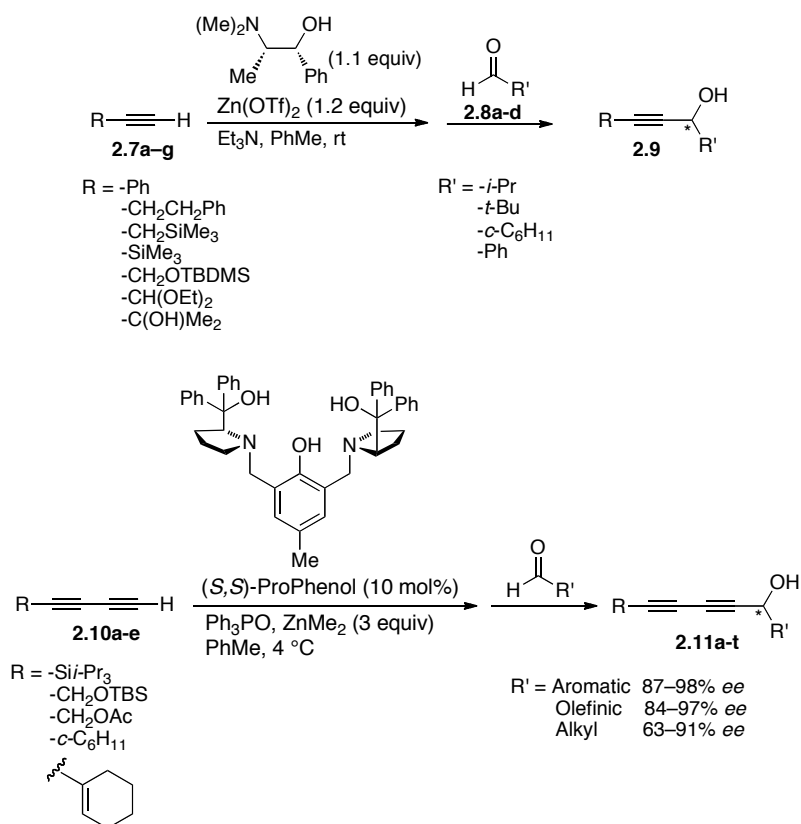
Scheme 2.2. Carreira (top) and Trost (bottom) protocols for enantioselective propargylic alcohol synthesis.

More recently, Trost and co-workers have shown that the asymmetric addition of diynes to a range of aldehydes can be carried out by using dimethylzinc in the presence of the catalyst (*S,S*)-ProPhenol, giving propargylic

alcohols in good to excellent yields and enantiomeric excess (Scheme 2.2).[25] The substrates that work best with the Trost protocol are α,β-unsaturated or non-α-branched aldehydes. This is the opposite trend to that observed by Carreira and coworkers, making the two methods complementary.

While the Trost protocol has been optimized for the asymmetric addition of diynes to aldehydes, the only examples of an asymmetric diyne addition with the Carreira protocol is the syntheses of strongylodiols A and B.[26] In these syntheses, four equivalents of the *N*-methylephedrine ligand are used and enantioselectivities of only 80 and 82% *ee* are obtained, suggesting that either these conditions are not optimized or this procedure does not work well for diyne additions. Also, to our knowledge, neither the Carreira nor the Trost protocols have been extended to the asymmetric addition of 1,3,5-hexatriynes to aldehydes. In this chapter, attempts to provide a general method for the asymmetric addition of diynes and triynes to aldehydes are outlined.

2.2 Results and discussion

2.2.1 Preparation of starting material diynes and triynes.

Diynes and triynes used in this study have been formed via a Fritsch–Buttenberg–Wiechell (FBW) rearrangement (except for **2.18f**),[27-37] as outlined in Scheme 2.3. Briefly, an acid chloride was subjected to a Friedel-Crafts acylation reaction with bis(trimethylsilyl)-acetylene or -1,4-butadiyne in the presence of

AlCl₃ to produce a ketone (**2.12** or **2.13**).[38] The resulting ketone was transformed

to the corresponding dibromoolefin (**2.14** or **2.15**) using the conditions reported

by Ramirez and coworkers.[39] The dibromoolefin then underwent a FBW

rearrangement in the presence of *n*-BuLi to give either the corresponding di- or

triyne (**2.16** or **2.17**) in good to excellent yield. The trimethylsilyl protecting

group was removed via reaction of the respective di- or triyne (**2.18** or **2.19**) with

K₂CO₃ in a 3:1 mixture of MeOH and THF. Due to its intrinsic instability, the

resulting terminal polyyne (**2.18** or **2.19**) was, following workup, carried on

immediately to the asymmetric addition reaction.
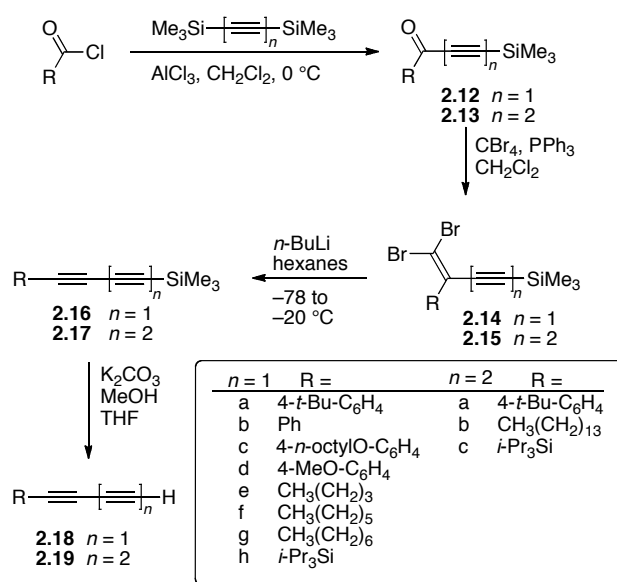
Scheme 2.3. Schematic outline of the synthesis of di- and triynes **2.18** and **2.19**.

A different approach was used in the synthesis of **2.18f**. Diyne **2.18f** was

formed via the cross–coupling reaction of **2.20** with **2.21**, as demonstrated in

Scheme 2.4 to give **2.22** in a 45% yield. Removal of the acetone protecting group

was performed by combining **2.22** and NaOH in refluxing toluene to give **2.18f** in a quantitative yield. Compound **2.18f**, like the other terminal diynes was added directly to the asymmetric addition reaction after removal of the protecting group, to prevent decomposition of the reagent.
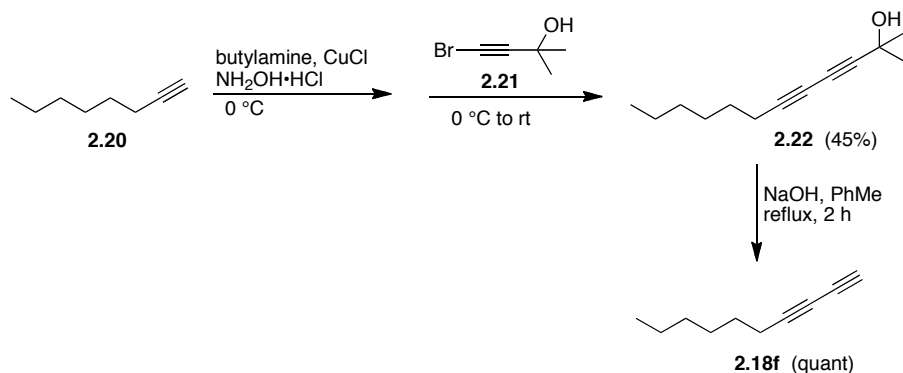
Scheme 2.4. Synthesis of **2.18f** via oxidative cross–coupling.

2.2.2 *t*-Butyl-phenyl end capped diyne 2.18a additions to aldehydes.

Initial synthetic explorations using the Carreira protocol for additions to aldehydes used *t*-Bu-phenyl endcapped diyne **2.18a** as a substrate due to its stability in comparison to other diyne derivatives. The results are summarized in Table 2.1. When the reaction was performed with α-branched aldehydes, isobutyraldehyde and cyclohexanecarboxaldehyde, products **2.23** and **2.24** were formed in good yield and enantioselectivities of 90–95%. With the more sterically hindered pivalaldehyde, the yield dropped significantly for **2.25**, but the enantioselectivity remained similar (90% *ee*) to that of **2.23** and **2.24**. On the other hand, when the reaction was performed with the non α-branched aldehyde

propanal to give **2.26**, a significantly lower enantioselectivity resulted (64% *ee*), consistent with that previously observed.[17]

Reactions of **2.18a** with α,β-unsaturated aldehydes acrolein and (*E*)-4-methylpent-2-enal were not successful, giving byproducts and <20% yield of the desired products as estimated by ^{1}H NMR spectroscopy. The reaction of **2.18a** with acrolein under Carreira conditions gave a low yield, possibly due to the volatile nature of the acrolein limiting reagent. The reaction of **2.18a** with (*E*)-4-methylpent-2-enal resulted in an inseparable mixture of **2.27** and **2.28** (Equation 2.4). These two isomers were identified by ^{1}H NMR spectroscopy, based on the signals of the vinyl protons which showed two different doublet of doublet of doublets (ddd) with a large trans coupling constant of 15.6 Hz for **2.27** (5.90 and 5.57 ppm) and a multiplet at 5.28 ppm for **2.28**.

It was found that, as with the monoyne addition,[17] enantiomers of the *N*-methylephedrine ligand gave equal enantioselectivities with the opposite optical rotation, as demonstrated by, for example, the synthesis of **2.23** and **2.25** (entries 1–2 and 4–5), as expected. Finally, it is worth noting that the presence of water in the reaction leads to a dramatic lowering of the observed enantioselectivity of the reaction.

Table 2.1. Reaction of diyne **2.18a** with various aldehydes[a]
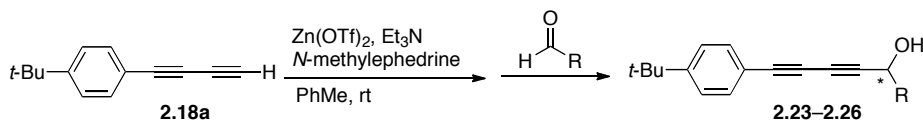
Entry	Ligand[b]	R	Product[c]	Yield[d]	% ee
1	(1*R*, 2*S*)	*i*-Pr	(*S*)-(+)-**2.23**	89%	95[e]
2	(1*S*,2*R*)	*i*-Pr	(*R*)-(−)-**2.23**	83%	94[e]
3	(1*R*,2*S*)	*c*-C$_6$H$_{11}$	(*S*)-(+)-**2.24**	73%	90[f]
4	(1*S*,2*R*)	*t*-Bu	(*R*)-(−)-**2.25**	33%	90[e]
5	(1*R*,2*S*)	*t*-Bu	(*S*)-(+)-**2.25**	37%	90[e]
6	(1*R*,2*S*)	Et	(*S*)-(−)-**2.26**	45%	64[f]

[a]Reaction conditions: Alkyne (1.2 equiv), Zn(OTf)$_2$ (ca. 1.2 equiv), *N*-methylephedrine (ca. 1.2 equiv), Et$_3$N (ca. 1.2 equiv), aldehyde (1 equiv); ca. 0.5 mmol scale, toluene (1 mL). [b]Ligand (1*R*,2*S*)-(−)- or (1*S*,2*R*)-(+)-*N*-methylephedrine. [c]Absolute stereochemistry established by Mosher ester method. [d]Isolated yields under optimized conditions. [e]Enantioselectivity determined via HPLC analysis. [f]Enantioselectivity determined via the modified Mosher method.
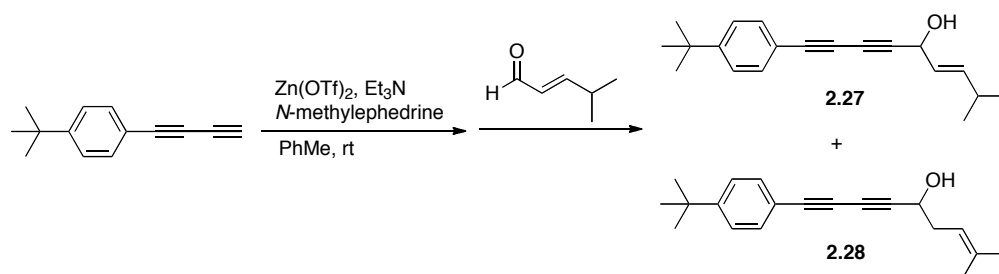
Equation 2.4. Asymmetric addition reaction of **2.18a** with (*E*)-4-methylpent-2-enal, giving an inseparable mixture of **2.27** and **2.28**.

2.2.3 First reaction optimization conditions.

Typical reaction times required for completion of the initial test reactions were 72 hours, which is less than ideal for reactions with terminal polyynes. A number of factors were thus examined towards optimizing the rate of the reaction using alkyne **2.18a** and isobutyraldehyde (Table 2.1). Increasing the amount of $Zn(OTf)_2$ from 1.2 to 1.6 equivalents cut the reaction time nearly in half, while yields and enantioselectivities held steady (Entries 1 and 2). Further increasing the amount of $Zn(OTf)_2$ to ca. 2.2 equivalents had little effect on either yield or enantioselectivity (entries 3 and 4).

Table 2.2. Results toward optimizing reaction time[a]
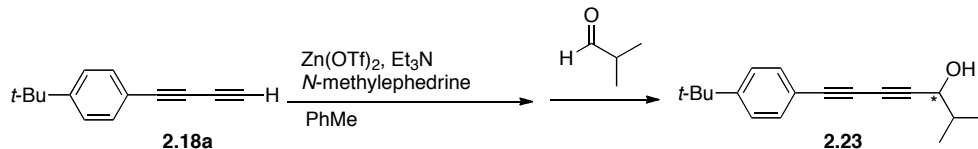
Entry	Zn(OTf)$_2$	Ligand[b]	Temp/°C	Time/h	Product[c]	Yield[d]	ee[e]
1	1.2 equiv	(1R,2S)	rt	72	(S)-(+)-**2.23**	89%	95%
2	1.6 equiv	(1R,2S)	rt	37	(S)-(+)-**2.23**	82%	94%
3	2.2 equiv	(1S,2R)	rt	36	(R)-(−)-**2.23**	83%	94%
4	2.1 equiv	(1S,2R)	37	48	(R)-(−)-**2.23**	79%	93%
5	1.6 equiv	(1S,2R)	40	13	(R)-(−)-**2.23**	89%	92%
6	1.6 equiv	(1S,2R)	50	14	(R)-(−)-**2.23**	89%	73%
7	1.6 equiv	(1S,2R)	60	3	(R)-(−)-**2.23**	88%	58%
8	1.6 equiv	(1S,2R)	80	2.5	(R)-(−)-**2.23**	89%	53%

[a]Reaction conditions: Alkyne (1.2 equiv), N-methylephedrine (ca. 1.2 equiv), Et$_3$N (ca. 1.2 equiv), isobutyraldehyde (1 equiv); ca. 0.5 mmol scale, toluene (1 mL). [b]Ligand (1R,2S)-(−)- or (1S,2R)-(+)-N-methylephedrine. [c]Absolute stereochemistry established by Mosher ester method. [d]Isolated yields. [e]Enantioselectivity determined via HPLC analysis.

The effect of temperature was then explored. When heated to 40 °C, using 1.6 equivalents of Zn(OTf)$_2$, a yield of 89% was obtained with 92% *ee* in only 13 hours (entry 5). When the reaction was performed at higher temperatures (entries 6–8), significant decreases in enantioselectivity were observed. The ideal reaction conditions were thus suggested as 1.6 equivalents of Zn(OTf)$_2$ with heating to 40

°C. Due to the instability of most terminal diynes, however, there was hesitation to use heat when exploring the diyne scope for this reaction. Since heating the reaction helped increase the rate of the reaction, but had no effect toward increasing enantioselectivities, it was ultimately decided to vary the diynes while continuing to perform these reactions at room temperature.

2.2.4 Diyne addition substrate scope

Table 2.3. Substrate scope for diyne addition to α-branched aldehydes[a]
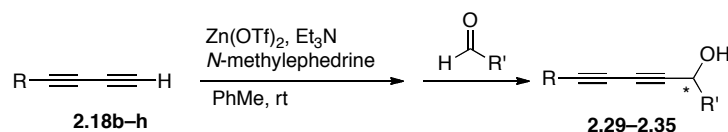
Diyne	R	Ligand[b]	R'	Product[c]	Yield[d]	% ee
2.18b	Ph	(1S,2R)	i-Pr	(R)-(−)-**2.29**	88%	92[e]
2.18c	4-n-octylO-C$_6$H$_4$	(1R,2S)	c-C$_6$H$_{11}$	(S)-(+)-**2.30**	82%	97[f]
2.18d	4-MeO-C$_6$H$_4$	(1R,2S)	i-Pr	(S)-(+)-**2.31**	93%	98[e]
2.18e	CH$_3$(CH$_2$)$_3$	(1S,2R)	i-Pr	(R)-(−)-**2.32**	43%	88[f]
2.18f	CH$_3$(CH$_2$)$_5$	(1R,2S)	i-Pr	(S)-(+)-**2.33**	65%	93[f]
2.18g	CH$_3$(CH$_2$)$_6$	(1R,2S)	i-Pr	(S)-(+)-**2.34**	77%	90[f]
2.18h	i-Pr$_3$Si	(1R,2S)	i-Pr	(S)-(+)-**2.35**	89%	91[e]

[a]Reaction conditions: Alkyne (1.2 equiv), Zn(OTf)$_2$ (ca. 1.6 equiv), N-methylephedrine (ca. 1.2 equiv), Et$_3$N (ca. 1.2 equiv), aldehyde (1.0 equiv); ca. 0.5 mmol scale, toluene (1 mL). [b]Ligand (1R,2S)-(−)- or (1S,2R)-(+)-N-methylephedrine. [c]Absolute stereochemistry established by Mosher ester method. [d]Isolated yields under optimized conditions. [e]Enantioselectivity determined via HPLC analysis. [f]Enantioselectivity determined via the modified Mosher method.

The scope of the reaction was then explored using diynes **2.18b–h** in reactions with α-branched aldehydes cyclohexanecarboxaldehyde and isobutyraldehyde. Enantioselectivities ranging from 88% to 98% *ee,* in typically respectable yields were obtained (Table 2.3). Arylbutadiynes **2.18b–d** reacted with aldehydes to give products **2.29–2.31** in excellent yield, and in good (92%) to excellent (98%) *ee*. Alkyl substituted diynes also worked well, giving propargylic alcohols **2.32–2.34** with 88–93% *ee* and increasing yields as a function of length of the alkyl chain. The observed increase in yield is likely related to the stability of the terminal diynes during the desilylation step, i.e., the longer the alkyl chain the greater the stability of the terminal polyyne.[40] Finally, the reaction of the triisopropylsilyl diyne **2.18h** with isobutyraldehyde gave **2.35** in 89% yield and 91% *ee*. Given the ability to remove the triisopropylsilyl-group of **2.35** with a fluoride source, compound **2.35** offers a potential building block for other chiral derivatives (*vide infra*).

2.2.5 Determining absolute configuration.
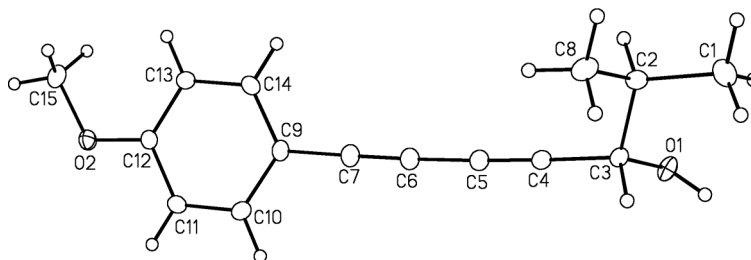
Figure 2.2. ORTEP drawing of **2.31** (20% probability level). Hydrogen atoms are shown with arbitrarily small thermal parameters. Selected interatomic distances (Å): O1–C3, 1.4357(15); O2–C12, 1.3578(15); O2–C15, 1.428(2); C1–C2, 1.521(2); C2–C3, 1.5385(19); C2–C8, 1.524(2); C3–C4, 1.4687(17); C4≡C5, 1.2002(19); C5–C6, 1.3778(19); C6≡C7, 1.2014(19); C7–C9, 1.4321(18). Selected interatomic angles (deg): C3–C4–C5, 177.57(14); C4–C5–C6, 178.33(15); C5–C6–C7, 177.40(15); C6–C7–C8, 178.27(15).

Crystals of **2.31** suitable for X-ray diffraction have been obtained from a concentrated solution of diethyl ether at room temperature (Figure 2.2) and offer a chance to explore molecular structure and, potentially, stereochemistry at C3. Crystallographic analysis shows that bond angles and lengths for **2.31** are unremarkable. While the structure suggests a (*S*)-configuration at C3, the obtained Flack parameter is not sufficient to assign reliably the absolute stereochemistry.[41] Formation of (*S*)-**2.31** is, however, expected when using (1*R*,2*S*)-(−)-*N*-methylephedrine based on literature reports.[42]

72

To confirm the stereochemistry at C3 experimentally both the (*R*)- and (*S*)-Mosher esters of **2.31** have been synthesized to give diastereomers **2.36** and **2.37** (Scheme 2.5). The ^{1}H NMR spectra of both **2.36** and **2.37** have been compared and the differences in shielding and deshielding used to determine the absolute configuration. The differences in signal assignment for **2.36** and **2.37** are tabulated in Table 2.4.
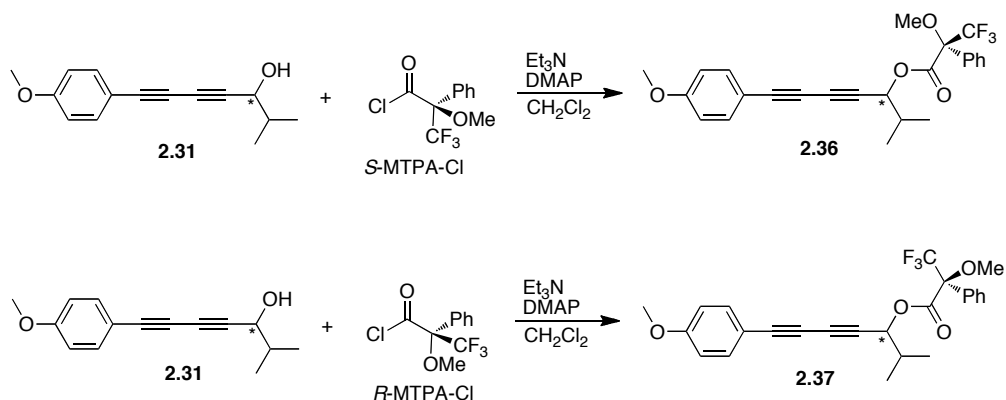
Scheme 2.5. Synthesis of both the (*R*)- and (*S*)-Mosher esters **2.36** and **2.37**, respectively.
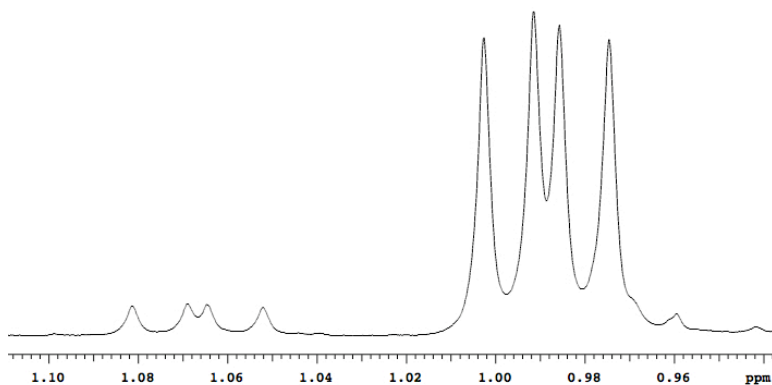
Figure 2.3. ^{1}H NMR spectrum of the (*S*)-Mosher ester **2.37** (upfield), with a small amount of the (*R*)-Mosther ester **2.36** (downfield).

73

Table 2.4. Differences between the (*R*)- and (*S*)- Mosher esters (**2.36** and **2.37**) of polyynol **2.31**.
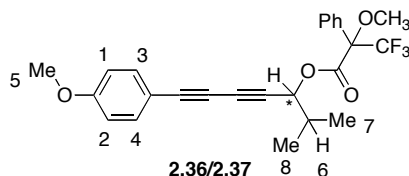
Signal	(*R*)–**2.36**	(*S*)–**2.37**	Δ ppm	Δ hertz
1	7.54	7.57	−0.03	−11.5
2	7.44	7.45	−0.01	−6.3
3	6.84	6.85	−0.01	−4.4
4	5.47	5.51	−0.04	−16
5	3.82	3.83	−0.01	−4.3
6	2.14	2.09	+0.05	26.0
7	1.07	1.00	+0.07	28.3
8	1.06	0.98	+0.08	32.0

The signals of the phenyl group in the (*R*)-Mosher ester **2.36** is shielded in comparison to the (*S*)-Mosher ester **2.37**, while those of the isopropyl group in **2.36** are deshielded in comparison to the (*S*)-Mosher ester (Table 2.4, Figure 2.4). Therefore by aligning the structure in the validated conformational picture[43] where the methine proton, carbonyl oxygen and CF_3 are in the same plane, **2.31** is deduced to be the (*S*)-enantiomer.
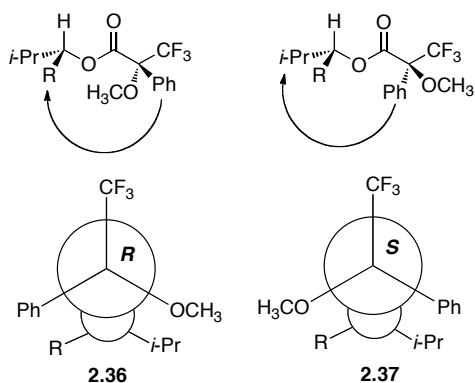
Figure 2.4. Conformational analysis of diastereomers **2.36** and **2.37** used to determine absolute configuration.

2.2.6 Triyne addition to aldehydes substrate scope

Encouraging results with the asymmetric addition of diynes to aldehydes led to the examination of reactions with triynes. Due to the intrinsic instability typically observed for terminal triynes (even in solution), however, their use as starting materials is more challenging than the corresponding diynes.[40] Nevertheless, these examples establish the viability of this route. When triyne **2.19a** was reacted with either isobutyraldehyde or cyclohexanecarboxaldehyde, enantioselectivities of 89 and 90% (**2.38** and **2.39**) were obtained, respectively (Table 2.5). The yield of **2.39** was, however, lower as observed in the analogous reaction of diyne **2.18a** with cyclohexanecarboxaldehyde. The reaction of 1,3,5-icosatriyne **2.19b** with isobutyraldehyde gave **2.40** in a good yield (80%) and enantioselectivity (89% *ee*), while the triisopropylsilyl terminated triyne **2.19c** was reacted to give both (+)-**2.41** and (−)-**2.41** in ca. 80% yield.

75

Table 2.5. Substrate scope for triyne addition into α-branched aldehydes[a]

R—≡—≡—≡—H →(Zn(OTf)₂, Et₃N, *N*-methylephedrine, PhMe, rt)→ aldehyde → R—≡—≡—≡—CH(OH)R'

$$R\text{---}{\equiv}\text{---}{\equiv}\text{---}{\equiv}\text{---}H \xrightarrow[\text{PhMe, rt}]{\substack{\text{Zn(OTf)}_2,\ \text{Et}_3\text{N}\\ N\text{-methylephedrine}}} \xrightarrow{\underset{H}{\overset{O}{\|}}\!\!-R'} R\text{---}{\equiv}\text{---}{\equiv}\text{---}{\equiv}\overset{OH}{\underset{R'}{-}}$$

2.19a–c   **2.38–2.41**
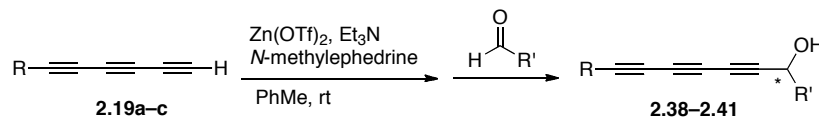
Triyne	R	Ligand[b]	R'	Product[c]	Yield[d]	% ee
2.19a	$4\text{-}t\text{-Bu-C}_6\text{H}_4$	(1R,2S)	*i*-Pr	(S)-(+)-**2.38**	69%	89[e]
2.19a	$4\text{-}t\text{-Bu-C}_6\text{H}_4$	(1R,2S)	$c\text{-C}_6\text{H}_{12}$	(S)-(+)-**2.39**	36%	90[e]
2.19b	$\text{CH}_3(\text{CH}_2)_{13}$	(1S,2R)	*i*-Pr	(R)-(−)-**2.40**	80%	89[e]
2.19c	$i\text{-Pr}_3\text{Si}$	(1S,2R)	*i*-Pr	(R)-(−)-**2.41**	78%	94[f]
2.19c	$i\text{-Pr}_3\text{Si}$	(1R,2S)	*i*-Pr	(S)-(+)-**2.41**	81%	98[f]

[a]Reaction conditions: Alkyne (1.2 equiv), Zn(OTf)₂ (ca. 1.6 equiv), *N*-methylephedrine (ca. 1.2 equiv), Et₃N (ca. 1.2 equiv), aldehyde (1.0 equiv); ca. 0.5 mmol scale, toluene (1 mL). [b]Ligand (1R,2S)-(−)- or (1S,2R)-(+)-*N*-methylephedrine. [c]Absolute stereochemistry established by Mosher ester method. [d]Isolated yields under optimized conditions. [e]Enantioselectivity determined via the modified Mosher method. [f]Enantioselectivity based on derivatization, see Scheme 2.6.

2.2.7 Further derivatization of polyynols

Unfortunately, the enantiomers of **2.41** were inseparable by HPLC and attempted Mosher ester formation was not efficient (full conversion to the ester could not be achieved). Thus the enantiomeric excess could not be established directly for **2.41**. As with diyne **2.35**, triynol **2.41** is a masked terminal acetylene, which allows for further functionalization. To establish this possibility, the triisopropylsilyl-group of (S)-(+)-**2.35** (91% *ee*) was removed using TBAF, and, after aqueous work up, the resulting terminal diyne was trapped with benzyl

azide[44,45] via a CuAAC reaction[46-49] to give the 1,4-disubstituted 1,2,3-triazole product (S)-(−)-**2.42** in a 51% yield and a 91% *ee* (Scheme 2.6). In an analogous reaction sequence, triyne (S)-(+)-**2.41** gave (S)-(−)-**2.43** in a 65% yield and 98% *ee,* while (R)-(−)-**2.41** gave (R)-(+)-**2.43** in the same yield and 94% *ee.* Once **2.41** is converted to the triazole, the two enantiomers were separable by HPLC allowing for the determination of enantiomeric excess. Thus, the removal of the silyl protecting group and further functionalization does not appear to impact enantiopurity.
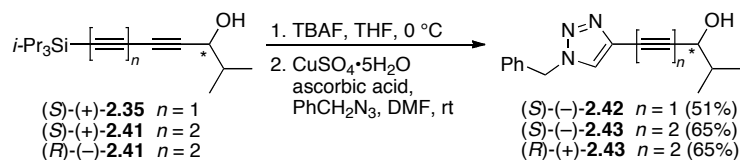
Scheme 2.6. Triazole formation using diyne **2.35** and triyne **2.41**.

2.2.8 Further optimization conditions

As our work was nearing completion, a publication by Trost and co-workers appeared,[25] which described rate enhancement and increased enantioselectivities using additives such as triphenylphosphine oxide, prompting us to explore such effects in our protocol (Table 2.6). In comparison to our initial result (Entry 1), using triphenylphosphine oxide as an additive in the reaction of **2.18a** with isobutyraldehyde gave a slight decrease in the reaction time, and the enantioselectivity also decreased slightly (Table 2.6, entry 2).

Table 2.6. The effect of PPh$_3$O additive on formation of (R)-$(-)$-**2.23**[a]
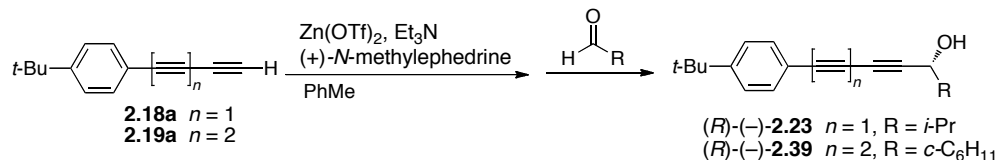
Entry	Product	Base	Additive	Time /h	Yield[b]	% ee[c]
1	(R)-$(-)$-**2.23**	Et$_3$N	—	36	83%	94
2	(R)-$(-)$-**2.23**	Et$_3$N	PPh$_3$O (1 equiv)	20	79%	88
3	(R)-$(-)$-**2.23**	i-Pr$_2$NEt	—	19	80%	98
4	(R)-$(-)$-**2.23**	i-Pr$_2$NEt	PPh$_3$O (1 equiv)	20	79%	95
5	(R)-$(-)$-**2.23**	i-Pr$_2$NEt	PPh$_3$O (0.2 equiv)	20	83%	97
6	(R)-$(-)$-**2.23**	i-Pr$_2$NEt	—	4[d]	83%	95
7	(R)-$(-)$-**2.39**	i-Pr$_2$NEt	—	30	52%	94

[a]Reaction conditions: Alkyne (1.2 equiv), Zn(OTf)$_2$ (ca. 1.6 equiv), $(1S,2R)$-$(+)$-N-methylephedrine (ca. 1.2 equiv), base (ca. 1.2 equiv), aldehyde (1.0 equiv): ca. 0.5 mmol scale, toluene (1 mL), rt. [b]Isolated yields. [c]Enantioselectivity determined via HPLC. [d]Reaction was performed at 40 °C instead of rt.

When switching from triethylamine to diisopropylethylamine (Hünig's base), the reaction time decreased somewhat, while the enantioselectivity increased slightly (entry 3). When triphenylphosphine oxide was used in conjunction with Hünig's base, the enantioselectivity remained approximately constant (entries 4 and 5). With Hünig's base and heating to 40 °C, the reaction was complete in 4 hours to give an 83% yield and a 95% *ee* (Table 2.6, entry 6). Since these optimizations resulted in only a significant decrease in the reaction time, and not a substantial increase in yield or enantioselectivity, we did not

pursue repeating this reaction with all the other substrates. Because the reaction of **2.19a** with cyclohexanecarboxaldehyde had resulted in such a low yield, it was revisited with the optimized conditions of diisopropylethylamine. The results for this were encouraging, as the yield increased from 36 to 52% and the enantioselectivity went from 90 to 94% *ee*, in 30 h, instead of the original 90 h.

2.2.9 Steps towards the total synthesis of Montiporyne I

After developing this method for the asymmetric addition of di- and triynes to aldehydes the next logical step was to apply this methodology towards the synthesis of a natural product. As mentioned in Chapter 1 montiporyne I was isolated from *Monitpora sp.* coral and found to have similar or better cytotoxicity to cisplatin toward human skin and ovarian cancer cell lines. Because the absolute stereochemistry of montiporyne I has never been established it was therefore pursued as the natural product target to showcase this methodology. A distinct disconnection point is shown in Figure 2.5 where the aldehyde **2.45** was synthesized from ethylacetoacetate in two steps and 70% overall yield. With **2.18g** and **2.45** in hand many attempts were made toward acquiring the dithiane protected montiporyne I (**2.46**) under our asymmetric alkynylation conditions, however, the best result obtained for the asymmetric alkynylation step gave only a 11% yield (Equation 2.5). It was assumed that the low yield was likely due to the dithiane protecting group because the analogous reaction with 2.18g with aldehydes protected with, for example, ethylene glycol gave a much better yield

(60%). Due to the acid lability of the montiporyne I product to become the α,β-unsaturated ketone, however, the use of such protecting groups was not practical. Due to this dilemma, the synthesis of montiporyne I was abandoned.
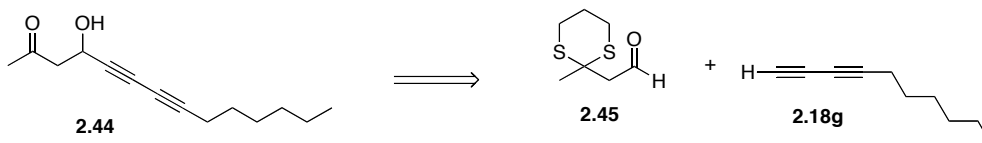
Figure 2.5. Proposed retrosynthetic pathway for the synthesis of montiporyne I (**2.44**).
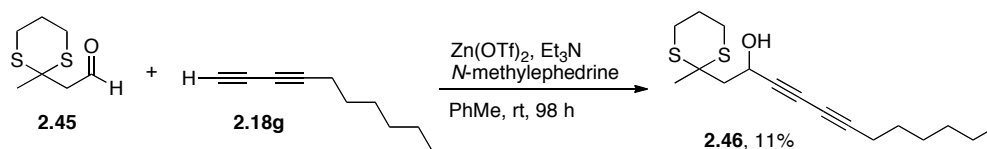
Equation 2.5. Attempted synthesis of montiporyne I (**2.44**) intermediate **2.46**.

2.2.10 In-situ polyyne formation and asymmetric addition reaction

Due to the instability of terminal polyynes, it was hypothesized that in situ formation and derivatization of a polyyne could offer higher yields. Thus starting with the more stable dibromoolefin, a one–pot procedure could arrive at the chiral polyynol. The process starts with desilylation of dibromoolefin **2.14** (Equation 2.6) to form the stable dibromoolefin **2.47**, which would be subjected to a FBW rearrangement conditions to give the lithium acetylide **2.48**. Lithium acetylides have been shown previously in the Tykwinski group to undergo transmetallation to the zinc acetylide *in situ* via the addition of a zinc salt.[50] Using conditions

80

similar to this protocol, the goal was to obtain the zinc acetylide and then subject it to the previously applied asymmetric addition reaction conditions.
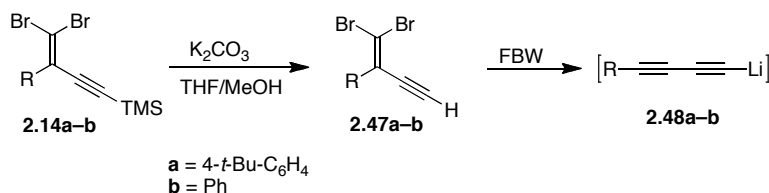
Equation 2.6. Desilylation of **2.14a–b** gives stable dibromoolefins **2.47a–b** that can then undergro a FBW rearrangement to the lithium acetylides **2.48a–b**.

In a first attempt, removal of the silyl protecting group of **2.14b** gave **2.47b**, which was subjected to a FBW rearrangement with hexanes as the reaction solvent to give **2.48b** (Equation 2.7). Transmetallation to the zinc acetylide via the addition of $Zn(OTf)_2$ and Et_3N was followed by the reaction with isobutyraldehyde in the presence of *N*-methylephedrine, resulting in a 50% yield, but only a 9% *ee*. Previously, toluene had been determined as the optimal solvent with the monoyne alkynylation; therefore, even though *n*-BuLi is stored as a 2.5 M solution in hexanes, the reaction solvent for this one–pot protocol was switched to toluene. In toluene, starting again from the dibromoolefin **2.47b** the same reaction was performed, resulting in a 41% yield and a 63% *ee* (Equation 2.8). Even though the yield was lower, there was a significant increase in the enantioselectivity.
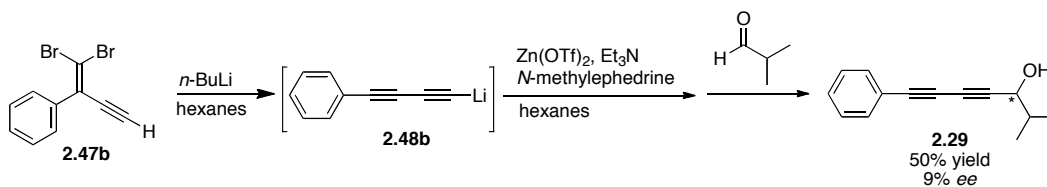
Equation 2.7. One-pot protocol of dibromoolefin **2.47b** with hexanes as solvent.
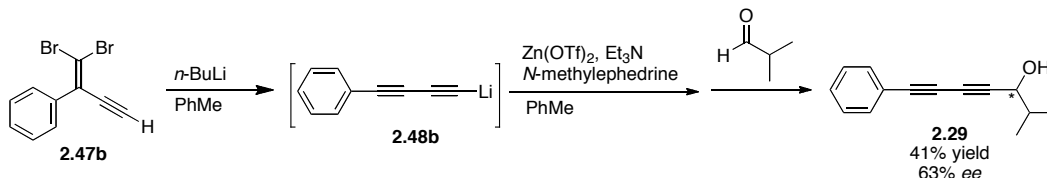
Equation 2.8. One-pot protocol of dibromoolefin **2.47b** with toluene as solvent.

It was postulated that a higher yield and enantioselectivity might be obtained with the more stable 4-*tert*-butylphenyl substituted dibromoolefin **2.14a**. Dibromoolefin **2.47a** was subjected to the same one–pot protocol as described above for dibromoolefin **2.47b**, to give **2.23** in a 48% yield and 65% *ee* (Equation 2.9), i.e., results nearly identical to that in Equation 2.8 for **2.29**.
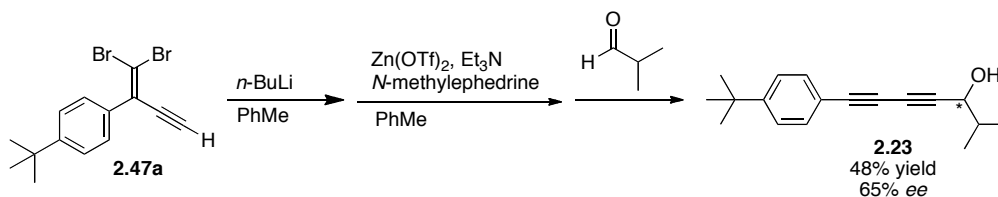
Equation 2.9. One-pot protocol with dibromoolefin **2.47a**.

The next optimization step targeted an increased reaction concentration. The reaction in Equation 2.10 was performed in only one fifth the amount of

toluene (2 mL, instead of 10 mL). This resulted in an inhomogeneous mixture that was difficult to stir properly. Therefore the reaction was quenched early to give a 7% yield and a 68% *ee*. A byproduct, from this reaction, isolated in a 8% yield, was compound **2.49**. This confirms that the dibromoolefin had not fully rearranged to the lithiated diyne before being cannulated over to the addition reaction. With **2.49** in hand, it was postulated that an alternative route to a chiral polyynol backbone would be to subject **2.49** to the FBW rearrangement conditions. This was attempted, giving **2.23** in a low yield (24%) and only a 29% *ee* (Equation 2.11). Due to the poor performance of this protocol, it was therefore abandoned.
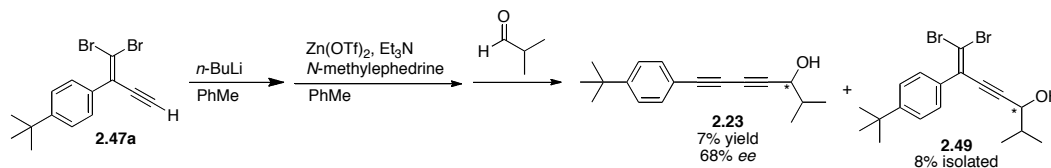
Equation 2.10. One-pot protocol of dibromoolefin **2.47a** with minimal solvent.
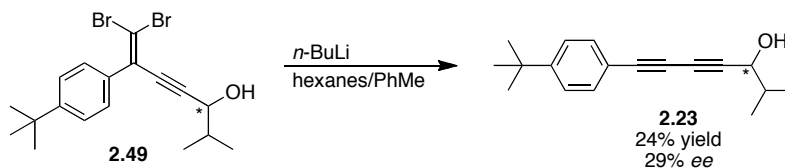
Equation 2.11. FBW rearrangement of **2.46**.

The next attempt towards optimization was to first make the zinc acetylide and then cannulate it into a mixture of Zn(OTf)$_2$, Et$_3$N, *N*-methylephedrine and toluene; instead of cannulating over the lithium acetylide into the same mixture to

form the zinc acetylide before the aldehyde is added. This however still resulted in a low yield (33%), however the enantioselectivity had now increased to 78% *ee* (Equation 2.12). Further attempts made with this procedure included varying the amount of Zn(OTf)$_2$ added, along with varying the time waited before cannulating the acetylide into the reaction mixture and varying when the aldehyde is then added. All attempts gave lower yields (7–29%) and similar enantioselectivities (54–68% *ee*). This low yield was postulated to be a result of decomposition due to warming up during cannulation into the reaction flask. A final optimization attempt was then performed, where, instead of cannulating the acetylide into the mixture of Zn(OTf)$_2$, *N*-methylephedrine, Et$_3$N, and toluene, this mixture was cannulated into the flask containing the zinc acetylide cooled to −30 °C. This might decrease the amount of decomposition of the acetylide and lead to a cleaner reaction. In addition the low temperature of the reaction could be maintained until after the addition of the aldehyde. With this procedure a 57% yield was obtained and an 88% *ee* (Equation 2.13). This is a substantial improvement over the previous procedures and further optimization of this should be pursued in the future.
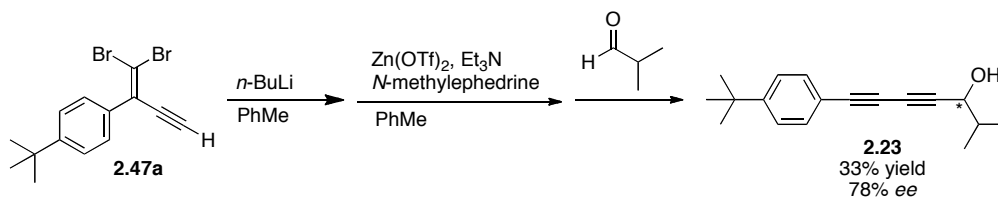
Equation 2.12. One-pot protocol of dibromoolefin **2.47a**, two separate additions of Zn(OTf)$_2$.
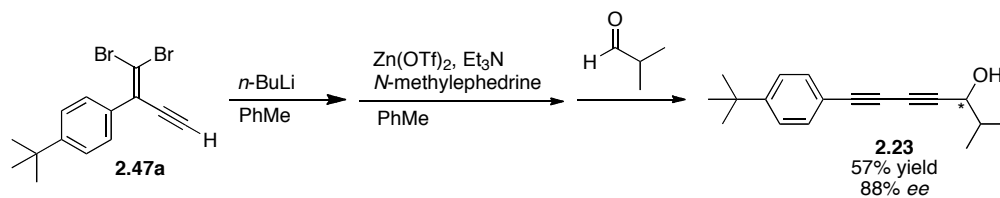
Equation 2.13. One-pot protocol of dibromoolefin **2.47a**, reversing addition protocol.

2.3   Conclusions

In summary, the asymmetric addition of terminal diynes and triynes to aldehydes described in this chapter provides a direct route to obtain optically active propargylic alcohols, often with good to excellent yields and enantioselectivities. Optimization of these conditions decreased the reaction time from 72 h to less than 4 h, while still maintaining high yields and enantioselectivities. This method works best with α-branched aldehydes, and is thus complementary to the recently published Trost protocol. This study offers the first examples of an asymmetric triyne addition to an aldehyde.

From the optimization data, the slightly more basic Hünig's base produced both a faster reaction and a slight increase in enantioselectivity, in comparison to reactions that used triethylamine. This fact suggests that deprotonation of the terminal acetylene may be the rate limiting step or at least change the equilibrium within the reaction. The equilibrium for a reversible step could be shifted due to the fact that a stronger base would result in a higher concentration of zinc acetylide. Also, the use of a more electron rich diyne gives slightly better

enantioselectivities, which seems counterintuitive, as the terminal proton of a more electron rich diyne is less acidic. Subtle changes in electronics can alter the binding affinity of the zinc acetylide with the amino alcohol giving slight variations in the enantioselectivity. Numerous mechanistic studies have been performed on the alkylzinc addition to aldehydes[51,52] however, further mechanistic investigations into the relationship of the electronics of the acetylide versus the enantioselectivity need to be performed. In performing mechanistic studies on the alkylzinc additions Goldfuss and Houk stated that "interactions between alkyl groups at zinc and the ligand are essential factors for the mechanisms of enantioselection."[52] This is likely more pronounced in the alkynyl additions. It is known that a diyne, which is more electron deficient than an alkyne, has a slower reaction rate than the corresponding monoyne. This observation is again observed when comparing addition rate of diynes to that of the corresponding triynes. Another future area of study would be to screen other amine bases to assess the effects of nucleophilicity versus basicity on the reaction rate.

The length of the polyyne has little effect on enantioselectivity, although, the yields do trend lower as a function of polyyne length. The trend observed here could be due to the reaction rate, but is also likely a result of decreased stability of the terminal triyne precursor. Even though the terminal triyne is used directly in the asymmetric addition reaction after desilylation, this procedure only reduces the extent of decomposition but does not eliminate it. An option to alleviate the

problem would be to increase the amount of the terminal polyyne (currently 1.1 equiv). Because using more reagent would be a less atom economical route, until now this has been avoided as an alternative.

In an attempt to further increase the yield of the reaction with less stable terminal polyynes, we looked at developing a one-pot protocol. The one-pot protocol might be the most viable route to this polyynol backbone after further optimization, as it does not require the isolation of an unstable intermediate. Parameters that still need to be optimized include the reaction temperature, as lower temperatures may provide better enantioselectivities. Another variable would be to modify the wait time before the aldehyde is added to the mixture; a longer equilibration time could allow the zinc acetylide and *N*-methylephedrine to get in the ideal orientation before the aldehyde is added, which might also result in increased enantioselectivities.

A final optimization step for either the stepwise or the in situ protocol would be to look at other possible amino alcohols. Both Jiang[22,53] and Tomioka[54] have independently shown that either the (1*R*,2*R*)- or (1*S*,2*S*)-amino alcohols give better yields and enantioselectivities than the (1*R*,2*S*)-derivatives for the monoyne addition to aldehydes. Also Jiang and Sui demonstrated that a *para*-nitro group on the phenyl ring of the amino alcohol gives a better enantioselectivity.[22] This demonstrates that electronics play a role in the ligand binding and reactivity. A plan would be to apply these and possibly other amino alcohols with this diyne addition reaction. With a more active amino alcohol ligand such as either **2.50** or

2.51 (Figure 2.6), higher enantioselectivities might be obtainable for aldehydes without a large α-substituent. If a better amino alcohol can be achieved, another route would be to apply this chiral amino alcohol in a sub-stoichiometric fashion (i.e. catalytic).
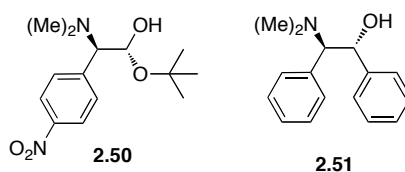
Figure 2.6. Reactions Jiang's amino alcohol ligand **2.50** and Yamashita's amino alcohol ligand **2.51**.

With these different optimization plans in hand, we are not far from developing a highly efficient and generalized route for the enantioselective formation of propargylic alcohol polyynes. An optimized one-pot protocol may allow for a tetrayne polyynol backbone to be obtained in a single step, such as that of the natural product minquartynoic acid, which would be a substantial improvement over the current synthesis that requires three cross-coupling reactions to produce the tetrayne backbone (Figure 1.15, Chapter 1).

2.4 References

(1)   Pan, Y.; Lowary, T. L.; Tykwinski, R. R. *Can. J. Chem.* **2009**, *87*, 1565-1582.

(2)   Gung, B. W. *C. R. Chim.* **2009**, *12*, 489-505.

(3)   Minto, R.; Blacklock, B. *Prog. Lipid Res.* **2008**, *47*, 233-306.

(4)   Shi Shun, A. L. K.; Tykwinski, R. R. *Angew. Chem. Int. Ed.* **2006**, *45*, 1034-1057.

(5)   Bohlmann, F.; Burkhardt, T.; Zdero, C. *Naturally Occurring Acetylenes*; Academic Press: New York, 1973.

(6)   Dembitsky, V. *Lipids* **2006**, *41*, 883-924.

(7)   Trost, B. M.; Weiss, A. H. *Adv. Synth. Catal.* **2009**, *351*, 963-983.

(8)   Pu, L. *Tetrahedron* **2003**, *59*, 9873-9886.

(9)   Cozzi, P. G.; Hilgraf, R.; Zimmermann, N. *Eur. J. Org. Chem.* **2004**, 4095-4105.

(10)   Mukaiyama, T.; Suzuki, K.; Soai, K.; Sato, T. *Chem. Lett.* **1979**, 447-448.

(11)   Niwa, S.; Soai, K. *J. Chem. Soc., Perkin Trans. 1* **1990**, 937-943.

(12)   Tombo, R. G. M.; Didier, E.; Loubinoux, B. *Synlett* **1990**, 547-548.

(13)   Corey, E.; Cimprich, K. *J. Am. Chem. Soc.* **1994**, *116*, 3151-3152.

(14)   Frantz, D.; Fässler, R.; Carreira, E. *J. Am. Chem. Soc.* **1999**, *121*, 11245-11246.

(15)   Frantz, D. E.; Fässler, R.; Tomooka, C. S.; Carreira, E. M. *Acc. Chem. Res.* **2000**, *33*, 373-381.

(16)   Ashwanden, P.; Carreira, E. M. *Acetylene Chemistry: Chemistry, Biology and Material Science* **2005**, 101-138.

(17)   Frantz, D. E.; Fässler, R.; Carreira, E. M. *J. Am. Chem. Soc.* **2000**, *122*, 1806-1807.

(18)   When non–α- or β-branched aldehydes were used the enantioselectivities were lower (70–88% ee), see reference 17. When unsaturated aldehydes were used a competing Cannizaro reaction resulted in lower than desirable yields, see reference 7.

(19)   Chen, Z.; Xiong, W.; Jiang, B. *Chem. Commun.* **2002**, 2098-2099.

(20)   Jiang, B.; Chen, Z.; Tang, X. *Org. Lett* **2002**, *4*, 3451-3453.

(21)   Jiang, B.; Feng, Y. *Tetrahedron Lett.* **2002**, *43*, 2975-2977.

(22)   Jiang, B.; Si, Y.-G. *Angew. Chem. Int. Ed.* **2004**, *43*, 216-218.

(23)   Kamble, R. M.; Singh, V. K. *Tetrahedron Lett.* **2003**, *44*, 5347-5349.

(24)   Prior to Trost's recent work in reference 25, only a single example of asymmetric addition of a diyne to an aldehyde had been reported, using Carreira's protocol toward the synthesis of the natural products strongylodiols A and B, see: Reber, S.; Knöpfel, T. F.; Carreira, E. M. Tetrahedron 2003, 59, 6813-6817.

(25)   Trost, B.; Chan, V.; Yamamoto, D. *J. Am. Chem. Soc.* **2010**, *132*, 5186-5192.

(26)   Reber, S.; Knoepfel, T.; Carreira, E. *Tetrahedron* **2003**, *59*, 6813-6817.

(27)   Fritsch, P. *Liebigs Ann. Chem.* **1894**, *279*, 319-323.

(28)   Buttenberg, W. P. *Liebigs Ann. Chem.* **1894**, *279*, 324-337.

(29)   Wiechell, H. *Liebigs Ann. Chem.* **1894**, *279*, 337-344.

(30)   Jahnke, E.; Tykwinski, R. R. *Chem. Commun.* **2010**, *46*, 3235-3249.

(31)   Chalifoux, W. A.; Tykwinski, R. R. *C. R. Chim.* **2009**, *12*, 341-358.

(32)   Knorr, R. *Chem. Rev.* **2004**, *104*, 3795-3849.

(33)   Stang, P. J. *Chem. Rev.* **1978**, *78*, 383-405.

(34)   Bichler, P.; Chalifoux, W. A.; Eisler, S.; Shi Shun, A. L. K.; Chernick, E. T.; Tykwinski, R. R. *Org. Lett.* **2009**, *11*, 519-522.

(35)   Eisler, S.; Chahal, N.; McDonald, R.; Tykwinski, R. R. *Chem. – Eur. J.* **2003**, *9*, 2542-2550.

(36)   Shi Shun, A. L. K.; Chernick, E. T.; Eisler, S.; Tykwinski, R. R. *J. Org. Chem.* **2003**, *68*, 1339-1347.

(37)   Eisler, S.; Tykwinski, R. R. *J. Am. Chem. Soc.* **2000**, *122*, 10736-10737.

(38)   Walton, D. R. M.; Waugh, F. *J. Organomet. Chem.* **1972**, *37*, 45-56.

(39)   Ramirez, F.; Desai, N. B.; McKelvie, N. *J. Am. Chem. Soc.* **1962**, *84*, 1745-1747.

(40)   Luu, T.; Tykwinski, R. R. *J. Org. Chem.* **2006**, *71*, 8982-8985.

(41)   The Flack parameter value obtained was –0.1(9).

(42)   See, for example, reference 24.

(43)   Hoye, T. R.; Jeffrey, C. S.; Shao, F. *Nat. Protoc.* **2007**, *2*, 2451-2458.

(44)   Luu, T.; Medos, B.; Graham, E.; Vallee, D.; McDonald, R.; Ferguson, M.; Tykwinski, R. *J. Org. Chem.* **2010**, *75*, 8498-8507.

(45)   Luu, T.; McDonald, R.; Tykwinski, R. R. *Org. Lett.* **2006**, *8*, 6035-6038.

(46)   Huisgen, R. In *1,3-Dipolar Cycloaddition Chemistry*; Padwa, A., Ed.; Wiley: New York, 1984, p 1-176.

(47)   Hein, J. E.; Fokin, V. V. *Chem. Soc. Rev.* **2010**, *39*, 1302-1315.

(48)   Amblard, F.; Cho, J.; Schinazi, R. *Chem. Rev.* **2009**, *109*, 4207-4220.

(49)   Meldal, M.; Tornoee, C. *Chem. Rev.* **2008**, *108*, 2952-3015.

(50)   Morisaki, Y.; Luu, T.; Tykwinski, R. R. *Org. Lett.* **2006**, *8*, 689-692.

(51)   Goldfuss, B.; Houk, K. N. *J. Org. Chem.* **1998**, *63*, 8998-9006.

(52)   Goldfuss, B.; Steigelmann, M.; Khan, S. I.; Houk, K. N. *J. Org. Chem.* **2000**, *65*, 77-82.

(53)   Jiang, B.; Chen, Z.; Xiong, W. *Chem. Commun.* **2002**, 1524-1525.

(54)   Yamashita, M.; Yamada, K.-i.; Tomioka, K. *Adv. Synth. Catal.* **2005**, *347*, 1649-1652.

Chapter 3- Enantioselective Allylboration of Propargylic Aldehydes.

3.1   Homoallylic propargylic alcohols as building blocks

As previously discussed in Chapter 1, there is a genuine need to find better synthetic routes toward the enantioselective formation of propargylic alcohols. Homoallylic propargylic alcohols (**3.1**, Figure 3.1) are another prevalent propargylic alcohol backbone in natural product synthesis that requires more focus on the development of better synthetic routes. The alkyne-alkene functionality of this backbone provides two different synthetic handles, which can be manipulated to arrive at a wide variety of building blocks. In the past 10 years, this backbone has been used as a building block in numerous natural product syntheses, including Nicolaou's syntheses of sanglifehrin[1] and apoptolidin[2] as well as other syntheses by Roush,[3,4] Pilli,[5] Ardisson,[6] Férézou,[7] Curran[8] and Fürstner,[9] to name a few.
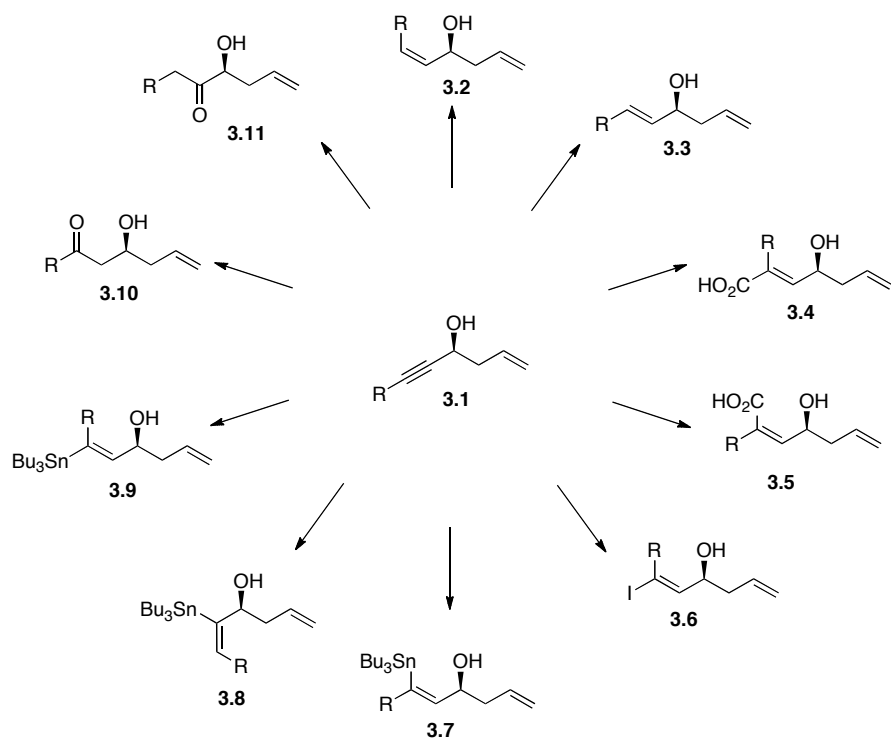
Figure 3.1. Examples of manipulations that can be performed on the alkyne functionality of homoallylic propargylic alcohols.

Figure 3.1 shows that a variety of building blocks of synthetic interest can be obtained by manipulation of the alkyne within this backbone. An alkyne can act as either a masked *cis* or *trans* double bond (**3.2**, **3.3**).[10,11] *Cis* or *trans* hydroalumination followed by the addition of CO_2 can give either acid **3.4** or **3.5**,[12,13] while following the hydroalumination with the addition of iodine can give the iodoalkene **3.6**.[14,15] Hydrostannation with different conditions can give building blocks **3.7**, **3.8**, or **3.9** selectively, demonstrating how an alkyne can act as a masked coupling partner.[16-18] Alkynes can also undergo hydroboration to again act as a masked coupling partner. The resulting boronic acid can also be

hydrated to act as a masked carbonyl (**3.10**)[19] or the alkyne itself can be hydrated to act as a masked carbonyl group (**3.11**).[20]

$$R \overset{O}{\underset{\textbf{3.12}}{\diagdown\!\!\!\diagup}}\!\!H \quad \underset{M = B, Si, Ti, Cr, Zr, Sn}{\diagup\!\!\!\diagdown MX} \quad \longrightarrow \quad R \overset{OH}{\underset{\textbf{3.1}}{\diagdown\!\!\!\diagup}}$$
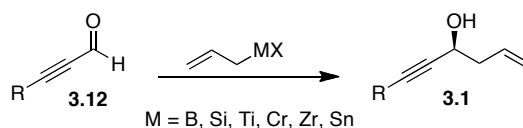
Equation 3.1. Allylation of a propargylic aldehyde (**3.12**).

The most common route of forming this optically active homoallylic propargylic alcohol backbone is by reacting a propargylic aldehyde with an allylmetal reagent (Equation 3.1). There are many different allylmetal reagents (boron, silicon, titanium, chromium, zirconium, tin) that have a wide scope of reactivity and selectivity. Denmark has classified these allylmetal reagents into three different classes based on their mechanims.[21] Type I reagents go through a highly diastereoselective chair-like Zimmermann-Traxler transition state, as depicted in Figure 3.2. Boron, aluminum, and trihalosilicon are all considered Type I reagents. Type II reagents consist of both organotrialkyltin and organotrialkylsilane; these reagents react through an open transition state. For this they require an external Lewis acid and are generally found to be *syn* selective. Conversely Type III reagents, which include trisubstituted organochromium, organotitanium and organozirconium, are found to be *anti* selective, undergoing fast equilibrium to the more stable (*E*)-isomer before reacting.
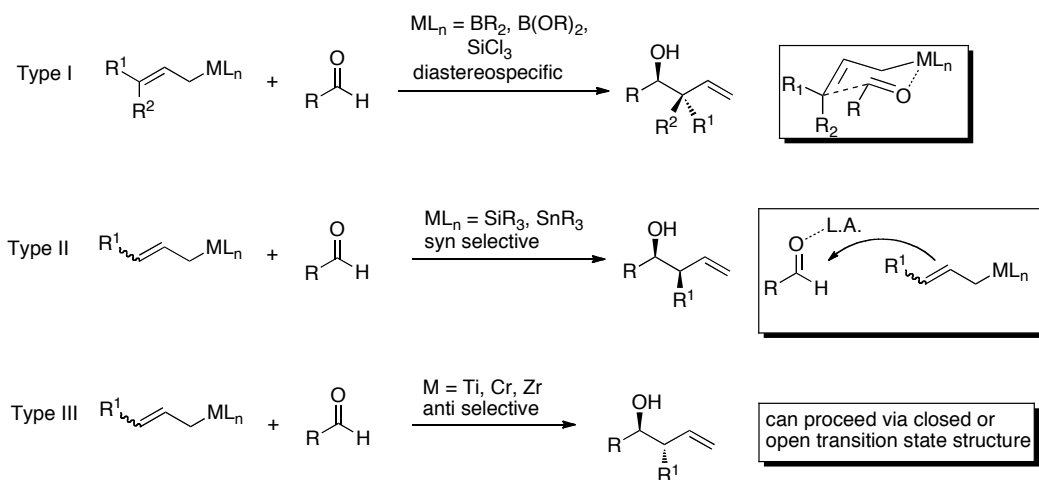
Figure 3.2. Denmark's classification of mechanisms for the different allylation reactions: Type I, Type II and Type III mechanisms.[21]

3.2 History of allylation of propargylic aldehydes

Many reviews on allylation chemistry have been presented;[22-25] however, few focus on the allylation of propargylic aldehydes. When reporting new allylation methodologies, most publications have excluded propargylic aldehydes from the reaction scope. BouzBouz *et al.* have been one of the few research groups who observed the vast difference between an aromatic and propargylic aldehyde, and focused on the asymmetric allylation of propargylic aldehydes.[26] Their procedure applied a stoichiometric amount of a chiral cyclopentadienyldialkoxyallyltitanium species (Equation 3.2). Using stoichiometric amounts of tin, titanium and chromium is less desirable than other

possible less toxic methodologies and catalytic processes. Lewis acids have been found to increase the rate of the reaction; however, this procedure still requires a stoichiometric amount of a toxic allylmetal species. To our knowledge, the first reported Lewis acid assisted asymmetric allylation of a propargylic aldehyde was performed by Marshall and Gung in 1989 (Equation 3.3).[27] The stereoselectivity for this reaction is attributed to the use of a chiral allylstannane **3.16** as a starting material, synthesized in four steps from the corresponding α,β-unsaturated aldehyde.
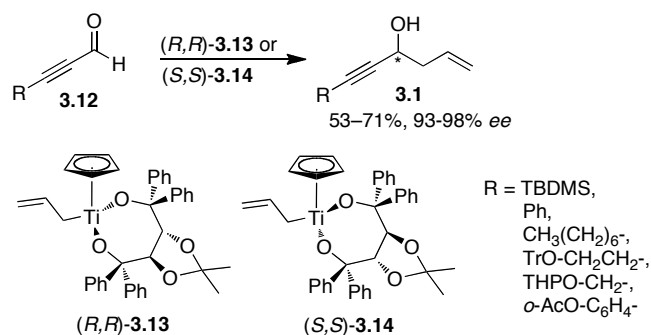
Equation 3.2. Cyclopentadienyldialkoxyallyltitanium chiral Lewis acid catalyzed allylation of propargylic aldehydes.[26]
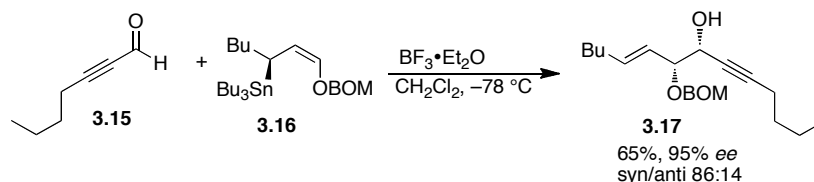
Equation 3.3. Marshall's Lewis acid catalyzed allylation of a propargylic aldehyde.[27]

97

Besides trying to get away from using stoichiometric toxic allyltin or chromium species, there also existed a need for a substochiometric/catalytic chiral reagent. Catalytic chiral reagents were first demonstrated in the early 1990s for aliphatic, aromatic, and α,β-unsaturated aldehydes, however, the first application of this strategy with a propargylic aldehyde was not demonstrated until 1998. Marshall and Palovich have studied a reaction scope utilizing Yamamoto's chiral acyloxy borane catalyst **3.18** with an allylstannane and aldehydes, with one being the propargylic aldehyde **3.19** (Equation 3.4).[28] The resulting homoallylic propargylic alcohol **3.20** was isolated with a 71% *ee*, substantially lower than those obtained using the aliphatic, aromatic and α,β-unsaturated aldehydes (89–96% *ee*). Although many research groups have applied either the use of Keck's BINOL-Ti(O*i*-Pr)$_4$/BINAP-Ti(O*i*-Pr)$_4$ complexes or the BINOL-Zr variant in 10–20 mol% catalyst loading for the asymmetric allylation of propargylic aldehydes, these methods still require stoichiometric amounts of toxic tin (Figure 3.3).[29-32] Moreover, *ee*s barely make the 90% mark in most cases.
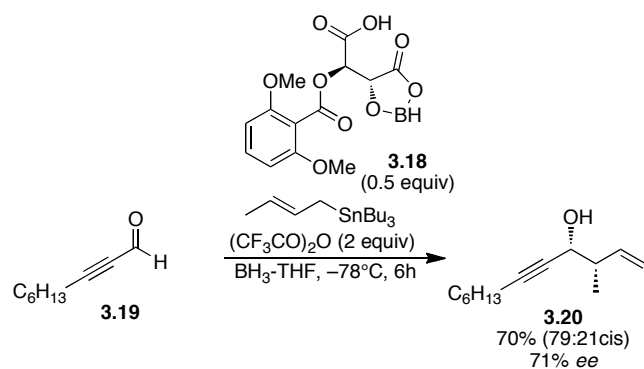
Equation 3.4. Marshall and Palovich showed the first catalytic enantioselective allylation of a propargylic aldehyde in 1998.[28]
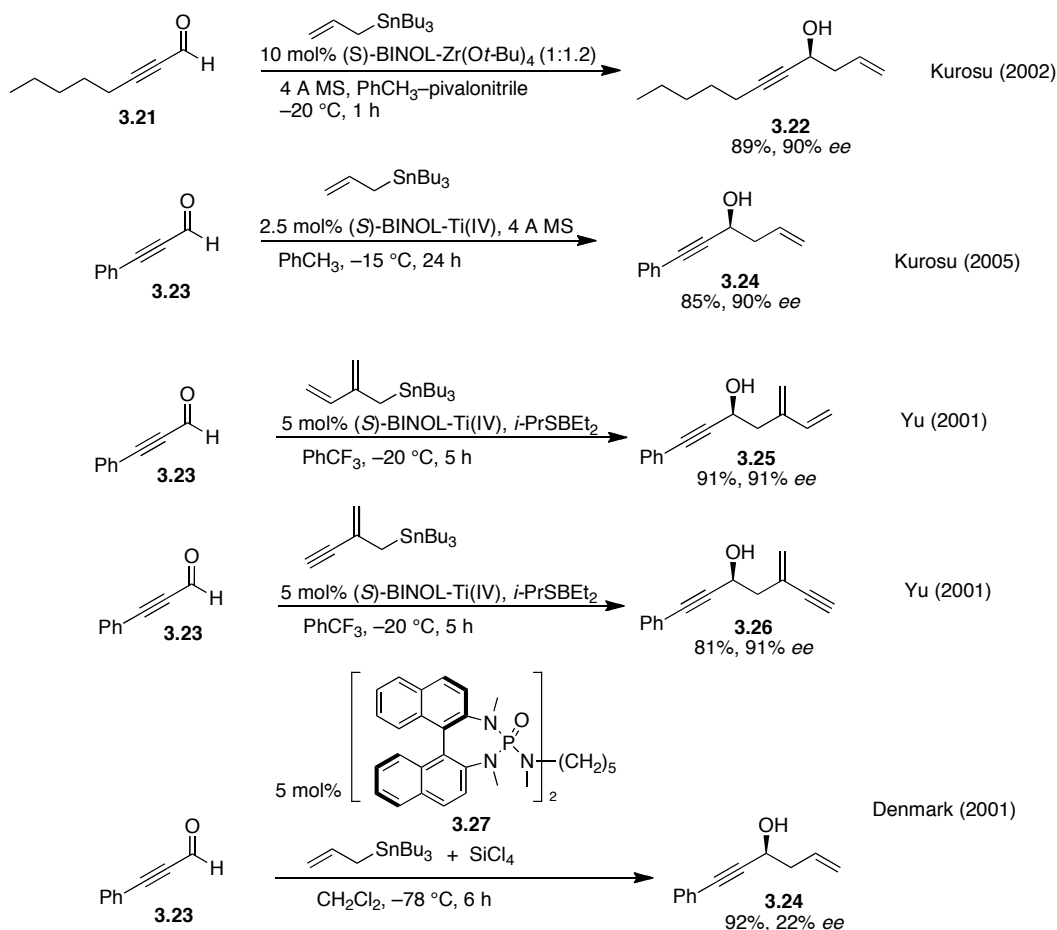
Figure 3.3. Enantioselective allylstannations with propargylic aldehydes.[29-32]

3.3 Allylboration

An environmentally–benign alternative is to perform an allylation reaction with boron reagents. Boron residues have a low level of toxicity, and a higher stability than most other allylmetal reagents making them ideal for these types of reactions. As stated by Cossy: "Additions of chiral allylboranes to α,β-acetylenic aldehydes is one of the more general routes to enantioenriched propargylic alcohols."[26] An allylation reaction that utilizes boron is commonly referred to as an allylboration reaction.[33] There are two different types of boron reagents that can undergo this allylation reaction: allylboranes, containing two alkyl groups along with the allyl substituent, and allylboronates (allyl boronic esters), which contain two alkoxy groups along with the allyl substituent (see Figure 3.4).[33]
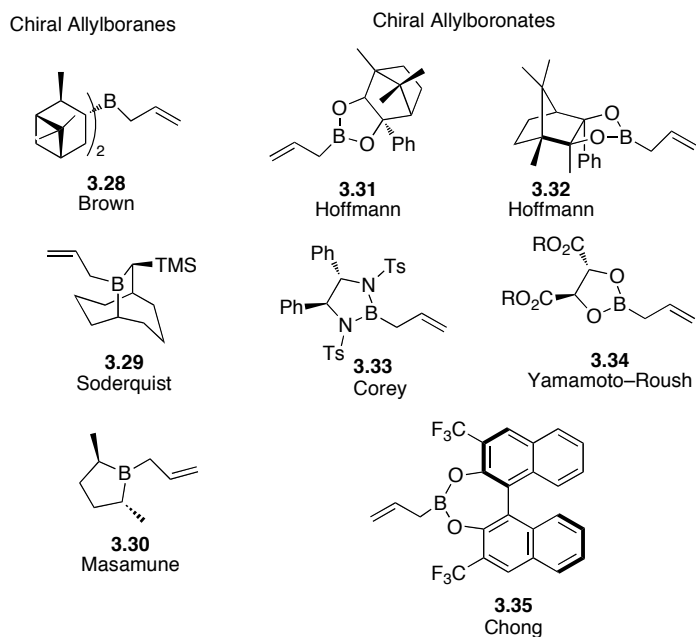
Figure 3.4. Different chiral allylboranes (**3.28–3.30**) and allylboronates (**3.31–3.35**).[33]

Although Mikhailov and Bubnov performed the first allylboration reaction in 1964,[34] it was not until 1978 that Hoffmann performed the first enantioselective allylboration.[35-37] Since the report of Hoffmann's chiral allylboronate (**3.31**), many other groups have developed similar chirality transfer reagents and today many different chiral auxiliaries exist for both allylboranes and allylboronates (Figure 3.4). An allylborane is significantly less air stable than an allylboronate[33] and unlike an allylboronate, an allylborane usually has to be prepared *in situ* directly before use. Even though allylboranes have stability issues, their high reactivity in comparison to allylboronates allows for the highly selective, low temperature reactions of chiral allylboranes, as first demonstrated by Brown.[38] Most natural product syntheses that require the formation of a homoallylic propargylic alcohol today use Brown's diisopinocamphenyl allylborane.[1-4,39-41] An example of this is shown in Figure 3.5 with Roush's synthesis of Cochleamycin A, a natural product isolated from *Streptomyces* DT136, which displays strong antimicrobial activity as well as being cytotoxic against a variety of tumor cell lines.[3]
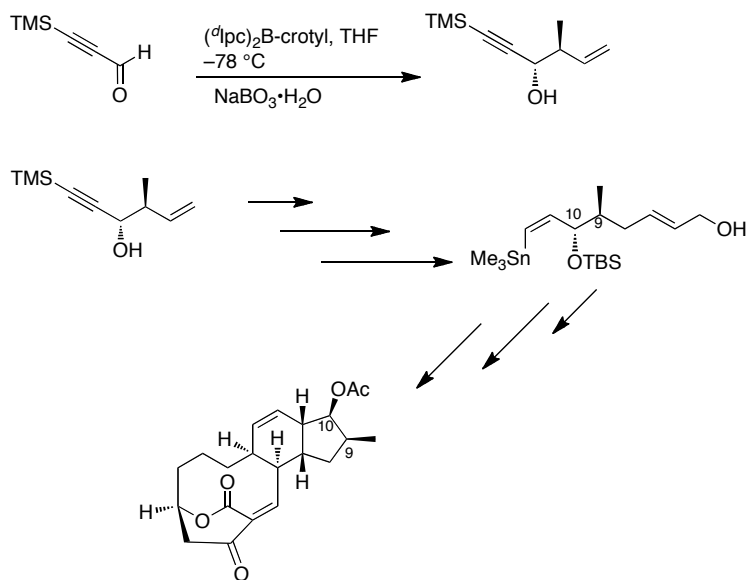
Figure 3.5. An example of a recent application of Brown's diisopinocamphenyl allylborane in Roush's synthesis of cochleamycin A in 23 steps and a 2.4% overall yield.[3]

Intrigued by the fact that dicobalt hexacarbonyl complexes of propargylic aldehydes gave enhanced diastereoselectivities in aldol reactions,[42] Roush and coworkers reacted this complex **3.37** with his tartrate ester–derived chiral allylboronate. In a comparison, he found increased enantioselectivities for homoallylic propargylic alcohols **3.38–3.40**, 86–96% *ee*, compared to 58–72% *ee* for the reaction with the free propargylic aldehyde **3.36**.[43] Oxidative decomplexation of the dicobalt hexacarbonyl unit was achieved by reacting with $Fe(NO_3)_3$, in 85–96% yield over the two steps (**3.38–3.40**, Scheme 3.1). Even though this method does not apply a stoichiometric amount of a toxic allylmetal reagent, it does still require a stoichiometric amount of a chiral auxiliary and two

extra steps for the complexation and decomplexation of dicobalt hexacarbonyl. Because of these shortfalls there remains a need for a more streamlined route to access homoallylic propargylic alcohols.
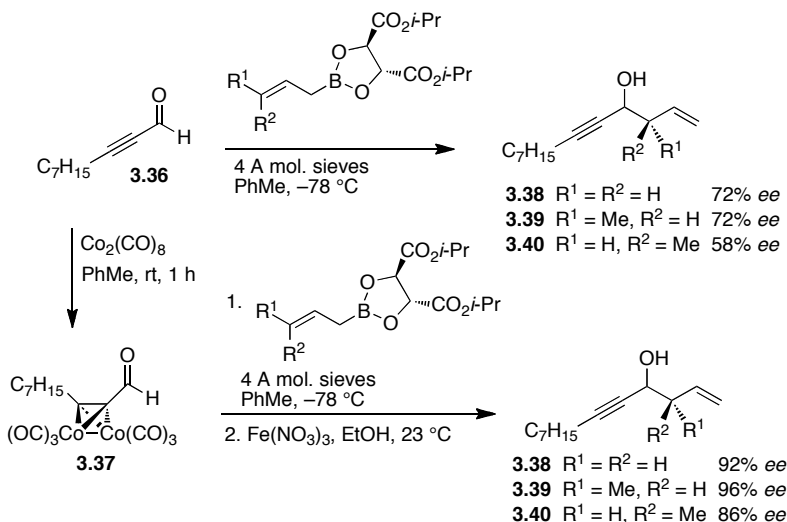
Scheme 3.1. Roush's dicobalt hexacarbonyl complex procedure used to obtain homoallylic propargylic alcohols in high enantioselectivities.[43]

Until recently, no catalytic variant of the allylboration reaction seemed plausible. This is possibly due to the fact that an allylboration reaction takes place through a Type I, closed Zimmerman-Traxler chair-like transition state (Figure 3.2), making it difficult for an external chiral reagent to work in a catalytic fashion. It was originally proposed that if an external Lewis acid were added to the system it could bind with the carbonyl lone pair and switch the reactivity of the allylboronate to a Type II open transition state, thus possibly resulting in complete loss of the stereospecificity seen with the Zimmermann-Traxler transition state.[44]
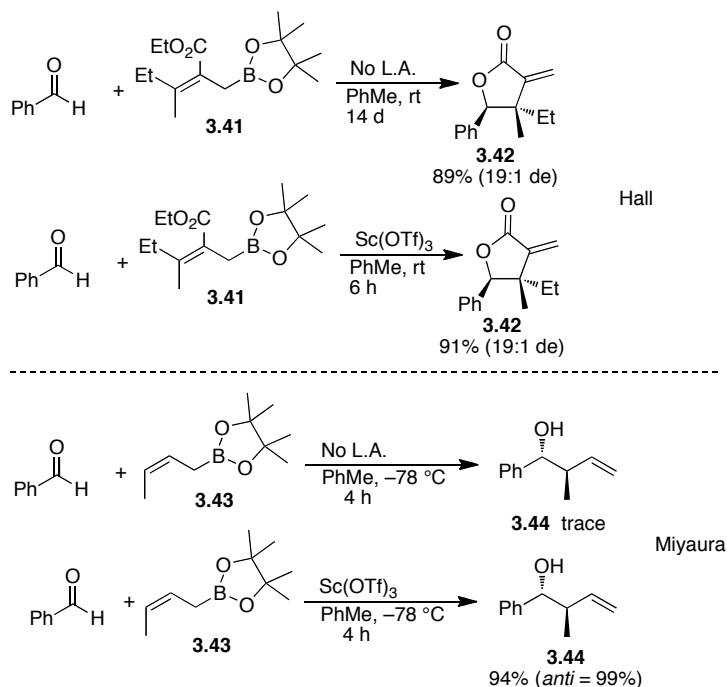
Figure 3.6. Lewis acid catalyzed reaction rate enhancement observed by Hall[44] and Miyaura.[45] L.A. = Lewis acid.

It was not until 2002 that Hall[44] and later Miyaura,[45] showed that metal salts like Sc(OTf)$_3$ were able to act as Lewis acids in catalyzing the allylboration of aldehydes. Using this Lewis acid, the reaction rate is increased by up to 35 fold while still maintaining high diastereoselectivity of the chair-like transition state (Figure 3.6). After numerous studies, it was eventually demonstrated by Rauniyar *et al.* that the Lewis acid binds to one of the oxygens of the allylboronate resulting in more acidic character for the boron, which leads to a stronger interaction with the aldehyde and therefore a faster reaction rate.[44,46,47] This proposed transition state agrees with Brown's demonstration that the electrophilicity of the boron atom is directly related to the rate of the reaction.[48] Later, the quantum chemical

calculations of Fujimoto and Sakata agreed with the activation of an oxygen in the allylboronate and more specifically that this activation was from the equatorial oxygen (Figure 3.7).[49]
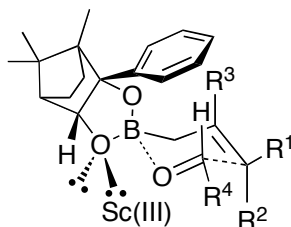
Figure 3.7. Proposed transition state of Lewis acid activation of an allylboration reaction.

Hall and coworkers went on to show that Sc(OTf)$_3$ could enhance the reactivity when using Hoffmann's chiral boronate auxiliary to many aldehydes at –78 °C, resulting in high enantioselectivities (and with high diastereoselectivities when using a crotylboronate). They also performed this reaction on a propargylic aldehyde to give a 86% yield and 97% *ee* (Equation 3.5).[50-52] Even though high yields and enantioselectivities have been obtained, a drawback is that the chirality transfer reagent is bound to the boron; therefore at least one equivalent of the chiral auxiliary is needed for the reaction.
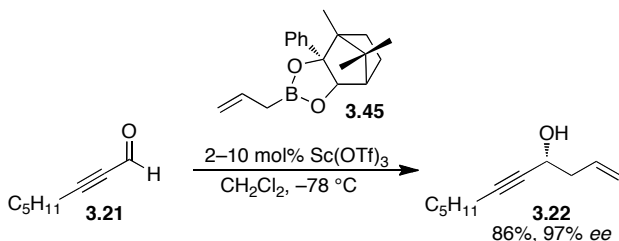
Equation 3.5. Scandium triflate rate enhancement with Hoffmann's chiral allylboronate on a propargylic aldehyde.

105

Since the addition of Sc(OTf)$_3$ resulted in a 35 time rate enhancement in comparison to the background reaction (Figure 3.6), it seemed apparent that to make the reaction more atom economical, one could apply an external chiral Lewis acid. Miyaura and coworkers were the first to demonstrate that a chiral Lewis acid could indeed catalyze an enantioselective allylboration, however low enantioselectivities were obtained (Equation 3.6).[45]
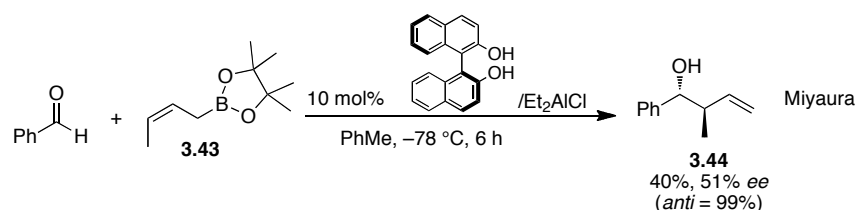
Equation 3.6. The first catalyzed asymmetric allylboration reaction.[45]

Intrigued by the possibility of developing a Lewis acid catalyzed enantioselective allylboration route, Hall and coworkers went on to attempt many different chiral Lewis acid salts, however most likely due to steric effects, the results were less than ideal.[53] In 2005 Yu and Hall were the first to show that H$^+$ could catalyze the allylboroation reaction by incorporating triflic acid instead of Sc(OTf)$_3$.[54] Inspired by this and recent publications about chiral Brønsted acid catalysis,[55] the Hall group found that Yamamoto's model of a Lewis acid assisted chiral Brønsted acid (**3.47**) gave some promising results.[56,57] Enantioselectivities up to 80% *ee* were observed for aliphatic aldehydes, while aromatic and propargylic aldehydes afforded enantioselectivities around 12% *ee* (Equation 3.7).[53] With a focus now on aliphatic aldehydes further optimizations by Rauniyar

et al. showed that a catalytic asymmetric allylboration can be performed, giving high yields and enantioselectivities with their new catalyst, which they coined as "Vivol" (**3.48**, Figure 3.8).[58] When looking at an aldehyde scope they observed substantially lower enantioselectivities for unsaturated aldehydes.[58]
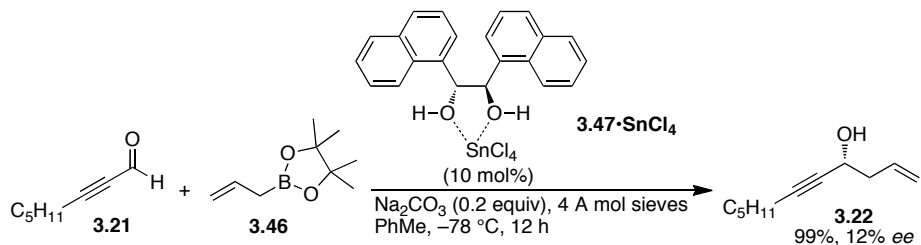
Equation 3.7. Catalytic asymmetric allylboration of a propargylic aldehyde using Yamamoto's Lewis acid assisted chiral Brønsted acid catalyst system.[58]

3.48
Vivol-8

3.49
F–Vivol-8
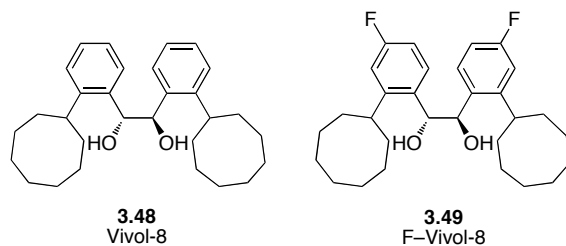
Figure 3.8. Second and third generation allylboration catalysts Vivol-8 (**3.48**) and F-Vivol-8 (**3.49**).

When investigating ways to further optimize the catalyst, Hall and coworkers rationalized that electron withdrawing groups on the aryl substituents could result in a more acidic diol, meaning a more active Brønsted acid.[59] A more active Brønsted acid would shorten the reaction time and possibly suppress the background reaction that was found to account for a 3-4% loss of

107

enantioselectivity. From the crystallographic data of the Vivol-SnCl$_4$ complex,[58] they determined that substituents at the *para*-position would disrupt the catalyst's spatial arrangement to the smallest degree. Placing fluorines in the 4-position of both phenyl groups resulted in higher enantioselectivities, even when the catalyst loading was decreased to 2.5 mol% (Equation 3.8).[59] This new catalyst was given the name "F-Vivol" (**3.49**). The most suitable substrates for this allylboration are still aliphatic aldehydes, however, with F-Vivol-8 (**3.49**) the electron deficient aromatic aldehyde **3.55** reacted to give **3.59** in a high yield and enantioselectivity (Equation 3.9).

Diol	yield (%)	*ee* (%)
(10 mol%) **3.48**	99	93
(2.5 mol%) **3.49**	95	96
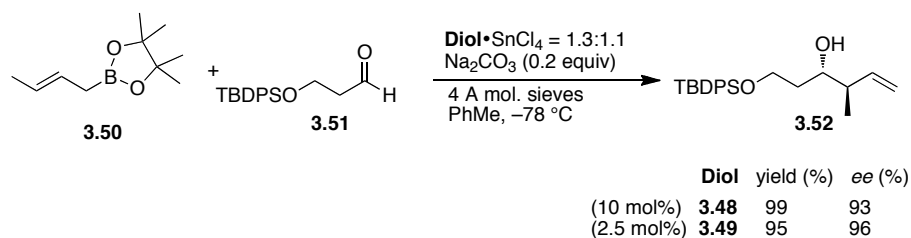
Equation 3.8. Comparison of Vivol-8 (**3.48**) and F-Vivol-8 (**3.49**).[59]
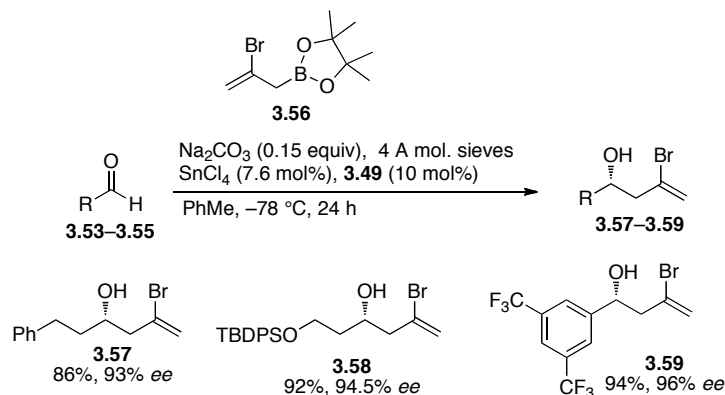
Equation 3.9. Selected examples of a substrate scope with F-Vivol-8 (**3.49**).[59]

Recently Antilla[60] reported a procedure using a highly substituted phosphoric acid **3.60** developed in 2006 by List[61] and coworkers based on a concept of Brønsted acid catalysis developed independently by both Terada[62] and Akiyama[63] in 2004. Catalyst **3.60** was found to work well for the allylboration of aryl and α,β-unsaturated aldehydes (Equation 3.10), however with the aliphatic cyclohexanecarboxaldehyde, lower enantioselectivities were observed. This method is therefore found to be a complementary method to that developed by Hall and coworkers. Of the routes known, no one has focused on optimizing conditions for the catalytic asymmetric allylboration of propargylic aldehydes. Neither Antilla's method with a phosphoric acid or Hall's F-Vivol diol/SnCl$_4$ complex were attempted with propargylic aldehydes. From here the plan was to further develop this area to find a catalytic route for the asymmetric allylboration of a propargylic aldehyde. By applying both Antilla's method using List's chiral phosphoric acid and Hall's F-Vivol catalyst steps were taken to determine the optimal conditions for the catalytic enantioselective allylboration of propargylic aldehydes.
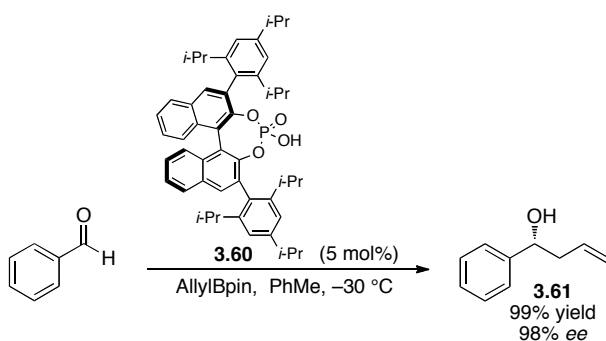
Equation 3.10. Antilla's chiral phosphoric acid catalyzed allylboration methodology.[60]

3.4 Results

3.4.1 Study of the background reaction

As shown by Hall and Miyaura, the background (uncatalyzed) reaction with both aliphatic and aromatic aldehydes at -78 °C plays a negligible role to that of the catalyzed reaction.[44,45] Therefore the first question proposed was what role does the background (uncatalyzed) allylboration of propargylic aldehydes at -78 °C play? If the racemic background reaction were to play a significant role, there would be competition between the background and catalyzed reaction, which would diminish the enantioselectivity in the catalyzed reaction. Propargylic aldehydes were synthesized by reacting the corresponding terminal acetylene with *n*-BuLi and either excess dimethylformamide (DMF) or ethylformate (1 equiv) to give the corresponding propargylic aldehydes in good yields (78–82%).[64] As Rauniyar *et al.* demonstrated previously,[58] the reaction is concentration dependent; therefore special care was used to mimic the identical conditions by including the 4 A molecular sieves and Na_2CO_3 in the background (uncatalyzed) reaction. The aldehydes 3-phenyl-2-propynal (**3.23**), 5-phenyl-2-pentynal (**3.63**) and triisopropylsilyl-propynal (**3.66**) were all reacted at -78 °C in the presence of allylBpin (**3.46**), Na_2CO_3, 4 A molecular sieves and toluene. All three background reactions were run overnight and then quenched via the cannulated addition of 1.2 equivalents of diisobutylaluminum hydride (DIBAL-H) cooled to -78 °C prior to addition (Figure 3.9).
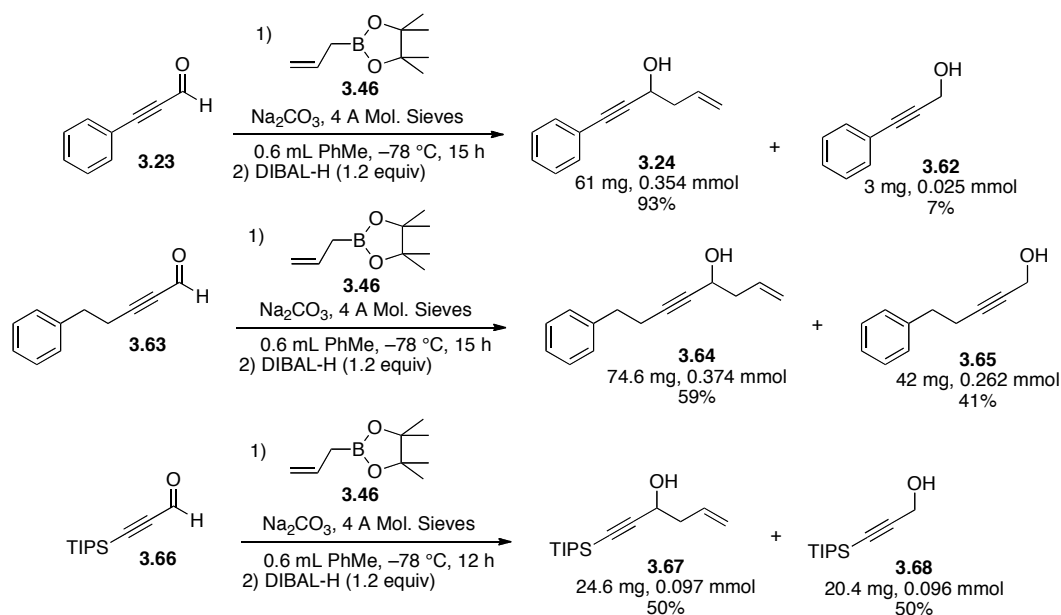
Figure 3.9. Comparing the background reactions for different propargylic aldehydes.

When a more conjugated aldehyde (**3.23**) is utilized, the background reaction was increased in comparison to that of the less conjugated aldehydes 5-phenyl-2-pentynal (**3.63**) and triisopropylsilylpropynal (**3.66**). In comparing the three aldehydes, **3.23** had the fastest background reaction, where only 7% of the reduced starting material was isolated from the reaction mixture. The reaction rates for both **3.63** and **3.66** were approximately half that of the fully conjugated aldehyde **3.23** (Figure 3.9). The background reaction for 5-phenyl-2-pentynal (**3.63**) was also examined at different concentrations. At increased concentration the background reaction went further to completion (Table 3.1).

Table 3.1. Background reaction at different concentrations.
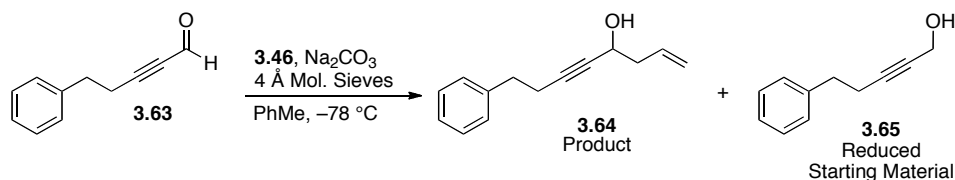
Temp	Toluene	Time	Yield^a	Rxn conc.
−85 °C	0.45 mL	6 h	43%	2 M
−78 °C	0.5 mL	10 h	59%	1.9 M
−78 °C	0.6 mL	12 h	46%	1.3 M
−78 °C	1.2 mL	9 h	23%	0.33 M

^{a}Isolated yield.

3.4.2 Catalytic enantioselective allylboration of propargylic aldehydes

We first looked at the catalyzed reaction with both 3-phenyl-2-propynal (**3.23**) and 5-phenyl-2-propynal (**3.63**). 3-Phenyl-2-propynal (**3.23**) is reacted with allylBpin under F-Vivol-8 (**3.49**) catalysis in 1 mL of toluene to give a 55% *ee*. As found previously, the reaction is concentration dependent; therefore, decreasing the amount of solvent to 0.5 mL (going from 1 M to 2 M) with F-Vivol-8 (**3.49**) gave a 69% *ee*. When switching to the smaller ring sized catalyst, F-Vivol-7 (**3.69**), with a 1 M solution a 59% *ee* was obtained and when increased to 2 M gave a 63% *ee*. To maximize on this trend, we further increased the concentration for both the reaction with F-Vivol-8 (**3.49**) and F-Vivol-7 (**3.69**) to a 4 M concentration; however, this gave inferior results at 53% and 43% *ee*, respectively (Table 3.2). Therefore it was thought possible that when increasing the concentration to 4 M, most likely not enough solvent was present to make a homogeneous mixture between the reagents and catalyst. Because of this issue, all future reactions were performed at a 2 M concentration.

Table 3.2. Concentration effects on enantioselectivity with catalysts F-Vivol-8 (**3.49**) and F-Vivol-7 (**3.69**).
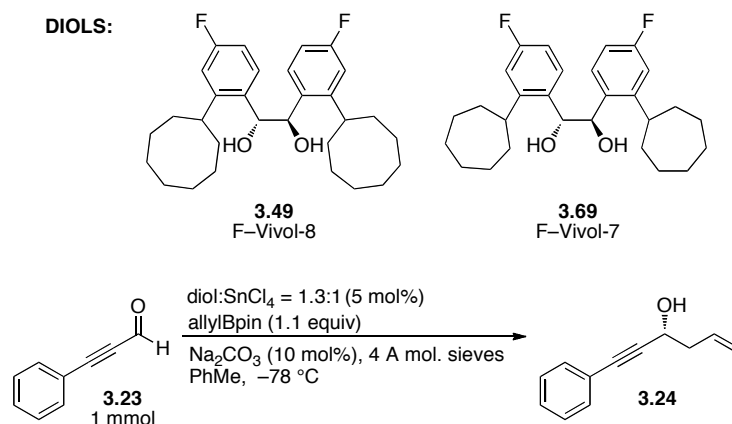
Entry	Catalyst	Toluene	Temp.	Time	Yield[a]	% ee[b]
1	F-Vivol-8	1 mL	−78 °C	41.5 h	77%	55% ee
2	F-Vivol-7	1 mL	−78 °C	41.5 h	70%	59% ee
3	F-Vivol-7	0.5 mL	−78 °C	13 h	72%	63% ee
4	F-Vivol-8	0.5 mL	−78 °C	13 h	70%	69% ee
5	F-Vivol-8	0.25 mL	−78 °C	14 h	71%	53% ee
6	F-Vivol-7	0.25 mL	−78 °C	14 h	75%	43% ee

[a]Isolated yield. [b]Enantioselectivity determined via HPLC analysis.

With 5-phenyl-2-pentynal (**3.63**, Table 3.3), which had a slower background reaction, a 1 M concentration with F-Vivol-8 (**3.49**) gave a 63% *ee*, while a 60% *ee* was obtained with F-Vivol-7 (**3.69**). From all the above conditions it can be seen that usually F-Vivol-8 (**3.49**) gave a slightly better enantioselectivity than that of F-Vivol-7 (**3.69**); however when increasing the catalyst loading to 10 mol% and a 2 M concentration, with F-Vivol-7 (**3.69**) the enantioselectivity was 76% *ee* while with F-Vivol-8 (**3.49**) it was only 73% *ee*

(Table 3.4). This led to confusion on whether a seven– or eight–membered ring substituent on F-Vivol would give superior enantioselectivities.

Table 3.3. 5 mol% F-Vivol-7 and F-Vivol-8 comparison with aldehyde **3.63**.
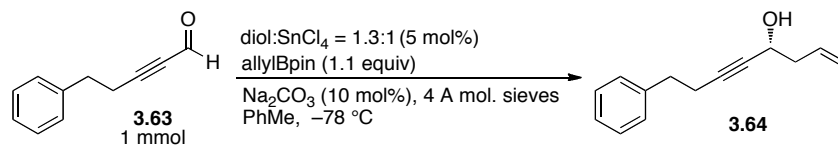
Entry	Catalyst	Toluene	Temp.	Time	Yield^a	% ee^b
1	F-Vivol-8	0.6 mL	−78 °C	17 h	87%	63% *ee*
2	F-Vivol-7	0.6 mL	−78 °C	17 h	93%	60% *ee*

^{a}Isolated yield. ^{b}Enantioselectivity determined via HPLC analysis.

Table 3.4. 10 mol% F-Vivol-7 and F-Vivol-8 comparison with aldehyde **3.63**.
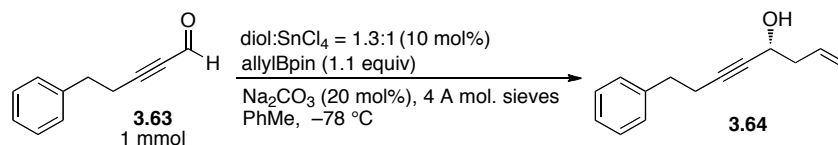
Entry	Catalyst	Toluene	Temp.	Time	Yield^a	% ee^b
1	F-Vivol-8	0.6 mL	−78 °C	4 h	75%	73% *ee*
2	F-Vivol-7	0.6 mL	−78 °C	4 h	74%	76% *ee*

^{a}Isolated yield. ^{b}Enantioselectivity determined via HPLC analysis.

Because there was no conclusion on which ring sized F-Vivol gave the best enantioselectivity, the task was undertaken to investigate the two extremes on ring size and synthesize both F-Vivol-5 and F-Vivol-12. The syntheses of both

derivatives followed the same procedure as that for the syntheses of **3.49** and **3.69**. Starting from the commercially available 2-bromo-4-fluorobenzaldehyde, a McMurray coupling to provide the *trans*-stilbene **3.70** was followed by a Sharpless asymmetric dihydroxylation using (DHQD)$_2$PHAL as the chiral ligand to give the diol **3.71** in a 65% yield over the two steps after recrystallization from hexanes/CH$_2$Cl$_2$ (Scheme 3.2). The diol **3.71** was then protected as the acetonide **3.72** before a Suzuki–Miyaura cross coupling to both aryl rings with either cyclopentenylpinacol boronate (**3.73**) or cyclododecenylpinacol boronate (**3.74**) to give either the F-Vivol-5 (**3.75**) or F-Vivol-12 (**3.76**) precursor in 86% and 80% yield, respectively, after recrystallization from methanol. Finally, removal of the protecting group under acidic conditions and hydrogenation gave the final products F-Vivol-5 (**3.79**) and F-Vivol-12 (**3.80**) in 95% and 88% yield, respectively (Scheme 3.2).
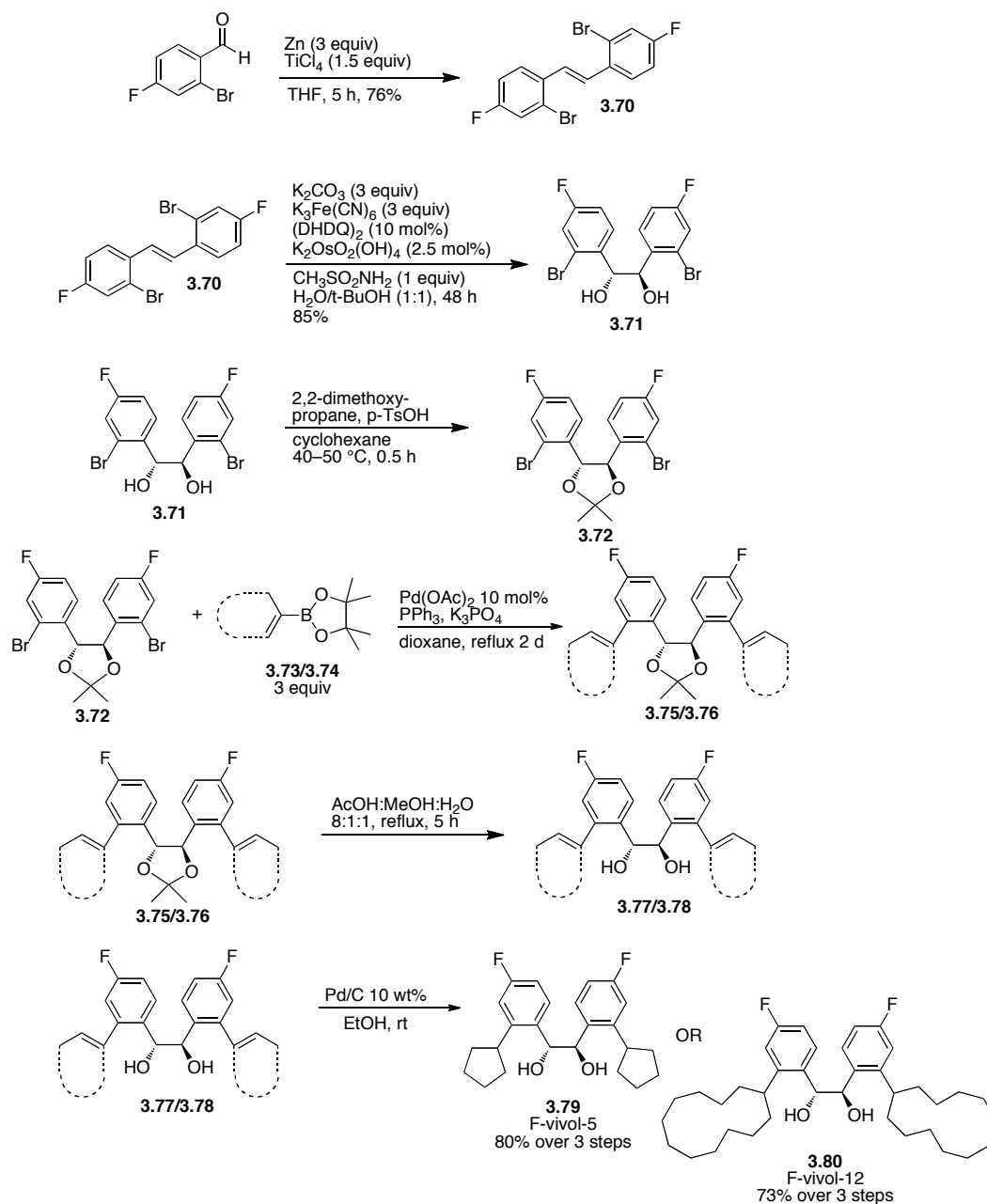
Scheme 3.2. Synthesis of F-Vivol analogues F-Vivol-5 (**3.79**) and F-Vivol-12 (**3.80**).

As Penner *et al.* have shown in the synthesis of Palmerolide A,[65,66] the seven membered ring catalyst gave a better enantioselectivity when compared to

the eight for their crotylation step. To determine whether a smaller or larger ring

size would give enhanced enantioselectivities for the catalytic asymmetric

allylboration of propargylic aldehydes; reactions were performed with both F-

Vivol-5 (**3.79**) and F-Vivol-12 (**3.80**) at 10 mol% catalyst loading.

Disappointingly, only a 27% and 23% *ee* were obtained for the allylboration of

3.63 with F-Vivol-5 and F-Vivol-12, respectively (Table 3.5). This outcome is

similar to results observed by Rauniyar *et al.* with aliphatic aldehydes: the best

ring size is either the seven membered (**3.69**) or eight membered (**3.49**), and going

to a larger or smaller ring size resulted in a decrease in enantioselectivity.[58]

Table 3.5. Comparison of F-Vivol-5 (**3.79**) and F-Vivol-12 (**3.80**).
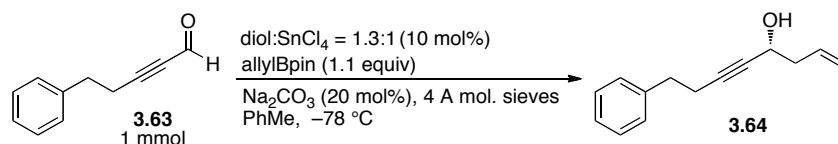
Entry	Catalyst	Toluene	Temp.	Time	Yield^a	% ee^b
1	F-Vivol-5	0.6 mL	−78 °C	1 h	60%	27% *ee*
2	F-Vivol-12	0.6 mL	−78 °C	9 h	74%	23% *ee*

^{a}Isolated yield. ^{b}Enantioselectivity determined via HPLC analysis.

The temperature of the reaction was also a variable that could be

controlled. By further decreasing the reaction temperature the goal was to

diminish the background/uncatalyzed reaction while still maintaining a fast

catalyzed reaction. Since toluene had previously been established as the optimal

solvent, we were limited to temperatures above the freezing point of −93 °C.
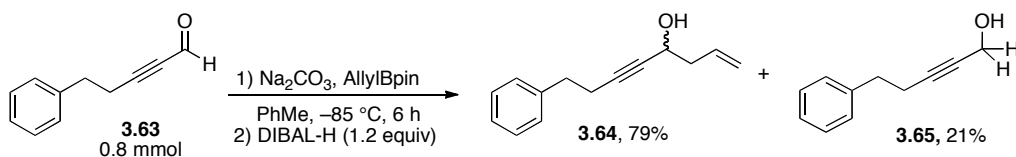
Equation 3.11. Background reaction of aldehyde **3.63** at −85 °C.
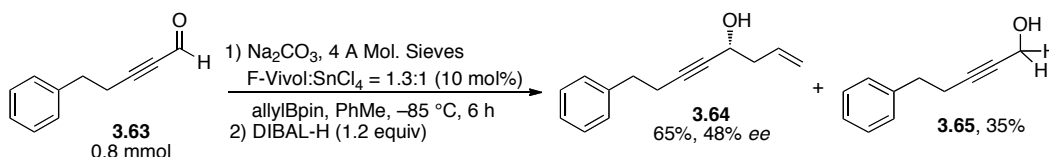
Equation 3.12. F-Vivol-7•SnCl$_4$ catalyzed reaction at −85 °C.

A background reaction performed at −85 °C showed that it still played a significant role in the reaction (Equation 3.11). Because the background reaction still played a significant role, the catalyzed reaction performed with **3.69** at −85 °C gave results that were similar to the catalyzed reaction at −78 °C (Equation 3.12). The product **3.64** was only obtained in a 48% *ee* after stirring for 6 hours at a temperature between −85 and −90 °C. This attempt demonstrates that at lower temperatures the catalyst is less active but the background reaction still proceeds to a significant extent.

3.4.3 Application of dicobalt hexacarbonyl complex

As previously mentioned, Roush used the dicobalt hexacarbonyl complexes of the propargylic aldehydes with his chiral, tartrate–derived allylboronate to give higher enantioselectivities than the allylboration reaction of

the uncomplexed propargylic aldehydes.[43] By increasing the steric bulk of the alkynyl substituent, a larger difference in steric interactions is observed between the R-substituent and the aldehyde proton, therefore leading to higher enantioselectivities because of the closed 6-membered ring transition state. It was therefore postulated that if this dicobalt hexacarbonyl complexed propargylic aldehyde could be applied, an increase of 25–30% *ee* would be observed for our catalytic enantioselective allylboration, just like the enhancement observed by Roush and coworkers.
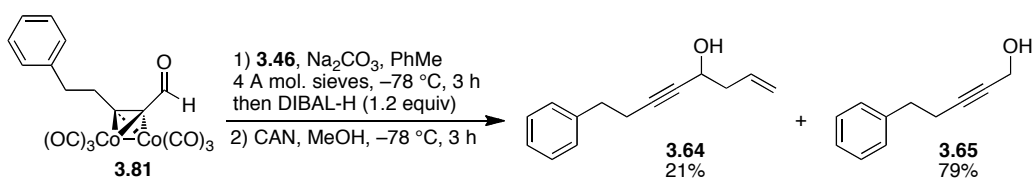
Equation 3.13. Background reaction with the dicobalt hexacarbonyl complex **3.81**.
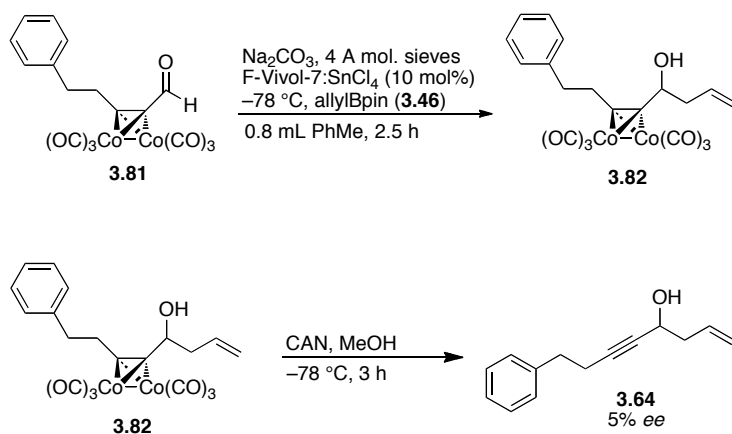
Scheme 3.3. Application of Roush's approach using dicobalt hexacarbonyl complex.

119

To this end, 5-phenyl-2-pentynal (**3.63**) was mixed with dicobalt octacarbonyl at room temperature to give the dicobalt hexacarbonyl complex of 5-phenyl-2-pentynal (**3.81**) in an 86% yield. First a background reaction was performed to give 21% product after only 3 h (Equation 3.13). The catalyzed reaction was then performed with 10 mol% F-Vivol-7 catalyst loading to give only a 5% *ee* after decomplexation with ceric ammonium nitrate ($(NH_4)_2Ce(NO_3)_6$, Scheme 3.3). Initially it was postulated that this extremely low enantioselectivity was due to epimerization occurring under the decomplexation conditions. To determine whether this was the case a test reaction was performed where (**3.64**), which had originally been obtained in a 73% *ee*, was reacted with dicobalt octacarbonyl to give to the complex **3.82** (Scheme 3.4). The same decomplexation conditions as before was then performed on **3.82**, resulting in a 73% *ee* which proved that the decomplexation reaction conditions did not contribute to the reduction in enantioselectivity.
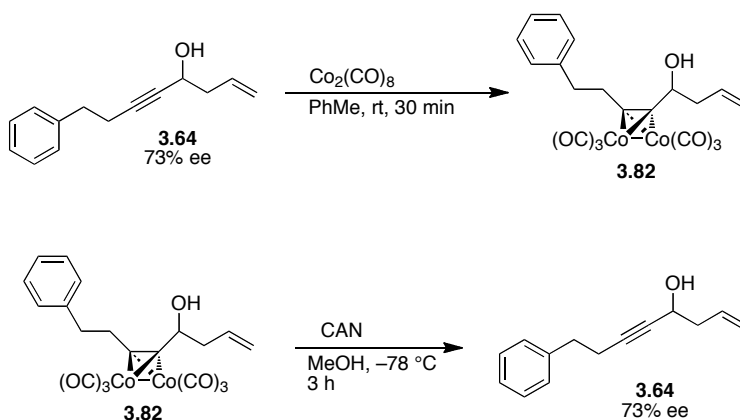
Scheme 3.4. Dicobalt hexacarbonyl complexation and decomplexation with optically enriched **3.64**.

3.4.4   Chiral phosphoric acid catalysis

Recently Antilla and coworkers published a methodology that applies a chiral phosphoric acid (**3.60**) in 5 mol% catalyst loading to catalyze the addition of allylBpin to aromatic and α,β-unsaturated aldehydes.[60] When Jian and Antilla investigated aliphatic aldehydes, lower than optimal results were obtained. Being complimentary to the F-Vivol method, it was proposed that using Antilla's procedure would give the desired enantioselectivity for the allylboration of a propargylic aldehyde. The reaction was first set up under the optimal published reaction conditions and then both the temperature and concentration were varied. In spite of this, under all conditions attempted, the enantioselectivities were found to be less than ideal. With 5 mol% **3.60** only a 50% *ee* was obtained when the reaction was cooled to –45 °C with a *m*-xylene/CO_2 bath (Equation 3.14).
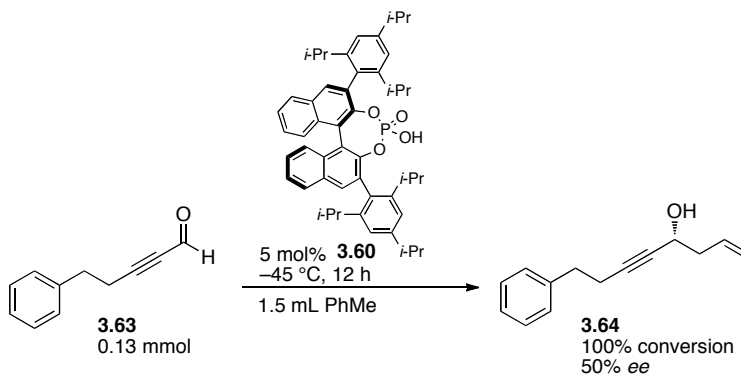
Equation 3.14. Antilla's method on aldehyde **3.63** with 5 mol% catalyst loading.
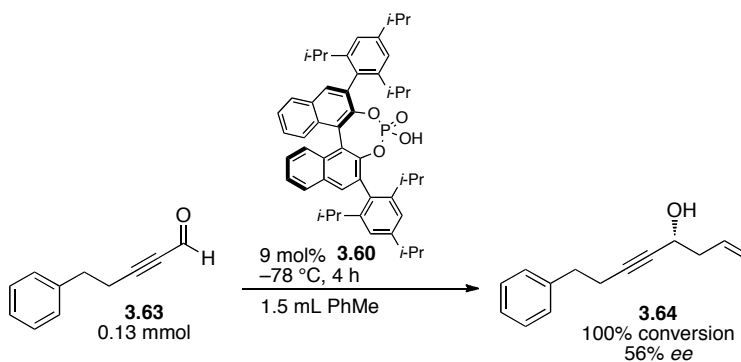
Equation 3.15. Application of Antilla's method with 9 mol% catalyst loading.

In an attempt to increase the enantioselectivity, the temperature was decreased to −78 °C and the catalyst loading increased to 9.3 mol%, however, under these modified conditions, product **3.64** was obtained with a 56% *ee* (Equation 3.15).
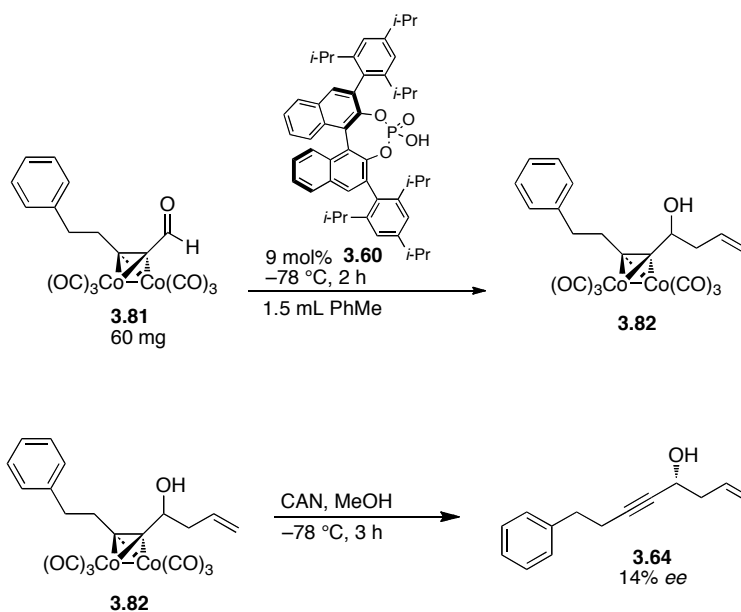
Scheme 3.5. Use of dicobalt hexacarbonyl **3.81** with Antilla's method.
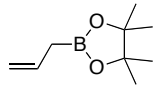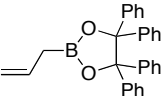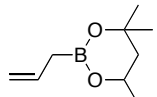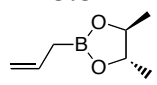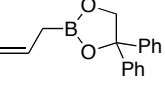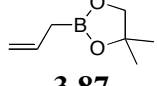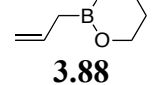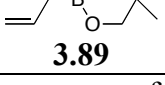
The dicobalt hexacarbonyl **3.81** also underwent the same phosphoric acid catalyzed allylboration conditions to give a slightly higher enantioselectivity of 14% *ee* (Scheme 3.5).

3.4.5 Examination of different allyl boronic esters

Another route that could increase the enantioselectivity would be to utilize allylboronates other than allylBpin; this might suppress the background reaction while still maintaining a fast catalyzed reaction. All the allylboronates looked at are shown in Table 3.6. Table 3.6 compares the speed of the background reaction for all the different allylboronates in reactions with aldehyde **3.63**. With the highly congested allylboronates **3.83** and **3.84** the background reactions were slower than the reaction with allylBpin (**3.46**). The background reactions of the allylboronates with steric congestion on only one side (**3.86** and **3.87**) had a similar background reaction to that of allylBpin, however they were less air stable and harder to synthesize. When switching to 6-membered ring allylboronates, **3.88** had a similar reaction rate to **3.85**, while the speed of the background reaction for neopentylallylboronate **3.89** was approximately half that of allylBpin.

Table 3.6. Background reaction of **3.63** with different allylboronates.[a]

Allylboronate	Reaction time	Product	Reduced Starting Material
3.46	12 h	59%	41%
3.83	16 h*	43%	57%
3.84	9 h	4%	96%
3.85	5 h	18%	82%
3.86	7 h	18%	82%
3.87	7 h	35%	65%
3.88	5 h	25%	75%
3.89	9 h	26%	74%

[a]All reactions were performed at a 2 M concentration and quenched via the −78 °C cannulated addition of 1.2 equiv DIBAL-H.
* Reaction warmed to −10 °C over the 16 hours.

For the catalyzed reaction, the first allylboronates investigated were the highly congested tetraphenyl substituted 5-membered ring allylboronate **3.83** and the congested 6-membered ring allylboronate **3.84**. With more steric congestion on the boronic ester, the background reaction could slow down while still having

a fast catalyzed reaction. Both background reactions gave a minimal amount of product overnight in comparison to allylBpin, even with allowing the temperature for allylboronate **3.83** to slowly increase to –10 °C the reaction only went to 43% completion over 16 hours.

Due to the difficulty of preparing the sterically hindered tetraphenyl substituted allylboronate **3.83** in good yields, the catalyzed reaction with a sterically hindered allylboronate was first attempted with the more accessible allylboronate **3.84**. The allylboronate **3.84** was used in a reaction with 8 mol% F-Vivol-7 (**3.69**) and only a 19% yield was obtained overnight with a 7.8% *ee* (Equation 3.16). This reaction was then reattempted at 0 °C and special care was taken to use new starting materials. In re-performing this reaction at a warmer temperature of 0 °C, 100% conversion was seen overnight to give only a 3% *ee* (Equation 3.17).
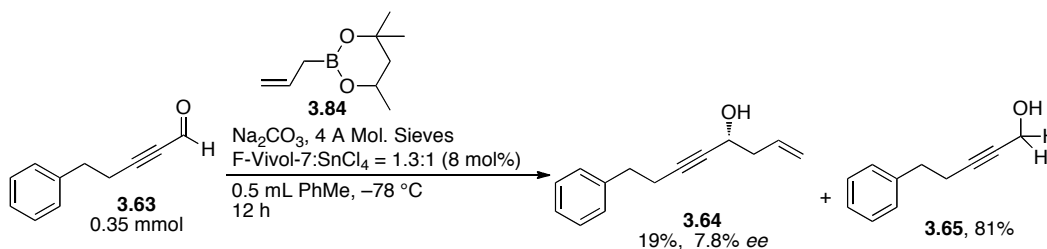
Equation 3.16. F-Vivol-7 (8 mol%) catalyzed reaction with allylboronate **3.73**.
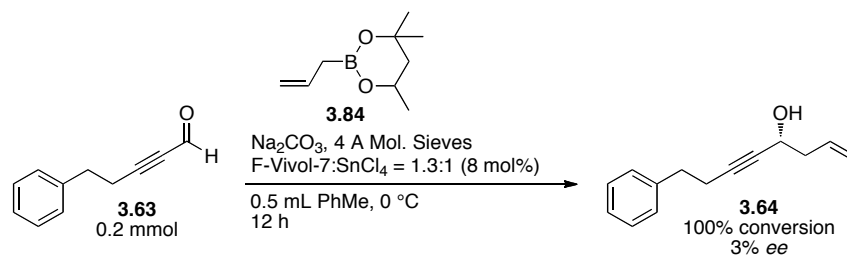
Equation 3.17. F-Vivol-7 (8 mol%) catalyzed reaction with allylboronate **3.84** at 0 °C.
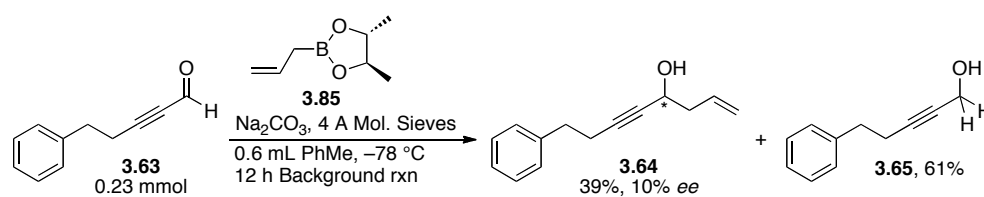
Equation 3.18. Background reaction with allylboronate **3.85**.

The 2,3-butanediol protected allylboronate **3.85** is a chiral allylboronate and therefore without a chiral catalyst can still give an optically enriched product. The background reaction was performed overnight to give a 39% yield and 10% *ee* (Equation 3.18). Starting with an initial 10% *ee*, by adding the chiral catalyst F-Vivol-7 (**3.69**), it was postulated that the enantioselectivity for the allylboration of **3.63** would most likely increase by at least 10%, giving a desired enantioselectivity in the high 80s or 90 percentile. Disappointingly, this was not the case; when adding 10 mol% F-Vivol-7 catalyst the resulting product gave a 0% *ee* (Equation 3.19). It was therefore postulated that this was a case of mismatching, and if either the other chiral diol was used to protect the

126

allylboronic acid or the other enantiomeric F-Vivol-7 catalyst was used a higher desirable enantioselectivity could be obtained. This, however, was not pursued because the main goal of this research was to develop a route that did not require the use of a stoichiometric amount of chiral reagent.
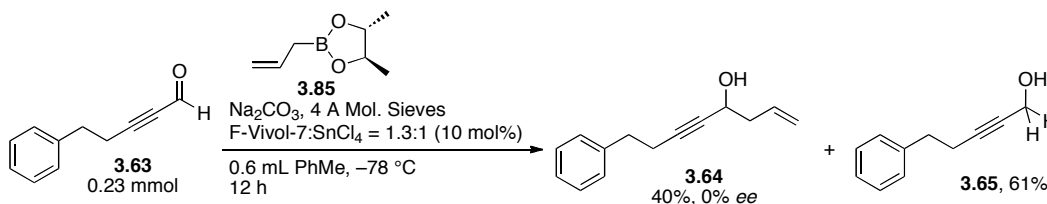
Equation 3.19. F-Vivol-7 catalyzed reaction with allylboronate **3.85**.

The allylboronates **3.86** and **3.87** contain steric congestion on one side of the diol (either two methyl or phenyl groups) and no steric congestion (a CH_2 group) on the other side. Both of these allylboronates were quite difficult to synthesize and even after purification needed to be used right away due to their instability. Although the background reaction for both of these allylboronates was slower than allylBpin, due to the tedious preparation of the starting materials, these allylboronates were abandoned as viable routes.

The next allylboronate to be explored was the six-membered allylboronate *B*-allyl-1,3,2-dioxaborinane **3.88**. The background reaction with *B*-allyl-1,3,2-dioxaborinane (**3.88**) was comparable to that of the reaction with allylBpin, while the catalyzed reaction gave 60% yield and a 38% *ee* (Equation 3.20). This outcome is possibly due to the fact that the six-membered allylboronate **3.88** is slightly less sterically hindered than allylBpin (**3.46**). In a comparison, with

hydrocinnamaldehyde (**3.90**) the same reaction with *B*-allyl-1,3,2-dioxaborinane

3.88 and 5 mol% F-Vivol-7 gave complete conversion and only a 20% *ee* in 5 h

(Equation 3.21). *B*-allyl-1,3,2-dioxaborinane **3.88** was also utilized under

Antilla's phosphoric acid catalyzed conditions to give full conversion overnight at

–78 °C with a 55% *ee* (Equation 3.22).
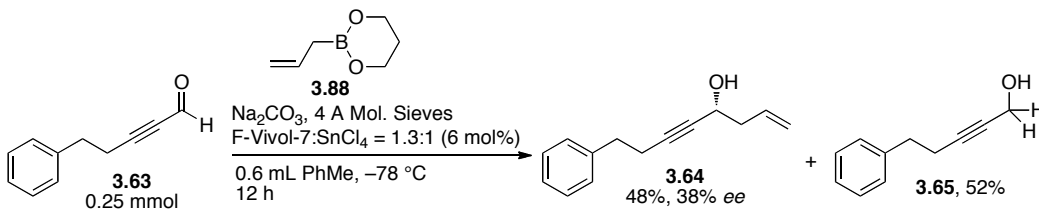
Equation 3.20. Allylboration with the allylboronate **3.88** and aldehyde **3.63** in the

presence of 6 mol% F-Vivol-7 catalyst.
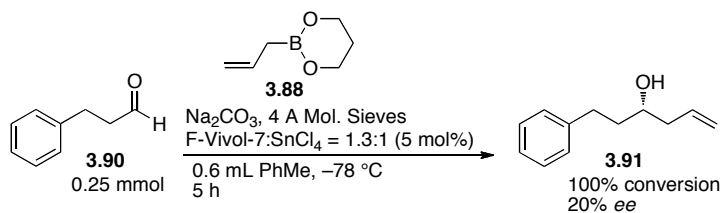
Equation 3.21. Allylboration of hydrocinnamaldehyde (**3.90**) and allylboronate

3.88 catalyzed by 5 mol% F-Vivol-7 (**4.69**).
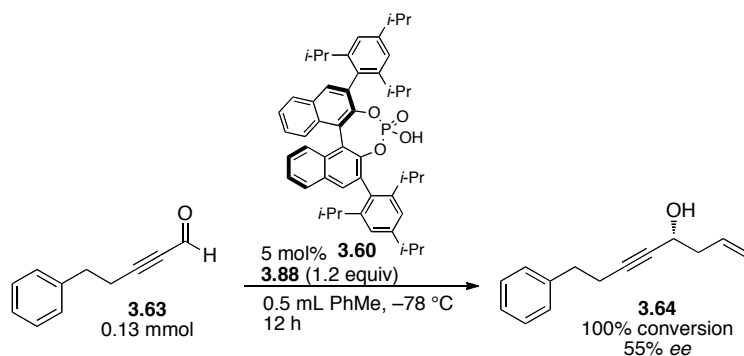
Equation 3.22. Allylboration on **3.63** with *B*-allyl-1,3,2-dioxaborinane **3.88** and 5 mol% catalyst **3.60**.

The similar neopentylallylboronate **3.89** had an uncatalyzed reaction that gave only 26% yield after 9 h, where allylboronate **3.88** had reached 25% completion in approximately half that time (5 h). The catalyzed allylboration of **3.63** with neopentylallylboronate **3.89** and 6 mol% F-Vivol-7 catalyst went to completion overnight and gave a 66% *ee* (Equation 3.23). Increasing the F-Vivol-7 catalyst loading to 10.6 mol% of F-Vivol-7 gave full conversion overnight, however to our satisfaction the enantioselectivity had now increased to 83% *ee* (Equation 3.24).
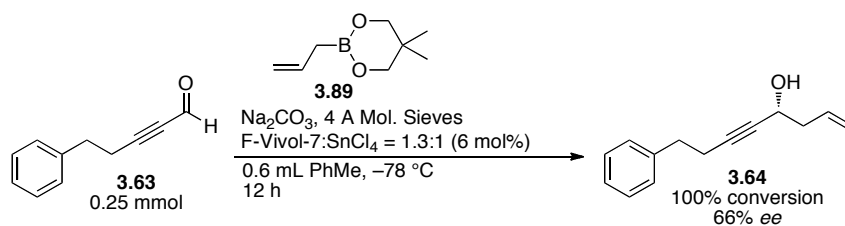
Equation 3.23. Allylboration of **3.63** with neopentylallylboronate **3.89** and 6 mol% F-Vivol-7.
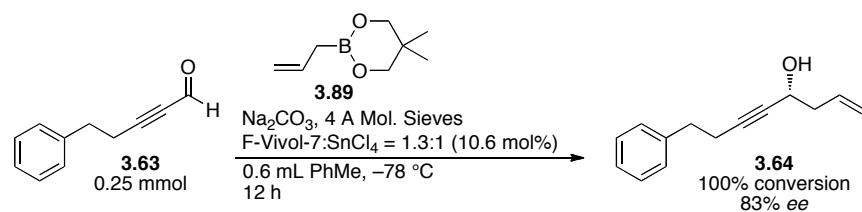
Equation 3.24. F-Vivol-7 catalyzed reaction with neopentylallylboronate **3.89**.

At the exact same time as the reaction shown in Equation 3.24 was performed, the same reaction was set up with allylBpin; giving a 90% conversion and 61% *ee* overnight (Equation 3.25). This result demonstrates that the neopentylallylboronate **3.89** is clearly superior to that of allylBpin (**3.46**); one can conclude that with neopentylallylboronate **(3.89)** the F-Vivol-7 catalyzed reaction is faster than the reaction with allylBpin (**3.46**), however without the catalyst the reaction with neopentylallylboronate **(3.89)** is slower. Another possible cause for the reduction in enantioselectivity for the reaction with allylBpin (**3.46**) could be due to the presence of free boronic acid. Free boronic acid would react with the substrate faster than that of the catalyzed allylboronic ester allylboration, resulting in a larger proportion of racemic product. This possibility was assessed by performing ^{11}B NMR analysis of both allylboronates before and after the reaction; in both cases only a single peak representing the ester derivative was observed.
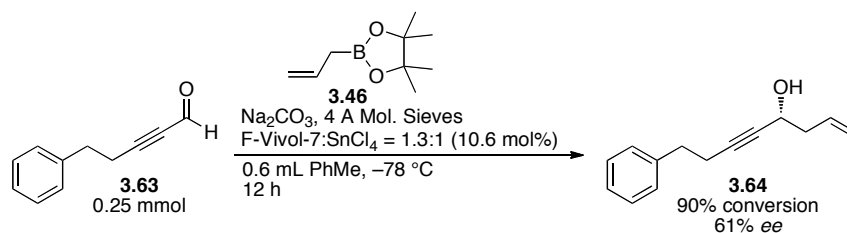
Equation 3.25. Allylboration of **3.63** with allylBpin **3.46** performed under the exact same conditions and at the same time as Equation 3.24.

3.5 Conclusion

In determining that neopentylallylboronate (**3.89**) is found to be a better allylboronate reagent than allylBpin (**3.46**) for the allylboration of propargylic aldehydes in the presence of F-Vivol-7•SnCl$_4$ catalyst (**3.69**), the major goal for this project was accomplished. Even though an enantioselectivity of only 83% *ee* was achieved, with increasing the F-Vivol-7 catalyst (**3.69**) loading a desirable enantioselectivity could be obtained. Another parameter that should be investigated in the future would be to perform the same allylboration conditions with the homologous F-Vivol-8 based catalyst (**3.49**).

Another factor that can be examined is other allylboronic esters with a similar backbone to that of neopentylallylboronate (**3.89**). Other diols similar to the neopentyl diol **3.90** are shown in Figure 3.10. By incorporating further steric congestion that is slightly removed from the diol system, this could have an effect on the activity of the diol•SnCl$_4$ species. Although allylBpin is the workhorse for

131

allylboration reactions, it is possible that better, more active allylboronates exist. Both of these situations should be addressed in the near future.
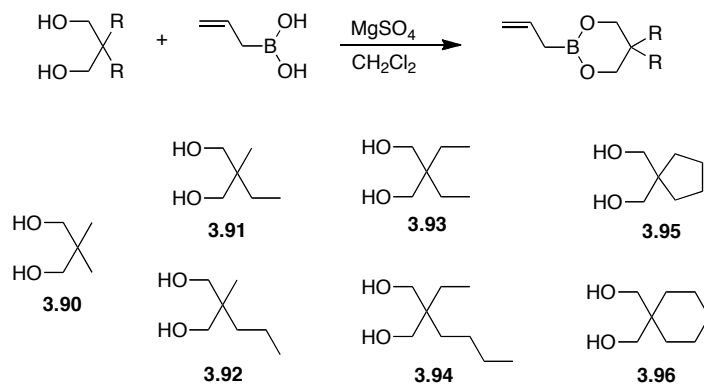
Figure 3.10. Examples of other diols that could be employed for the synthesis other allylboronic esters which could be used for further studies with the catalytic enantioselective allylboration of aldehydes.

The efficacy of other allylboronic esters may not be limited to allylborations with the diol•SnCl₄ complexes. This allylboronate should be examined in other catalytic enantioselective allylboration reactions, such as Antilla's methodology. A study should explore whether the structure-reactivity relation applies to other allylboration methods. If this were true it could eventually change the entire face of allylation chemistry, as we know it. However, if neopentylallylboronate is found to be the best option, there is a possibility that we might be reaching the limits of the F-Vivol catalyst system and future research in this area should focus on the development of a new catalyst system.

3.6 References

(1)   Nicolaou, K.; Murphy, F.; Barluenga, S.; Ohshima, T.; Wei, H.; Xu, J.; Gray, D.; Baudoin, O. *J. Am. Chem. Soc.* **2000**, *122*, 3830-3838.

(2)   Nicolaou, K.; Fylaktakidou, K. C.; Monenschein, H.; Li, Y.; Weyershausen, B.; Mitchell, H. J.; Wei, H.; Guntupalli, P.; Hepworth, D.; Sugita, K. *J. Am. Chem. Soc.* **2003**, *125*, 15433-15442.

(3)   Dineen, T. A.; Roush, W. R. *Org. Lett.* **2004**, *6*, 2043-2046.

(4)   Shotwell, J. B.; Roush, W. R. *Org. Lett.* **2004**, *6*, 3865-3868.

(5)   Fátima, Ā. d.; Pilli, R. A. *Tetrahedron Lett.* **2003**, *44*, 8721-8724.

(6)   Razon, P.; N'zoutani, M.-A.; Dhulut, S.; Bezzenine-Lafollée, S.; Pancrazi, A.; Ardisson, J. *Synthesis* **2005**, 109-121.

(7)   Madec, D.; Férézou, J.-P. *Eur. J. Org. Chem.* **2006**, 92-104.

(8)   Jung, W.-H.; Guyenne, S.; Riesco-Fagundo, C.; Mancuso, J.; Nakamura, S.; Curran, D. P. *Angew. Chem. Int. Ed.* **2008**, *47*, 1130-1133.

(9)   Fürstner, A.; Schlecker, A. *Chem. Eur. J.* **2008**, *14*, 9181-9191.

(10)   Denmark, S. E.; Jones, T. K. *J. Org. Chem.* **1982**, *47*, 4595-4597.

(11)   Brown, C. A.; Ahuja, V. K. *J. Org. Chem.* **1973**, *38*, 2226-2230.

(12)   Zweifel, G.; Steele, R. *J. Am. Chem. Soc.* **1967**, *89*, 5085-5086.

(13)   Zweifel, G.; Steele, R. *J. Am. Chem. Soc.* **1967**, *89*, 2754-2755.

(14)   Marshall, J. A.; DeHoff, B. S. *J. Org. Chem.* **1986**, *51*, 863-872.

(15)   Chemin, D.; Gueugnot, S.; Linstrumelle, G. *Tetrahedron* **1992**, *48*, 4369-4378.

(16)   Zhang, H.; Guibé, F.; Balavoine, G. *J. Org. Chem.* **1990**, *55*, 1857-1867.

(17)   Russel, G. A.; Ngoviwatchai, P. *Tetrahedron Lett.* **1985**, *26*, 4975-4978.

(18)   Stoltz, B. M.; Kano, T.; Corey, E. J. *J. Am. Chem. Soc.* **2000**, *122*, 9044-9045.

(19)   Brown, H.; Ravindran, N.; Kulkarni, S. *J. Org. Chem.* **1980**, *45*, 384-389.

(20)   Sayo, N.; Nakai, E.; Nakai, T. *Chem. Lett.* **1985**, 1723-1724.

(21)   Denmark, S. E.; Weber, E. J. *Helv. Chim. Acta* **1983**, *66*, 1655-1660.

(22)   Denmark, S. E.; Fu, J. *Chem. Rev.* **2003**, *103*, 2763-2794.

(23)   Denmark, S. E.; Almstead, N. G. In *Modern Carbonyl Chemistry*; Otera, J., Ed.; Wiley–VCH: Weinheim, 2000, p 299-402.

(24)   Chemler, S. R. R., W. R. In *Modern Carbonyl Chemistry*; Otera, J., Ed.; Wiley–VCH: Weinheim, 2000, p 403-490.

(25)   Yamamoto, Y.; Asao, N. *Chem. Rev.* **1993**, *93*, 2207-2293.

(26)   BouzBouz, S.; Pradaux, F.; Cossy, J.; Ferroud, C.; Falguières, A. *Tetrahedron Lett.* **2000**, *41*, 8877-8880.

(27)   Marshall, J. A.; Gung, W. Y. *Tetrahedron Lett.* **1989**, *30*, 2183-2186.

(28)   Marshall, J. A.; Palovich, M. R. *J. Org. Chem.* **1998**, *63*, 4381-4384.

(29)   Kurosu, M.; Lorca, M. *Tetrahedron Lett.* **2002**, *43*, 1765-1769.

(30)   Kurosu, M.; Lorca, M. *Synlett* **2005**, 1109-1112.

(31)   Yu, C. M.; Jeon, M.; Lee, J. Y.; Jeon, J. *Eur. J. Org. Chem.* **2001**, 1143-1148.

(32)   Denmark, S. E.; Wynn, T. *J. Am. Chem. Soc.* **2001**, *123*, 6199-6200.

(33)   Hall, D. G. *Boronic Acids: Preparation and Application in Organic Synthesis and Medicine*; Wiley-VCH: Weinheim, 2005.

(34)   Mikhailov, B. M.; Bubnov, Y. N. *Izv. Akad. Nauk. SSSR, Ser. Khim.* **1964**, 1874.

(35)   Herold, T.; Hoffmann, R. W. *Angew. Chem. Int. Ed.* **1978**, *17*, 768-769.

(36)   Hoffmann, R. W.; Zeiss, H.-J. *Angew. Chem. Int. Ed.* **1979**, *18*, 306-307.

(37)   Hoffmann, R. W.; Ladner, W. *Tetrahedron Lett.* **1979**, *20*, 4653-4656.

(38)   Brown, H. C.; Jadhav, P. K. *J. Am. Chem. Soc.* **1983**, *105*, 2092-2093.

(39)   Smith III, A. B.; Ott, G. R. *J. Am. Chem. Soc.* **1998**, *120*, 3935-3948.

(40)   Sonawane, R.; Joolakanti, S.; Arseniyadis, S.; Cossy, J. *Synlett* **2009**, 213-216.

(41)   Robles, O.; McDonald, F. E. *Org. Lett.* **2008**, *10*, 1811-1814.

(42)   Ju, J.; Reddy, B.; Khan, M.; Nicholas, K. M. *J. Org. Chem.* **1989**, *54*, 5426-5428.

(43)   Roush, W. R.; Park, J. C. *J. Org. Chem.* **1990**, *55*, 1143-1144.

(44)   Kennedy, J. W. J.; Hall, D. G. *J. Am. Chem. Soc.* **2002**, *124*, 11586-11587.

(45)   Ishiyama, T.; Ahiko, T.; Miyaura, N. *J. Am. Chem. Soc.* **2002**, *124*, 12414-12415.

(46)   Lachance, H.; Lu, X.; Gravel, M.; Hall, D. G. *J. Am. Chem. Soc.* **2003**, *125*, 10160-10161.

(47)   Rauniyar, V.; Hall, D. G. *J. Am. Chem. Soc.* **2004**, *126*, 4518-4519.

(48)   Brown, H.; Racherla, U. S.; Pellechia, P. J. *J. Org. Chem.* **1990**, *55*, 1868-1874.

(49)   Sakata, K.; Fujimoto, H. *J. Am. Chem. Soc.* **2008**, *130*, 12519-12526.

(50)   Gravel, M.; Lachance, H.; Lu, X.; Hall, D. G. *Synthesis* **2004**, 1290-1302.

(51)   Peng, F.; Hall, D. G. *J. Am. Chem. Soc.* **2007**, *129*, 3070-3071.

(52)   Hall, D. G. *Synlett* **2007**, 1644-1655.

(53)   Rauniyar, V.; Hall, D. G. *Angew. Chem. Int. Ed.* **2006**, *45*, 2426-2428.

(54)   Yu, S. H.; Ferguson, M. J.; McDonald, R.; Hall, D. G. *J. Am. Chem. Soc.* **2005**, *127*, 12808-12809.

(55)   Pihko, P. M. *Angew. Chem. Int. Ed.* **2004**, *43*, 2062-2064.

(56)   Ishihara, K.; Nakamura, S.; Kaneeda, M.; Yamamoto, H. *J. Am. Chem. Soc.* **1996**, *118*, 12854-12855.

(57)   Nakamura, S.; Kaneeda, M.; Ishihara, K.; Yamamoto, H. *J. Am. Chem. Soc.* **2000**, *122*, 8120-8130.

(58)   Rauniyar, V.; Zhai, H.; Hall, D. G. *J. Am. Chem. Soc.* **2008**, *130*, 8481-8490.

(59)   Rauniyar, V.; Hall, D. G. *J. Org. Chem.* **2009**, *74*, 4236-4241.

(60)   Jain, P.; Antilla, J. *J. Am. Chem. Soc.* **2010**, *132*, 11884-11886.

(61)   Seayad, J.; Seayad, A. M.; List, B. *J. Am. Chem. Soc.* **2006**, *128*, 1086-1087.

(62)   Uraguchi, D.; Terada, M. *J. Am. Chem. Soc.* **2004**, *126*, 5356-5357.

(63)   Akiyama, T.; Itoh, J.; Yokota, K.; Fuchibe, K. *Angew. Chem. Int. Ed.* **2004**, *43*, 1566-1568.

(64)   Journet, M.; Cai, D.; DiMichele, L. M.; Larsen, R. D. *Tetrahedron Lett.* **1998**, *39*, 6427-6428.

(65)   Penner, M.; Rauniyar, V.; Kaspar, L. T.; Hall, D. G. *J. Am. Chem. Soc.* **2009**, *131*, 14216-14217.

(66)   Rauniyar, V. Ph.D. Thesis, 2009.

Chapter 4- Conclusions and Future Outlook

In summary, the work presented in this thesis has been directed towards the asymmetric formation of propargylic alcohols. Prior to this research, minimal work had focused on the enantioselective synthesis of propargylic alcohols, even though they are found to be prevalent in natural products. Two divergent methodologies to acquiring propargylic alcohols have been demonstrated. The first route applied the asymmetric addition of polyynes to aldehydes. In contrast, the second approach had the alkynyl unit as part of the aldehyde, where steps were taken to develop a catalytic asymmetric allylboration method for propargylic aldehydes.

When first investigating the alkynylation of aldehydes, the reaction conditions had only been studied for the monoyne addition, while the sole example of a diyne addition found in the literature had given modest results. In addition, no attempt had ever been demonstrated towards the triyne addition to aldehydes. In this project great strides were made as both the asymmetric addition of diynes and triynes gave high enantioselectivities (89–98% *ee*) and respectable yields (36–89%). Although the reaction with polyynes is found to be slower than the previously described monoyne addition, optimization decreased the typical reaction time from 72 h to 4 h while still maintaining high yields and enantioselectivities. As previously discussed, this protocol would be a more expedient route to the synthesis of natural products with this polyynol backbone than the current methodologies that exist. By circumventing the use of low

138

yielding tedious cross-coupling reactions, polyynol natural products could be synthesized in fewer steps and higher yields, while still maintaining high enantioselectivities.

Since lower yields were observed with the less stable triyne precursors, additional studies looked at a one-pot protocol where both the polyyne and the enantioselective propargylic alcohol are formed in a single step. Initial studies of this reaction have resulted in 88% *ee*. While a long list of possible optimization protocols are discussed in Chapter 2, including looking further into the effect of basicity and electronic properties of either the polyynol precursor or amino alcohol, only a small increase in enantioselectivity is needed in order to make this a viable expedient route in polyynol natural product syntheses.

Despite a strong focus on the catalytic enantioselective allylboration reaction recently, the allylboration of propargylic aldehydes has been elusive. When this research commenced, the only published example of a catalytic enantioselective allylboration of a propargylic aldehyde had produced a disappointing 12% *ee*. The efforts described within this thesis have increased the enantioselectivity for the allylboration of propargylic aldehydes to 83% *ee*, giving comparable enantioselectivities to the one-pot polyynol protocol. The factor that played the biggest role in this enantioselectivity increase was the switch from allylBpin to the similar neopentyl allyl boronate. When neopentyl allyl boronate is utilized, the uncatalyzed reaction is significantly slower to that of the catalyzed reaction, leading to higher enantioselectivities than the allylboration with

allylBpin. Although allylBpin is the most widely applied reagent for allylboration reactions, it is now postulated that maybe a better and more active allylboronate exists for the catalytic asymmetric allylboration process.

The work presented in this thesis shows that substantial progress has been made on both areas of research. The asymmetric addition of polyynes to aldehydes is shown as a viable route to propargylic polyynol natural products. In both the allylboration and one-pot rearrangement/alkynylation methodologies described the enantioselectivities are only just shy of ideal. With further optimization these methodologies offer new opportunities to access propargylic alcohols in an enantioselective fashion. Once optimized, these protocols would be substantially more appealing as more direct routes than those currently applied today. As such, my contribution has stimulated continued efforts along these directions in the Tykwinski and Hall laboratories.

Chapter 5- Experimental Details for the Enantioselective Addition of Terminal Di– and Triynes to Aldehydes[†]

5.1 General experimental details:

All reactions were performed in standard, dry glassware under an inert atmosphere of N_2. Unless otherwise specified, reagents were purchased from commercial suppliers and used without further purification. Toluene was distilled from sodium/benzophenone ketyl, while hexanes and dichloromethane were distilled from CaH_2 immediately prior to use. Anh. $MgSO_4$ was used as the drying agent after aqueous work-up. $Zn(OTf)_2$ was dried in a Schlenk flask under vacuum (ca. 1 mmHg) for at least 12 h, while heating to 100 °C to remove any water. Cyclohexanecarboxaldehyde and isobutyraldehyde were dried over $CaSO_4$ and fractionally distilled directly before use, while pivalaldehyde and propionaldehyde were dried over $CaCl_2$ and fractionally distilled directly before use. Unless otherwise stated, trimethylsilyl-protected diynes and triynes were synthesized as previously reported[1,2] and the protecting group was removed immediately prior to use via General Procedure A. Evaporation and concentration *in vacuo* was done at H_2O-aspirator pressure. Column chromatography: *silica gel-60* (230-400 mesh). Thin Layer Chromatography (TLC): pre-coated plastic sheets

covered with 0.2 mm silica gel with fluorescent indicator UV 254 nm; visualization by UV light, KMnO$_4$ or anisaldehyde stain. IR spectra (cm^{-1}): *Nicolet Magna-IR 750* (cast film or neat). ^{1}H, ^{19}F and ^{13}C NMR: *Varian Inova-300, 400* or *Varian Unity- 500* instruments, at 27 °C in CD$_2$Cl$_2$, CDCl$_3$, (CD$_3$)$_2$CO or CD$_3$CN; solvent peaks (5.32, 7.26, 2.05 and 1.96 ppm, respectively, for ^{1}H and 53.8, 77.0, 206.26/29.84 and 118.26/1.32 ppm, respectively, for ^{13}C) as reference. EI MS (*m/z*): *Kratos MS50* instrument. Optical rotation was recorded using a Perkin Elmer 241 Polarimeter using the sodium D line (589 nm) with a cell length of 10.002 cm. For simplicity, the coupling constants of the aryl protons for *para*-substituted phenyl groups have been reported as pseudo first-order, even though they are second-order spin systems. For mass spectral analyses, low resolution data is provided in cases when M$^+$ is not the base peak; otherwise, only high resolution data is provided. Optical purities of the products were measured by chiral HPLC using either a Chiralcel OD or Chiralpak AS column or by formation of the Mosher ester and subsequent ^{1}H or ^{19}F NMR analysis of the product along with the racemic product.[3-6] Procedures for the synthesis of compounds **2.18a**,[1] **2.18b**,[7] **2.18c**,[8] **2.18d**,[1] **2.18e**,[7] **2.18f**,[9,10] **2.18h**,[11] **2.19a**,[1] and **2.19c**[12] have been reported. All racemic mixtures unless otherwise specified were synthesized in accordance with General Procedure B.

5.2   General procedures

5.2.1   A: Removal of trimethylsilyl groups.

Unless otherwise noted, the following procedure was followed. To the appropriate silyl protected diyne or triyne (0.65 mmol) in a solution of wet MeOH/THF (5 mL, 4:1 v/v) was added K_2CO_3 (6 mg, 0.04 mmol), and the mixture stirred at rt until TLC analysis no longer showed the presence of the starting material, ca. 0.5–1.5 h. Et_2O (30 mL) and saturated aq. NH_4Cl (30 mL) were added, the organic layer separated, washed with saturated aq. NH_4Cl (2 × 30 mL), dried over $MgSO_4$, filtered, and the solvent volume reduced *in vacuo* to ca. 5 mL. Toluene (0.5 mL) was added and the remainder of the Et_2O was then removed *in vacuo*. The terminal diyne/triyne in toluene solvent was then added directly into the asymmetric addition reaction.

5.2.2   B: Synthesis of racemic propargylic alcohols

Unless otherwise specified the following procedure was used for the synthesis of the racemic compounds. Following the General Procedure A, the appropriate diyne or triyne (1 equiv) in 1 mL of toluene was combined with 50 mL of Hexanes. The reaction was cooled to −78 °C and *n*-BuLi (2.5 M in hexanes, 1.2 equiv) was added. The reaction stirred and was slowly warmed to −20 °C over 0.5 h. The solution was cooled back down to −78 °C and the corresponding aldehyde (1 equiv) was added. The resulting reaction stirred while slowly warming to 0 °C over 1–2 h, until complete by TLC analysis. The reaction was quenched via the addition of saturated aq. NH_4Cl (20 mL) and extracted with

Et$_2$O (30 mL). The organic layer was further washed with saturated aq. NH$_4$Cl (2 × 20 mL), dried over MgSO$_4$, filtered, and the solvent removed *in vacuo*. Unless otherwise specified, column chromatography (silica gel, hexanes/EtOAc 10:1) gave the corresponding racemic propargylic alcohol diyne or triyne in (30–90% yield).

5.2.3   C: Asymmetric diyne and triyne addition to aldehydes.

Zn(OTf)$_2$ (0.90 mmol, 1.6 equiv) and *N*-methylephedrine (0.65 mmol, 1.2 equiv) were charged under N$_2$ for 10 min in an 10 mL round bottom flask. Toluene (1 mL) and Et$_3$N (90 μL, 0.65 mmol, 1.2 equiv) were then added. The mixture was stirred for 2 h at rt, followed by the addition of the terminal diyne/triyne (0.60 mmol, 1.1 equiv) in toluene (0.5 mL). The flask containing the diyne was then washed with additional toluene (0.5 mL), which was added to the reaction flask. The reaction was stirred for 20 min and freshly purified aldehyde (0.55 mmol, 1.0 equiv) was added. The reaction was stirred at rt until deemed complete by TLC analysis. The reaction was quenched via the addition of saturated aq. NH$_4$Cl (3 mL) and extracted with Et$_2$O (30 mL). The aqueous layer was further extracted with Et$_2$O (4 × 30 mL). The combined organic phase was dried over MgSO$_4$, filtered, and the solvent removed *in vacuo*. Unless otherwise stated, column chromatography (silica gel, hexanes/EtOAc 5:1) afforded the product.

5.2.4 D: Reaction of di- and triynes with benzyl azide.

A mixture of the appropriate triisopropylsilyl-protected polyyne and TBAF (2.0 equiv) in THF (5 mL) was combined and stirred at 0 °C until TLC analysis showed complete conversion to the terminal alkyne. Et_2O (25 mL) and saturated aq. NH_4Cl (25 mL) were added, the organic phase was separated, washed with saturated aq. NH_4Cl (2 × 10 mL), saturated aq. NaCl (10 mL), and then dried over $MgSO_4$. DMF (1 mL) was then added, the solution was filtered and then concentrated to 1–2 mL via rotary evaporation. To the mixture above, DMF (10 mL) was added, followed by benzyl azide (1.0 equiv based on the starting silylated polyyne), $CuSO_4 \cdot 5H_2O$ (0.1 g), ascorbic acid (0.1 g), and H_2O (2 mL). This mixture was then stirred at rt until TLC analysis no longer showed the presence of the terminal alkyne. Saturated aq. NH_4Cl (10 mL) and Et_2O (10 mL) were added, the organic phase was separated, washed with saturated aq. NaCl (2 × 10 mL), and dried over $MgSO_4$. The mixture was then filtered and the solvent removed *in vacuo*. Purification via column chromatography gave the pure product.

5.2.5 E: Mosher ester formation[3-6]

The corresponding alcohol was added to CH_2Cl_2 (1 mL) along with either the (*R*)- or (*S*)-Mosher acid chloride (1.5 equiv), DMAP (1.0 equiv), and Et_3N (5.0 equiv). When the reaction was judged to be complete by TLC analysis, diisopropylethylamine (0.2 mL) was added and the mixture passed through a one-inch silica column (in a 9" pipette eluting with 30% EtOAc/hexanes). The mixture

145

was analyzed by ^{19}F and/or ^{1}H NMR spectroscopy to determine the diastereomeric ratio.

5.3   Preparation of terminal polyynes

5.3.1   [3-(Dibromomethylene)-1-decynyl]trimethylsilane (2.14g)

Thionyl chloride (17 g, 0.14 mol) was added to octanoic acid (2.50 g, 17.5 mmol) in a dry flask protected from moisture with a drying tube containing $CaCl_2$, and the mixture was stirred at rt for 24 h. The excess thionyl chloride was removed *in vacuo* to provide the acid chloride. CH_2Cl_2 (100 mL) was added and the temperature of the solution was lowered to 0 ˚C. Bis(trimethylsilyl)acetylene (3.00 g, 17.6 mmol) and $AlCl_3$ (2.7 g, 20 mmol) were added and the reaction mixture warmed to rt over 3 h. The reaction was carefully quenched by the addition of the reaction mixture to 10% HCl (50 mL) in 10 g of ice. The organic layer was separated, washed with saturated aq. $NaHCO_3$ (50 mL), NaCl (50 mL), dried over $MgSO_4$, filtered, and the solvent removed *in vacuo*. The crude ketone was carried on to the next step.

CBr_4 (6.6 g, 20 mmol) and PPh_3 (11 g, 42 mmol) were added to CH_2Cl_2 (125 mL) and allowed to stir for 5 min at rt. The crude ketone in 10 mL CH_2Cl_2 was slowly added to the mixture over 10 min and the progress of the reaction was then monitored by TLC analysis until the ketone was no longer observed (ca. 30 min). Solvent was reduced to ca. 10 mL, hexanes added (125 mL), the inhomogeneous mixture filtered through a silica gel plug with hexanes, and

146

solvent removed *in vacuo* to yield the desired product (4.7 g, 71% over 3 steps) as a yellow oil. R_f = 0.9 (hexanes/EtOAc 10:1). IR (neat): 2958 (s), 2928 (s), 2858 (s), 2153 (m-w), 1251 (m) cm^{-1}. ^{1}H NMR (400 MHz, CDCl$_3$) δ 2.31 (t, J = 7.6 Hz, 2H), 1.57 (quintet, J = 7.5 Hz, 2H), 1.33–1.29 (m, 8H), 0.9 (t, J = 6.9, 3H), 0.22 (s, 9H). ^{13}C NMR (100 MHz, CDCl$_3$) δ 131.3, 103.3, 102.9, 97.6, 36.9, 31.9, 29.2, 29.0, 27.6, 22.8, 14.3, –0.1. EIMS *m/z* 379.9 (M$^+$, 12), 137.0 ([C$_4$H$_9$Br]$^+$, 65) 73.0 ([Me$_3$Si]$^+$, 100).

5.3.2 Trimethyl-1,3-undecadiynylsilane (2.16g)

[3-(Dibromomethylene)-1-decynyl]-trimethylsilane (2.53 g, 6.64 mmol) was added to hexanes (50 mL) and cooled to –78 °C. *n*-BuLi (3.2 mL of 2.5 M *n*-BuLi in hexanes, 8.0 mmol, 1.2 equiv) was added and the reaction slowly warmed to 0 °C over 1 h. The reaction was quenched via the addition of saturated aq. NH$_4$Cl (20 mL) and extracted with Et$_2$O (30 mL). The organic phase was then washed with saturated aq. NH$_4$Cl (3 × 20 mL), dried (MgSO$_4$), filtered, and the solvent removed *in vacuo*. The crude product was passed through a plug of silica gel and column chromatography (silica gel, hexanes) gave **2.16g** (1.3 g, 90%) as a yellow oil. R_f = 0.85 (10:1 hexanes/EtOAc). IR (neat): 2958 (s), 2930 (s), 2858 (m), 2226 (m), 2109 (m), 1251 (m), 845 (s) cm^{-1}. ^{1}H NMR (400 MHz, CDCl$_3$) δ 2.26 (t, J = 7.0 Hz, 2H), 1.52 (app. quintet, J = 7.3 Hz, 2H), 1.41–1.26 (m, 8H), 0.88 (t, J = 6.9 Hz, 3H), 0.18 (s, 9H). ^{13}C NMR (100 MHz, CDCl$_3$) δ 88.6, 83.1, 80.4, 65.6, 31.8, 29.0, 28.9, 28.3, 22.8, 19.4, 14.2, –0.2. EIMS m/z 220.2 (M$^+$, 1), 205.1 ([M – Me]$^+$, 100). EI HRMS calcd. for C$_{14}$H$_{24}$Si (M$^+$) 220.1647, found

220.1645.

5.3.3 [5-(Dibromomethylene)-1,4-nonadecadiynyl]trimethylsilane (2.15b)

This compound was formed in the same manner as [3-(dibromomethylene)-1-decynyl]trimethylsilane above, using myristic acid and bis(trimethylsilyl)acetylene. R_f = 0.83 (10:1 hexanes/EtOAc). IR (neat): 2957 (m), 2925 (s), 2854 (s), 2225 (w), 2156 (w) cm^{-1}. ^{1}H NMR (500 MHz, CDCl$_3$) δ 2.33 (t, J = 7.0 Hz, 2H), 1.72–1.57 (m, 4H), 1.54–1.10 (m, 20H), 0.91–0.70 (m, 3H), 0.22 (s, 9H). ^{13}C NMR (125 MHz, acetone d$_6$) δ 115.4, 108.5, 102.5, 101.5, 99.6, 78.2, 32.7, 28.8, 23.4, 19.9, 14.4, –0.4. EIMS m/z 504.1 (M$^+$, 3), 502.1 (M$^+$, 5), 500.1 (M$^+$, 3), 73.0 ([Me$_3$Si]$^+$, 100). EI HRMS calcd. for C$_{23}$H$_{38}$^{81}Br$_2$Si (M$^+$) 504.1069, found 504.1068. Calcd. for C$_{23}$H$_{38}$^{79}Br^{81}BrSi 502.1089, found 502.1090. Calcd. for C$_{23}$H$_{38}$^{79}Br$_2$Si 500.1110, found 500.1104.

5.3.4 Trimethyl-1,3,5-eicosyltriynylsilane (2.17b)

[5-(Dibromomethylene)-1,4-nonadecadiynyl]-trimethylsilane (0.83 g, 1.7 mmol) was added to hexanes (50 mL), cooled to –78 °C. n-BuLi (0.8 mL of 2.5 M n-BuLi in hexanes, 2.0 mmol, 1.2 equiv) was added and the reaction slowly warmed to 0 °C over 1 h. The reaction was quenched via the addition of saturated aq. NH$_4$Cl (20 mL) and extracted with Et$_2$O (30 mL). The organic phase was then washed with saturated aq. NH$_4$Cl (3 × 20 mL), dried (MgSO$_4$), filtered, and the solvent removed *in vacuo*. The crude product was passed through a plug of silica gel, and column chromatography (silica gel, hexanes) gave **2.17b** (0.5 g, 88%) as

a yellow-brown oil. $R_f = 0.85$ (10:1 hexanes/EtOAc). IR (film cast, CHCl$_3$): 2957 (m), 2925 (m), 2854 (m), 2212 (m), 2167 (w), 2080 (m) cm^{-1}. ^{1}H NMR (400 MHz, CDCl$_3$) δ 2.30 (t, $J = 7.2$ Hz, 2H), 1.54 (quintet, $J = 7.2$ Hz, 2H), 1.40–1.22 (m, 22H), 0.89 (t, $J = 6.6$ Hz, 3H) 0.20 (s, 9H). ^{13}C NMR (100 MHz, CDCl$_3$) δ 88.4, 85.3, 81.0, 65.5, 62.6, 59.9, 31.9, 29.69, 29.66, 29.6, 29.44, 26.36, 29.0, 28.8, 28.0, 22.7, 19.4, 14.1, –0.5 (two signals coincident or not observed). EIMS m/z 342.3 (M$^+$, 2), 327.2 ([M – Me]$^+$, 9), 73.0 ([Me$_3$Si]$^+$, 100). EI HRMS calcd for C$_{23}$H$_{38}$Si (M$^+$) 342.2743, found 342.2741.

5.4 Synthesis of polyynol products

5.4.1 (3S)-(+)-7-(4-*tert*-Butylphenyl)-2,2-dimethylhepta-4,6-diyn-3-ol ((3S)-(+)-2.23)

2.23
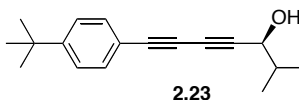
(Table 2.1, entry 1). Compound **2.18a** (130 mg, 0.70 mmol, 1.2 equiv) was combined with Zn(OTf)$_2$ (254 mg, 0.699 mmol, 1.2 equiv), (−)-N-methylephedrine (118 mg, 0.658 mmol, 1.1 equiv), Et$_3$N (91 µL, 0.65 mmol, 1.1 equiv) and isobutyraldehyde (55 µL, 43 mg, 0.60 mmol, 1.0 equiv) in toluene (1 mL) as per the general procedure for 72 h to yield (S)-(+)-**2.23** (136 mg, 89%) as a pale yellow waxy oil. A 95% ee was determined by HPLC analysis (Chiralcel OD column, 1% i-PrOH in hexanes, 0.5 mL/min λ = 254 nm, column temperature 10 °C) T$_{major}$ = 38.1 min, T$_{minor}$ = 41.7 min. [α]$^{22}_D$ = 3.53 (c = 1.00, CHCl$_3$).

149

5.4.2 (3R)-(–)-7-(4-*tert*-Butylphenyl)-2,2-dimethylhepta-4,6-diyn-3-ol ((R)-(–)-2.23)

2.23
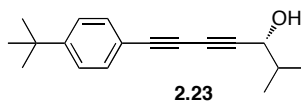
The other enantiomer, (Table 2.1, entry 2), was synthesized from **2.18a** (109 mg, 0.598 mmol, 1.2 equiv), $Zn(OTf)_2$ (390 mg, 1.1 mmol, 2.2 equiv), (+)-*N*-methylephedrine (110 mg, 0.61 mmol, 1.2 equiv), Et_3N (84 µL, 61 mg, 0.60 mmol, 1.2 equiv) and isobutyraldehyde (46 µL, 36 mg, 0.50 mmol, 1.0 equiv) in toluene (1 mL) as per the general procedure for 36 h to yield (R)-(–)-**2.23** (105 mg, 83%) as a pale yellow waxy oil in 94% *ee*. $[\alpha]^{22}_D = -4.05$ (c = 1.12, $CHCl_3$). $R_f = 0.33$ (hexanes/EtOAc 5:1). IR (film cast, $CHCl_3$): 3352 (m, broad), 3086 (w), 3038 (w), 2964 (s), 2905 (s), 2872 (s), 2239 (m), 1604 (w), 1024 (s) cm^{-1}. ^{1}H NMR (400 MHz, $CDCl_3$) δ 7.44 (d, J = 8.5 Hz, 2H), 7.34 (d, J = 8.5 Hz, 2H), 4.31 (t, J = 5.8 Hz, 1H), 1.95 (app. octet, J = 6.6, 1H), 1.83 (d, J = 5.9, 1H) 1.32 (s, 9H), 1.06 (d, J = 6.7 Hz, 3H), 1.04 (d, J = 6.8 Hz, 3H). ^{13}C NMR (100 MHz, $CDCl_3$) δ 152.7, 132.3, 125.4, 118.4, 82.0, 78.6, 72.7, 70.4, 68.5, 34.9, 34.7, 31.1, 18.1, 17.5. EIMS *m/z* 254.2 (M$^+$, 38), 211.1 ([M$^+$ – *i*-Pr]$^+$, 100). EI HRMS calcd. for $C_{18}H_{22}O$ (M$^+$) 254.1671, found 254.1671.

5.4.3 (1S)-(+)-5-(4-*tert*-Butylphenyl)-1-cyclohexylpenta-2,4-diyn-1-ol ((S)-(+)-2.24)

2.24

150
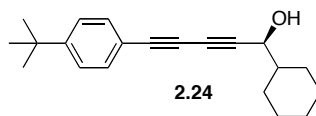
(Table 2.1, entry 3). Compound **2.18a** (158 mg, 0.867 mmol, 1.2 equiv) was combined with Zn(OTf)$_2$ (371 mg, 1.02 mmol, 1.4 equiv), (–)-*N*-methylephedrine (160 mg, 0.89 mmol, 1.3 equiv), Et$_3$N (120 μL, 89 mg, 0.88 mmol, 1.3 equiv), and cyclohexanecarboxaldehyde (85 μL, 79 mg, 0.70 mmol, 1.0 equiv) in toluene (1 mL) as per the general procedure for 80 h to yield (*S*)-(+)-**2.24** (150 mg, 73%) as a yellow oil. A 90% *ee* was determined by ^{19}F NMR analysis of the corresponding ester derived from (*S*)-MTPA chloride (–72.92 ppm (major), –71.91 ppm (minor)). $[\alpha]^{22}_D$ = 11.8 (c = 1.00, CHCl$_3$). R_f = 0.4 (CH$_2$Cl$_2$/hexanes 2:1). IR (film cast, CHCl$_3$): 3346 (m, broad), 3086 (w), 3037 (w), 2928 (s), 2854 (s), 2236 (w), 1604 (w), 1503 (m), 1016 (s) cm^{-1}. ^{1}H NMR (300 MHz, CDCl$_3$) δ 7.43 (d, *J* = 8.5 Hz, 2H), 7.34 (d, *J* = 8.5 Hz, 2H), 4.31 (t, *J* = 5.3 Hz, 1H), 2.10 (d, 4.7 Hz, 1H), 1.95–1.85 (m, 2H), 1.82–1.78 (m, 2H), 1.71–1.59 (m, 2H), 1.32–1.09 (m, 14H). ^{13}C NMR (125 MHz, CDCl$_3$) δ 152.9, 132.5, 125.6, 118.6, 82.4, 78.8, 72.8, 70.7, 68.0, 44.4, 35.1, 31.2, 28.7, 28.3, 26.4, 25.82, 25.86. EIMS *m/z* 294.2 (M$^+$, 21), 211.1 ([M – C$_6$H$_{11}$]$^+$, 100). EI HRMS calcd. for C$_{21}$H$_{26}$O (M$^+$) 294.1984, found 294.1985.

### 5.4.4   (3*R*)-(–)-7-(4-*tert*-Butylphenyl)-2,2-dimethylhepta-4,6-diyn-3-ol ((R)-(–)-2.25)

2.25
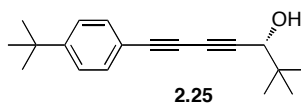
(Table 2.1, entry 4). Compound **2.18a** (97 mg, 0.52 mmol, 1.1 equiv) was combined with Zn(OTf)$_2$ (231 mg, 0.635 mmol, 1.3 equiv), (+)-*N*-

methylephedrine (122 mg, 0.681 mmol, 1.4 equiv), Et$_3$N (83 μL, 60 mg, 0.59

mmol, 1.2 equiv), and pivalaldehyde (53 μL, 42 mg, 0.49 mmol, 1.0 equiv) in

toluene (1 mL) as per the general procedure for 1 week to yield (*R*)-(–)-**2.25** (43

mg, 33%) as a beige waxy solid. A 90% *ee* was determined by HPLC analysis

(Chiralcel OD column, 5% *i*-PrOH in hexanes, 0.5 mL/min, λ = 254 nm, column

temperature = 25 °C) T$_{major}$ = 11.4 min, T$_{minor}$ = 10.3 min. [α]$^{22}_D$ = –5.2 (c = 0.39,

CHCl$_3$).

5.4.5   (3*S*)-(+)-7-(4-*tert*-Butylphenyl)-2,2-dimethylhepta-4,6-diyn-3-ol (2.25)

2.25
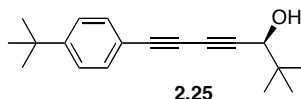
The other enantiomer (*S*)-(+)-**2.25** (Table 2.1, entry 5) was synthesized

from **2.18a** (93 mg, 0.51 mmol, 1.3 equiv), Zn(OTf)$_2$ (220 mg, 0.61 mmol, 1.6

equiv), (–)-*N*-methylephedrine (86 mg, 0.48 mmol, 1.2 equiv), Et$_3$N (66 μL, 48

mg, 0.47 mmol, 1.2 equiv), and pivalaldehyde (43 μL, 34 mg, 0.39 mmol, 1.0

equiv) in toluene (1 mL) as per the general procedure for 1 week to give (*S*)-(+)-

2.25 (38 mg, 37%) as a beige waxy solid in 90% *ee*. [α]$^{22}_D$ = 3.9 (c = 0.21,

CHCl$_3$). R_f = 0.5 (hexanes/EtOAc 5:1). IR (film cast, CHCl$_3$): 3398 (m, broad),

3037 (w), 2963 (s), 2930 (s), 2869 (m), 2244 (w) cm^{-1}. ^{1}H NMR (400 MHz,

CDCl$_3$) δ 7.44 (d, *J* = 8.4 Hz, 2H), 7.35 (d, *J* = 8.4 Hz, 2H), 4.15 (d, *J* = 5.7 Hz,

1H), 1.80 (d, *J* = 6.1 Hz, 1H), 1.31 (s, 9H), 1.04 (s, 9H). ^{13}C NMR (125 MHz,

CDCl$_3$) δ 152.7, 132.3, 125.5, 118.4, 82.0, 78.5, 72.7, 72.0, 70.6, 36.4, 34.9, 31.1,

25.3. EIMS m/z 268.2 (M$^+$, 20), 253.2 ([M – Me]$^+$, 15), 211.1 ([M – t-Bu]$^+$, 100).

EI HRMS calcd. for $C_{19}H_{24}O$ (M$^+$) 268.1827, found 268.1826.

5.4.6   (3S)-(–)-7-(4-$tert$-Butylphenyl)hetpa-4,6-diyn-3-ol ((S)-(–)-2.26)

2.26
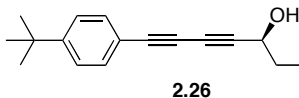
(Table 2.1, entry 6). Compound **2.18a** (181 mg, 0.993 mmol, 1.3 equiv) was combined with Zn(OTf)$_2$ (430 mg, 1.2 mmol, 1.5 equiv), (–)-N-methylephedrine (190 mg, 1.1 mmol, 1.3 equiv), Et$_3$N (140 μL, 1.0 mmol, 1.1 equiv) and propionaldehyde (57 μL, 46 mg, 0.79 mmol, 1.0 equiv) in toluene (1 mL) as per the general procedure for 68 h to give (S)-(–)-**2.26** (86 mg, 45%) as an off white-yellow waxy solid. A 64% ee was determined by ^{19}F NMR analysis of the corresponding ester derived from (R)-MTPA chloride (–71.99 ppm (major), –72.31 ppm (minor)). $[\alpha]^{22}_D$ = –0.99 (c = 0.24, CHCl$_3$). R_f = 0.6 (CH$_2$Cl$_2$). IR (film cast, CHCl$_3$): 3347 (m, broad), 3086 (w), 3038 (w), 2966 (s), 2906 (m), 2873 (m), 2239 (m), 1603 (w) cm^{-1}. ^{1}H NMR (400 MHz, CHCl$_3$) δ 7.43 (d, J = 8.6 Hz, 2H), 7.34 (d, J = 8.5 Hz, 2H), 4.46 (dd, J = 12.2, 6.3 Hz, 1H), 1.84 (d, J = 5.8, 1H), 1.82–1.76 (m, 2H), 1.31 (s, 9H), 1.06 (t, J = 7.4 Hz, 3H). ^{13}C NMR (125 MHz, CHCl$_3$) δ 152.8, 132.3, 125.5, 118.4, 82.8, 78.8, 72.6, 69.8, 64.3, 34.9, 31.1, 30.7, 9.4. EIMS m/z 240.2 (M$^+$, 42), 225.1 ([M – Me]$^+$, 52), 211.1 ([M – Et]$^+$, 100). EI HRMS calcd. for $C_{17}H_{20}O$ (M$^+$) 240.1514, found 240.1516.

5.4.7 (6*E*)-1-(4-*tert*-Butylphenyl)-8-methylnon-6-ene-1,3-diyn-5-ol (2.27) and 1-(4-*tert*-Butylphenyl)-8-methylnon-7-ene-1,3-diyn-5-ol (2.28)
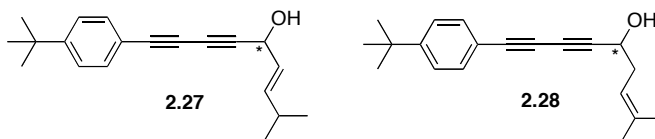
Compound **2.18a** (56 mg, 0.31 mmol, 1.3 equiv) was combined with Zn(OTf)$_2$ (189 mg, 0.520 mmol, 2.2 equiv), (+)-*N*-methylephedrine (70 mg, 0.39 mmol, 1.6 equiv), Et$_3$N (42 μL, 30 mg, 0.30 mmol, 1.3 equiv), and (*E*)-4-methylpent-2-enal (24 mg, 0.24 mmol, 1.0 equiv) in toluene (1 mL) as per the general procedure for 56 h. After column chromatography (silica gel, 10:1 hexanes/EtOAc, and then 2:1 hexanes/CH$_2$Cl$_2$) gave an inseparable mixture of **2.27** and **2.28** (7 mg, 10%) as a yellow oil. ^{1}H NMR (400 MHz, CDCl$_3$) δ 7.43–7.32 (m, 8H), 5.90 (ddd, *J* = 15.6, 5.6, 1.2 Hz, 1H), 5.57 (ddd, *J* = 15.6, 5.6, 1.2 Hz, 1H), 5.28 (triplet of quintet, *J* = 7.6, 1.2 Hz, 2H), 4.96 (t, *J* = 6 Hz, 1H), 4.50 (q, *J* = 6 Hz, 2H), 2.55–2.44 (m, 2H), 2.38–2.31 (m, 1H), 1.77 (s, 3H), 1.68 (s, 3H), 1.31 (s, 18H), 0.89 (d, *J* = 6.4 Hz, 3H), 0.88 (d, *J* = 7.2 Hz, 3H).

5.4.8 (3*R*)-(−)-2-Methyl-7-phenylhepta-4,6-diyn-3-ol ((*R*)-(−)-2.29)
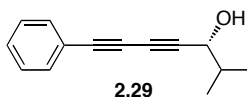
Compound **2.18b** (88 mg, 0.70 mmol, 1.4 equiv) was combined with Zn(OTf)$_2$ (363 mg, 1.00 mmol, 2.0 equiv), (+)-*N*-methylephedrine (134 mg, 0.748 mmol, 1.5 equiv), Et$_3$N (98 μL, 71 mg, 0.70 mmol, 1.4 equiv) and

154

isobutyraldehyde (46 μL, 36 mg, 0.50 mmol, 1.0 equiv) in toluene (1 mL) as per the general procedure for 48 h to yield (*R*)-(–)-**2.29** (87 mg, 88%) as a yellow waxy thick oil. A 92% *ee* was determined by HPLC analysis (Chiralcel OD column, 50% *i*-PrOH in hexanes, 0.5 mL/min, λ = 254 nm, column temperature = 25 °C) T_{major} = 9.0 min, T_{minor} = 9.8 min. $[\alpha]^{22}_D$ = –3.68 (c = 1.00, CHCl$_3$). R_f = 0.3 (hexanes/EtOAc 5:1). IR (film cast, CHCl$_3$): 3442 (s, broad), 3081 (w), 3064 (w), 2964 (s), 2930 (m), 2873 (m), 2242 (w), 1569 (w), 1025 (s) cm^{-1}. ^{1}H NMR (400 MHz, CDCl$_3$) δ 7.52–7.49 (m, 2H), 7.39–7.30 (m, 3H), 4.32 (t, *J* = 5.8 Hz, 1H), 1.96 (app. octet, *J* = 6.6 Hz, 1H), 1.86 (d, *J* = 5.9 Hz, 1H), 1.06 (d, *J* = 6.7 Hz, 3H), 1.04 (d, *J* = 6.8 Hz, 3H). ^{13}C NMR (100 MHz, CDCl$_3$) δ 132.7, 129.4, 128.6, 121.7, 82.5, 78.4, 73.4, 70.4, 68.7, 34.8, 18.2, 17.7. EIMS *m/z* 198.1 (M$^+$, 17), 155.0 ([M$^+$ – *i*-Pr]$^+$, 100). EI HRMS calcd. for C$_{14}$H$_{14}$O (M$^+$) 198.1045, found 198.1045.

5.4.9 (1*S*)-(+)-1-Cyclohexyl-5-[4-(octyloxy)phenyl]penta-2,4-diyn-1-ol ((*S*)-(+)-2.30)
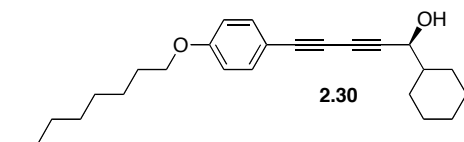
Compound **2.18c** (153 mg, 0.601 mmol, 1.2 equiv) was combined with Zn(OTf)$_2$ (298 mg, 0.820 mmol, 1.6 equiv), (–)-*N*-methylephedrine (110 mg, 0.63 mmol, 1.3 equiv), Et$_3$N (84 μL, 61 mg, 0.60 mmol, 1.2 equiv) and cyclohexanecarboxaldehyde (56 mg, 0.50 mmol, 1.0 equiv) in toluene (1 mL) as

per the general procedure for 74 h to yield (*S*)-(+)-**2.30** (150 mg, 82%) as a pale yellow waxy oil. A 97% *ee* was determined by ^{19}F NMR analysis of the corresponding ester derived from (*R*)-MTPA chloride (–71.89 ppm (major), –72.27 ppm (minor)). $[\alpha]^{22}_D$ = 9.5 (c = 0.76, CHCl$_3$). R_f = 0.2 (hexanes/EtOAc 10:1). IR (film cast, CHCl$_3$): 3372 (m), 2927 (s), 2854 (s), 2237 (m), 1603 (s), 1567 (w), 1509 (s), 1251 (s) cm^{-1}. ^{1}H NMR (500 MHz, CDCl$_3$) δ 7.42 (d, *J* = 8.9 Hz, 2H), 6.83 (d, *J* = 8.9 Hz, 2H), 4.30 (t, *J* = 6.0 Hz, 1H), 3.96 (t, *J* = 6.6 Hz, 1H), 1.89 (bd, *J* = 12.7 Hz, 2H), 1.82–1.72 (m, 5H), 1.72–1.56 (m, 2H), 1.49–1.42 (m, 2H), 1.39–1.08 (m, 14H), 0.90 (t, *J* = 7.0 Hz, 3H). ^{13}C NMR (125 MHz, CDCl$_3$) δ 160.2, 134.3, 114.8, 113.3, 82.2, 78.9, 72.2, 70.8, 68.3, 68.0, 44.4, 31.9, 29.5, 29.4, 29.3, 28.7, 28.3, 26.4, 26.1, 26.01, 25.99, 22.8, 14.2. EIMS *m/z* 366.3 (M$^+$, 34), 283.2 ([M – C$_6$H$_{11}$]$^+$, 64), 55 (C$_4$H$_7$$^+$, 100). EI HRMS calcd. for C$_{25}$H$_{34}$O$_2$ (M$^+$) 366.2559, found 366.2566.

5.4.10 (3*S*)-(+)-7-(4-Methoxyphenyl)-2-methylhepta-4,6-diyn-3-ol ((*S*)-(+)-2.31)

2.31
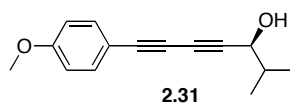
Compound **2.18d** (132 mg, 0.709 mmol, 1.1 equiv) was combined with Zn(OTf)$_2$ (406 mg, 1.12 mmol, 1.7 equiv), (–)-*N*-methylephedrine (129 mg, 0.720 mmol, 1.1 equiv), Et$_3$N (110 µL, 77 mg, 0.76 mmol, 1.2 equiv) isobutyraldehyde (59 µL, 47 mg, 0.65 mmol, 1.0 equiv) in toluene (1 mL) as per the general procedure for 48 h to yield (*S*)-(+)-**2.31** (138 mg, 93%) as a pale yellow waxy

solid. A 98% *ee* was determined by HPLC analysis (Chiralcel OD column, 5% *i*-PrOH in hexanes, 0.5 mL/min, λ = 254 nm, column temperature = 25 °C) T_{major} = 42.6 min, T_{minor} = 49.4 min. $[\alpha]^{22}_D$ = 2.5 (c = 0.90, CHCl$_3$). R_f = 0.3 (hexanes/EtOAc 5:1). IR (film cast, CHCl$_3$): 3386 (m, broad), 2963 (s), 2933 (m), 2873 (m), 2839 (m), 2237 (m), 1604 (s), 1567 (w), 1510 (s) cm^{-1}. ^{1}H NMR (400 MHz, CDCl$_3$) δ 7.44 (d, *J* = 8.9 Hz, 2H), 6.84 (d, *J* = 8.9 Hz, 2H), 4.31 (d, *J* = 5.7 Hz, 1H), 3.82 (s, 3H), 1.94 (app. octet, *J* = 6.4 Hz, 2H), 1.88 (bs, 1H), 1.06 (d, *J* = 6.8 Hz, 3H), 1.04 (d, *J* = 6.8 Hz, 3H). ^{13}C NMR (100 MHz, CDCl$_3$) δ 160.4, 134.2, 114.1, 113.4, 81.8, 78.5, 72.1, 70.5, 68.6, 55.3, 34.8, 18.1, 17.6. EIMS *m/z* 288.1 (M$^+$, 37), 185.1 ([M − *i*-Pr]$^+$, 100). EI HRMS calcd. for C$_{15}$H$_{16}$O$_2$ (M$^+$) 228.1150, found 228.1153.

Single crystals for **2.31** suitable for X-ray crystallographic analysis were grown by slow evaporation of Et$_2$O at room temperature. X-ray crystallographic data for 7-(4-methoxyphenyl)-2-methylhepta-4,6-diyn-3-ol (**2.31**): C$_{15}$H$_{16}$O$_2$, *Mw* = 228.28; crystal dimensions 0.58 ´ 0.53 ´ 0.26 mm; crystal system: orthorhombic; space group $P2_12_12_1$ (No. 19); *a* = 5.08550(10) Å, *b* = 9.6271(3) Å, *c* = 25.6576(7) Å^3; *V* = 1256.16(6) Å^3; *Z* = 4; ρ_{calcd} = 1.207 g cm^{-3}; μ = 0.079 mm^{-1}; λ = 0.71073 Å; T = −100 °C; $2\theta_{max}$ = 55.06°; total data collected = 11130; R_1 = 0.0312 for 1683 observed reflections with [$F_o^2 \geq 2\sigma(F_o^2)$]; wR_2 = 0.0872 for 155 variables and all 1721 unique reflections; residual electron density = 0.199 and −0.158 e Å^{-3}. CCDC 818624.

5.4.11 (3R)-(−)-2-Methylundeca-4,6-diyn-3-ol ((R)-(−)-2.32)
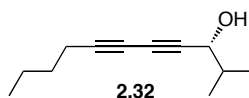
Compound **2.18e** (53 mg, 0.50 mmol, 1.3 equiv) was combined with Zn(OTf)$_2$ (348 mg, 0.957 mmol, 2.5 equiv), (+)-*N*-methylephedrine (132 mg, 0.736 mmol, 1.9 equiv), Et$_3$N (98 μL, 71 mg, 0.70 mmol, 1.8 equiv) and isobutyraldehyde (35 μL, 28 mg, 0.39 mmol, 1.0 equiv) in toluene (1 mL) as per the general procedure for 60 h to yield (*R*)-(−)-**2.32** (30 mg, 43%) as a yellow oil. An 88% *ee* was determined by ^{19}F NMR analysis of the corresponding ester derived from (*R*)-MTPA chloride (−72.34 ppm (major), −71.97 ppm (minor)). $[\alpha]^{22}_D$ = −3.5 (c = 0.87, CHCl$_3$). R_f = 0.4 (hexanes/EtOAc 5:1). IR (film cast, CHCl$_3$): 3354 (m, broad), 2961 (s), 2934 (s), 2874 (m), 2254 (m), 1467 (m) cm^{-1}. ^{1}H NMR (400 MHz, CDCl$_3$) δ 4.21 (d, *J* = 5.7 Hz, 1H), 2.29 (dt, *J* = 7.0, 0.9, 2H), 1.95–1.83 (m, 2H), 1.56–1.37 (m, 4H), 1.01 (d, *J* = 6.8 Hz, 3H), 0.99 (d, *J* = 6.8 Hz, 3H), 0.91 (t, *J* = 7.3 Hz, 3H). ^{13}C NMR (100 MHz, CDCl$_3$) δ 81.4, 75.3, 70.6, 68.3, 64.4, 34.6, 30.2, 21.9, 18.9, 18.0, 17.4, 13.2. EIMS *m/z* 178.1 (M$^+$, 4), 149.1 ([M − Et]$^+$, 6), 135.1 ([M − *i*-Pr]$^+$, 100). EI HRMS calcd. for C$_{12}$H$_{18}$O (M$^+$) 178.1358, found 178.1362.

### 5.4.12 (3*S*)-(+)-2-Methyltrideca-4,6-diyn-3-ol ((*S*)-(+)-2.33)

2.33
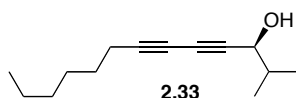
Compound **2.18f** (92 mg, 0.76 mmol, 1.2 equiv) was combined with Zn(OTf)$_2$ (312 mg, 0.858 mmol, 1.3 equiv), (−)-*N*-methylephedrine (125 mg, 0.700 mmol, 1.1 equiv), Et$_3$N (110 μL, 77 mg, 0.76 mmol, 1.2 equiv), and isobutyraldehyde (59 μL, 47 mg, 0.65 mmol, 1.0 equiv) in toluene (1 mL) as per the general procedure for 60 h to yield (*S*)-(+)-**2.33** (87 mg, 65%) as a yellow liquid. An 93% *ee* was determined by ^{19}F NMR analysis of the corresponding ester derived from (*R*)-MTPA chloride (−71.98 ppm (major), −72.35 ppm (minor)). [α]^{22}$_D$ = 4.2 (c = 0.25, CHCl$_3$). R_f = 0.4 (hexanes/EtOAc 5:1). IR (film cast, CHCl$_3$): 3361 (m, broad), 2960 (s), 2932 (s), 2872 (m), 2860 (m), 2254 (m) 1028 (m) cm^{-1}. ^{1}H NMR (400 MHz, CDCl$_3$) δ 4.21 (t, *J* = 5.6 Hz, 1H), 2.28 (td, *J* = 7.1, 0.9 Hz, 2H), 1.89 (app. octet, *J* = 6.9 Hz, 1H), 1.79 (d, *J* = 5.9 Hz, 1H), 1.53 (quintet, *J* = 7.3 Hz, 2H), 1.42–1.24 (m, 6H), 1.01 (d, *J* = 6.7, Hz, 3H), 0.99 (d, *J* = 6.8, Hz, 3H), 0.89 (t, *J* = 7.0 Hz, 3H). ^{13}C NMR (100 MHz, CDCl$_3$) δ 81.5, 75.3, 70.6, 68.4, 64.4, 34.7, 31.2, 28.5, 28.1, 22.5, 19.3, 18.0, 17.5, 14.0. EIMS *m/z* 206.2 (M$^+$, 2), 191.1 ([M − CH$_3$]$^+$, 4), 177.1 ([M − C$_2$H$_5$]$^+$, 6), 163.1 ([M − C$_3$H$_7$]$^+$, 100). EI HRMS calcd. for C$_{14}$H$_{22}$O (M$^+$) 206.1671, found 206.1665.

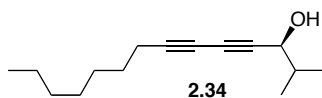### 5.4.13 (3*S*)-(+)-2-Methyltetradeca-4,6-diyn-3-ol ((*S*)-(+)-2.34)

2.34

159

Compound **2.18g** (82 mg, 0.55 mmol, 1.2 equiv) was combined with Zn(OTf)$_2$ (210 mg, 0.58 mmol, 1.3 equiv), (–)-*N*-methylephedrine (112 mg, 0.625 mmol, 1.4 equiv), Et$_3$N (90 μL, 61 mg, 0.60 mmol, 1.3 equiv) and isobutyraldehyde (41 μL, 32 mg, 0.45 mmol, 1.0 equiv) in toluene (1 mL) as per the general procedure for 48 h to yield (*S*)-(+)-**2.34** (76 mg, 77%) as a yellow oil. A 90% *ee* was determined by ^{19}F NMR analysis of the corresponding ester derived from (*R*)-MTPA chloride (–71.99 ppm (major), –72.36 ppm (minor)). $[\alpha]^{22}_D$ = 3.74 (c = 1.00, CHCl$_3$). R_f = 0.3 (hexanes/EtOAc 5:1). IR (film cast, CHCl$_3$): 3344 (m, broad), 2959 (s), 2930 (s), 2872 (m), 2858 (m), 2254 (m), 1028 (m) cm^{-1}. ^{1}H NMR (400 MHz, CDCl$_3$) δ 4.23 (d, *J* = 5.7 Hz, 1H), 2.27 (t, *J* = 7.0 Hz, 2H), 1.95–1.84 (m, 2H), 1.53 (quintet, *J* = 7.3, 2H), 1.41–1.26 (m, 8H), 1.01 (d, *J* = 6.8 Hz, 3H), 0.99 (d, *J* = 6.8 Hz, 3H), 0.88 (t, *J* = 6.8 Hz, 3H). ^{13}C NMR (100 MHz, CDCl$_3$) δ 81.7, 75.5, 70.8, 68.5, 64.6, 34.8, 31.8, 29.0, 28.9, 28.3, 22.8, 19.4, 18.2, 17.6, 14.2. EIMS *m/z* 220.2 (M$^+$, 1), 177.1 ([M – *i*-Pr]$^+$, 100). EI HRMS calcd. for C$_{15}$H$_{24}$O (M$^+$) 220.1827, found 220.1825.

5.4.14 (3*S*)-(+)-2-Methyl-7-[tri(propan-2-yl)silyl]hepta-4,6-diyn-3-ol ((*S*)-(+)-2.35)

2.35
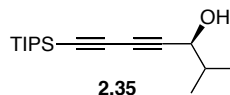
Compound **2.18h** (105 mg, 0.510 mmol, 1.3 equiv) was combined with Zn(OTf)$_2$ (338 mg, 0.930 mmol, 2.4 equiv), (–)-*N*-methylephedrine (99 mg, 0.55 mmol, 1.4 equiv), Et$_3$N (77 μL, 56 mg, 0.55 mmol, 1.4 equiv) and

isobutyraldehyde (34 μL, 28 mg, 0.38 mmol, 1.0 equiv) in toluene (1 mL) as per the general procedure for 40 h to yield (S)-(+)-**2.35** (95 mg, 89%) as a yellow oil. A 91% *ee* was determined by HPLC (Chiralpak AS column, 1% *i*-PrOH in heptane, 0.5 mL/min, λ = 254 nm, column temperature = 2.5 °C) T_{minor} = 20.0 min, T_{major} = 22.5 min. $[\alpha]^{22}_D$ = 2.35 (c = 2.00, CHCl$_3$). R_f = 0.5 (hexanes/EtOAc 5:1). IR (film cast, CHCl$_3$): 3314 (m, broad), 2961 (s), 2945 (s), 2867 (s), 2219 (w), 2103 (m), 1464 (m) cm^{-1}. ^{1}H NMR (400 MHz, CDCl$_3$) δ 4.23 (d, *J* = 5.8, 1H), 1.98 (broad singlet, 1H), 1.91 (app. octet, *J* = 6.6, 1H), 1.08 (s, 21H), 1.03 (d, *J* = 6.8, 3H) 1.01 (d, *J* = 6.9, 3H). ^{13}C NMR (100 MHz, CDCl$_3$) δ 88.9, 84.4, 76.5, 70.9, 68.3, 34.6, 18.5, 18.0, 17.6, 11.2. EIMS *m/z* 278.2 (M$^+$, 9), 235.2 ([M − *i*-Pr]$^+$, 100); EI HRMS calcd. for C$_{17}$H$_{30}$OSi (M$^+$) 278.2066, found 278.2065.

Mosher esters 2.36 and 2.37 were synthesized according to the general procedure for Mosher ester formation, using both the *R*-MTPA-Cl and the *S*-MTPA-Cl.[3-6]

5.4.15 (3*S*)-(+)-9-(4-*tert*-Butylphenyl)-2-methylnona-4,6,8-triyn-3-ol ((*S*)-(+)-2.38)

2.38
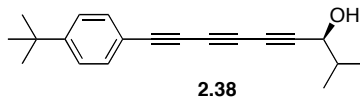
Compound **2.19a** (32 mg, 0.16 mmol, 1.1 equiv) was combined with Zn(OTf)$_2$ (210 mg, 0.59 mmol, 4.9 equiv),[13] (−)-*N*-methylephedrine (81 mg, 0.45 mmol, 3.8 equiv), Et$_3$N (60 μL, 44 mg, 0.43 mmol, 3.6 equiv), and

isobutyraldehyde (11 µL, 8.7 mg, 0.12 mmol, 1.0 equiv) in toluene (1 mL) as per

the general procedure for 72 h to yield (S)-(+)-**2.38** (23 mg, 69%) as a beige waxy

solid. An 89% *ee* was determined by ^{19}F NMR analysis of the corresponding ester

derived from (R)-MTPA chloride (−71.92 ppm (major), −72.27 ppm (minor)).

$[\alpha]^{22}_D$ = 11 (c = 0.50, CHCl$_3$). R_f = 0.5 (hexanes/EtOAc 5:1). IR (film cast,

CHCl$_3$): 3359 (m, broad), 3086 (w), 3039 (w), 2964 (s), 2928 (s), 2872 (m), 2191

(m), 2103 (w), 1603 (w), 1503 (w), 1464 (m) cm^{-1}. ^{1}H NMR (400 MHz, CDCl$_3$) δ

7.46 (d, J = 8.3 Hz, 2H), 7.35 (d, J = 8.4 Hz, 2H), 4.27 (t, J = 5.8 Hz, 1H), 1.94

(app. octet, J = 6.7 Hz, 1H), 1.81 (d, J = 5.9 Hz, 1H), 1.31 (s, 9H), 1.04 (d, J = 6.7

Hz, 3H) 1.03 (d, J = 6.7 Hz, 3H). ^{13}C NMR (125 MHz, CDCl$_3$) δ 153.6, 133.0,

125.7, 117.8, 79.9, 77.7, 73.8, 70.9, 68.6, 65.8, 63.6, 35.2, 34.9, 31.2, 18.2, 17.6.

EIMS *m/z* 278.2 (M$^+$, 26), 235.1 ([M$^+$ − *i*-Pr]$^+$, 100). EI HRMS calcd. for C$_{20}$H$_{22}$O

(M$^+$) 278.1671, found 278.1674.

5.4.16 (1S)-(+)-7-(4-*tert*-Butylphenyl)-1-cyclohexylhepta-2,4,6-triyn-1-ol ((S)-(+)-2.39)


2.39
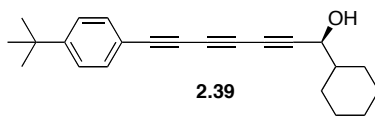
Compound **2.19a** (82 mg, 0.40 mmol, 1.2 equiv) was combined with

Zn(OTf)$_2$ (182 mg, 0.501 mmol, 1.4 equiv), (−)-N-methylephedrine (81 mg, 0.45

mmol, 1.3 equiv), Et$_3$N (65 µL, 45 mg, 0.45 mmol, 1.3 equiv) and cyclohexane-

carboxaldehyde (42 µL, 39 mg, 0.35 mmol, 1.0 equiv) in toluene (1 mL) as per

the general procedure for 90 h to yield (S)-(+)-**2.39** (40 mg, 36%) as a pale yellow

oil. A 90% *ee* was determined by ^{19}F NMR analysis of the corresponding ester derived from (*S*)-MTPA chloride (−72.26 ppm (major), −71.89 ppm (minor)). $[\alpha]^{22}_D$ = 7.56 (c = 1.00, CHCl$_3$). R_f = 0.5 (hexanes/EtOAc 5:1). IR (film cast, CHCl$_3$): 3351 (m, broad), 3086 (w), 3038 (w), 2929 (s), 2854 (s), 2189 (m), 2104 (w), 1603 (w), 1503 (w) cm^{-1}. ^{1}H NMR (500 MHz, CDCl$_3$) δ 7.45 (d, *J* = 8.3 Hz, 2H), 7.35 (d, *J* = 8.4 Hz, 2H), 4.27 (t, *J* = 6.0 Hz, 1H), 1.86 (bd, *J* = 12.8 Hz, 2H), 1.80–1.78 (m, 3H), 1.69 (bd, *J* = 12.3 Hz, 1H), 1.65–1.58 (m, 1H), 1.32–1.05 (m, 14H). ^{13}C NMR (100 MHz, CDCl$_3$) δ 153.4, 132.8, 125.5, 117.7, 80.0, 77.5, 73.6, 70.8, 67.8, 65.4, 63.4, 44.2, 35.0, 31.0, 28.5, 28.1, 26.2, 25.80, 25.77. EIMS *m/z* 318.2 (M$^+$, 61), 303.2 ([M − Me]$^+$, 26), 235.1 ([M − C$_6$H$_{11}$]$^+$, 100). EI HRMS calcd. for C$_{23}$H$_{26}$O (M$^+$) 318.1984, found 318.1987.

5.4.17 (3*R*)-(−)-2-Methyltricosa-4,6,8-triyn-3-ol ((*R*)-(−)-2.40)
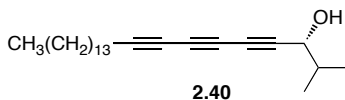
Compound **2.19b** (162 mg, 0.600 mmol, 1.2 equiv) was combined with Zn(OTf)$_2$ (254 mg, 0.699 mmol, 1.4 equiv), (+)-*N*-methylephedrine (108 mg, 0.602 mmol, 1.2 equiv), Et$_3$N (85 μL, 62 mg, 0.61 mmol, 1.2 equiv) and isobutyraldehyde (46 μL, 36 mg, 0.50 mmol, 1.0 equiv) toluene (1 mL) as per the general procedure for 61 h to yield (*R*)-(−)-**2.40** (137 mg, 80%) as a white waxy solid that turned purple upon decomposition. A 89% *ee* was determined by ^{1}H NMR analysis of the corresponding ester derived from (*R*)-MTPA chloride (−71.95 ppm (minor), −72.30 ppm (major)). $[\alpha]^{22}_D$ = −1.60 (c = 1.00, CHCl$_3$). R_f =

0.2 (hexanes/EtOAc 10:1). IR (film cast, CHCl$_3$): 3344 (m, broad), 2959 (s), 2925 (s), 2854 (s), 2218 (m), 1467 (m) cm^{-1}. ^{1}H NMR (400 MHz, CDCl$_3$) δ 4.23 (d, J = 5.6 Hz, 1H), 2.30 (t, J = 7.0 Hz, 2H), 1.91 (app. octet, J = 6.6 Hz, 1H), 1.80 (broad singlet, 1H), 1.54 (quintet, J = 7.3 Hz, 2H), 1.40–1.27 (m, 22H), 1.01 (t, J = 6.8 Hz, 6H), 0.89 (t, J = 6.8 Hz, 3 H). ^{13}C NMR (100 MHz, CDCl$_3$) δ 81.3, 70.8, 68.4, 65.4, 64.0, 59.0, 34.7, 31.9, 29.7, 29.65, 29.57, 29.49, 29.4, 29.0, 28.2, 28.0, 25.4, 22.7, 19.4, 18.0, 17.4, 14.1 (two signals coincident or not observed). EIMS m/z 342.3 (M$^+$, 2), 327.3 ([M − Me]$^+$, 7), 299.2 ([M − i-Pr]$^+$, 100). EI HRMS calcd. for C$_{24}$H$_{38}$O (M$^+$) 342.2923, found 342.2919.

5.4.18 (3R)-(−)-2-Methyl-9-[tri(propan-2-yl)silyl]nona-4,6,8-triyn-3-ol ((R)-(−)-2.41)

2.41
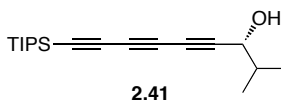
(Table 2.5, entry 4). Compound **2.19c** (120 mg, 0.52 mmol, 1.2 equiv) was combined with Zn(OTf)$_2$ (260 mg, 0.72 mmol, 1.6 equiv), (+)-N-methylephedrine (108 mg, 0.602 mmol, 1.3 equiv), Et$_3$N (80 µL, 0.57 mmol, 1.3 equiv) and isobutyraldehyde (41 µL, 32 mg, 0.45 mmol, 1.0 equiv) in toluene (1 mL) as per the general procedure for 35 h to yield (R)-(−)-**2.41** (106 mg, 78%) as a yellow   waxy solid. [α]$^{22}_D$ = −2.64 (c =1.00, CHCl$_3$). Determination of enantiomeric excess by HPLC analysis and Mosher ester formation was unsuccessful.

5.4.19 (3*S*)-(+)-2-Methyl-9-[tri(propan-2-yl)silyl]nona-4,6,8-triyn-3-ol ((*S*)-(+)-2.41)

2.41

The other enantiomer, (*S*)-(+)-**2.41** (Table 2.5, entry 5) was synthesized from **2.19c** (120 mg, 0.52 mmol, 1.2 equiv.), Zn(OTf)$_2$ (260 mg, 0.72 mmol, 1.6 equiv), (–)-*N*-methylephedrine (101 mg, 0.563 mmol, 1.3 equiv), Et$_3$N (38 μL, 53 mg, 0.52 mmol, 1.2 equiv) and isobutyraldehyde (40 μL, 31 mg, 0.44 mmol, 1.0 equiv) in toluene (1 mL) as per the general procedure for 36 h to yield (*S*)-(+)-**2.41** (108 mg, 81%) as a yellow waxy solid. Determination of enantiomeric excess by HPLC analysis and Mosher ester formation was unsuccessful.

Data for (*S*)-(+)-**24**: $[\alpha]^{22}_D$ = 1.9 (c = 0.29, CHCl$_3$). R_f = 0.4 (hexanes/EtOAc 5:1). IR (film cast, CHCl$_3$): 3328 (m, broad), 2961 (s), 2945 (s), 2892 (m), 2867 (s),2163 (w), 2077 (m), 1463 (m) cm^{-1}. ^{1}H NMR (400 MHz, CDCl$_3$) δ 4.23 (t, *J* = 4.4 Hz, 1H), 1.98 (d, *J* = 3.9 Hz, 1H), 1.91 (app. octet, *J* = 6.6 Hz, 1H), 1.08 (s, 21H), 1.00 (dd, *J* = 6.8, 8.5 Hz, 6H). ^{13}C NMR (125 MHz, CDCl$_3$) δ 89.5, 85.3, 77.9, 70.5, 68.3, 63.9, 60.1, 34.7, 18.5, 18.0, 17.4, 11.2. EIMS *m/z* 302.2 (M$^+$, 2), 259.2 ([M – *i*-Pr]$^+$, 100). EI HRMS calcd. for C$_{19}$H$_{30}$OSi (M$^+$) 302.2066, found 302.2057.

5.4.20 (3*S*)-(−)-1-(1-Benzyl-1*H*-1,2,3-triazol-4-yl)-4-methylpent-1-yn-3-ol ((*S*)-(−)-2.42)

2.42
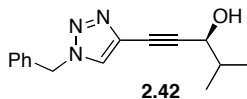
Compound (*S*)-(+)-**2.35** (13 mg, 0.047 mmol), benzyl azide (6 mg, 0.04 mmol), CuSO$_4$•5H$_2$O (100 mg, 0.4 mmol), ascorbic acid (100 mg, 0.6 mmol), and H$_2$O (0.5 mL) were reacted in DMF (3 mL) as per the general procedure and the reaction was quenched after 30 min. Column chromatography (silica gel, CH$_2$Cl$_2$) afforded (*S*)-(−)-**2.42** (6 mg, 51%) as a slightly off-white solid. [α]$^{22}_D$ = −1.7 (c = 0.50, CHCl$_3$). A 91% *ee* was determined by HPLC analysis (Chiralcel OD column, 10% *i*-PrOH/hexanes, 0.5 mL/min, λ= 254, column temperature = 25 °C) T$_{minor}$ = 74.5 min, T$_{major}$ = 82.2 min.

The racemic triazole *rac*-**2.42** was synthesized from *rac*-**2.35** (3 mg, 0.011 mmol), benzyl azide (3 mg, 0.023 mmol), CuSO$_4$•5H$_2$O (100 mg, 0.4 mmol), ascorbic acid (100 mg, 0.6 mmol), and H$_2$O (0.5 mL) reacted in DMF (3 mL) via the general procedure and the reaction was quenched after 30 min. Column chromatography (silica gel, CH$_2$Cl$_2$) afforded *rac*-**2.42** (1.5 mg, 53%), which was used for determining HPLC conditions to calculate the enantiomeric excess.

Data for (*S*)-(−)-**2.42**. R_f = 0.4 (hexanes/EtOAc 1:1). IR (film cast, CHCl$_3$): 3362 (m, broad), 3140 (m), 3066 (w), 3034 (w), 2962 (s), 2927 (s), 2872 (s), 1458 (s), 1054 (s) cm^{-1}. ^{1}H NMR (700 MHz, CDCl$_3$) δ 7.52 (s, 1H), 7.40–7.37 (m, 3H), 7.27–7.25 (m, 2H), 5.52 (s, 2H), 4.37 (d, *J* = 5.6 Hz, 1H), 1.99–1.92 (m, 2H), 1.05

(d, J = 6.8 Hz, 3H), 1.03 (d, J = 6.8 Hz, 3H). ^{13}C NMR (175 MHz, CDCl$_3$) δ

134.0, 130.9, 129.2, 129.0, 128.1, 125.9, 92.7, 75.0, 68.3, 54.3, 34.4, 18.1, 17.6.

EIMS m/z 255.1 (M$^+$, 4), 237.1 ([M – H$_2$O]$^+$, 6), 212.1 ([M – CH$_3$N$_2$]$^+$, 25), 184.1

([M – C$_3$H$_7$ – N$_2$]$^+$, 37), 91.1 ([C$_7$H$_7$]$^+$, 100). EI HRMS calcd. for C$_{15}$H$_{17}$N$_3$O

255.1372, found 255.1366.

5.4.21 (3*S*)-(–)-7-(1-Benzyl-1*H*-1,2,3-triazol-4-yl)-2-methylhepta4,6-diyn-3-ol ((*S*)-(–)-2.43)

2.43
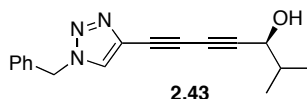
Compound (*S*)-(+)-**2.41** (13 mg, 0.043 mmol), benzyl azide (6 mg, 0.04

mmol), CuSO$_4$•5H$_2$O (100 mg, 0.4 mmol), ascorbic acid (100 mg, 0.6 mmol), and

H$_2$O (0.5 mL) were reacted in DMF (3 mL) as per the general procedure and the

reaction quenched after 40 min. Column chromatography (silica gel,

hexanes/EtOAc, 3:1) afforded (*S*)-(–)-**2.43** (8 mg, 65%) as a yellow liquid. $[\alpha]^{22}_D$

= –13 (c = 0.13, CHCl$_3$). A 98% *ee* was determined by HPLC analysis (Chiralcel

OD column, 40% *i*-PrOH/hexanes, 0.5 mL/min, λ = 254, column temperature =

25 °C) T_{major} = 18.8 min, T_{minor} = 21.4 min with (*S*)-(–)-**2.43**.

5.4.22 (3R)-(+)-7-(1-Benzyl-1*H*-1,2,3-triazol-4-yl)-2-methylhepta4,6-diyn-3-ol ((R)-(+)-2.43)

2.43
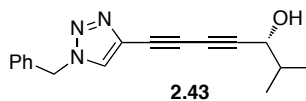
The other enantiomer (3R)-(−)-7-(1-benzyl-1*H*-1,2,3-triazol-4-yl)-2-methylhepta4,6-diyn-3-ol ((R)-(+)-**2.43**) was synthesized from (R)-(−)-**2.41** (13 mg, 0.043 mmol), benzyl azide (6 mg, 0.04 mmol), CuSO$_4$•5H$_2$O (100 mg, 0.4 mmol), ascorbic acid (100 mg, 0.6 mmol), and H$_2$O (0.5 mL) in DMF (3 mL) as per the general procedure and the reaction quenched after 40 min. Column chromatography (silica gel, hexanes/EtOAc, 3:1) afforded (R)-(+)-**2.43** (7.8 mg, 65%) as a yellow liquid. [α]$^{22}_D$ = 2.7 (c = 0.06, CHCl$_3$). A 94% *ee* for (R)-(+)-**2.43** was determined using the conditions outlined above for (S)-(−)-**2.43**.

Data for (R)-(+)-**2.43**: R_f = 0.5 (hexanes/EtOAc 1:1). IR (film cast, CHCl$_3$): 3362 (m, broad), 3141 (m), 3067 (w), 3034 (w), 2963 (s), 2930 (m), 2873 (m), 2243 (w), 1457 (s) cm^{-1}. ^{1}H NMR (400 MHz, CDCl$_3$) δ 7.59 (s, 1H), 7.40–7.38 (m, 3H), 7.28–7.25 (m, 2H), 5.53 (s, 2H), 4.30 (d, *J* = 5.6, 1H), 1.93 (app. octet, *J* = 5.6 Hz, 1H), 1.75 (broad singlet, 1H), 1.03 (d, *J* = 6.8 Hz, 3H), 1.01 (d, *J* = 7.2 Hz, 3H). ^{13}C NMR (175 MHz, CDCl$_3$) δ 133.8, 130.2, 129.3, 129.1, 128.2, 127.4, 83.6, 76.9, 69.6, 68.4, 67.1, 54.4, 34.6, 18.0, 17.4. ESI HRMS calcd. for C$_{17}$H$_{17}$N$_3$O$_2$Na ([M + Na]$^+$) 302.1264, found 302.1262; calcd. for C$_{17}$H$_{18}$N$_3$O$_2$ ([M + H]$^+$) 280.1444, found 280.1446.

168

5.5 Steps towards the synthesis of montiporyne I

5.5.1 Synthesis of aldehyde 2.45.
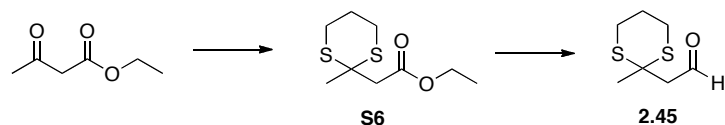
Ethylacetoacetate (1.26 mL, 1.30 g, 10.0 mmol, 1.0 equiv) was combined with $AlCl_3$ (1.73 g, 13 mmol, 1.3 equiv) and 1,3-propanedithiol (1.30 mL, 1.41 g, 13 mmol, 1.3 equiv) in 1,2-dichloroethane (20 mL) at room temperature. The reaction was quenched after 1 h via the addition of H_2O (16 mL). The resulting biphasic mixture was separated with CH_2Cl_2 (2 × 30 mL), dried over anhydrous $MgSO_4$, filtered, and solvent removed *in vacuo*. Column chromatography (silica gel, 10:1 hexanes/EtOAc) gave **S6** (1.78 g, 81%) as a yellow oil. **S6** (0.913 g, 4.14 mmol, 1.0 equiv) was added to a round bottom flask with toluene (15 mL) and cooled to 78 °C. DIBAL-H (1 M in hexanes, 4.2 mL, 4.2 mmol 1.01 equiv) was added and the reaction stirred for 2 h. The reaction was quenched via the slow addition of H_2O (4 mL) and extracted with CH_2Cl_2 (2 × 30 mL), dried over anhydrous $MgSO_4$, filtered, and the solvent removed *in vacuo*. Column chromatography (silica gel, 4:1 hexanes/Et$_2$O) gave **2.45** (0.628 mg, 86%) as a yellow oil. Spectral data for compound **2.45** matched that previously published.[14]

5.5.2 Synthesis of 2.46.

2.46
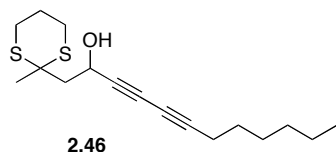
Compound **2.18g** (139 mg, 0.938 mmol, 1.80 equiv) was combined with Zn(OTf)$_2$ (344 mg, 0.946 mmol, 1.81 equiv), (+)-*N*-methylephedrine (138 mg, 0.770 mmol, 1.6 equiv), Et$_3$N (84 mg, 0.83 mmol, 1.6 equiv) and **2.45** (92 mg, 0.52 mmol, 1.0 equiv) toluene (3 mL) as per the general procedure for 98 h to yield **2.46** (18 mg, 11%) as a dark yellow oil which turned dark brown upon decomposition. R_f = 0.2 (hexanes/EtOAc 10:1). ^{1}H NMR (400 MHz, acetone d$_6$) δ 4.39 (t, *J* = 6.0 Hz, 1H), 3.55 (t, *J* = 6.0 Hz, 2H), 2.29 (td, *J* = 6.8, 0.4 Hz, 2H), 1.76–1.70 (m, 2H), 1.68–1.63 (m, 2H), 1.54–1.47 (m, 2H), 0.87 (t, *J* = 7.2 Hz, 3H). A 81% *ee* was suggested by HPLC analysis (Chiralcel OD column, 50% *i*-PrOH/hexanes, 0.5 mL/min, λ = 254, column temperature = 25 °C) T$_{minor}$ = 6.6 min, T$_{major}$ = 15.8 min.

5.6 One-pot protocol
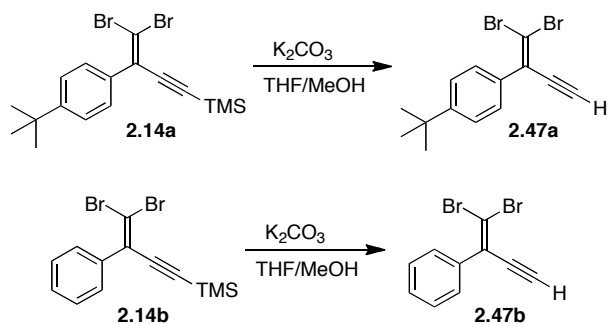
Both **2.47a** and **2.47b** were synthesized according to General Procedure A to give **2.47a** in a 97%, and **2.47b** in a 93% yield. Spectral and analytical properties of **2.47a** and **2.47b** match those previously reported.[1,15]

5.6.1 Procedure 1.
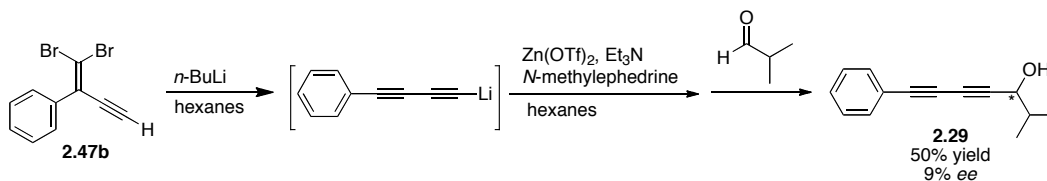
One-pot protocol of dibromoolefin 2.47b with hexanes as solvent.
Dibromoolefin **2.47b** (150 mg, 0.59 mmol, 1.1 equiv) was combined with hexanes (12 mL) in a flame-dried 25 mL pear shaped flask (flask A) equipped with a stirbar and septum. The flask was placed under N_2 and cooled to −78 °C before the addition of *n*-BuLi (0.38 mL of 2.5 M *n*-BuLi in hexanes, 0.95 mmol, 1.7 equiv). The solution stirred at −78 °C for 1.5 h, before being slowly warmed to −30 °C over 30 min. In a separate flame dried 25 mL round bottom flask (flask B) was combined Zn(OTf)$_2$ (361 mg, 0.993 mmol, 1.81 equiv), (−)-*N*-

methylephedrine (168 mg, 0.937 mmol, 1.70 equiv), Et$_3$N (110 μL, 80 mg, 0.79 mmol, 1.4 equiv) and hexanes (2 mL) and stirred for 2 h. The reaction was cooled to –30 °C before the contents of flask A were cannulated into the reaction mixture in flask B. After cannulating, flask A was rinsed with hexanes (2 mL). The reaction mixture was stirred at –30 °C for 15 min and then warmed to 0 °C over 10 min. At 0 °C isobutyraldehyde (40 mg, 0.55 mmol, 1.0 equiv) was added and the reaction was then warmed to room temperature. After 96 h at rt, the reaction was quenched via the addition of saturated aq NH$_4$Cl and extracted with Et$_2$O (4 × 20 mL). The combined organic extracts were dried over MgSO$_4$, filtered, and concentrated *in vacuo*. The crude product was purified by column chromatography (silica gel, 10:1 hexanes/EtOAc) to give **2.29** (54 mg, 50%) as a yellow waxy thick oil in a 9% *ee* (for HPLC conditions and spectral properties please see the procedure above for the stepwise reaction).

5.6.2   Procedure 2.

2.47b

2.29
41% yield
63% *ee*
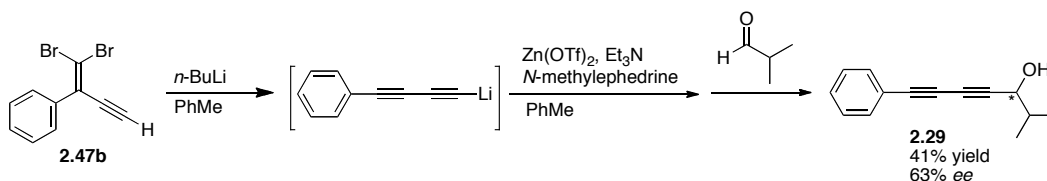
One-pot protocol of dibromoolefin 2.47b with toluene as solvent. Dibromoolefin **2.47b** (120 mg, 0.46 mmol, 1.1 equiv) was combined with toluene (12 mL) in a flame-dried 25 mL pear shaped flask (flask A) equipped with a stirbar and septum. The flask was placed under N$_2$ and cooled to –60 °C before

172

the addition of *n*-BuLi (0.32 mL of 2.5 M *n*-BuLi in hexanes, 0.8 mmol, 1.9 equiv). The solution stirred at −78 °C for 1.5 h, before being slowly warmed to − 30 °C over 30 min. In a separate flame dried 25 mL round bottom flask (flask B) was combined Zn(OTf)₂ (286 mg, 0.786 mmol, 1.72 equiv), (−)-*N*-methylephedrine (146 mg, 0.813 mmol, 1.78 equiv), Et₃N (90 μL, 61 mg, 0.60 mmol, 1.3 equiv) and toluene (1.3 mL) and stirred for 2 h. The reaction was cooled to −30 °C before the contents of flask A were cannulated into the reaction mixture in flask B. After cannulating, flask A was rinsed with toluene (2.5 mL). The reaction mixture was stirred at −30 °C for 15 min and then warmed to 0 °C over 10 min. At 0 °C isobutyraldehyde (30 mg, 0.42 mmol, 1.0 equiv) was added and the reaction was then warmed to room temperature. After 96 h at rt, the reaction was quenched via the addition of saturated aq NH₄Cl and extracted with Et₂O (4 × 20 mL). The combined organic extracts were dried over MgSO₄, filtered, and concentrated *in vacuo*. The crude product was purified by column chromatography (silica gel, 10:1 hexanes/EtOAc) to give **2.29** (34 mg, 41%) as a yellow waxy thick oil in a 63% *ee* (for HPLC conditions and spectral properties please see the procedure above for the stepwise reaction).

5.6.3 Procedure 3.

173
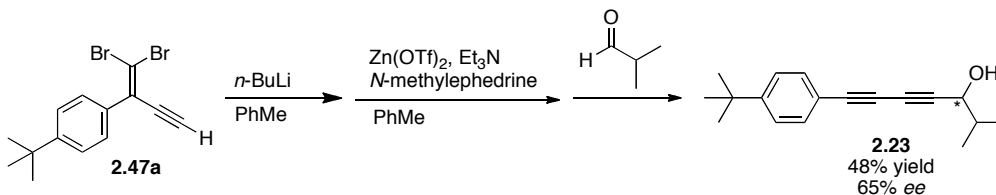
One-pot protocol with dibromoolefin 2.47a. The same procedure as shown above in the previous experiment was performed with Dibromoolefin **2.47a** instead of **2.47b**. Dibromoolefin **2.47a** (239 mg, 0.700 mmol, 1.4 equiv), *n*-BuLi (0.44 mL of 2.5 M *n*-BuLi in hexanes, 1.1 mmol, 2.2 equiv), Zn(OTf)$_2$ (410 mg, 1.1 mmol, 2.2 equiv), (−)-*N*-methylephedrine (135 mg, 0.753 mmol, 1.5 equiv), Et$_3$N (90 μL, 61 mg, 0.60 mmol, 1.2 equiv) toluene (10.0 + 2.0 mL) and isobutyraldehyde (45 μL, 36 mg, 0.50 mmol, 1.0 equiv) were used to give **2.23** (61 mg, 48%) as a pale yellow waxy oil in a 65% *ee* (for HPLC conditions and spectral properties please see the procedure above for the stepwise reaction).

5.6.4 Procedure 4.
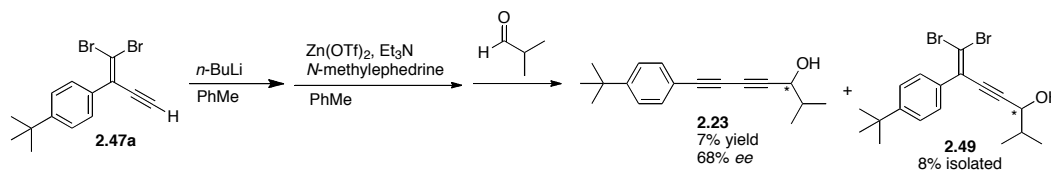
One-pot protocol of dibromoolefin 2.47a with minimal solvent. The same procedure as shown above in Procedure 2 was performed with a minimal amount of solvent (2.0 mL, instead of ~12 mL toluene). Dibromoolefin **2.47a** (207 mg, 0.605 mmol, 1.2 equiv), *n*-BuLi (0.53 mL of 2.5 M *n*-BuLi in hexanes, 1.3 mmol, 2.6 equiv), Zn(OTf)$_2$ (380 mg, 1.1 mmol, 2.2 equiv), (+)-*N*-methylephedrine (127 mg, 0.708 mmol, 1.42 equiv), Et$_3$N (90 μL, 61 mg, 0.60 mmol, 1.2 equiv) toluene (2.0 mL) and isobutyraldehyde (45 μL, 36 mg, 0.50 mmol, 1.0 equiv) were stirred in accordance with the Procedure 2. After 24 h the

reaction had hardened to the point that it could no longer stir, therefore the reaction was quenched via the above mentioned procedure to give **2.23** (9 mg, 7%) as a pale yellow waxy oil in a 68% *ee* (for HPLC conditions and spectral properties please see the procedure above for the stepwise reaction), along with **2.49** (17 mg, 8%).

5.6.5 Procedure 5.

2.49

n-BuLi
hexanes/PhMe

2.23
24% yield
29% *ee*
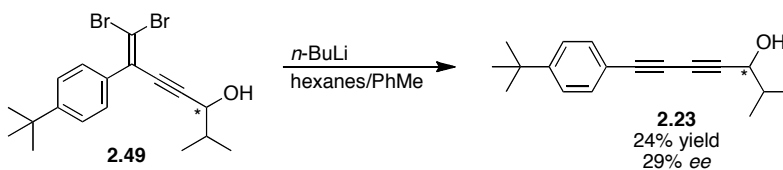
FBW rearrangement of dibromoolefin 2.49. Dibromoolefin **2.49** (17 mg, 0.041 mmol, 1.0 equiv) was added in a flame dried 10 mL round bottom flask equipped with a stirbar. Distilled hexanes (2.5 mL) was added and the reaction flushed with N_2 before being cooled to -78 °C. *n*-BuLi (0.02 mL of 2.5 M *n*-BuLi in hexanes, 0.05 mmol, 1.2 equiv) was added and the reaction was stirred until deemed complete by TLC (15 min). The reaction was quenched via the addition of saturated aq NH_4Cl and extracted with Et_2O (3 × 10 mL). The combined organic extracts were dried over $MgSO_4$, filtered, and concentrated *in vacuo*. The crude product was purified by column chromatography (silica gel, 5:1 hexanes/EtOAc) to give **2.23** (2.5 mg, 24%) as a pale yellow waxy oil in a 29% ee (for HPLC conditions and spectral properties please see the procedure above for the stepwise reaction).

175

5.6.6 Procedure 6.

2.47a

Zn(OTf)₂, Et₃N
N-methylephedrine
PhMe

n-BuLi
PhMe

2.23
33% yield
78% ee
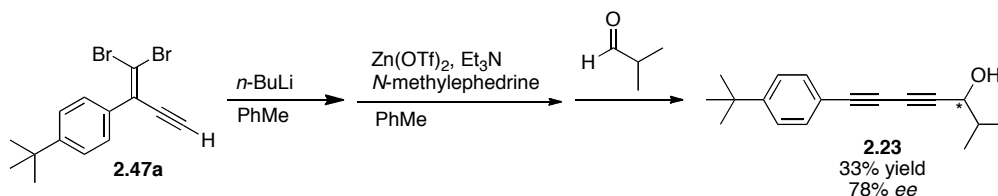
One-pot protocol of dibromoolefin 2.47a with two separate Zn(OTf)₂ additions. The same procedure as shown above in Procedure 2 was performed with two separate additions of Zn(OTf)$_2$. The first addition of Zn(OTf)$_2$ (330 mg, 0.91 mmol, 1.2 equiv) was added to flask A before it was cannulated into flask B. The second addition of Zn(OTf)$_2$ (297 mg, 0.819 mmol, 1.1 equiv) was added to flask B along with (+)-N-methylephedrine (178 mg, 0.993 mmol, 1.3 equiv), Et$_3$N (1.1 mL, 82 mg, 0.81 mmol, 1.1 equiv) and toluene (10 mL). Dibromoolefin **2.47a** (260 mg, 0.76 mmol, 1.0 equiv), n-BuLi (0.70 mL of 2.5 M n-BuLi in hexanes, 1.8 mmol, 2.3 equiv), and isobutyraldehyde (81 μL, 64 mg, 0.89 mmol, 1.2 equiv) were also used in accordance with the procedure for Equation 2.7 to give **2.23** (64 mg, 33%) as a pale yellow waxy oil in a 78% *ee* (for HPLC conditions and spectral properties please see the procedure above for the stepwise reaction).

5.6.7 Procedure 7.

2.47a

Zn(OTf)₂, Et₃N
N-methylephedrine
PhMe

n-BuLi
PhMe

2.23
57% yield
88% ee
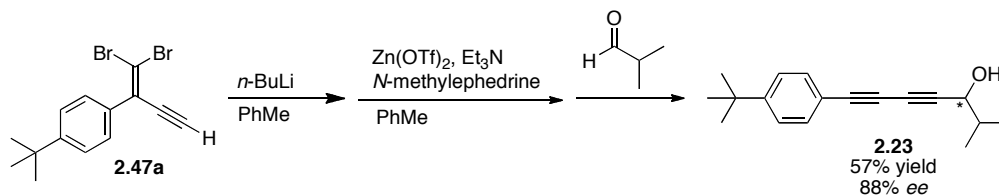
One-pot protocol of dibromoolefin 2.47a reversing cannulation protocol. The same procedure as shown above in Procedure 2 was employed again here, however the two separate additions of Zn(OTf)$_2$ from Procedure 6 was also employed. The difference between Procedure 6 and Procedure 7 shown here is that flask B containing Zn(OTf)$_2$ (222 mg, 0.611 mmol, 2.44 equiv), (−)-*N*-methylephedrine (109 mg, 0.608 mmol, 2.43 equiv), Et$_3$N (65 μL, 45 mg, 0.45 mmol, 1.8 equiv) and toluene (4.0 mL) were cannulated into flask A containing dibromoolefin **2.47a** (127 mg, 0.371 mmol, 1.5 equiv), *n*-BuLi (0.33 mL of 2.5 M *n*-BuLi in hexanes, 0.83 mmol, 3.3 equiv), Zn(OTf)$_2$ (120 mg, 0.33 mmol, 1.30 equiv) and toluene (10.0 mL) at −30 °C, the temperature was maintained at −30 °C for 30 min, then isobutyraldehyde (25 μL, 18 mg, 0.25 mmol, 1.0 equiv) was added. After 15 min at −30 °C the reaction was allowed to warm to room temperature to stir for 96 h. The reaction was quenched according to the procedure for Equation 2.7 to give **2.23** (36 mg, 57%) as a pale yellow waxy oil in a 88% ee (for HPLC conditions and spectral properties please see the procedure above for the stepwise reaction).

5.7 References

(1) Shi Shun, A. L. K.; Chernick, E. T.; Eisler, S.; Tykwinski, R. R. *J. Org. Chem.* **2003**, *68*, 1339-1347.

(2) Chalifoux, W. A.; Tykwinski, R. R. *Chem. Rec.* **2006**, *6*, 169-182.

(3)   Dale, J.; Mosher, H. *J. Am. Chem. Soc.* **1973**, *95*, 512-519.

(4)   Dale, J. A.; Dull, D. L.; Mosher, H. S. *J. Org. Chem.* **1969**, *34*, 2543-2549.

(5)   Dale, J. A.; S., M. H. *J. Am. Chem. Soc.* **1973**, *95*, 512-519.

(6)   Sullivan, G. R.; Dale, J. A.; Mosher, H. S. *J. Org. Chem.* **1973**, *38*, 2143-2147.

(7)   Bichler, P.; Chalifoux, W. A.; Eisler, S.; Shi Shun, A. L. K.; Chernick, E. T.; Tykwinski, R. R. *Org. Lett.* **2009**, *11*, 519-522.

(8)   Made from the corresponding dibromoolefin as per the general procedure reported in ref. 15.

(9)   Jiang, H. F.; Wang, A. Z. *Synthesis* **2007**, 1649-1654.

(10) Dabdoub, M. J.; Dabdoub, V. B.; Lenardão, E. J. *Tetrahedron Lett.* **2001**, *42*, 1807-1809.

(11) Luu, T.; McDonald, R.; Tykwinski, R. R. *Org. Lett.* **2006**, *8*, 6035-6038.

(12) Eisler, S.; Chahal, N.; McDonald, R.; Tykwinski, R. R. *Chem. – Eur. J.* **2003**, *9*, 2542-2550.

(13) An excess of reagents were inadvertently used in this case, discovered only after the conclusion of the project.

(14) Le Sann, C.; Simpson, T. J.; Smith, D. I.; Watts, P.; Willis, C. L. *Tetrahedron Lett.* **1999**, *40*, 4093-4096.

(15) Morisaki, Y.; Luu, T.; Tykwinski, R. R. *Org. Lett.* **2006**, *8*, 689-692.

Chapter 6- Experimental Details for the Enantioselective Allylboration of Propargylic Aldehydes.

6.1 General experimental details:

All reactions were performed in standard, dry glassware under an inert atmosphere of argon. Unless otherwise specified, reagents were purchased from commercial suppliers and used without further purification. Toluene was distilled from sodium/benzophenone ketyl or treated by Fisher Scientific MBraun MB SPS* Solvent system, while hexanes and dichloromethane were distilled from CaH_2 immediately prior to use. Anhydrous $MgSO_4$ was used as the drying agent after aqueous workup. All aldehydes were fractionally distilled directly before use. Evaporation and concentration in vacuo were done at H_2O aspirator pressure. Column chromatography: silica gel-60 (230–400 mesh). Thin layer chromatography (TLC): precoated plastic sheets covered with 0.2 mm silica gel with fluorescent indicator UV 254 nm; visualization by UV light, $KMnO_4$ or anisaldehyde stain. IR spectra: *Nicolet Magna-IR 750* (cm^{-1}, cast film or neat). ^{1}H, ^{11}B, and ^{13}C NMR: *Varian Inova- 300, 400* or *Varian Unity- 500* instruments, at 27 °C in $CDCl_3$, or $(CD_3)_2CO$; solvent peaks (7.26 and 2.05 ppm, respectively, for ^{1}H; 77.0, and 206.26/29.84 ppm, respectively, for ^{13}C) as reference. Accuracy for coupling constants (*J*–values) is +/-0.1 Hz. EI MS (*m/z*): *Kratos MS50* instrument. Optical rotation was recorded using a Perkin Elmer 241 Polarimeter using the sodium D line (589 nm) with a cell length of 10.002 cm. For simplicity,

the coupling constants of the aryl protons for para-substituted phenyl groups have been reported as pseudo first-order, even though they are second-order spin systems. For mass spectral analyses, low-resolution data is provided in cases when M^+ is not the base peak; otherwise, only high-resolution data are provided. Optical purities of the products were measured by chiral HPLC using either a Chiralcel OD or Chiralpak AS column or by formation of the Mosher ester and subsequent ^1H or ^{19}F NMR analysis of the product.

6.2 Preparation of aldehydes.

6.2.1 3-Phenylprop-2-ynal (3.23)

3.23
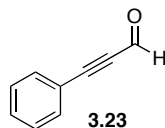
3-Phenylprop-2-ynal (**3.23**) was synthesized according to the published procedure.[1] Spectral data for compound **3.23** matched that previously published.[1]

6.2.2 5-Phenylpent-2-ynal (3.63)

3.63
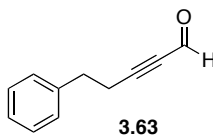
5-Phenylpent-2-ynal (**3.63**) was synthesized according to the published procedure.[1] Spectral data for compound **3.63** matched that previously published.[2]

6.2.3   Dicobalt hexacarbonyl complex of 5-phenylpent-2-ynal (3.81).

3.81
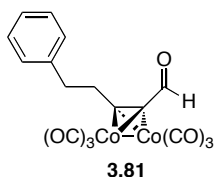
Dicobalt hexacarbonyl complex of 5-phenylpent-2-ynal (**3.81**). In a flame dried 3 neck round bottom flask aldehyde **3.63** (0.44 g, 2.78 mmol, 1.00 equiv) and toluene (12 mL) were added and stirred under argon before the addition of $Co_2(CO)_8$ (1.05 g, 3.07 mmol, 1.10 equiv). Upon the addition of $Co_2(CO)_8$ the reaction bubbled, and once the bubbling ceased (30 min) the reaction was determined complete by TLC analysis. A silica plug (10:1 hexanes/EtOAc) gave **3.81** (1.04 g, 82%) as a dark red thick oil. R_f = 0.38 (10:1 hexanes/EtOAc). IR (neat film, CHCl$_3$): 3088 (w), 3067 (w), 3031 (w), 2931 (w), 2809 (w), 2100 (s), 2060 (s), 2029 (s), 1668 (m), 1585 (w) cm^{-1}. ^{1}H NMR (400 MHz, CDCl$_3$) δ 9.98 (s, 1H), 7.29 (m, 5H), 3.38 (s, 2H), 3.06 (s, 2H). ^{13}C NMR (125 MHz, CDCl$_3$) δ 198.2, 190.2, 139.7, 128.9, 128.3, 126.8, 99.0, 87.8, 37.5, 36.0. EIMS *m/z* 415.9 (M$^+$, 2), 387.9 ($C_{15}H_{10}Co_2O_5$, 1), 359.9 ($C_{14}H_{10}Co_2O_4$, 57), 331.9 ($C_{13}H_{10}Co_2O_3$, 33), 303.9 ($C_{12}H_{10}Co_2O_2$, 31), 275.9 ($C_{11}H_{10}Co_2O$, 41), 247.9 ($C_{10}H_{10}Co_2$, 100). EI HRMS calcd. for $C_{16}H_{10}Co_2O_6$ (M$^+$) 415.9141, found 415.9152.

6.3 Preparation of allylboronates.

6.3.1 4,4,5,5-Tetramethyl-2-(prop-2-en-1-yl)-1,3,2-dioxaborolane (3.46)

3.46
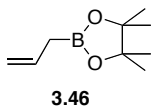
4,4,5,5-Tetramethyl-2-(prop-2-en-1-yl)-1,3,2-dioxaborolane (**3.46**) was synthesized according to the published procedure.[3]

6.3.2 4,4,5,5-Tetraphenyl-2-(prop-2-en-1-yl)-1,3,2-dioxaborolane (3.83)

3.83
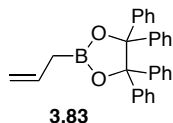
4,4,5,5-Tetraphenyl-2-(prop-2-en-1-yl)-1,3,2-dioxaborolane (**3.83**) was synthesized in accordance to the published procedure, where 1,1,2,2-tetraphenyl-1,2-ethanediol was substituted for pinacol[3] to give **3.83** (112 mg, 5%) as a white waxy solid. R_f = 0.48 (10:1 Hexanes/EtOAc). IR (film cast, CHCl$_3$): 3060 (m), 3037 (m), 2975 (w), 2928 (w), 1953 (w), 1890 (w), 1811 (w), 1638 (m), 1600 (m), 1494 (s) cm^{-1}. ^{1}H NMR (400 MHz, CDCl$_3$) δ 7.22–7.08 (m, 20H), 6.23–6.09 (m, 1H), 5.23 (d, J = 17.1 Hz, 1H), 5.10 (d, J = 10.1 Hz, 1H), 2.22 (d, J = 7.5 Hz, 2H). ^{13}C NMR (100 MHz, CDCl$_3$) δ 142.4, 133.6, 128.5, 128.4, 127.2, 126.9, 115.6, 95.9. ^{11}B NMR (128 MHz, CDCl$_3$) δ 33.81. EI MS m/z 416.2 (M$^+$, 29), 234.1 ([M–C$_{13}$H$_{10}$O]$^+$, 52), 165.1 (C$_{13}$H$_9$, 100). EI HRMS calcd. for C$_{29}$H$_{25}$^{11}BO$_2$ (M$^+$) 416.1948, found 416.1968.

6.3.3 4,4,6-Trimethyl-2-(prop-2-en-1-yl)1,3,2-dioxaborinane (3.84)

3.84
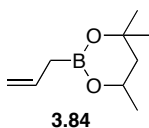
4,4,6-Trimethyl-2-(prop-2-en-1-yl)1,3,2-dioxaborinane (**3.84**) was synthesized in accordance to the published procedure[3] to give **3.84** (6.52 g, 86%) as a clear oil. Spectral data for compound **3.84** matched that previously published.[4]

6.3.4 (4*R*,5*R*)-4,5-Dimethyl-2-(prop-2-en-1-yl)-1,3,2-dioxaborolane (3.85)

3.85

(4*R*,5*R*)-4,5-Dimethyl-2-(prop-2-en-1-yl)-1,3,2-dioxaborolane (**3.85**) was synthesized according to the published procedure[3] to give **3.85** (1.24 g, 81%) as a clear oil. Spectral and analytical data for compound **3.85** matched that previously published.[3]

6.3.5 4,4-Diphenyl-2-(prop-2-en-1-yl)-1,3,2-dixoaborolane (3.86)

3.86
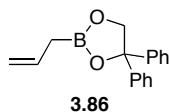
4,4-Diphenyl-2-(prop-2-en-1-yl)-1,3,2-dixoaborolane (**3.86**) was synthesized in accordance to the published procedure,[3] where pinacol was substituted for 1,1-diphenyl-1,1-ethanediol. The crude product was found to be unstable to silica and decomposed to the free boronic acid in the presence of air. Fractional distillation under reduced pressure was performed to give **3.86** (130

mg, 9%). R_f = 0.33 (10:1 hexanes/EtOAc). IR (film cast, CHCl$_3$): 3063 (m), 3028 (m), 2974 (m), 2908 (m), 1954 (w), 1881 (w), 1810 (w), 1726 (w), 1638 (m), 1599 (w), 1492 (s), 1449 (s) cm^{-1}. ^{1}H NMR (400 MHz, CDCl$_3$) δ 7.42–7.27 (m, 10H), 6.05–5.94 (m, 1H), 5.13–5.00 (m, 2H), 4.97 (s, 2H), 1.97 (d, J = 7.2 Hz, 2H). ^{13}C NMR (100 MHz, CDCl$_3$) δ 144.9, 133.7, 128.4, 127.5, 125.5, 115.3, 86.5, 78.2. Due to the high air instability of allylboronic ester **3.86**, mass spectral analysis was not performed. The major resulting product after distillation was the pinacol rearrangement of 1,1-diphenyl-1,2-ethanediol,[3] to give diphenylacetaldehyde. Spectral and analytical properties of diphenylacetaldehyde matched that previously recorded.

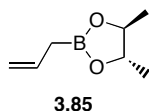### 6.3.6 4,4-Dimethyl-2-(prop-2-en-1-yl)-1,3,2-dioxaborolane (3.87)

3.87
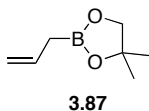
4,4-Dimethyl-2-(prop-2-en-1-yl)-1,3,2-dioxaborolane (**3.87**) was synthesized in accordance to the published procedure, where pinacol was substituted for 1,1-dimethyl-1,1-ethanediol to give **3.87** (130 mg, 9%) as a clear oil. R_f = 0.30 (10:1 hexanes/EtOAc). ^{1}H NMR (400 MHz, CDCl$_3$) δ 5.93–5.83 (m, 1H), 5.05–4.92 (m, 2H), 4.03–3.96 (m, 2H), 1.77 (d, J = 7.2 Hz, 2H), 1.32–1.28 (m, 6H). ^{11}B NMR (128 MHz, CDCl$_3$) δ 33.26. ^{13}C NMR (125 MHz, CDCl$_3$) δ 134.0, 114.9, 79.8, 77.2, 28.2. Due to the high air instability of allylboronic ester **3.87**, mass spectral analysis was not performed.

6.3.7 2-(Prop-2-en-1-yl)-1,3,2-dioxaborinane (3.88)
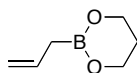
3.88

2-(prop-2-en-1-yl)-1,3,2-dioxaborinane **(3.88)** was synthesized according to the published procedure.[5]

6.3.8 5,5-Dimethyl-2-(prop-2-en-1-yl)-1,3,2-dioxaborinane (3.89)
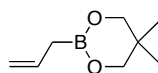
3.89

5,5-dimethyl-2-(prop-2-en-1-yl)-1,3,2-dioxaborinane **(3.89)** was synthesized according to the published procedure.[3]

6.4 Synthesis of Vivols

6.4.1 (1R,2R)-1,2-Bis(2-cyclooctyl-4-fluorophenyl)ethane-1,2-diol (3.49)
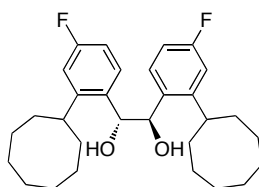
3.49
F–Vivol-8

(1R,2R)-1,2-Bis(2-cyclooctyl-4-fluorophenyl)ethane-1,2-diol **(3.49)** was synthesized according to the published procedure.[6]

6.4.2 (1*R*,2*R*)-1,2-Bis(2-cycloheptyl-4-fluorophenyl)ethane-1,2-diol (3.69)

3.69
F–Vivol-7
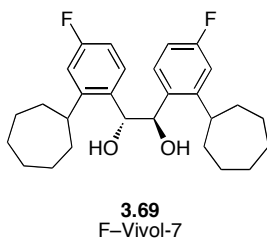
(1*R*,2*R*)-1,2-Bis(2-cycloheptyl-4-fluorophenyl)ethane-1,2-diol **(3.69)** was synthesized according to the published procedure.[6]

6.4.3 (4*R*,5*R*)-4,5-Bis(2-bromo-4-fluorophenyl)-2,2-dimethyl-1,3-dioxolane (3.72)

3.72
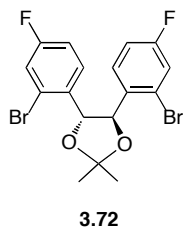
(4*R*,5*R*)-4,5-Bis(2-bromo-4-fluorophenyl)-2,2-dimethyl-1,3-dioxolane (**3.72**) was synthesized according to the published procedure.[6]

6.4.4 2-(Cyclopent-1-en-1-yl)-4,4,5,5-tetramethyl-1,3,2-dioxaborolane (3.73)

3.73
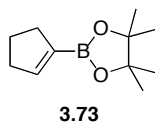
2-(Cyclopent-1-en-1-yl)-4,4,5,5-tetramethyl-1,3,2-dioxaborolane **(3.73)** was synthesized in a similar procedure to the published Shapiro protocol.[7] In a 250 mL round bottom flask *p*-tolylsulfonylhydrazine (18.0 g, 96.0 mmol, 1.0 equiv) was combined with 100% EtOH (20 mL). Cyclopentanone (8.6 mL, 8.1 g, 96 mmol, 1.0 equiv) was added and the reaction heated to reflux at 100 °C. After

5 min the suspension dissolved, and after another 15 min, a white solid appeared. After refluxing for 1.5 h the reaction was cooled to 0 °C and the resulting solid was then collected by filtration and washed with ice-cold EtOH. After drying under reduced pressure the hydrazone was isolated as a white powder in a quantitative yield. The cyclopentanone *p*-tolylsulfonylhydrazone (1.62 g, 5.40 mmol, 1.00 equiv) and 20 mL dry hexanes was added to a flame dried 250 mL round bottom flask equipped with a septum and magnetic stirbar. To this mixture anhydrous TMEDA (20 mL) was added and the reaction cooled to −78 °C, where it was maintained for 15 min, after which 2.5 M *n*-BuLi (10 mL, 25 mmol, 4.6 equiv) was added. The reaction mixture was then stirred at −78 °C for 1 h and then warmed to room temperature and stirred for 1.5 h. During this time N_2 was extruded from the reaction and after the allotted time the reaction was cooled back down to −78 °C and maintained for 15 min, after which pinacol isopropyl borate (5.5 mL, 4.5 g, 24 mmol, 4.4 equiv) was added. The reaction mixture was stirred at −78 °C for 1 h, and then at room temperature for 3 h, before being quenched via the addition of 10% HCl (50 mL) and extracted with Et_2O (4 × 50 mL), (10% HCl was used instead of saturated NH_4Cl, to increase the acidity on work–up. By increasing the acidity, this reduced the amount of an emulsion and allowed for easier work-up). The combined organic extracts were dried over anhydrous $MgSO_4$, filtered, and concentrated *in vacuo*. The crude product was purified via column chromatography (95:5 hexanes/EtOAc) to give **3.73** (0.90 g, 86%) as a

187

faint yellow oil. Spectral and analytical properties of **3.73** were in accordance

with the literature.[7]

6.4.5   2-[(1*Z*)-cyclododec-1-en-1-yl]-4,4,5,5-tetramethyl-1,3,2-dioxaborolane (3.74)
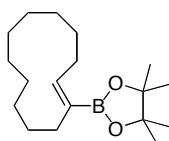
3.74

2-[(1*Z*)-cyclododec-1-en-1-yl]-4,4,5,5-tetramethyl-1,3,2-dioxaborolane

(3.74) was synthesized in a similar procedure to the published Shapiro protocol.[7]

In a 250 mL round bottom flask *p*-tolylsulfonylhydrazine (18.0 g, 96.0 mmol, 1.0

equiv) was combined with 100% EtOH (20 mL). Cyclododecanone (19.0 mL,

17.5 g, 96.0 mmol, 1.0 equiv) was added and the reaction heated to reflux at 100

°C. After 5 min the suspension dissolved, and after another 15 min, a white solid

appeared. After refluxing for 1.5 h the reaction was cooled to 0 °C and the

resulting solid was then collected by filtration and washed with ice-cold EtOH,

After drying under reduced pressure the hydrazone was isolated as a white

powder in a quantitative yield. The cyclododecanone *p*-tolylsulfonylhydrazone

(4.56 g, 13.0 mmol, 1.00 equiv) and 20 mL of dry hexanes was added to a flame

dried 250 mL round bottom flask equipped with a septum and magnetic stirbar.

To this mixture anhydrous TMEDA (40 mL) was added and the reaction cooled to

−78 °C, where it was maintained for 15 min, after which 2.5 M *n*-BuLi (21.0 mL,

53.0 mmol, 4.10 equiv) was added, turning the solution dark red in colour. The

reaction mixture was then stirred at −78 °C for 1 h and then warmed to room

temperature and stirred for 1.5 h. During this time N_2 was extruded from the reaction and after the allotted time the reaction was cooled back down to −78 °C and maintained for 15 min, after which pinacol isopropyl borate (12.4 mL, 10.1 g, 54.0 mmol, 4.20 equiv) was added. The reaction mixture was stirred at −78 °C for 1 h, and then at room temperature for 3 h, before being quenched via the addition of 10% HCl (50 mL) and extracted with Et_2O (4 × 50 mL), (10% HCl was used instead of saturated NH_4Cl, to increase the acidity on work-up. By increasing the acidity, this reduced the amount of an emulsion and allowed for easier work-up). The combined organic extracts were dried over anhydrous $MgSO_4$, filtered, and concentrated *in vacuo*. The crude product was purified via column chromatography (20:1 hexanes/EtOAc) to give **3.74** (1.94 g, 51%) as a colorless oil. Spectral and analytical properties of **3.74** were in accordance with the literature.[7]

6.4.6   (4*R*,5*R*)-4,5-Bis[2-(cyclopent-1-en-1-yl)-4-fluorophenyl]-2,2-dimethyl-1,3-dioxolane (3.75)

3.75
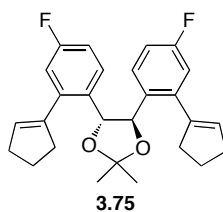
(4*R*,5*R*)-4,5-Bis[2-(cyclopent-1-en-1-yl)-4-fluorophenyl]-2,2-dimethyl-1,3-dioxolane (**3.75**). In a 250 mL round bottom flask equipped with a stir bar was charged cyclopentenylboronate **3.73** (2.66 g, 13.7 mmol, 3.17 equiv), dibromo-dioxalane **3.72** (1.94 g, 4.33 mmol, 1.00 equiv), Pd(OAc)$_2$ (126 mg, 0.550 mmol,

189

0.127 equiv), PPh$_3$ (720 mg, 2.8 mmol, 0.64 equiv), and K$_3$PO$_4$ (7.0 g, 33 mmol, 7.6 equiv). To this mixture was added 60 mL of anhydrous dioxane and 6 mL of degassed distilled water. The round bottom flask was then equipped with a condenser and then subjected to three freeze–pump–thaw cycles (to remove any dissolved oxygen) and heated at 111 ºC for 2 days. The reaction mixture was brought to room temperature and poured into a 250 mL separatory funnel and the residue in the flask was further rinsed with Et$_2$O (100 mL), and transferred into the separatory funnel. The combined organic layer was then washed with saturated aqueous NH$_4$Cl (30 mL), separated, dried over anhydrous Na$_2$SO$_4$, filtered and concentrated *in vacuo*. The dark oily residue was purified by a hexanes plug and recrystallization with methanol (1.51 g, 84% yield). When the recrystallization was performed in methanol, x-ray quality crystals were obtained, see appendix.

[α]$^{22}_D$ = 65.3 (c = 0.49, CHCl$_3$). R_f = 0.45 (10:1 hexanes/EtOAc). IR (cast film, CHCl$_3$): 3044 (w), 2983 (m), 2953 (m), 2933 (m), 2847 (m), 1611 (m), 1585 (m), 1236 (s), 1055 (s) cm^{-1}. ^{1}H NMR (500 MHz, CDCl$_3$) δ 7.55 (dd, J = 9.0, 6.0 Hz, 2H), 6.99 (dt, J = 8.5, 3.0 Hz, 2H), 6.71 (dd, J = 9.5, 3.0 Hz, 2H), 4.99 (s, 2H), 4.75 (quintet, J = 2.0 Hz, 2H), 2.37–2.16 (m, 6H), 1.92–1.69 (m, 6H), 1.65 (s, 6H). ^{13}C NMR (125 MHz, CDCl$_3$) δ 162.0 (J_{C-F} = 247.2 Hz), 141.7 (J_{C-F} = 8.0 Hz), 140.5, 130.5, 129.3 (J_{C-F} = 2.9 Hz), 129.1 (J_{C-F} = 8.8 Hz), 114.6 (J_{C-F} = 21.2 Hz), 114.1 (J_{C-F} = 21.4 Hz), 108.6, 81.4, 37.7, 33.5, 27.4, 23.5. EIMS *m/z* 422.2

(M^+, 1), 232.1 ($C_{15}H_{17}FO$, 89), 189.1 ($C_{12}H_{10}FO$, 100). EI HRMS calcd. for $C_{27}H_{28}F_2O_2$ (M^+) 422.2058, found 422.2055.

6.4.7   (1*R*,2*R*)-1,2-Bis[2-(cyclopent-1-en-1-yl)-4-fluorophenyl]ethane-1,2-diol (3.77)

3.77
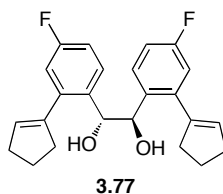
(1*R*,2*R*)-1,2-Bis[2-(cyclopent-1-en-1-yl)-4-fluorophenyl]ethane-1,2-diol (**3.77**). To a 100 mL round bottom flask equipped with a stir bar was added **3.75** (1.47 g, 3.48 mmol, 1.0 equiv), acetic acid (16 mL, 0.28 mol, 80 equiv), MeOH (2 mL) and H_2O (2 mL). The flask was equipped with a reflux condenser and the reaction was heated to 100 ºC for 13 h. The resulting mixture was added to a separatory funnel along with NaHCO$_3$ (30 mL) and the organic layer was extracted with Et$_2$O (4 × 30 mL) dried over MgSO$_4$, filtered, and the solvent removed *in vacuo.* The crude mixture was purified by flash chromatography (3:1 hexanes/EtOAc) and the resulting product was recrystallized from CH$_2$Cl$_2$/hexanes to give **3.77** (1.27 g, 95%) as a white crystals. $[\alpha]^{22}_D$ = 140 (c = 0.50, CHCl$_3$). R_f = 0.58 (3:2 hexanes/EtOAc). IR (cast film, CHCl$_3$): 3271 (strong-broad), 3046 (w), 2954 (m), 2891 (m), 2844 (m), 1889 (w), 1612 (s), 1583 (s), 1500 (s) cm^{-1}. ^{1}H NMR (500 MHz, CDCl$_3$) δ 7.45 (dd, *J* = 6.0, 8.5 Hz, 2H), 6.89 (dt, *J* = 8.5, 2.5 Hz, 2H), 6.66 (dd, *J* = 10.0, 2.5 Hz, 2H), 5.23 (quintet, *J* = 2.0 Hz, 2H), 5.04 (m, 2H), 2.81 (t *J* = 1.5 Hz, 2H), 2.53–2.38 (m, 6H), 2.00–1.82

(m, 6H). ^{13}C NMR (125 MHz, CDCl$_3$) δ 161.9 ($J_{C\text{-}F}$ = 245.8 Hz), 141.2 ($J_{C\text{-}F}$ = 7.7 Hz), 141.1, 133.0 ($J_{C\text{-}F}$ = 3.1 Hz), 130.5, 129.3 ($J_{C\text{-}F}$ = 8.5 Hz), 114.5 ($J_{C\text{-}F}$ = 20.9 Hz), 113.7 ($J_{C\text{-}F}$ = 21.1 Hz), 74.1, 37.5, 33.5, 23.6. EIMS m/z 382.2 (M$^+$, 1), 191.1 (C$_{12}$H$_{10}$FO, 100). EI HRMS calcd. for C$_{24}$H$_{24}$F$_2$O$_2$ (M$^+$) 382.1744, found 382.1740.

6.4.8   (1*R*,2*R*)-1,2-Bis(2-cyclopentyl-4-fluorophenyl)ethane-1,2-diol (3.79)
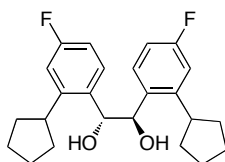
3.79

(1*R*,2*R*)-1,2-Bis(2-cyclopentyl-4-fluorophenyl)ethane-1,2-diol (**3.79**). Into a round bottom flask was charged 897 mg of diol **3.77**, and absolute EtOH (45 mL). The resulting solution was degassed and purged with argon. At this point, Pd/C (10 wt%, 0.90 g) was carefully added to the reaction flask. (**Caution!! Since this is a high loading of flammable palladium, the addition should take place strictly under argon**). After the completion of addition of Pd/C, the sidewalls of the flask were washed with EtOH (2.0 mL) and the reaction mixture was degassed and purged with hydrogen. This cycle was repeated three times, after which the reaction was let to stir for 17 h at rt. After the elapsed time, the reaction was tested for completion using ^{1}H NMR spectroscopy of a small aliquot. The reaction was judged complete, and the reaction mixture was filtered through a pad of Celite and concentrated *in vacuo* and the crude product was purified by flash chromatography (10-20% EtOAc/hexanes) and to give the title compound

3.79 (903 mg, quantitative) as white crystals. $[\alpha]^{22}_D$ = 7.9 (c = 0.30, CHCl$_3$). R_f = 0.6 (3:2 hexanes/EtOAc). IR (cast film, CHCl$_3$): 3333 (strong broad), 2962 (s), 2873 (m), 1896 (w), 1613 (m), 1590 (s), 1501 (s) cm^{-1}. ^{1}H NMR (400 MHz, CDCl$_3$) δ 7.55 (dd, J = 8.8, 6.0 Hz, 2H), 6.88 (dt, J = 8.8, 2.8 Hz, 2H) 6.79 (dd, J = 10.8, 2.8 Hz, 2H), 5.30 (s, 2H), 2.86 (s, 2H), 2.73–2.62 (m, 2H), 2.00–1.91 (m, 2H), 1.73–1.24 (m, 10H), 0.98–0.84 (m, 4H). ^{13}C NMR (100 MHz, CDCl$_3$) δ 162.7 ($J_{C\text{-}F}$ = 244.4 Hz), 147.6 ($J_{C\text{-}F}$ = 6.7 Hz), 133.1, 129.0 ($J_{C\text{-}F}$ = 8.4 Hz), 112.8 ($J_{C\text{-}F}$ = 14.5 Hz), 112.6 ($J_{C\text{-}F}$ = 14.5 Hz), 74.2, 40.5, 35.9, 34.2, 25.8, 25.6. ESI MS m/z 409.2 ([M + Na]$^+$, 100). ESI HRMS calcd. for C$_{24}$H$_{28}$F$_2$NaO$_2$ ([M + Na]$^+$) 409.195, found 409.195.

6.4.9 (4R,5R)-4,5-Bis{2-[(1E)-cyclododec-1-en-1-yl]-4-fluorophenyl}-2,2-dimethyl-1,3-dioxolane (3.76)

3.76
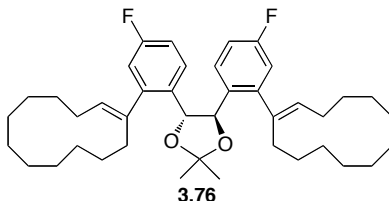
(4R,5R)-4,5-Bis{2-[(1E)-cyclododec-1-en-1-yl]-4-fluorophenyl}-2,2-dimethyl-1,3-dioxolane (**3.76**). In a 250 mL round bottom flask equipped with a stirbar was charged cyclododecenylboronate **3.74** (2.00 g, 6.84 mmol, 3.07 equiv), dibromo-dioxalane **3.72** (1.00 g, 2.23 mmol, 1.00 equiv), Pd(OAc)$_2$ (56 mg, 0.25 mmol, 0.10 equiv), PPh$_3$ (315 mg, 1.20 mmol, 0.54 equiv), and K$_3$PO$_4$ (3.00 g, 14.1 mmol, 6.32 equiv). To this mixture was added anhydrous dioxane (30 mL) and degassed distilled water (4 mL). The round bottom flask was then

equipped with a condenser and then subjected to three freeze thaw cycles (to remove any dissolved oxygen) and heated at 111 ºC for 3 days. The reaction mixture was brought to room temperature and poured into a 250 mL separatory funnel and the residue in the flask was further rinsed with Et_2O (100 mL), and transferred into a separatory funnel. The combined organic layer was then washed with saturated aqueous NH_4Cl (30 mL), separated, dried over anhydrous Na_2SO_4, filtered and concentrated *in vacuo*. The oily residue was purified by flash chromatography (2% EtOAc/hexanes) and recrystallized with methanol to afford 1.15 g, 1.86 mmol (83%) of **3.76** as clear crystals. R_f = 0.55 (10:1 hexanes/EtOAc). $[\alpha]^{22}_D$ = 106 (c = 1.25, $CHCl_3$). IR (cast film, $CHCl_3$): 3017 (w), 2981 (m), 2929 (s), 2858 (m), 1610 (m), 1584 (m), 1494 (m) 1220 (m), 1050 (m) cm^{-1}. ^1H NMR (500 MHz, $CDCl_3$) δ 7.51 (dd, *J* = 8.5, 6.0 Hz, 2H), 6.96 (dt, *J* = 8.5, 3.0 Hz, 2H), 6.63 (dd, *J* = 9.5, 2.5 Hz, 2H) 5.02 (s, 2H), 4.45 (broad singlet, 2H), 2.17–2.03 (m, 6H), 1.80–1.60 (m, 8H), 1.45–1.30 (m, 25H), 1.22–1.00 (m, 7H). ^{13}C NMR (125 MHz, $CDCl_3$) δ 161.7 (J_{C-F} = 247.1 Hz), 146.8 (J_{C-F} = 3.8 Hz), 137.9, 131.9, 129.4, 129.0, 115.9 (J_{C-F} = 19.1 Hz), 113.9 (J_{C-F} = 21.1 Hz), 108.6, 81.1, 28.3, 27.5, 26.8, 25.0, 24.9, 24.8, 24.7, 24.6, 24.4, 24.3, 22.4. EIMS *m/z* 618.4 (M$^+$, 1), 330.2 ($C_{22}H_{31}FO$, 77), 272.2 ($C_{19}H_{25}F$, 100). EI HRMS calcd. for $C_{41}H_{56}F_2O_2$ (M$^+$) 618.4249, found 618.4242.

6.4.10 (1R,2R)-1,2-Bis{2-[(1E)-cyclododec-1-en-1-yl]-4-fluorophenyl}ethane-1,2-diol (3.78)

3.78
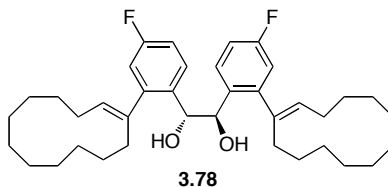
(1R,2R)-1,2-Bis{2-[(1E)-cyclododec-1-en-1-yl]-4-fluorophenyl}ethane-1,2-diol (**3.78**). To a 100 mL round bottom flask equipped with a stirbar was added **3.76** (400 mg, 0.646 mmol), acetic acid (16 mL, 0.28 mol, 80 equiv), MeOH (2 mL) and H_2O (2 mL). The flask was equipped with a reflux condenser and the reaction was heated to 100 ºC for 5 days. The resulting mixture was added to a separatory funnel along with $NaHCO_3$ (30 mL) and the organic layer was extracted with Et_2O (4 × 30 mL) dried over $MgSO_4$, filtered, and the solvent was evaporated *under vacuo.* The crude mixture was purified by flash chromatography (3:1 hexanes/EtOAc) and the resulting product was recrystallized from MeOH/CH_2Cl_2 to give **3.78** (328 mg, 88%) as white crystals. R_f = 0.7 (3:2 hexanes/EtOAc). $[\alpha]^{22}_D$ = 101 (c = 2.88, $CHCl_3$). IR (cast film, $CHCl_3$): 3353 (m, broad), 2928 (s), 2855 (s), 2673 (w), 1726 (w), 1609 (m), 1584 (m) 1489 (m), 1468 (m) 1446 (m) cm^{-1}. ^{1}H NMR (300, $CDCl_3$) δ 7.43 (dd, J = 9.0, 6.0 Hz, 2H), 6.88 (dt, J = 8.4, 2.7 Hz, 2H), 6.58 (dd, J = 9.6, 2.7 Hz, 2H), 4.92 (s, 2H), 4.58 (broad singlet, 2H), 3.48 (s, 2H), 2.79 (s, 2H), 2.54–2.08 (m, 4H), 1.96–1.80 (m, 2H), 1.56–1.45 (m, 32H). ^{13}C NMR (100 MHz, $CDCl_3$) δ 161.6 (J_{C-F} = 247.1 Hz), 146.2 (J_{C-F} = 7.4 Hz), 138.5, 132.9, 132.3, 129.4 (J_{C-F} = 8.6 Hz), 116.4 (J_{C-F} = 20.3 Hz), 113.4 (J_{C-F} = 21.1 Hz), 73.8, 28.4, 26.8, 25.2, 24.85, 24.79, 24.7, 24.5,

24.0, 22.6, 22.2. EIMS m/z 578.4 (M^+, 0.3), 560.4 ($[M–H_2O]^+$, 10), 272.2 ($C_{16}H_{27}F_2O_2$, 100). EI HRMS calcd. for $C_{38}H_{52}F_2O_2$ (M^+) 578.3936, found 578.3923.

6.4.11 (1R,2R)-1,2-Bis(2-cyclododecyl-4-fluorophenyl)ethane-1,2-diol (3.80)

3.80
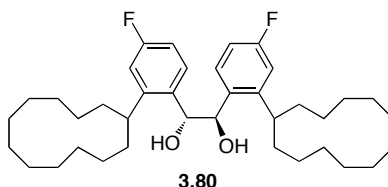
(1*R*,2*R*)-1,2-Bis(2-cyclododecyl-4-fluorophenyl)ethane-1,2-diol **(3.80)**. Into a round bottom flask was charged 210 mg of diol **3.78**, and absolute EtOH (25 mL). The resulting solution was degassed and purged with argon. At this point, Pd/C (10 wt%, 210 mg) was carefully added to the reaction flask. (**Caution!! Since this is a high loading of flammable palladium, the addition should take place strictly under argon**). After the completion of addition of Pd/C, the sidewalls of the flask were washed with EtOH (2.0 mL) and the reaction mixture was degassed and purged with hydrogen. This cycle was repeated twice, after which the reaction was let to stir for 17 h at rt. After the elapsed time, the reaction was tested for completion using ^{1}H NMR spectroscopy of a small aliquot and deemed complete. The reaction mixture was filtered through a pad of Celite and concentrated *in vacuo* and the crude product was purified by flash chromatography (CH_2Cl_2) and gave **3.80** (210 mg, quant) as a small white crystalline powder. R_f = 0.8 (3:2 hexanes/EtOAc). $[\alpha]^{22}_D$ = –2.6 (c = 0.30, $CHCl_3$). IR (cast film, $CHCl_3$): 3382 (broad, m), 2930 (s), 2862 (m), 1653 (w), 1612 (m),

1589 (m), 1495 (m), 1470 (m) cm^{-1}. ^{1}H NMR (400 MHz, CDCl$_3$) δ 7.57 (dd, J = 8.4, 6.0 Hz, 2H), 6.89 (dt, J = 8.4, 2.4 Hz, 2H), 6.75 (dd, J = 11.2, 2.4 Hz, 2H), 5.08 (s, 2H), 2.85 (s, 2H), 2.59–2.54 (m, 2H), 1.55–1.27 (m, 32H), 1.20–0.98 (m, 10H), 0.86–0.76 (m, 2H). ^{13}C NMR (125 MHz, CDCl$_3$) δ 162.4 ($J_{C\text{-}F}$ = 245.6 Hz), 148.0 ($J_{C\text{-}F}$ = 7.0 Hz), 133.3, 128.9 ($J_{C\text{-}F}$ = 8.5 Hz), 113.4 ($J_{C\text{-}F}$ = 21.4 Hz), 113.2 ($J_{C\text{-}F}$ = 21.4 Hz), 73.5, 35.3, 30.8, 29.2, 24.8, 24.49, 24.46, 23.5, 23.1, 22.9, 22.5, 21.2. EIMS m/z 582.4 (M$^+$, 0.3), 292.2 (C$_{19}$H$_{29}$FO, 94), 291.2 (C$_{19}$H$_{28}$FO, 100). EI HRMS calcd. for C$_{38}$H$_{56}$F$_2$O$_2$ (M$^+$) 582.4249, found 582.4271.

6.5   General procedure background reaction:

In a flame dried 10 mL round bottom flask equipped with a stirbar was added anhydrous Na$_2$CO$_3$ (0.2 equiv) and 4 A molecular sieves (25 mg, pre dried under vacuum at 100 °C overnight and then stored in an oven). The flask was equipped with a rubber septum and charged with argon, and freshly distilled toluene (0.25–1.0 mL) was added. After stirring for 5 min at rt, the reaction was cooled to −78 °C where it was maintained for 15 min. Allylboronic acid pinacol ester **3.46** (206 μL, 1.10 mmol, 1.10 equiv) was added dropwise, followed 30 min later by the addition of the aldehyde (1.0 mmol, 1.0 equiv). After the allotted time, diisobutylaluminum hydride (2.0 equiv) was cooled to −78 °C and cannulated into the reaction flask, maintaining the reaction at −78 °C. After all the remaining aldehyde was reduced (ca. 30-50 min), the excess DIBAL-H was quenched via the addition of 10% HCl (4.0 mL). The reaction was then allowed to

slowly warm to rt over 1 h and stirred for an additional 30 min. The reaction mixture was then extracted with Et$_2$O (4 × 15 mL) and the combined organic extracts were treated with saturated aq NaCl, dried over MgSO$_4$, filtered and concentrated *in vacuo*. Column chromatography (silica gel, hexanes/EtOAc 5–30%) gave the corresponding racemic product in fractions ~11-14 and the corresponding reduced starting material in fractions ~16-19.

6.6   General procedure for the F-Vivol catalyzed reaction:

In a flame dried 10 mL round bottom flask equipped with a stirbar, the corresponding F-Vivol (**3.49**, **3.69**, **3.79** or **3.80**) catalyst (0.05 mmol, 0.05 equiv), anhydrous Na$_2$CO$_3$ (0.1 equiv) and 4 A molecular sieves (50 mg, pre dried under vacuum at 100 °C overnight and then stored in an oven) were added. The flask was equipped with a rubber septum and charged with argon, freshly distilled Toluene (0.25–1.0 mL, (1–4 M)) was added. The mixture was stirred for 2 min and SnCl$_4$ (1.0 M in CH$_2$Cl$_2$, 38.5 μL, 0.0385 mmol, 0.0385 equiv) was added. After stirring for 5 min at rt the reaction was cooled to −78 °C where it was maintained for 15 min. Allylboronic acid pinacol ester **3.46** (206 μL, 1.10 mmol, 1.10 equiv) was added dropwise, followed 30 min later by the addition of the aldehyde (1.0 mmol, 1.0 equiv). The reaction was stirred at −78 °C until TLC analysis no longer showed presence of the aldehyde starting material. DIBAL-H (1.5 M in Toluene, 0.70 mL, 2.0 equiv) was cooled to −78 °C and cannulated into the reaction flask, maintain the reaction at −78 °C. After all the remaining

aldehyde was reduced (ca. 30-50 min), the excess DIBAL-H was quenched via the addition of 10% HCl (4.0 mL). The reaction was slowly warmed to rt over 1 h and stirred for an additional 30 min. The reaction mixture was then extracted with Et$_2$O (4 × 15 mL) and the combined organic extracts were extracted with saturated aq NaCl, dried over MgSO$_4$, filtered and concentrated *in vacuo*. Column chromatography (silica gel, 5–30% EtOAc in hexanes) gave the corresponding racemic product in fractions ~11-14 and the corresponding reduced starting material in fractions ~16-19.

6.6.1 1-[Tri(propan-2-yl)silyl]hex-5-en-1-yn-3-ol

3.67
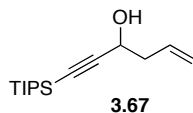
Na$_2$CO$_3$ (8 mg, 0.08 mmol, 0.3 equiv), 4 A molecular sieves (40 mg), allylboronic pinacol ester **3.46** (103 mg, 0.61 mmol, 2.2 equiv), toluene (0.6 mL) and **3.66** (60 mg, 0.28 mmol, 1.0 equiv) were added to a 10 mL round bottom flask in accordance with the general procedure to give 3.67 (25 mg, 50%) and the reduced starting material 3.68 (20 mg, 50%) after column chromatography (5-30% EtOAc in hexanes).Spectral and analytical properties of **3.67** were in accordance with the literature.[8] Spectral and analytical properties of **3.68** were in accordance with the literature.[9,10]

6.6.2 (3*R*)-1-Phenylhex-5-en-1-yn-3-ol (3.24)

3.24
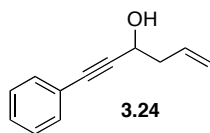
6.6.2.1 Table 3.2, entry 4

F-Vivol-8 (24 mg, 0.050 mmol, 0.050 equiv), Na_2CO_3 (8 mg, 0.08 mmol, 0.08 equiv), 4 A molecular sieves (59 mg) and freshly distilled toluene (1.0 mL) were added to a flame dried 10 mL round bottom flask, followed by the addition of $SnCl_4$ (1.0 M in CH_2Cl_2, 39 μL, 0.039 mmol, 0.039 equiv), allylboronic acid pinacol ester **4.46** (206 μL, 1.10 mmol, 1.10 equiv) and **3.23** (122 mg, 0.94 mmol, 1.0 equiv) in accordance with the general procedure to give 3.24 (120 mg, 70%) as a yellow oil. A 69% *ee* was determined by HPLC analysis (Chiralcel OD column, 50% *i*-PrOH in hexanes, 0.5 mL/min, λ = 210 nm, column temperature = 25 °C) T_{major} = 7.3 min, T_{minor} = 9.3 min. $[\alpha]^{22}_D$ = 26 (c = 0.36, $CHCl_3$). Spectral and analytical properties of **3.24** were in accordance with the literature.[11]

6.6.3 (4*R*)-8-Phenyloct-1-en-5-yn-4-ol (3.64)

3.64
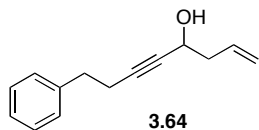
6.6.3.1 Table 3.4, entry 1

F-Vivol-8 (24 mg, 0.050 mmol, 0.10 equiv), Na_2CO_3 (8 mg, 0.08 mmol, 0.2 equiv), 4 A molecular sieves (59 mg) and freshly distilled toluene (0.6 mL) were added to a flame dried 10 mL round bottom flask, followed by the addition

of SnCl$_4$ (1.0 M in CH$_2$Cl$_2$, 39 μL, 0.039 mmol, 0.078 equiv), allylboronic acid

pinacol ester **4.46** (125 μL, 1.10 mmol, 1.10 equiv) and **3.63** (80 mg, 0.51 mmol,

1.0 equiv) in accordance with the general procedure to give **3.64** (77 mg, 75%) as

a yellow oil. A 73% *ee* was determined by HPLC analysis (Chiralcel OD column,

50% *i*-PrOH in hexanes, 0.5 mL/min, λ = 254 nm, column temperature = 25 °C)

T$_{major}$ = 7.2 min, T$_{minor}$ = 9.2 min. [α]$^{22}_D$ = 19.5 (c = 1.10, CHCl$_3$).

6.6.3.2   Table 3.4, entry 2

F-Vivol-7 (22 mg, 0.050 mmol, 0.10 equiv), Na$_2$CO$_3$ (8 mg, 0.08 mmol,

0.2 equiv), 4 A molecular sieves (61 mg) and freshly distilled toluene (0.6 mL)

were added to a flame dried 10 mL round bottom flask, followed by the addition

of SnCl$_4$ (1.0 M in CH$_2$Cl$_2$, 39 μL, 0.039 mmol, 0.078 equiv), allylboronic acid

pinacol ester **4.46** (125 μL, 1.10 mmol, 1.10 equiv) and **3.63** (80 mg, 0.51 mmol,

1.0 equiv) in accordance with the general procedure to give **3.64** (76 mg, 74%) as

a yellow oil. A 76% *ee* was determined by HPLC analysis (Chiralcel OD column,

50% *i*-PrOH in hexanes, 0.5 mL/min, λ = 254 nm, column temperature = 25 °C)

T$_{major}$ = 8.0 min, T$_{minor}$ = 11.2 min. [α]$^{22}_D$ = 19.1 (c = 1.24, CHCl$_3$).

6.6.3.3   Equation 3.24

F-Vivol-7 (13 mg, 0.029 mmol, 0.11 equiv), Na$_2$CO$_3$ (8 mg, 0.08 mmol,

0.31 equiv), 4 A molecular sieves (35 mg) and freshly distilled toluene (0.6 mL)

were added to a flame dried 10 mL round bottom flask, followed by the addition

of SnCl$_4$ (1.0 M in CH$_2$Cl$_2$, 19.5 μL, 0.0195 mmol, 0.0780 equiv), allylboronic

ester **3.89** (80 mg, 1.10 mmol, 1.10 equiv) and **3.63** (45 mg, 0.28 mmol, 1.0

equiv) in accordance with the general procedure to give **3.64** (40 mg, 72%) as a yellow oil. A 83% *ee* was determined by HPLC analysis (Chiralcel OD column, 10% *i*-PrOH in hexanes, 0.5 mL/min, λ = 254 nm, column temperature = 25 °C) T_{major} = 12.4 min, T_{minor} = 18.0 min. $[α]^{22}_D$ = 22.8 (c = 1.30, CHCl₃). R_f = 0.1 (hexanes/EtOAc 10:1). IR (film cast, CHCl₃): 3375 (broad, m), 3076 (m), 3063 (m), 3027 (m), 2978 (w), 2924 (s), 2859 (m), 2226 (w), 1641 (m), 1496 (m), 1453 (w), 1032 (s), 698 (s) cm⁻¹. ¹H NMR (500 MHz, CDCl₃) δ 7.33–7.29 (m, 2H), 7.24–7.21 (m, 3H), 5.90–5.80 (m, 1H), 5.20–5.15 (m, 2H), 4.39 (tt, J = 6.0, 2.0 Hz, 1H), 2.84 (t, J = 7.6 Hz, 2H), 2.52 (dt, J = 7.6, 2.0 Hz, 2H), 2.45–2.41 (m, 2H), 1.94 (s, 1H). ¹³C NMR (125 MHz, CDCl₃) δ 140.5, 133.2, 128.4, 128.3, 126.3, 118.7, 85.1, 81.4, 61.7, 42.4, 35.0, 20.8. EIMS *m/z* 200.1 (M⁺, 0.2), 199.1 ([M–H]⁺, 1), 182.1 ($C_{14}H_{14}$, 6), 159.1 ($C_{11}H_{11}O$, 73). EI HRMS calcd. for $C_{14}H_{14}^+$ ([M–H₂O]⁺) 182.1096, found 182.1093.

6.6.3.4   Scheme 3.3

F-Vivol-7 (13 mg, 0.05 mmol, 0.10 equiv), Na₂CO₃ (8 mg, 0.08 mmol, 0.2 equiv), 4 Å molecular sieves (61 mg) and freshly distilled toluene (0.6 mL) were added to a flame dried 10 mL round bottom flask, followed by the addition of SnCl₄ (1.0 M in CH₂Cl₂, 39 µL, 0.039 mmol, 0.078 equiv), allylboronic acid pinacol ester **3.46** (125 µL, 1.10 mmol, 1.10 equiv) and **3.81** (122 mg, 0.250 mmol, 1.00 equiv) in accordance with the general procedure. After aqueous work-up the crude product **3.82** was combined with MeOH (10 mL) in a round bottom flask and cooled to −78 °C. Ceric ammonium nitrate (137 mg, 0.250 mmol, 1.00

equiv) was then added and allowed to stir for 3 h. The mixture was then extracted with Et_2O (4×20 mL). The combined organic extracts were dried over anh. $MgSO_4$, filtered, and concentrated *in vacuo*. Column chromatography (silica gel, 5–30% EtOAc in hexanes) gave **3.64** (40 mg, 72%) as a yellow oil. A 5% *ee* was determined by HPLC analysis (Chiralcel OD column, 50% *i*-PrOH in hexanes, 0.5 mL/min, $\lambda = 254$ nm, column temperature = 25 °C) $T_{major} = 7.3$ min, $T_{minor} = 11.2$ min.

6.6.3.5 Equation 3.14

The reaction shown in equation 3.14 was performed in a similar manner to the published protocol.[12] In a flame dried 5 mL round bottom flask the (*R*)-TRIP-PA catalyst **3.60** (4 mg, 0.005 mmol, 0.005 mmol), **3.63** (16 mg, 0.10 mmol, 1.0 equiv), and toluene (1.5 mL) were combined and flushed with argon. The reaction mixture was cooled down to –45 °C before the addition of allylboronic pinacol ester **3.46** (20 mg, 0.12 mmol, 1.2 equiv). The reaction was stirred at –40–50 °C for 12 h, after which 1M HCl (1.0 mL) was added and the reaction stirred for 15 min before flash chromatography (silica gel, 10:1 hexanes/EtOAc) to give **3.64** in a nearly quantitative yield (20 mg, 90%). A 56% *ee* was established by HPLC analysis (Chiralcel OD column, 50% *i*-PrOH in hexanes, 0.5 mL/min, $\lambda = 254$ nm, column temperature = 25 °C) $T_{major} = 7.3$ min, $T_{minor} = 11.2$ min.

6.6.3.6 Equation 3.15

The reaction shown in equation 3.15 was performed in a similar manner to the published protocol.[12] In a flame dried 5 mL round bottom flask the (R)-TRIP-PA catalyst **3.60** (9 mg, 0.01 mmol, 9 mol%), **3.63** (21 mg, 0.14 mmol, 1.00 equiv), and Toluene (1.5 mL) were combined and flushed with argon. The reaction mixture was cooled down to −78 °C before the addition of allylboronic pinacol ester **3.46** (27 mg, 0.16 mmol, 1.2 equiv). The reaction was stirred at −78 °C for 4 h, after which 1 M HCl (1.0 mL) was added and the reaction stirred for 15 min flash chromatography (silica gel, 10:1 hexanes/EtOAc) to give **3.64** in a nearly quantitative yield (30 mg, 94%). A 56% *ee* was established by HPLC analysis (Chiralcel OD column, 50% *i*-PrOH in hexanes, 0.5 mL/min, λ = 254 nm, column temperature = 25 °C) T_{major} = 7.3 min, T_{minor} = 11.2 min.

6.6.3.7 Equation 3.16

The reaction shown in Equation 3.16 was performed in a similar manner to the published protocol.[12] In a flame dried 5 mL round bottom flask the (R)-TRIP-PA catalyst **3.60** (10 mg, 0.013 mmol, 9.4 mol%), **3.81** (60 mg, 0.14 mmol, 1.00 equiv), and Toluene (1.5 mL) were combined and flushed with argon. The reaction mixture was cooled down to −78 °C before the addition of allylboronic pinacol ester **3.46** (27 mg, 0.16 mmol, 1.2 equiv). The reaction was stirred at −78 °C for 4 h, after which 1 M HCl (1.0 mL) was added and the reaction stirred for 15 min before a silica plug (10:1 hexanes/EtOAc) gave **3.82**, which was subjected to the deprotection conditions. After flash chromatography (silica gel, 10:1

hexanes/EtOAc) **3.64** was obtained in a nearly quantitative yield (27 mg, 84%). A

14% *ee* was established by HPLC analysis (Chiralcel OD column, 50% *i*-PrOH in

hexanes, 0.5 mL/min, λ = 254 nm, column temperature = 25 °C) T_{major} = 7.3 min,

T_{minor} = 11.2 min. R_f = 0.1 (hexanes/EtOAc 10:1). IR (film cast, $CHCl_3$): 3375

(broad, m), 3076 (m), 3063 (m), 3027 (m), 2978 (w), 2924 (s), 2859 (m), 2226

(w), 1641 (m), 1496 (m), 1453 (w), 1032 (s), 698 (s) cm^{-1}. ^1H NMR (400 MHz,

$CDCl_3$) δ 7.33–7.29 (m, 2H), 7.24–7.21 (m, 3H), 5.90–5.80 (m, 1H), 5.20–5.15

(m, 2H), 4.39 (tt, J = 6.0, 2.0 Hz, 1H), 2.84 (t, J = 7.6 Hz, 2H), 2.52 (dt, J = 7.6,

2.0 Hz, 2H), 2.45–2.41 (m, 2H), 1.94 (s, 1H). ^{13}C NMR (125 MHz, $CDCl_3$) δ

140.5, 133.2, 128.4, 128.3, 126.3, 118.7, 85.1, 81.4, 61.7, 42.4, 35.0, 20.8. EIMS

m/z 200.1 (M^+, 0.2), 199.1 ($[M–H]^+$, 1), 182.1 ($C_{14}H_{14}$, 6), 159.1 ($C_{11}H_{11}O$, 73).

EI HRMS calcd. for $C_{14}H_{14}^+$ ($[M–H_2O]^+$) 182.1096, found 182.1093.

6.7   References

(1) Journet, M.; Cai, D.; DiMichele, L. M.; Larsen, R. D. *Tetrahedron Lett.*
1998, *39*, 6427-6428.

(2) Takai, K.; Morita, R.; Sakamoto, S. *Synlett* **2001**, *10*, 1614-1616.

(3) Roush, W. R.; Walts, A. E.; Hoong, L. K. *J. Am. Chem. Soc.* **1985**, *107*,
8186-8190.

(4) Blais, J.; L'Honore, A.; Soulie, J.; Cadiot, P. *J. Organomet. Chem.* **1974**, *78*, 323-337.

(5) Brown, H.; Racherla, U. S.; Pellechia, P. J. *J. Org. Chem.* **1990**, *55*, 1868-1874.

(6) Rauniyar, V.; Hall, D. G. *J. Org. Chem.* **2009**, *74*, 4236-4241.

(7) Rauniyar, V.; Zhai, H.; Hall, D. G. *Synthetic Comm.* **2008**, *38*, 3984-3995.

(8) Langille, N. F.; Panek, J. S. *Org. Lett.* **2004**, *6*, 3203-3206.

(9) Mori, M.; Tonogaki, K.; Kinoshita, A. *Org. Synth.* **2005**, *81*, 1-13.

(10) Egi, M.; Yamaguchi, Y.; Fujiwara, N.; Akai, S. *Org. Lett.* **2008**, *10*, 1867-1870.

(11) Denmark, S. E.; Wynn, T. *J. Am. Chem. Soc.* **2001**, *123*, 6199-6200.

(12) Jain, P.; Antilla, J. *J. Am. Chem. Soc.* **2010**, *132*, 11884-11886.

APPENDIX A: SUPPORTING SPECTRA
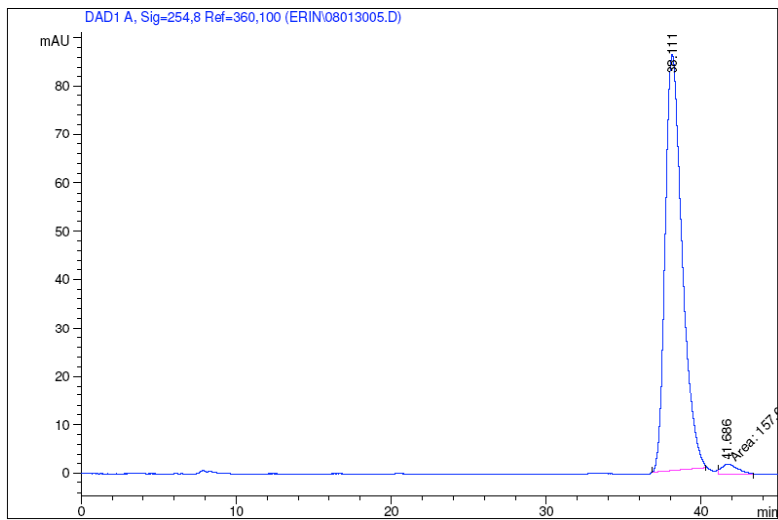
A.1. Optimization of reaction conditions:

A.1.1. Table 2. Results toward optimizing reaction time.

Entry	Zn(OTf)$_2$	Ligand	Temp/°C	Time /h	Yield	% *ee*
1	1.2 equiv	(1*R*, 2*S*)	rt	72	89%	95
2	1.6 equiv	(1*R*, 2*S*)	rt	37	82%	94
3	2.2 equiv	(1*S*, 2*R*)	rt	36	83%	94
4	2.1 equiv	(1*S*, 2*R*)	37 °C	48	79%	93
5	1.6 equiv	(1*S*, 2*R*)	40 °C	13	89%	92
6	1.6 equiv	(1*S*, 2*R*)	50 °C	14	89%	73
7	1.6 equiv	(1*S*, 2*R*)	60 °C	3	88%	58
8	1.6 equiv	(1*S*, 2*R*)	80 °C	2.5	89%	53

A.1.2. Optimization of reaction conditions for 2.23:

Zn(OTf)$_2$ and *N*-methylephedrine (118 mg, 0.658 mmol, 1.1 equiv) were charged under N$_2$ for 10 min if an additive was used it was also added at this point. PhMe (1 mL) and base (1.2 equiv) were then added. The mixture was stirred for 2 h at rt, followed by the addition of *para-tert*-butylphenyldiyne[1a] (120 mg, 0.66 mmol, 1.1 equiv) in PhMe (0.5 mL). The flask containing the diyne was then washed with additional PhMe (0.5 mL), which was added to the reaction mixture. The reaction was stirred for 20 min and freshly purified and fractionally distilled isobutyraldehyde (54 mL, 43 mg, 0.60 mmol, 1.0 equiv) was added. The reaction was then stirred at the specified temperature until deemed complete by TLC analysis. The reaction was quenched via the addition of saturated aq. NH$_4$Cl (3 mL) and extracted with Et$_2$O (30 mL). The aqueous layer was further extracted with Et$_2$O (4 × 30 mL). The combined organic phase was dried over MgSO$_4$, filtered, and the solvent removed *in vacuo*. Column chromatography (silica gel, hexanes/EtOAc 5:1) afforded the product. The yield was then calculated before the enantioselectivity was determined by HPLC (for HPLC conditions please see the experimental procedure for **2.23**, A1−A13).

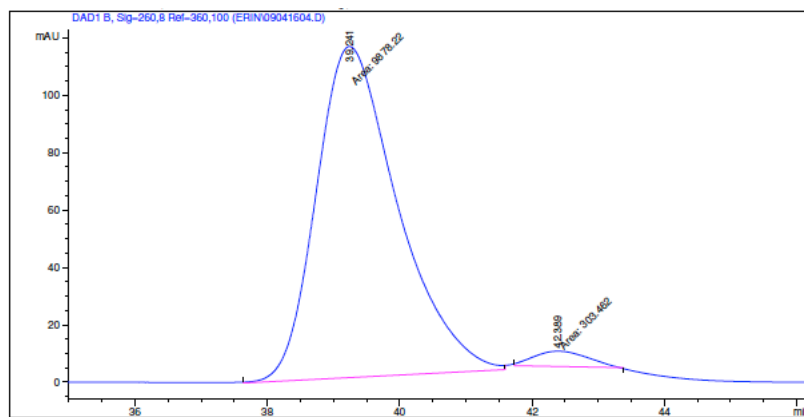*A.1.3. HPLC traces for reaction optimization conditions.*


```
                        Area Percent Report
=================================================================
Peak  RetTime  Type   Width      Area        Height     Area
 #     [min]          [min]    [mAU*s]       [mAU]        %
----|--------|----|--------|------------|-----------|--------|
  1   38.111  BB    1.1354  6571.26172    86.20113   97.6568
  2   41.686  MM    1.2794   157.67551     2.05406    2.3432

Totals :                     6728.93723    88.25519
```

Figure A1. HPLC trace of (*S*)-(+)-**2.23** performed with 1.2 equiv. Zn(OTf)$_2$ (Entry 1 of Table 2.2).


```
                        Area Percent Report
=================================================================
Peak  RetTime  Type   Width      Area        Height     Area
 #     [min]          [min]    [mAU*s]       [mAU]        %
----|--------|----|--------|------------|-----------|--------|
  1   39.241  MM    1.4247  9878.21680   115.56286   97.0195
  2   42.389  MM    0.9508   303.46231     5.31925    2.9805

Totals :                     1.01817e4   120.88210
```

Figure A2. HPLC trace of (*S*)-(+)-**2.23** performed with 1.6 equiv. Zn(OTf)$_2$ (Entry 2 of Table 2.2).
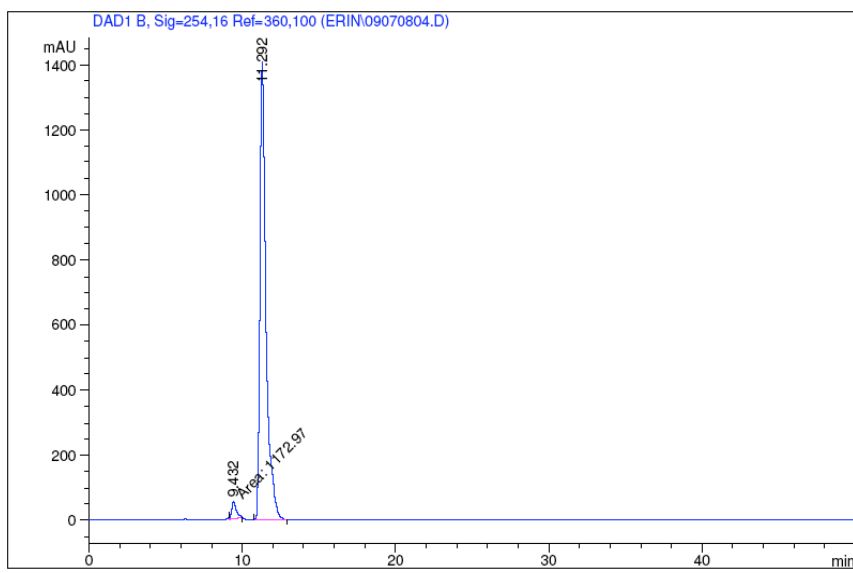
208

```
                        Area Percent Report
=========================================================================
Peak RetTime Type    Width      Area        Height      Area
  #    [min]         [min]     [mAU*s]       [mAU]        %
----|-------|----|-------|----------|----------|--------|
  1    9.432  MM    0.3590  1172.96936    54.45091    2.9146
  2   11.292  BB    0.4089  3.90710e4   1411.55530   97.0854

Totals :                     4.02439e4   1466.00621
```

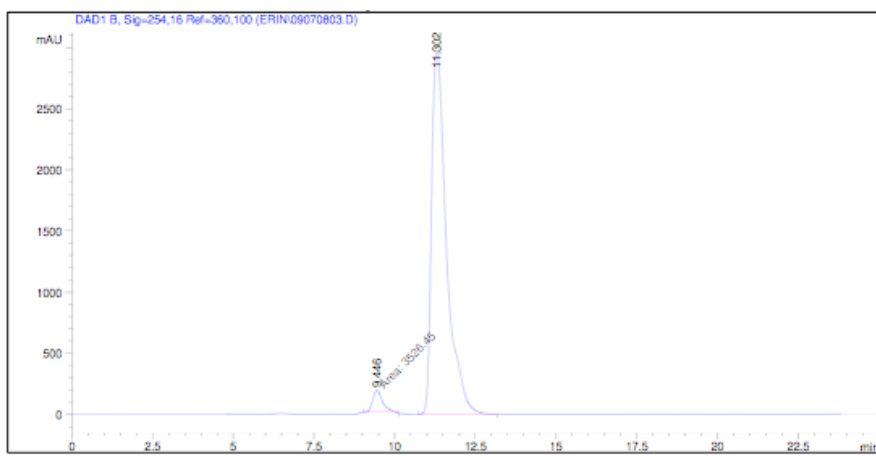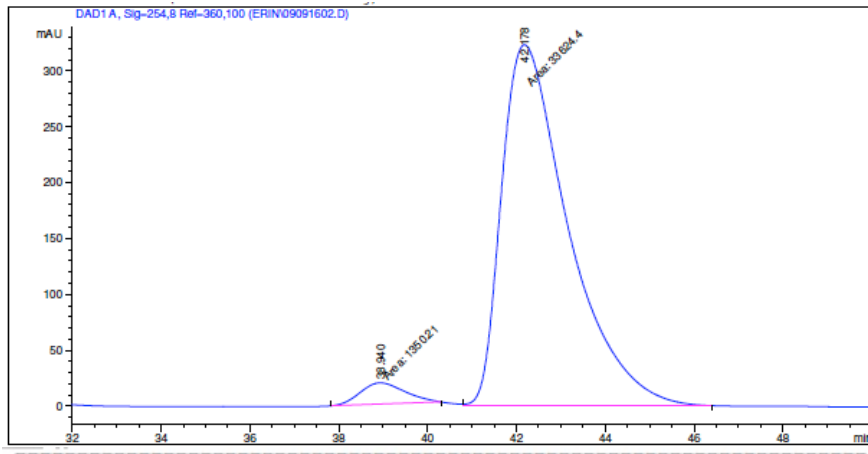Figure A3. HPLC trace of (*R*)-(–)-**2.23** performed with 2.2 equiv. Zn(OTf)$_2$ (Entry 3 of Table 2.2).


```
                        Area Percent Report
=========================================================================
Peak RetTime Type    Width      Area        Height      Area
  #    [min]         [min]     [mAU*s]       [mAU]        %
----|-------|----|-------|----------|----------|--------|
  1    9.446  MM    0.3361  3526.44604   174.89383    3.5539
  2   11.302  BB    0.4834  9.57007e4   2974.14233   96.4461

Totals :                     9.92271e4   3149.03616
```

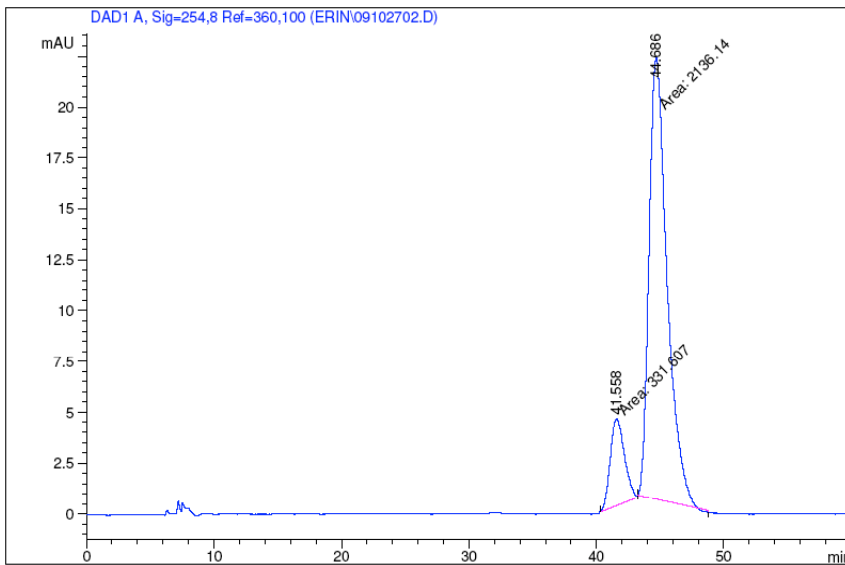Figure A4. HPLC trace of (*R*)-(–)-**2.23** performed at 37 °C (Entry 4 of Table 2.2).

```
DAD1 A, Sig=254,8 Ref=360,100 (ERIN\09091602.D)

                Area Percent Report
========================================================
Peak RetTime Type  Width     Area       Height    Area
  #    [min]        [min]   [mAU*s]      [mAU]      %
----|-------|----|-------|-----------|----------|--------|
  1  38.940 MM   1.1728 1350.21167   19.18803   3.8605
  2  42.178 MM   1.7362 3.36244e4   322.77121  96.1395

Totals :                3.49746e4   341.95924
```

Figure A5. HPLC trace of (*R*)-(−)-**2.23** performed at 40 °C (Entry 5 of Table 2.2).


```
DAD1 A, Sig=254,8 Ref=360,100 (ERIN\09102702.D)

                Area Percent Report
========================================================
Signal 1: DAD1 A, Sig=254,8 Ref=360,100

Peak RetTime Type  Width     Area       Height    Area
  #    [min]        [min]   [mAU*s]      [mAU]      %
----|-------|----|-------|-----------|----------|--------|
  1  41.558 MM   1.2904  331.60660    4.28303  13.4376
  2  44.686 MM   1.6399 2136.14209   21.70963  86.5624

Totals :                2467.74869   25.99266
```

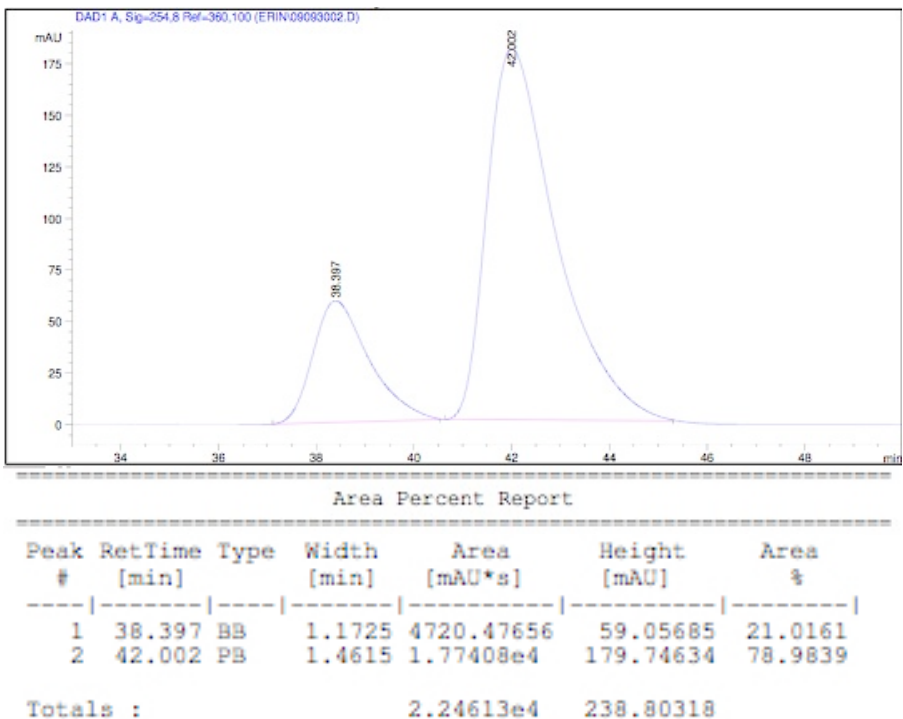Figure A6. HPLC trace of (*R*)-(−)-**2.23** performed at 50 °C (Entry 6 of Table 2.2).

210

```
Area Percent Report

Peak RetTime Type  Width     Area       Height      Area
 #    [min]        [min]    [mAU*s]      [mAU]        %
----|--------|----|-------|-----------|----------|--------|
  1  38.397 BB    1.1725  4720.47656   59.05685   21.0161
  2  42.002 PB    1.4615  1.77408e4   179.74634   78.9839

Totals :                  2.24613e4   238.80318
```

Figure A7. HPLC trace of (*R*)-(−)-**2.23** performed at 60 °C (Entry 7 of Table 2.2).


```
Area Percent Report

Peak RetTime Type  Width     Area       Height      Area
 #    [min]        [min]    [mAU*s]      [mAU]        %
----|--------|----|-------|-----------|----------|--------|
  1  36.316 BB    1.1140  5066.08936   66.55713   23.6099
  2  39.905 BB    1.3493  1.63914e4   177.84637   76.3901

Totals :                  2.14575e4   244.40350
```
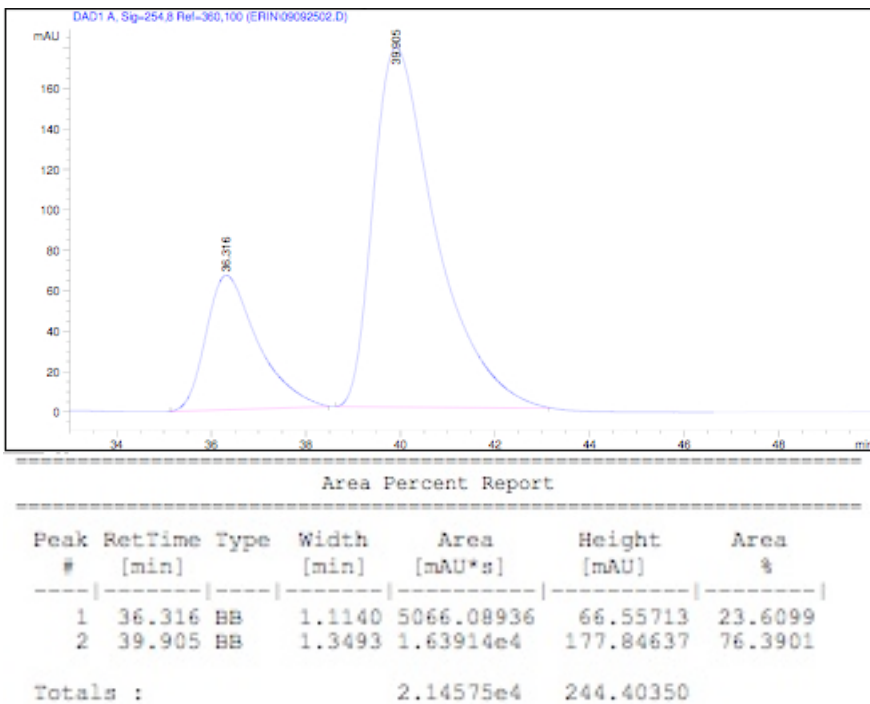
Figure A8. HPLC trace of (*R*)-(−)-**2.23** performed at 80 °C (Entry 8 of Table 2.2).

211

A.1.4. *Table 5.* ***The effect of PPh₃O additive on formation of (–)-2.23***

Entry	Base	Additive	Time /h	Yield	% ee[c]
1	Et₃N	—	36	83	94
2	Et₃N	PPh₃O (1 equiv)	20	79	88
3	Hünig's	—	19	80	98
4	Hünig's	PPh₃O (1 equiv)	20	79	95
5	Hünig's	PPh₃O (0.2 equiv)	20	83	97
6	Hünig's	—	4[d]	83	95
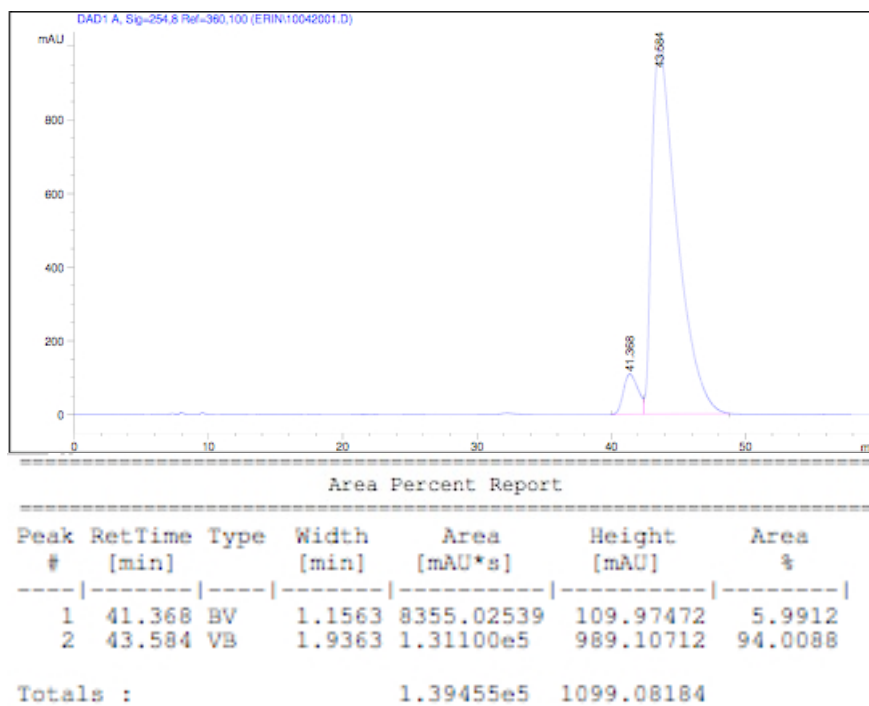
Figure A9. HPLC trace of (*R*)-(–)-**2.23** (Entry 2 of Table 2.6).
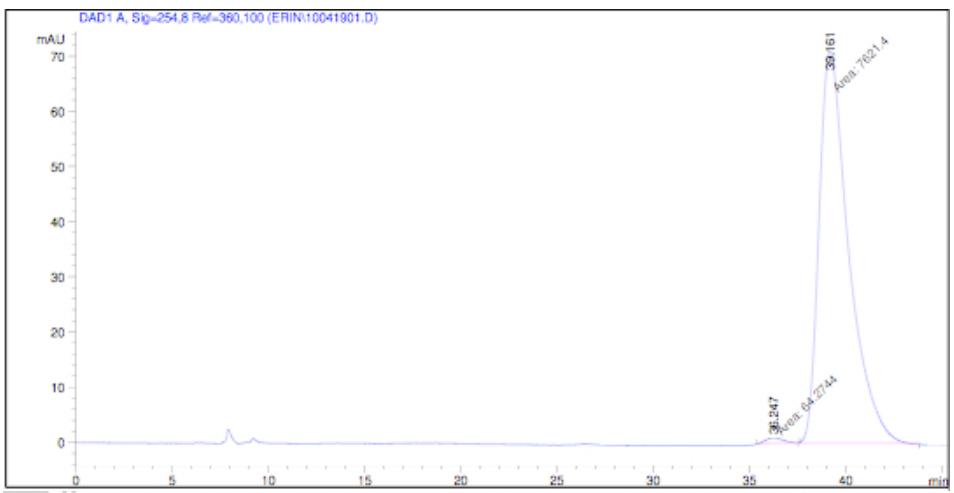
```
DAD1 A, Sig=254,8 Ref=360,100 (ERIN\10041901.D)
```

```
======================================================================
                        Area Percent Report
======================================================================

Peak RetTime Type  Width      Area       Height      Area
 #    [min]        [min]    [mAU*s]       [mAU]        %
----|-------|----|-------|----------|-----------|--------|
  1  36.247  MM   1.0602    64.27438    1.01039   0.8363
  2  39.161  MM   1.7878  7621.40039   71.04845  99.1637

Totals :                  7685.67477   72.05884
```

Figure A10. HPLC trace of (*R*)-(–)-**2.23** (Entry 3 of Table 2.6).
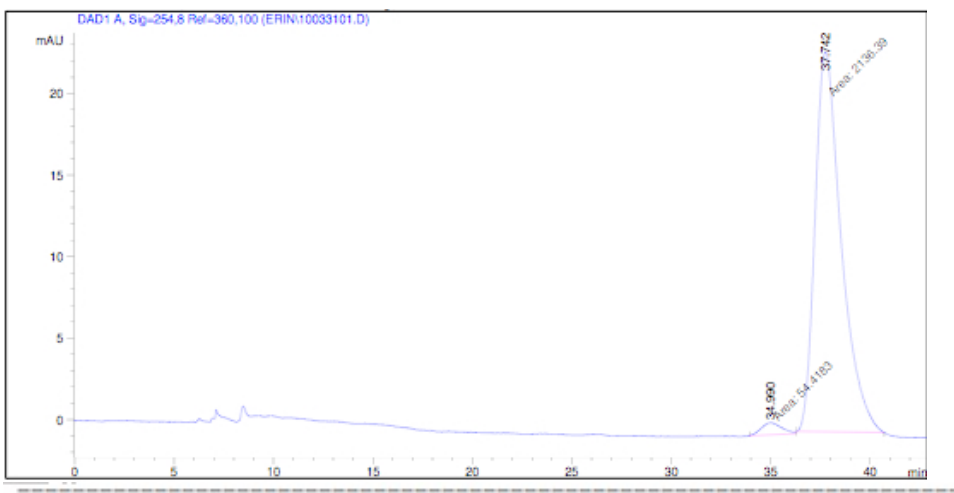

```
DAD1 A, Sig=254,8 Ref=360,100 (ERIN\10033101.D)
```

```
======================================================================
                        Area Percent Report
======================================================================

Peak RetTime Type  Width      Area       Height       Area
 #    [min]        [min]    [mAU*s]       [mAU]         %
----|-------|----|-------|----------|-----------|--------|
  1  34.990  MM   1.2076    54.41826  7.51083e-1   2.4839
  2  37.742  MM   1.5294  2136.38892   23.28159   97.5161

Totals :                  2190.80718   24.03267
```

Figure A11. HPLC trace of (*R*)-(–)-**2.23** (Entry 4 of Table 2.6).

```
Area Percent Report

Peak  RetTime Type  Width     Area       Height      Area
  #    [min]        [min]    [mAU*s]      [mAU]        %
----|-------|----|-------|----------|-----------|--------|
  1  41.486  MM   1.2296  313.75174     4.25275   1.6671
  2  44.105  MM   1.7867 1.85063e4    172.63089  98.3329

Totals :                 1.88200e4    176.88364
```
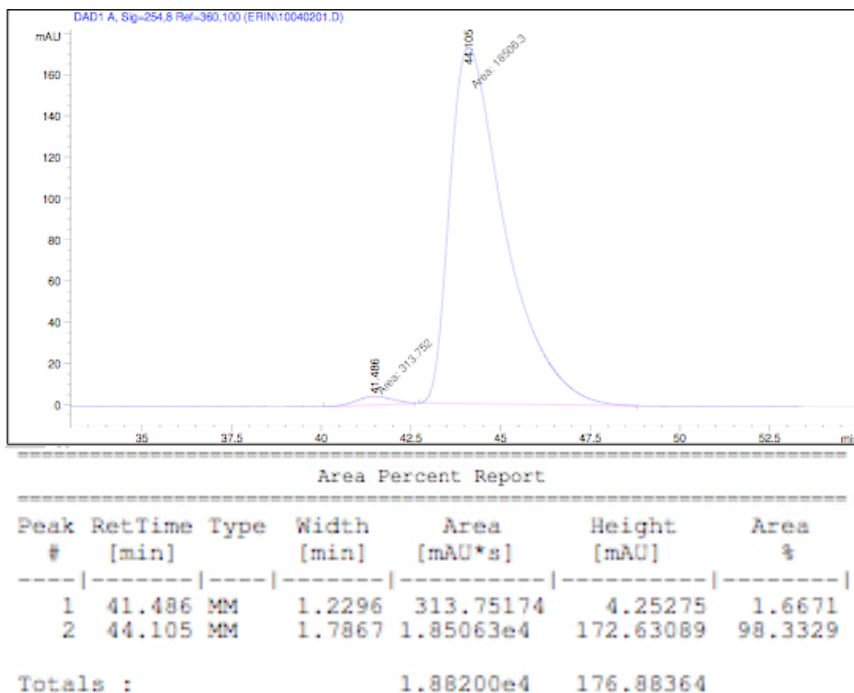
Figure A12. HPLC trace of (*R*)-(−)-**2.23** (Entry 5 of Table 2.6).


```
Area Percent Report

Peak  RetTime Type  Width     Area       Height      Area
  #    [min]        [min]    [mAU*s]      [mAU]        %
----|-------|----|-------|----------|-----------|--------|
  1  38.802  BB   0.8250  318.17697     4.58843   2.2695
  2  42.083  MM   1.6773 1.37013e4    136.14342  97.7305

Totals :                 1.40195e4    140.73184
```
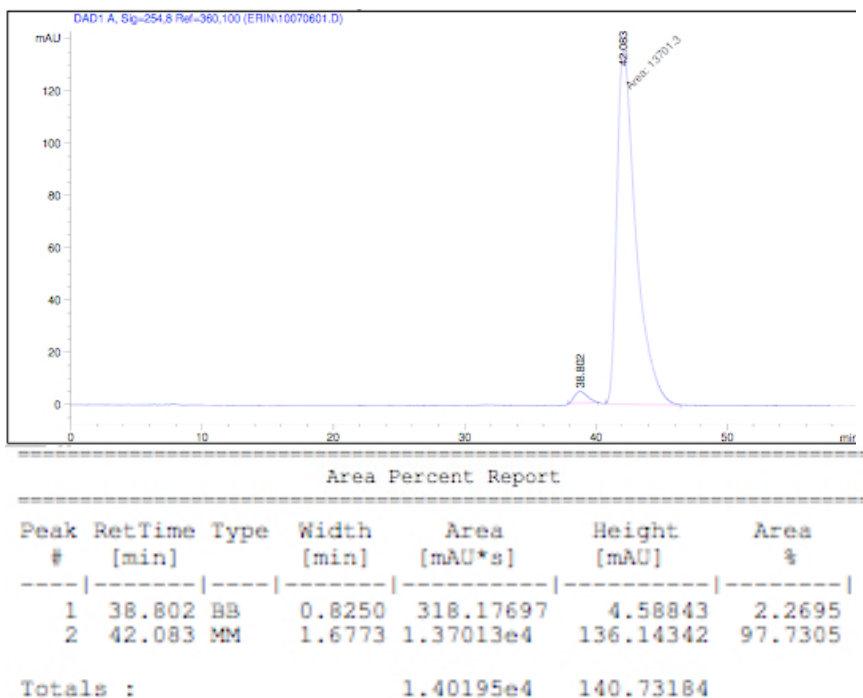
Figure A13. HPLC trace of (*R*)-(−)-**2.23** (Entry 6 of Table 2.6).

A.2. ^{1}H NMR and ^{13}C NMR spectra of new compounds of Chapter 2.
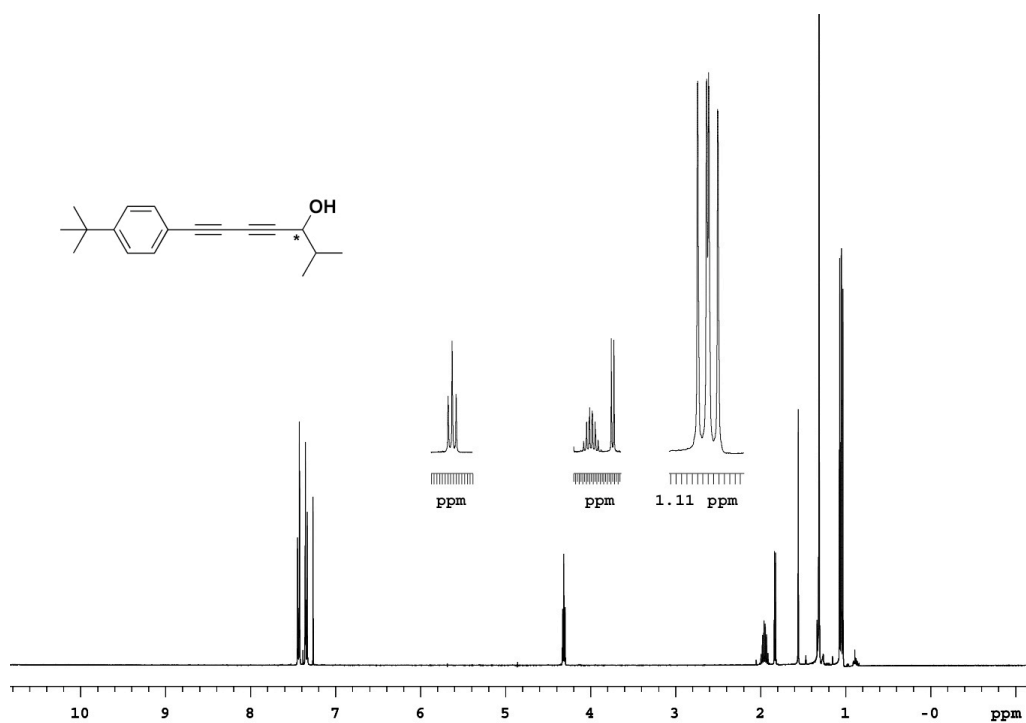
Figure A14. ^{1}H NMR spectrum of **2.23** in CDCl$_3$, 400 MHz.
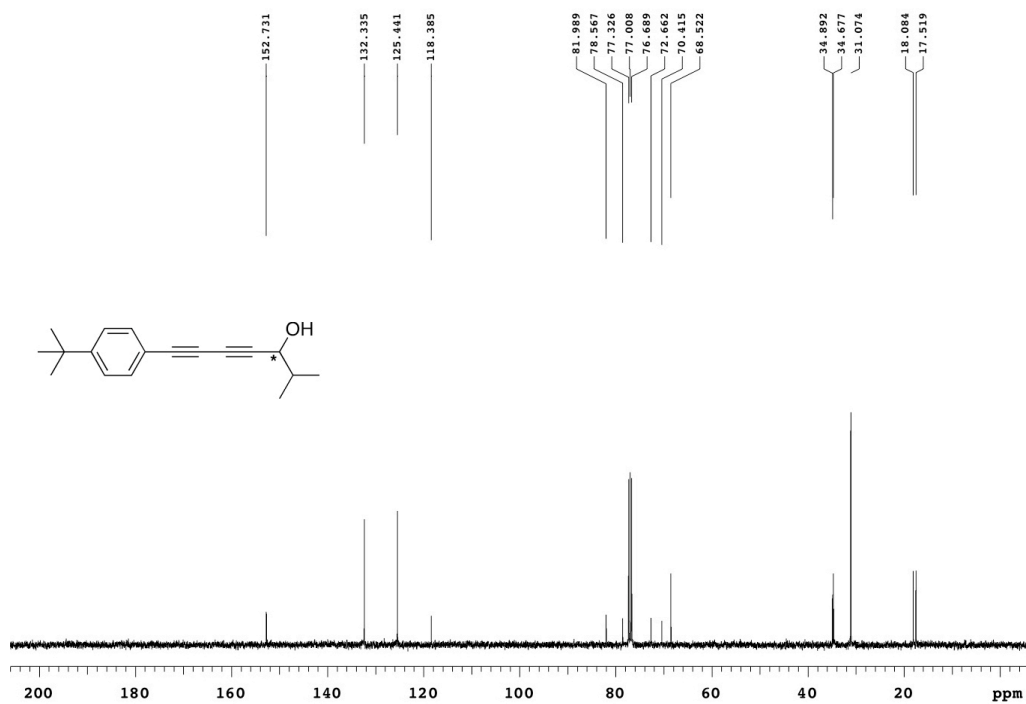
Figure A15. ^{13}C NMR spectrum of **2.23** in CDCl$_3$, 100 MHz.
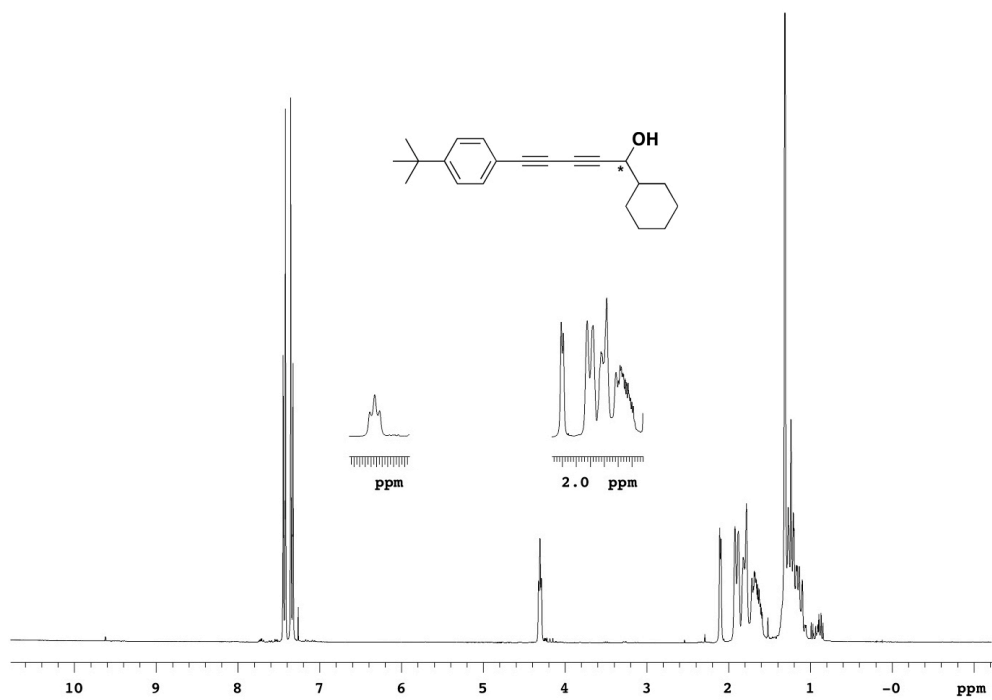
Figure A16. ^{1}H NMR spectrum of **2.24** in CDCl$_3$, 300 MHz.
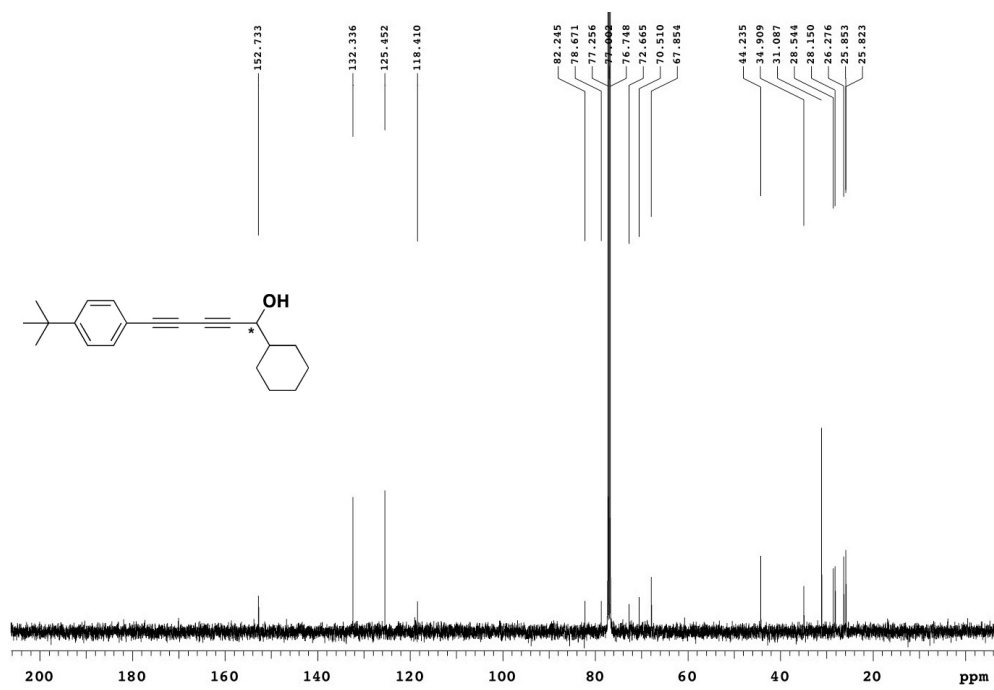
Figure A17. ^{13}C NMR spectrum of **2.24** in CDCl$_3$, 125 MHz.
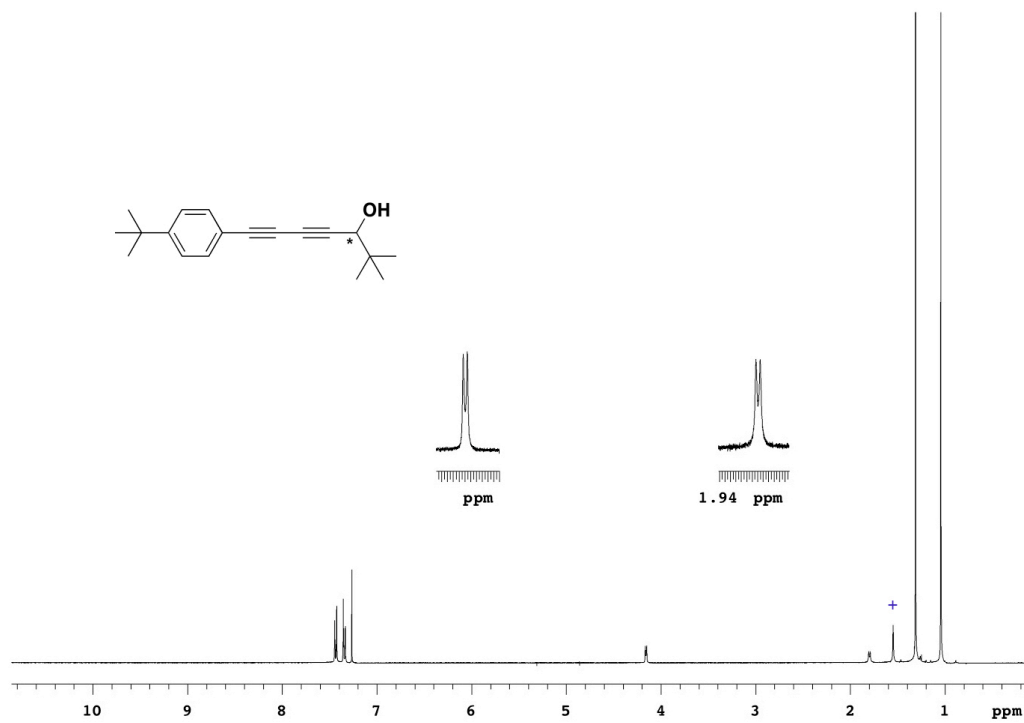
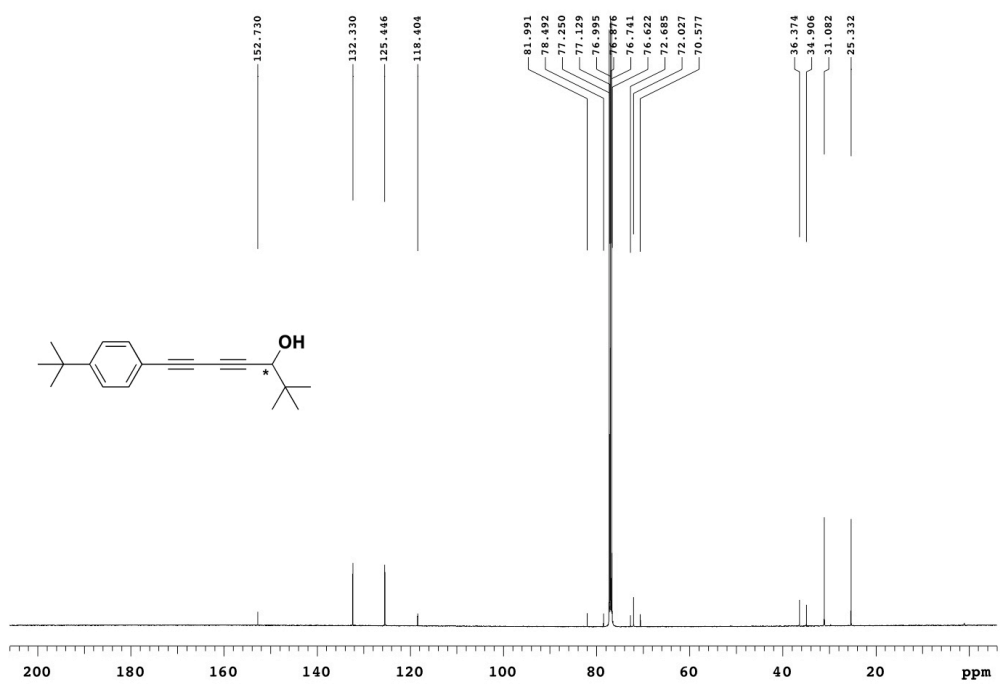Figure A18. ^{1}H NMR spectrum of **2.25** in CDCl$_3$, 400 MHz (+ = H$_2$O).

Figure A19. ^{13}C NMR spectrum of **2.25** in CDCl$_3$, 125 MHz.
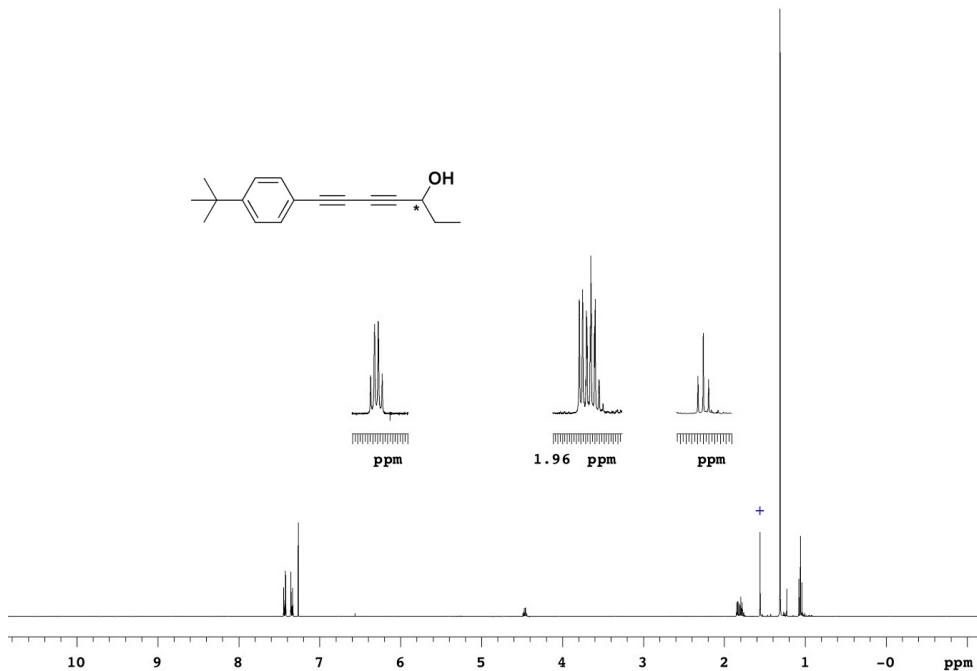
Figure A20. ^{1}H NMR spectrum of **2.26** in CDCl$_3$, 400 MHz (+ = H$_2$O).
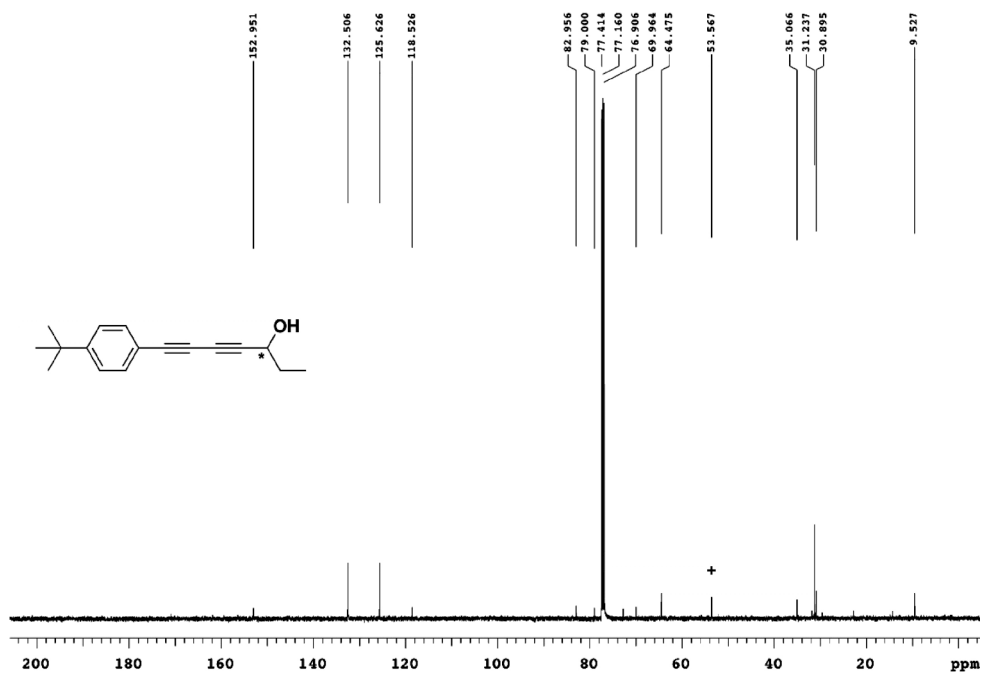
Figure A21. ^{13}C NMR spectrum of **2.26** in CDCl$_3$, 125 MHz (+ = CH$_2$Cl$_2$).

218
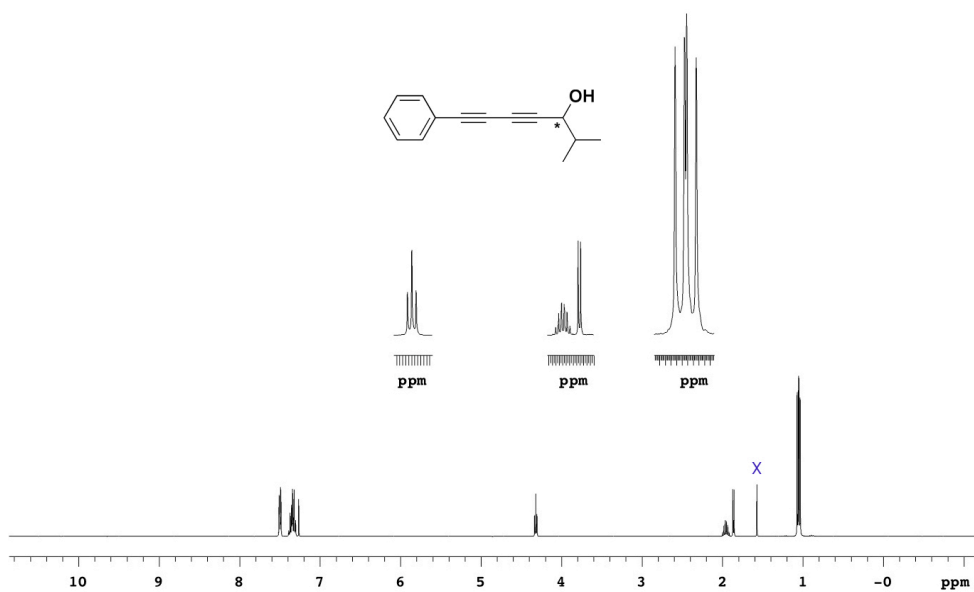
Figure A22. ^{1}H NMR spectrum of **2.29** in CDCl$_3$, 400 MHz (X = H$_2$O).
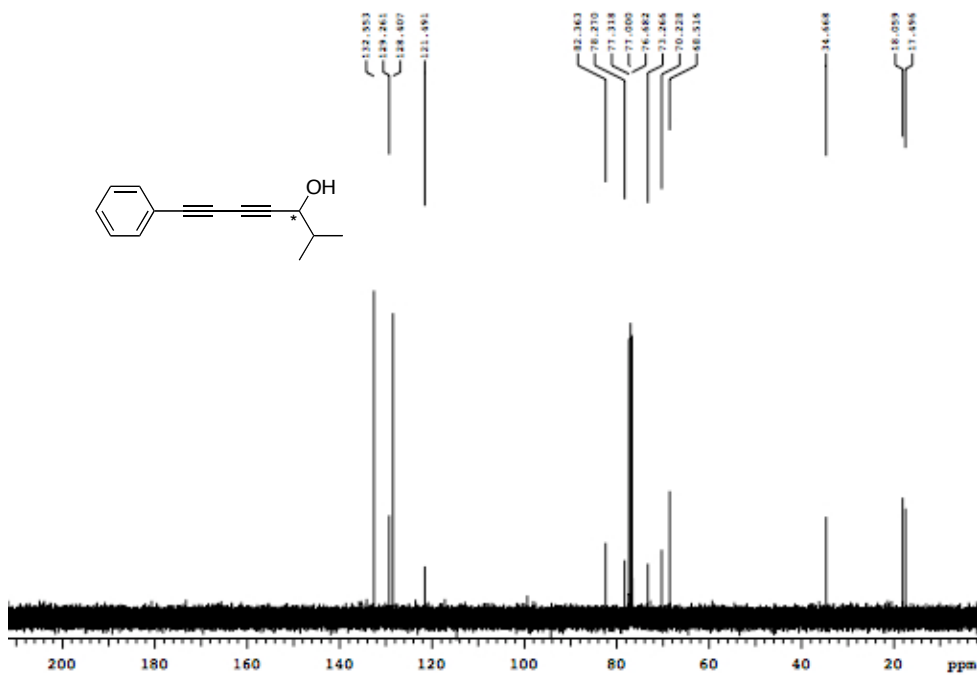
Figure A23. ^{13}C NMR spectrum of **2.29** in CDCl$_3$, 100 MHz.

219
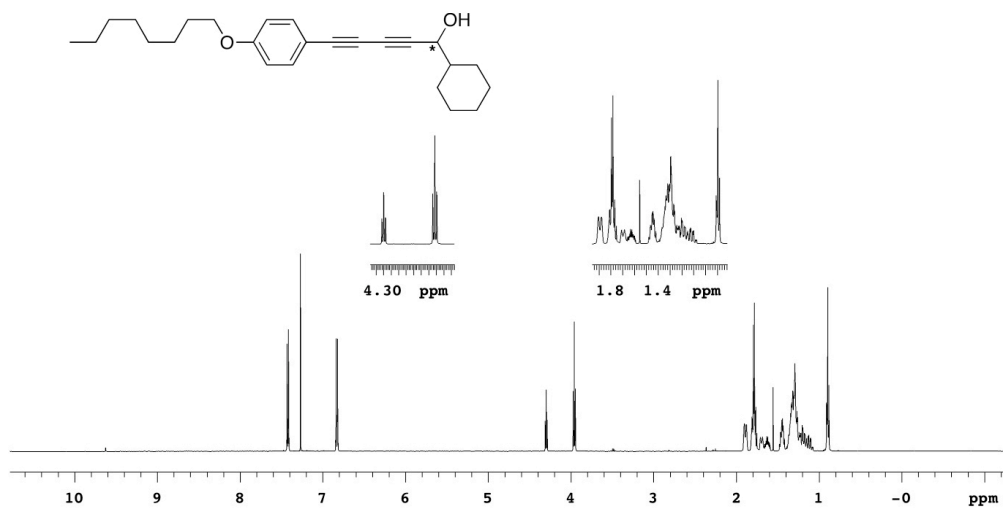
Figure A24. ^{1}H NMR spectrum of **2.30** in CDCl$_3$, 500 MHz.
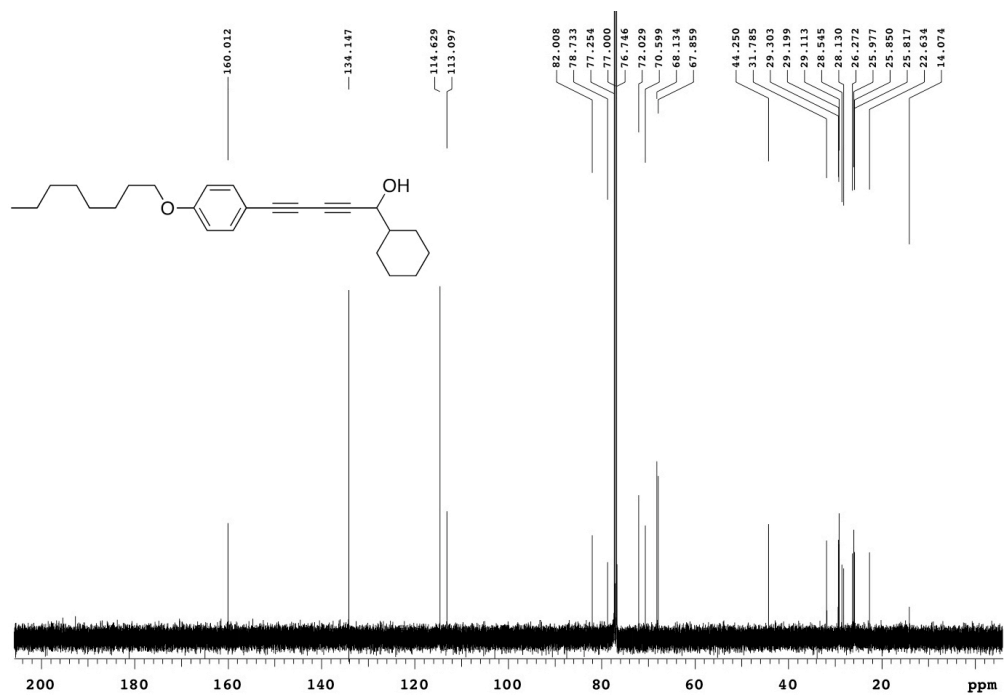
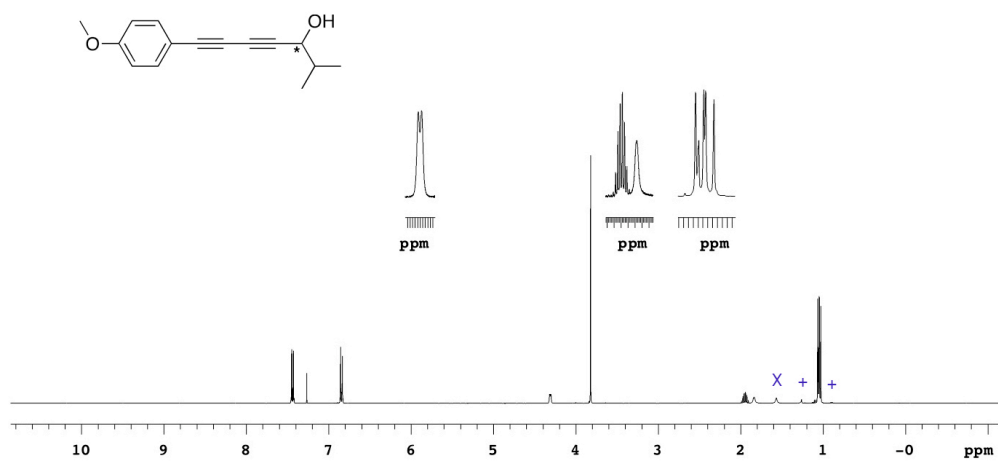Figure A25. ^{13}C NMR spectrum of **2.30** in CDCl$_3$, 125 MHz.

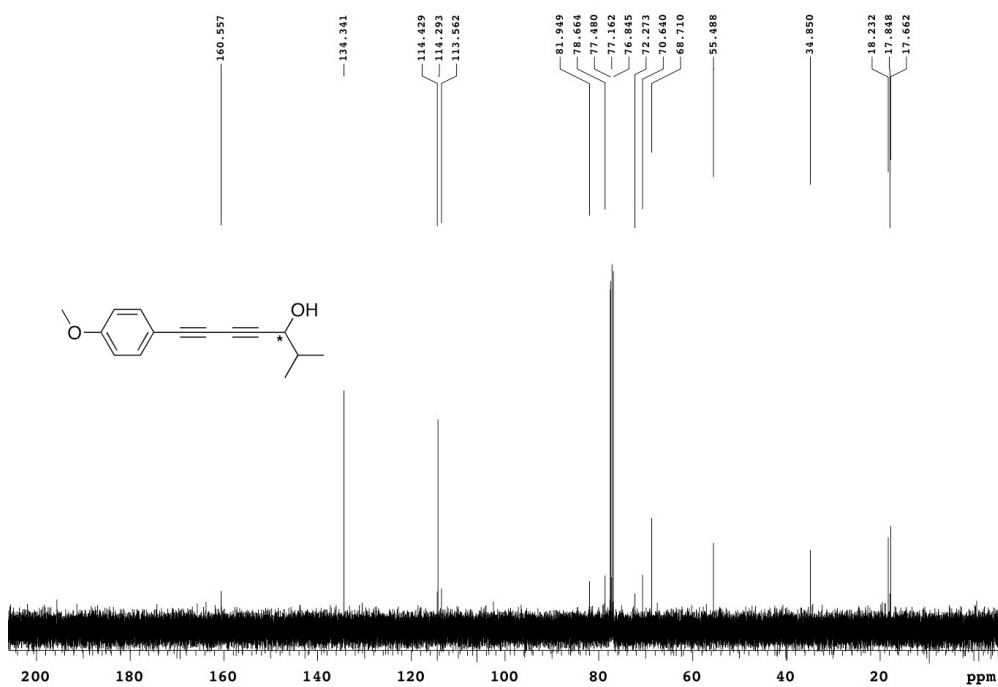Figure A26. ^{1}H NMR spectrum of **2.31** in CDCl$_3$, 400 MHz (X = H$_2$O, + = hexanes).
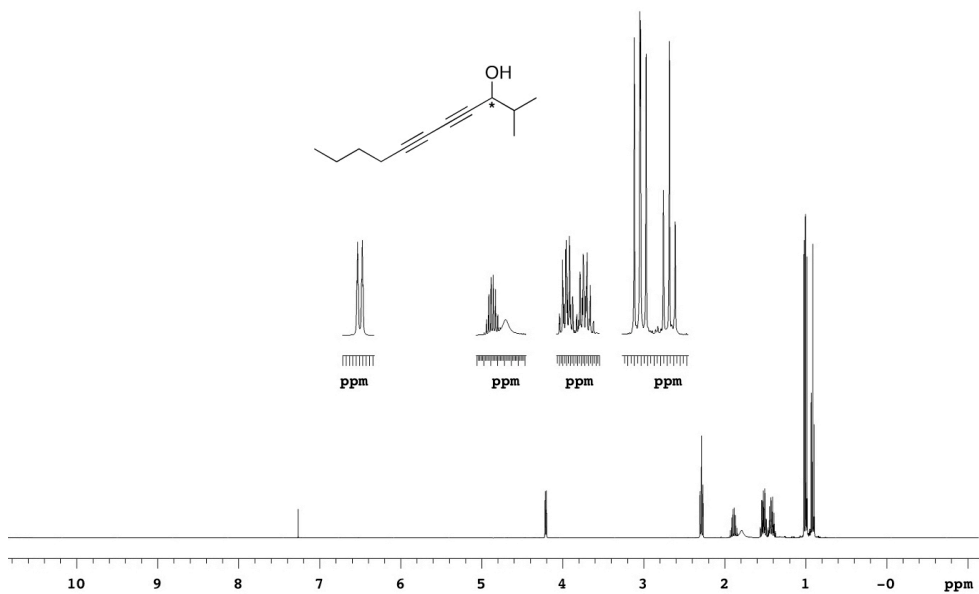

Figure A27. ^{13}C NMR spectrum of **2.31** in CDCl$_3$, 100 MHz.

Figure A28. ^{1}H NMR spectrum of **2.32** in CDCl$_3$, 400 MHz.

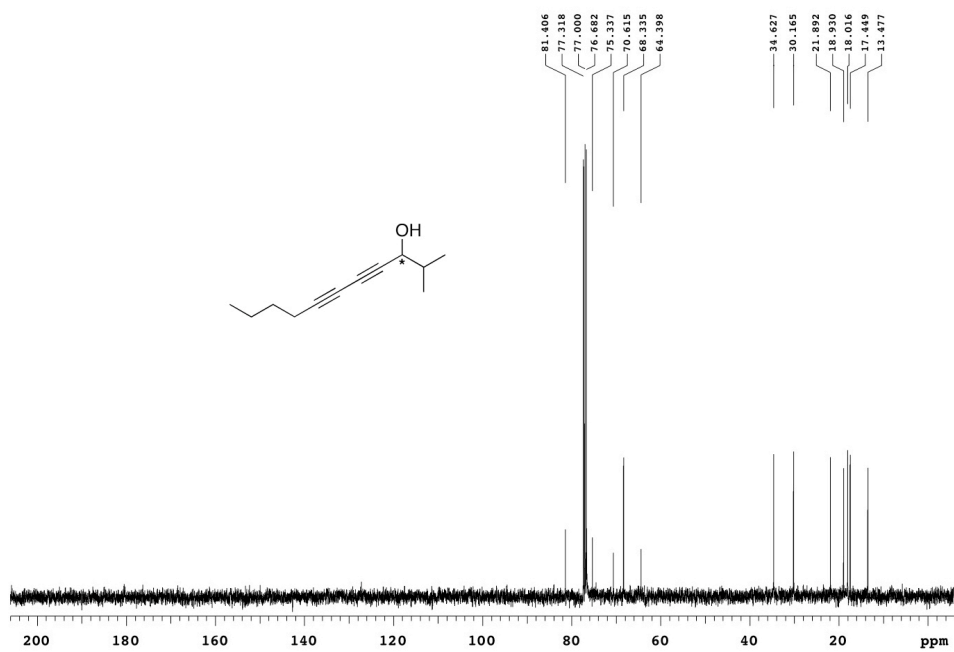Figure A29. ^{13}C NMR spectrum of **2.32** in CDCl$_3$, 100 MHz.
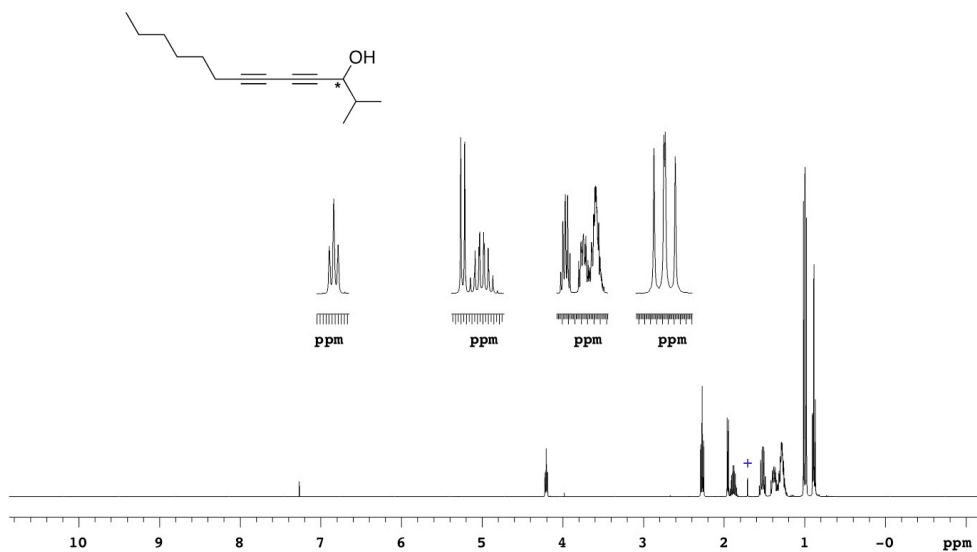
Figure A30. ^{1}H NMR spectrum of **2.33** in CDCl$_3$, 400 MHz (+ = H$_2$O).
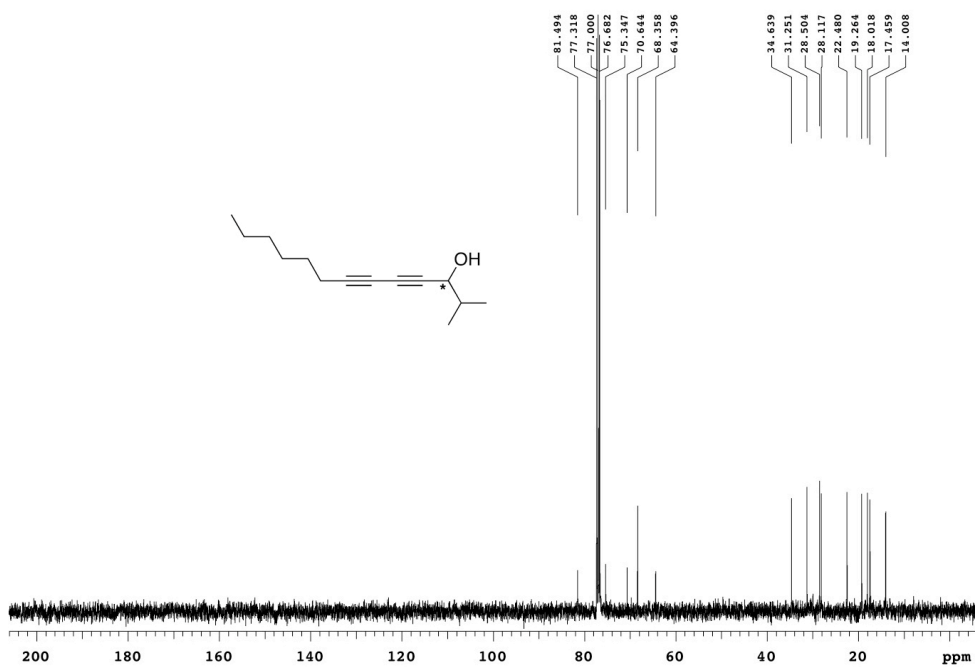
Figure A31. ^{13}C NMR spectrum of **2.33** in CDCl$_3$, 100 MHz.
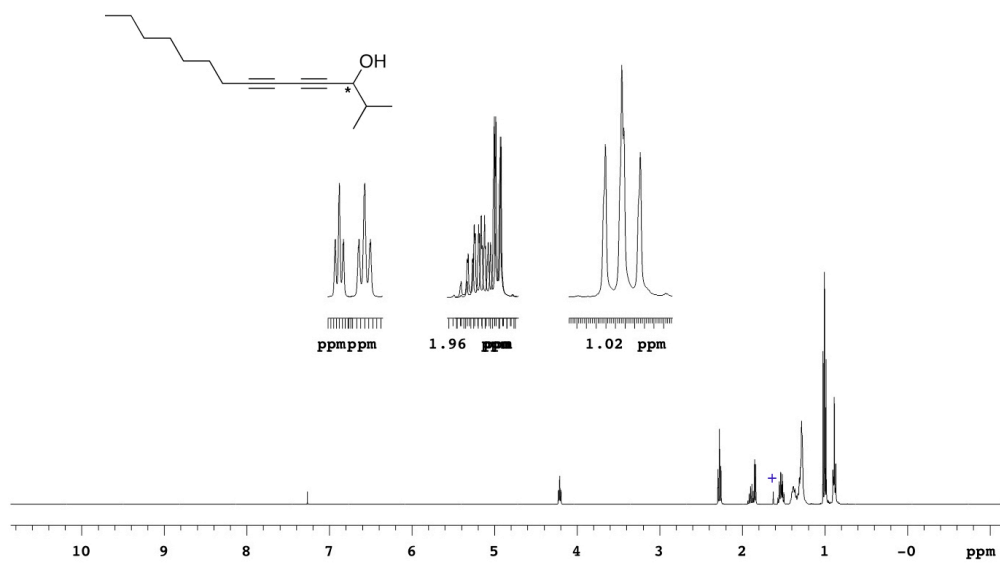
Figure A32. ^{1}H NMR spectrum of **2.34** in CDCl$_3$, 400 MHz (+ = H$_2$O).
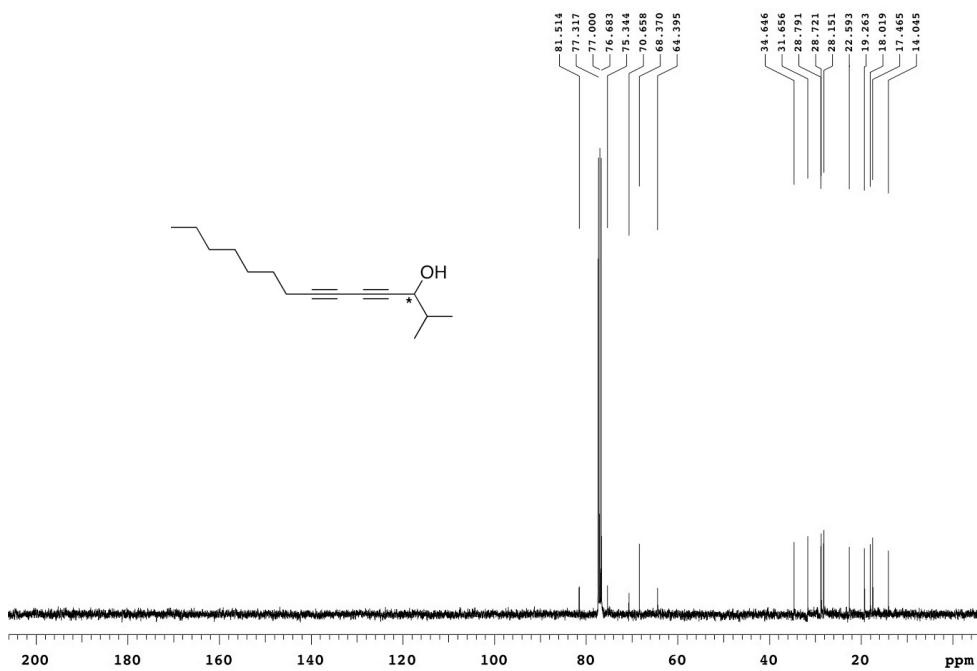
Figure A33. ^{13}C NMR spectrum of **2.34** in CDCl$_3$, 100 MHz.
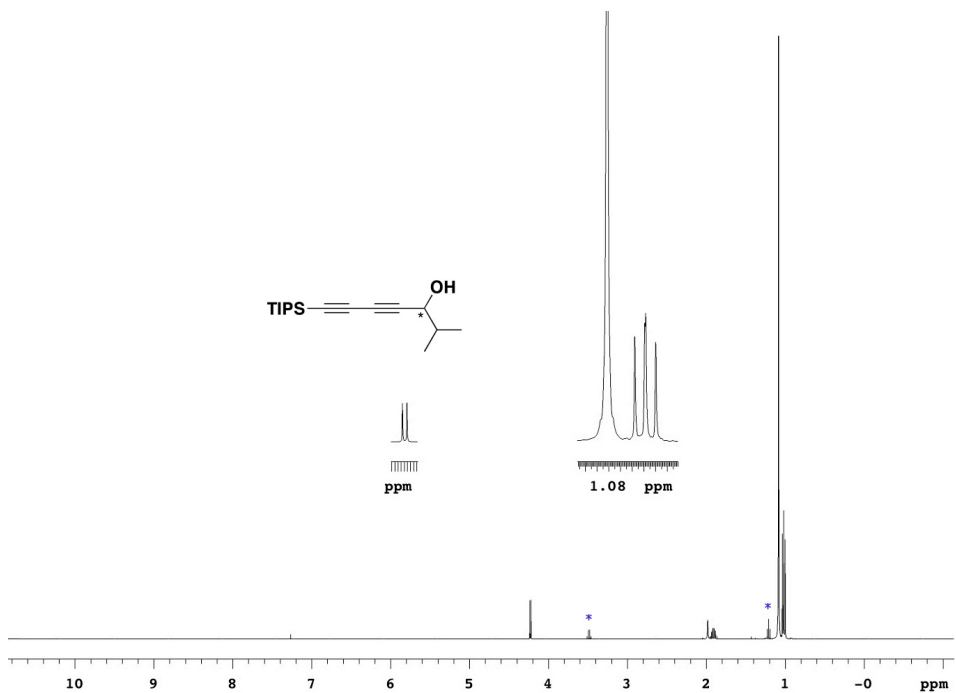
Figure A34. ^{1}H NMR spectrum of **2.35** in CDCl$_3$, 400 MHz (* = Et$_2$O).
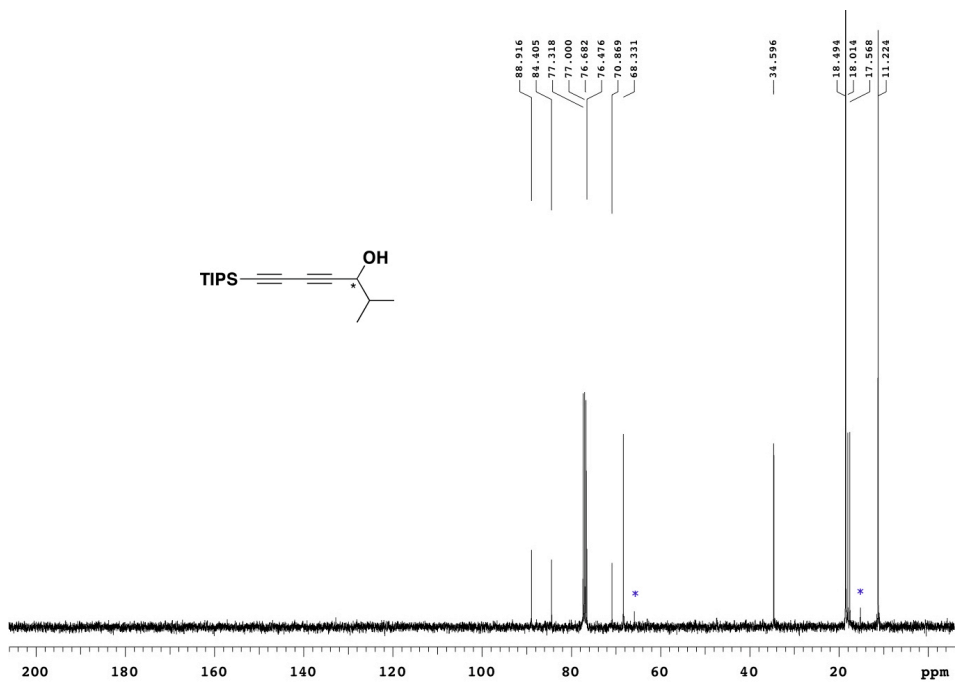
Figure A35. ^{13}C NMR spectrum of **2.35** in CDCl$_3$, 100 MHz (* = Et$_2$O).
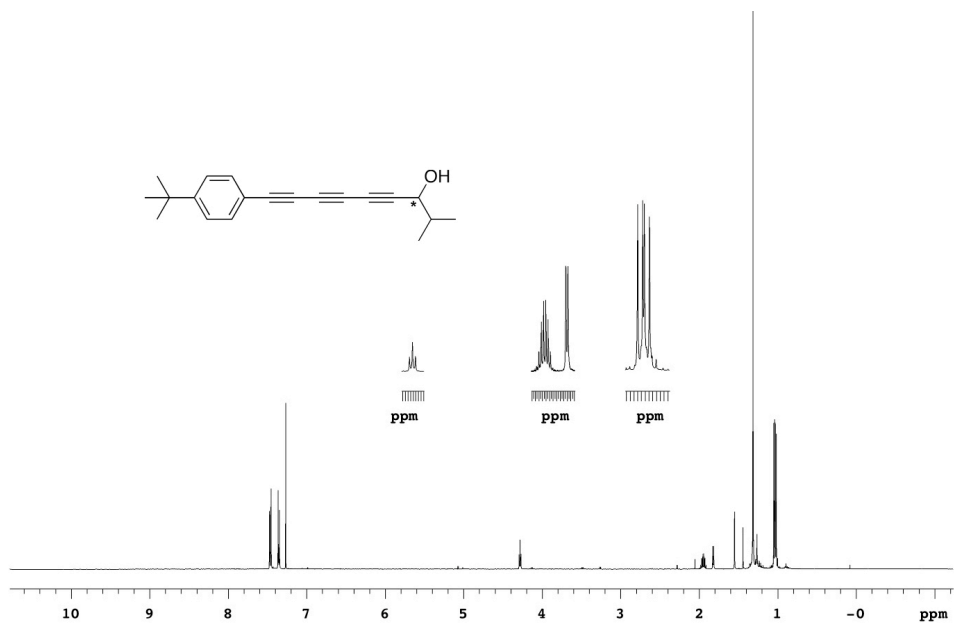
Figure A36. ^{1}H NMR spectrum of **2.38** in CDCl$_3$, 500 MHz.
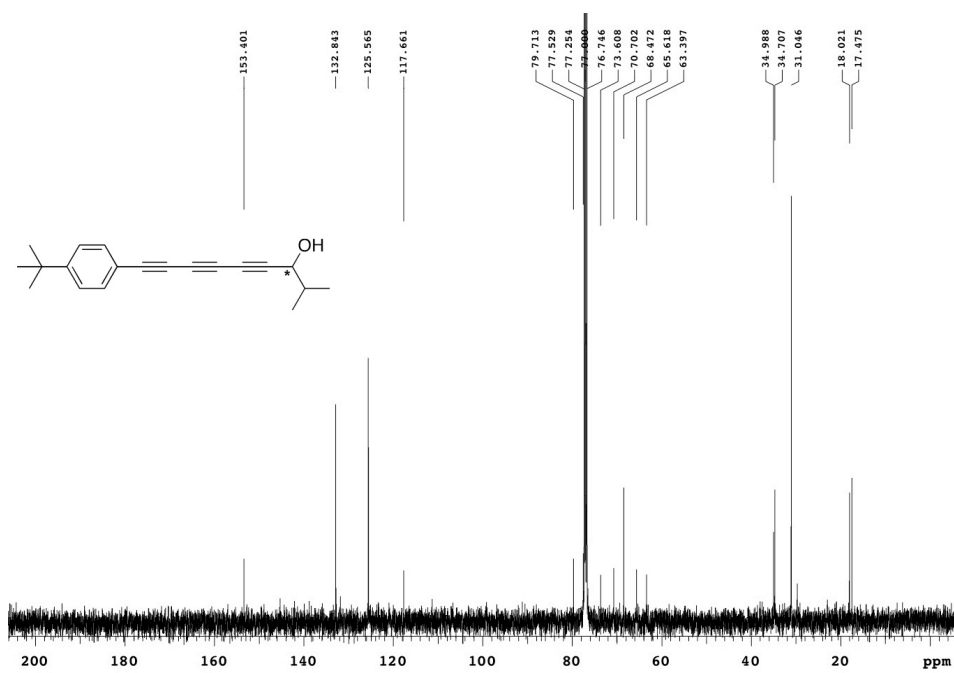
Figure A37. ^{13}C NMR spectrum of **2.38** in CDCl$_3$, 125 MHz.
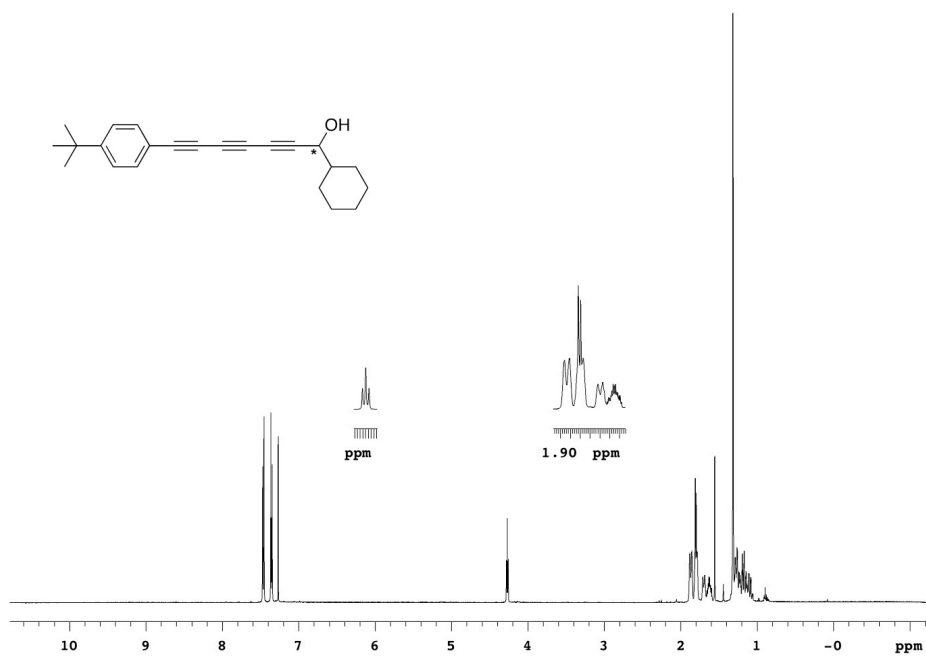
Figure A38. ^{1}H NMR spectrum of **2.39** in CDCl$_3$, 500 MHz.
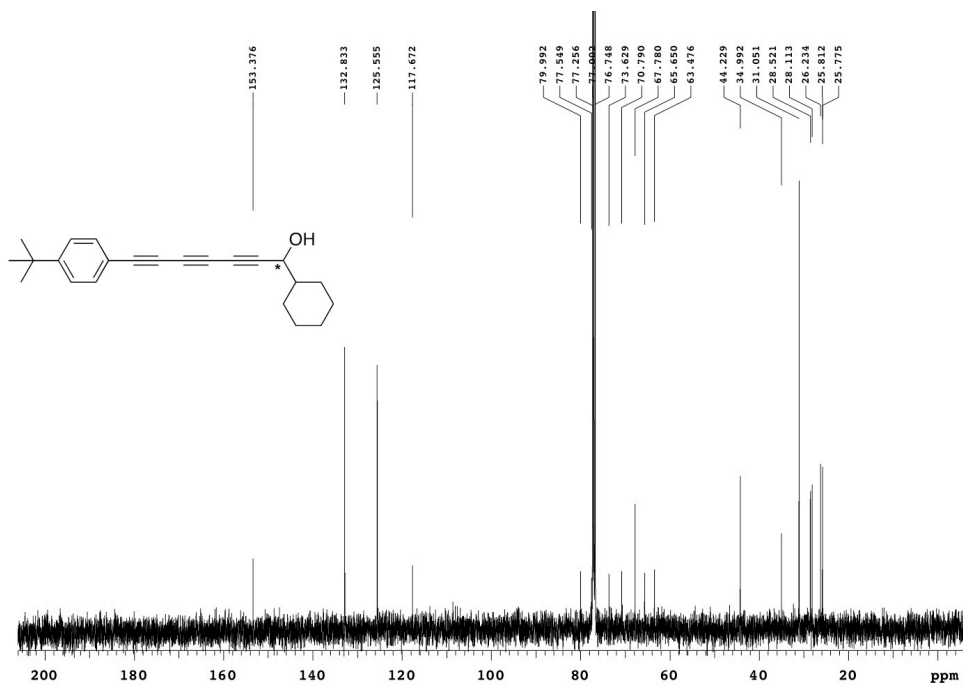
Figure A39. ^{13}C NMR spectrum of **2.39** in CDCl$_3$, 125 MHz.

227
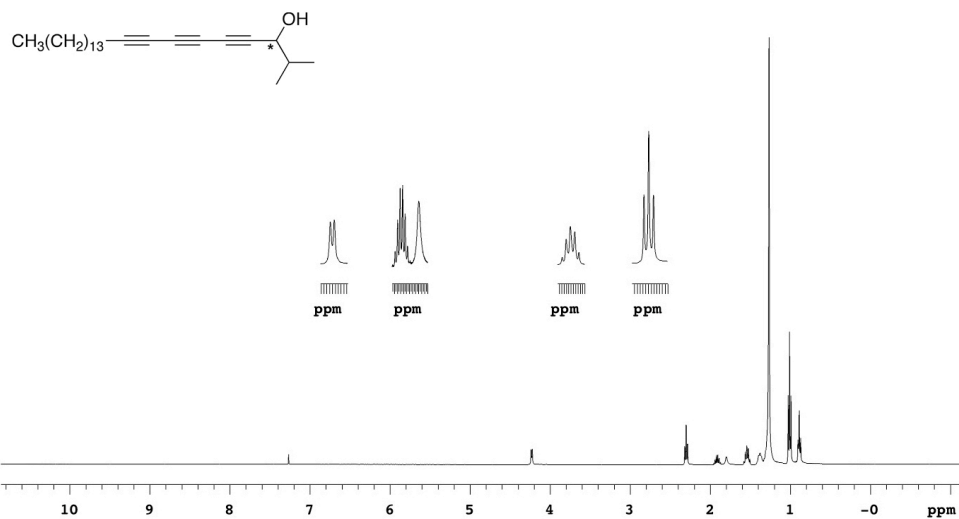
Figure A40. ^{1}H NMR spectrum of **2.40** in CDCl$_3$, 400 MHz.
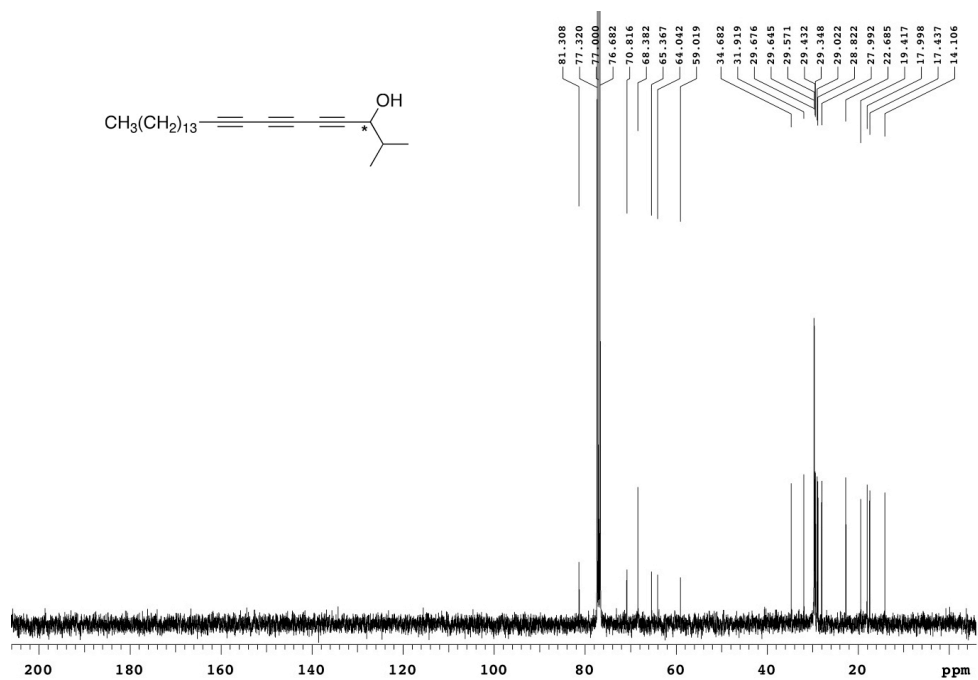
Figure A41. ^{13}C NMR spectrum of **2.40** in CDCl$_3$, 100 MHz.

228

Figure A42. ^{1}H NMR spectrum of **2.41** in CDCl$_3$, 400 MHz.

Figure A43. ^{13}C NMR spectrum of **2.41** in CDCl$_3$, 100 MHz.

229
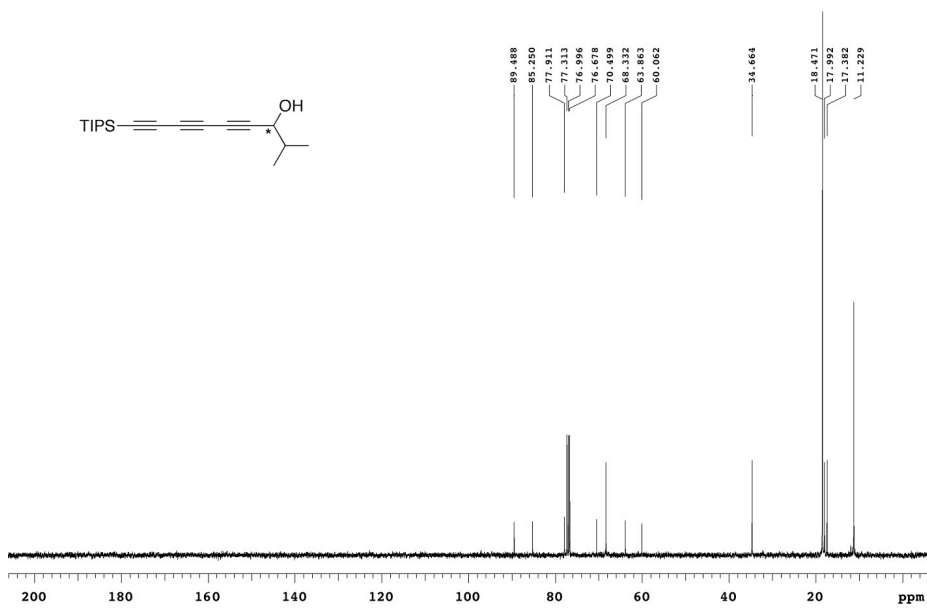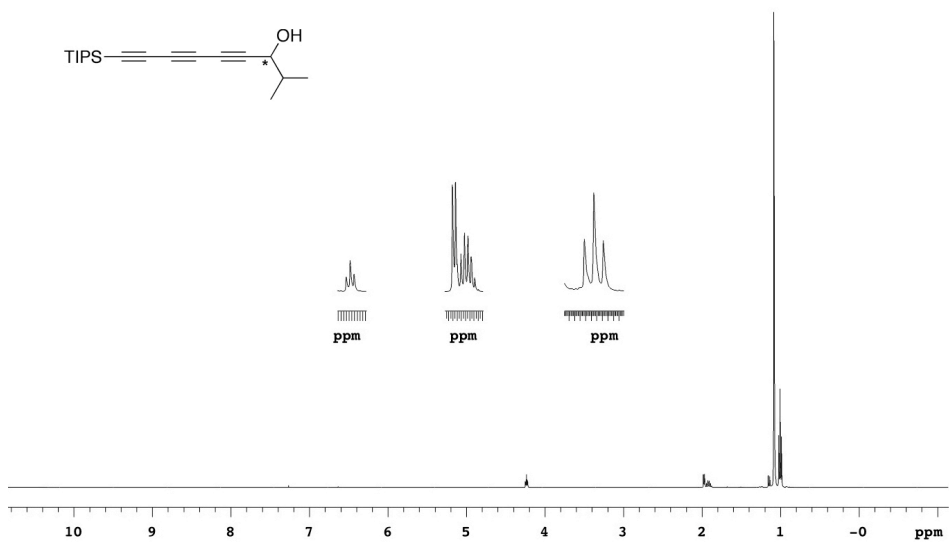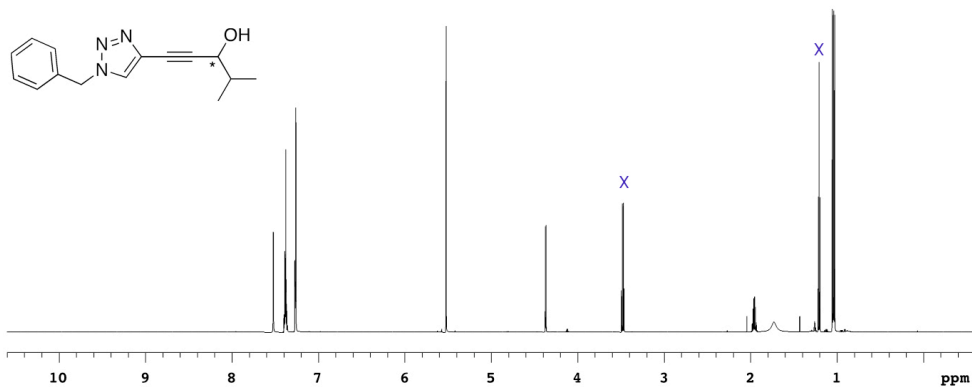
Figure A44. ^{1}H NMR spectrum of **2.42**, 700 MHz (X = Et$_2$O).
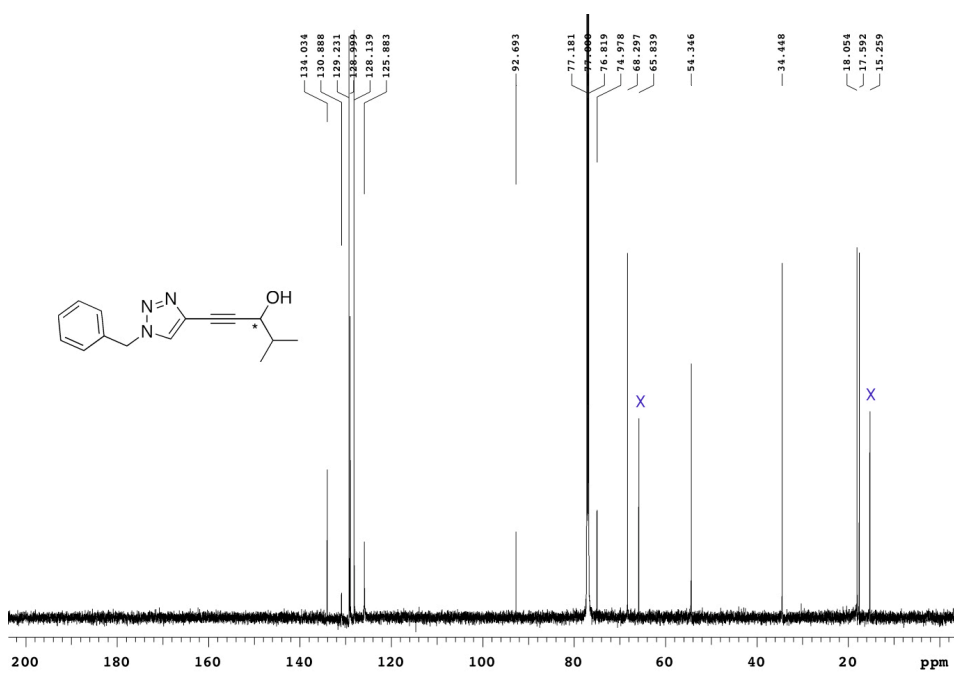
Figure A45. ^{13}C NMR spectrum of **2.42**, 175 MHz (X = Et$_2$O).
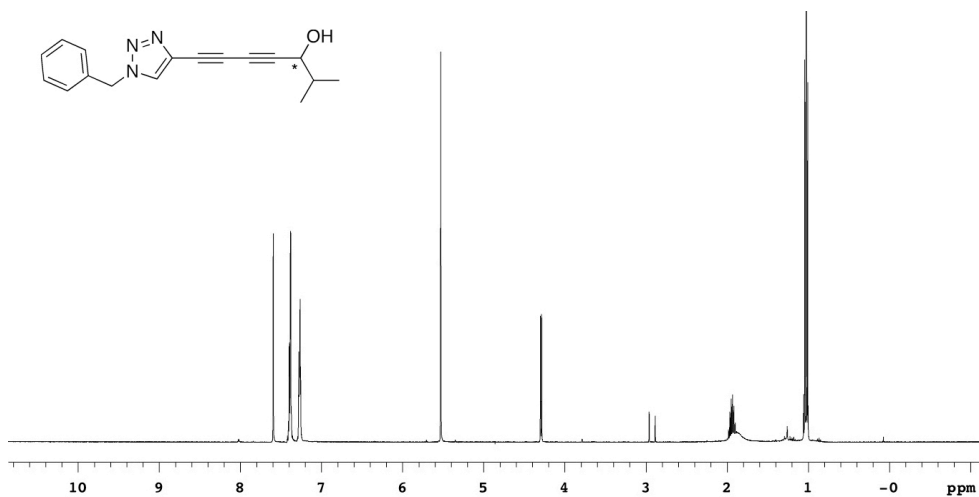
Figure A46. 1H NMR spectrum of **2.43**, 700 MHz.
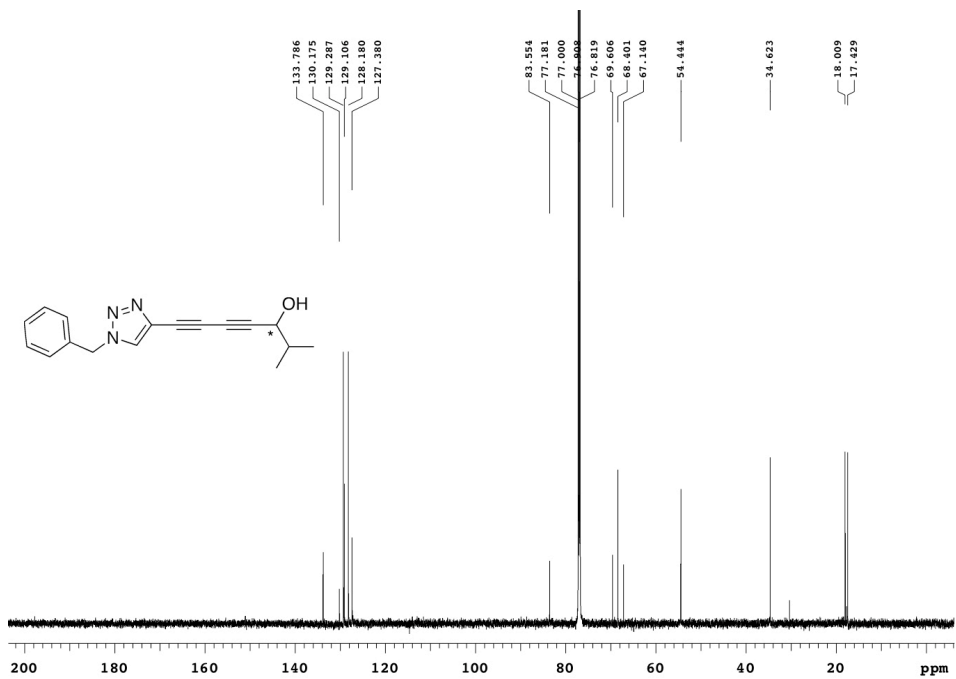
Figure A47. ^{13}C NMR spectrum of **2.43**, 175 MHz.

231

Figure   A48. ^{1}H   NMR   spectrum   of   2.46   (400MHz,   acetone   d$_6$).
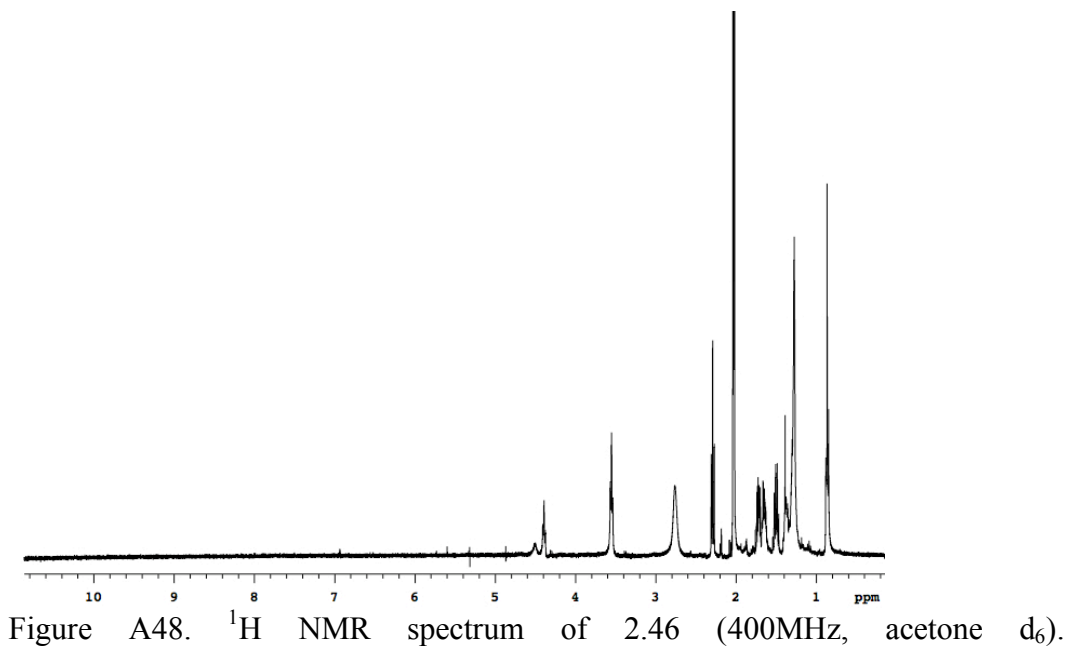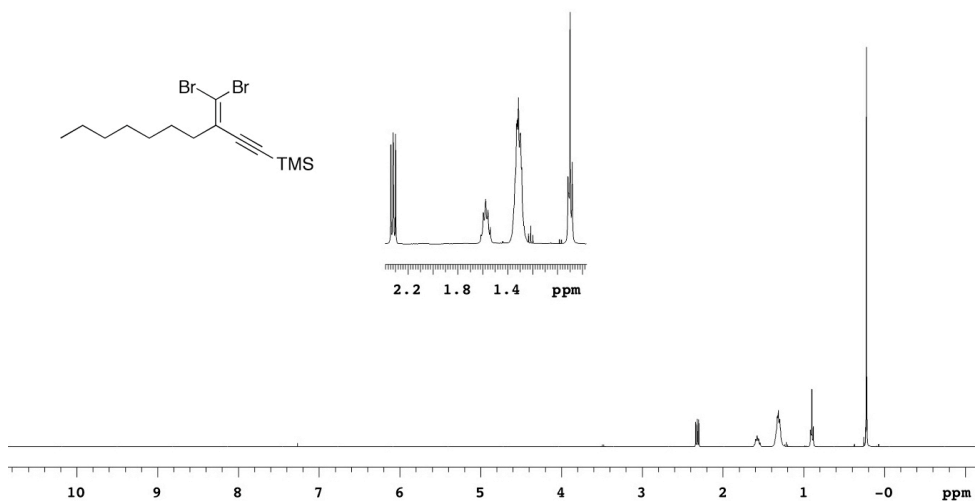
Figure A49. ^{1}H NMR spectrum of [3-(dibromomethylene)-1-decynyl]trimethylsilane in CDCl$_3$, 400 MHz.
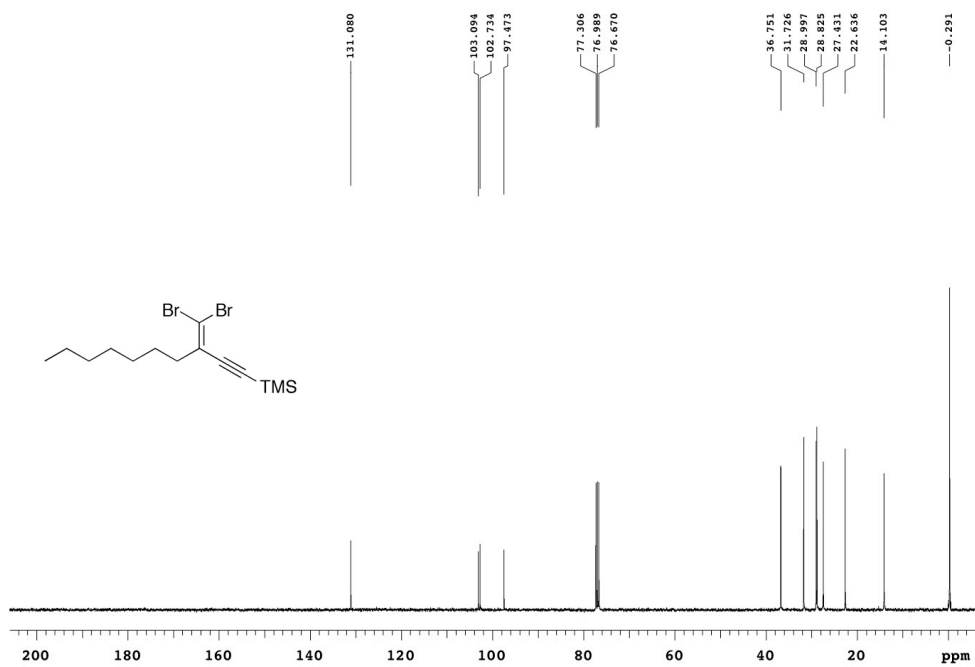
Figure A50. ^{13}C NMR spectrum of [3-(dibromomethylene)-1-decynyl]trimethylsilane in CDCl$_3$, 100 MHz.
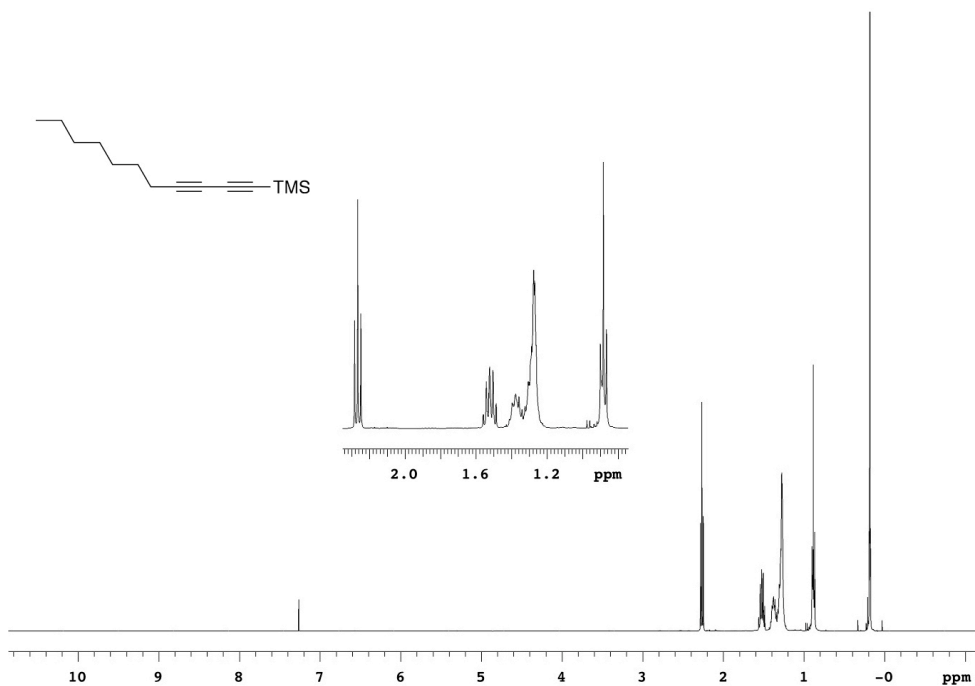
Figure A51. ^{1}H NMR spectrum of trimethyl-1,3-undecadiynylsilane in CDCl$_3$, 400 MHz.
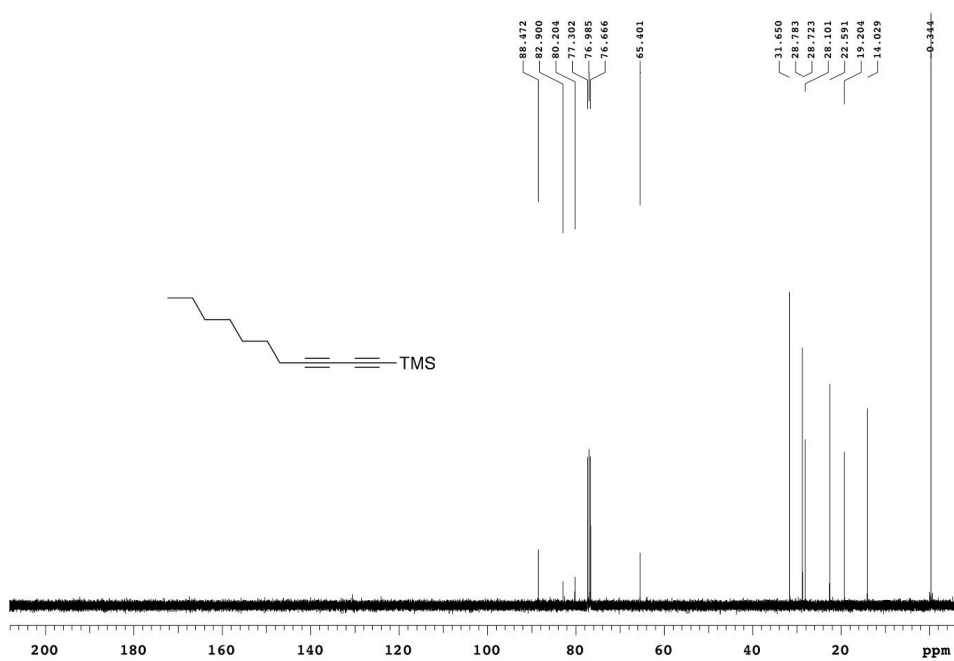
Figure A52. ^{13}C NMR spectrum of trimethyl-1,3-undecadiynylsilane in CDCl$_3$, 100 MHz.
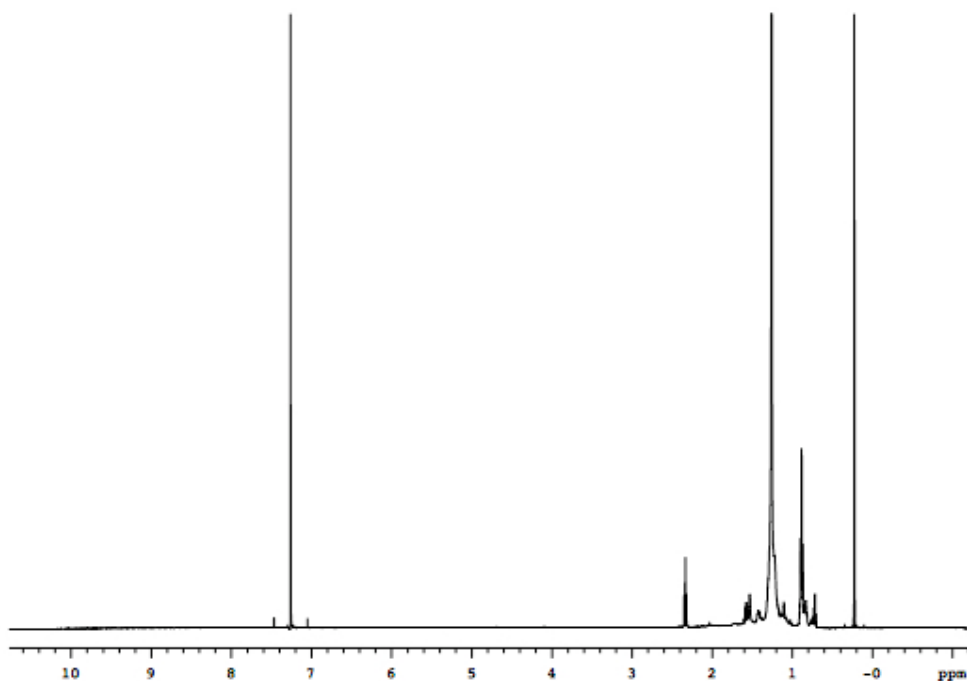
Figure A53. ^1H NMR spectrum of [5-(dibromomethylene)-1,4-nonadecadiynyl]trimethylsilane in CDCl₃, 500 MHz.
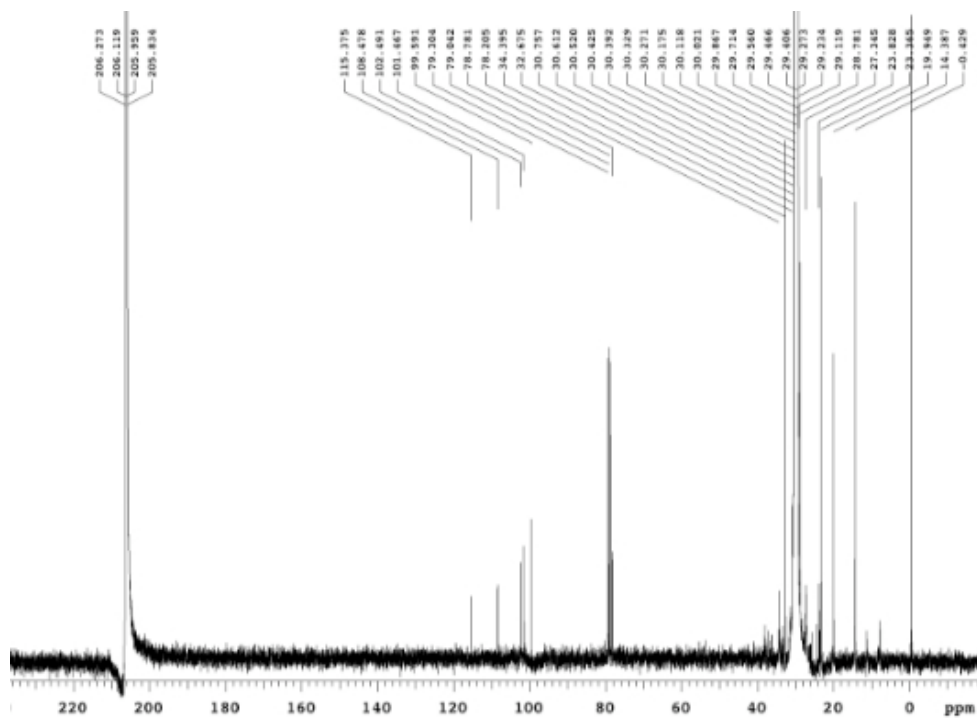
Figure A54. ^{13}C NMR spectrum of [5-(dibromomethylene)-1,4-nonadecadiynyl]trimethylsilane in (CD₃)₂CO, 125 MHz. Trace impurity CDCl₃.
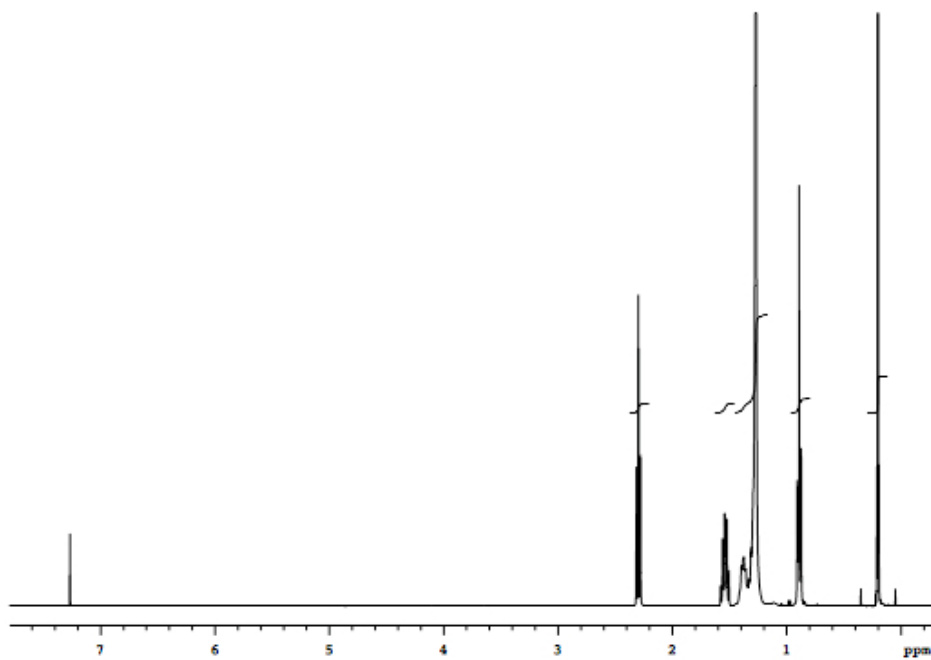
Figure A55. ^{1}H NMR of trimethyl-1,3,5-eicosyltriynylsilane in CDCl$_3$, 400 MHz.
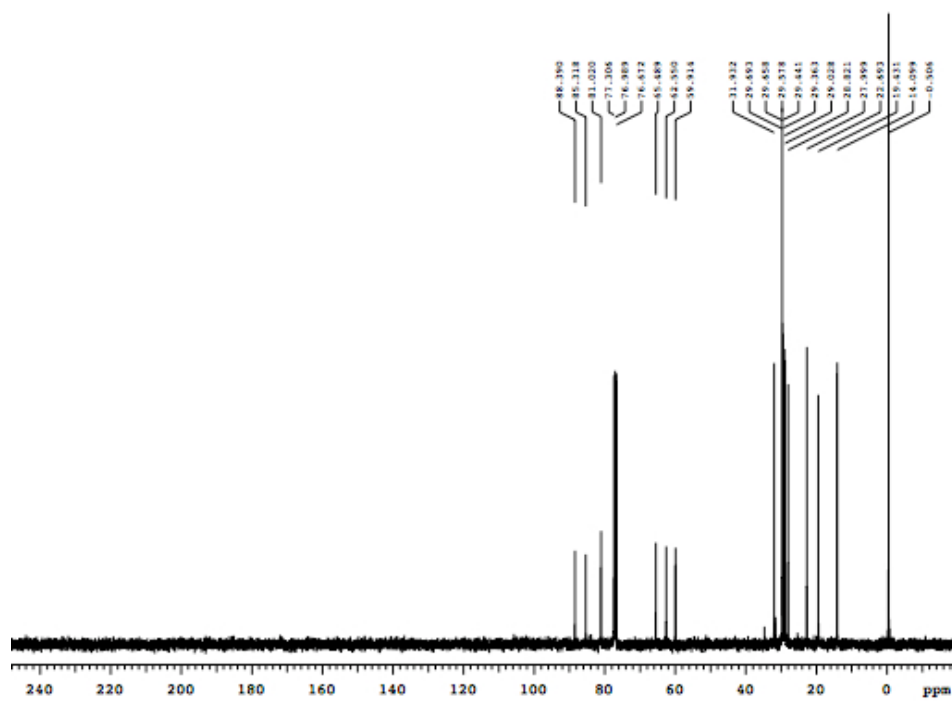
Figure A56. ^{13}C NMR of trimethyl-1,3,5-eicosyltriynylsilane in CDCl$_3$, 100 MHz.

A.3. HPLC traces and ^{19}F NMR spectra for new compounds from Chapter 2.


```
Area Percent Report
=============================================================================

Peak  RetTime Type  Width     Area       Height     Area
 #     [min]        [min]    [mAU*s]     [mAU]        %
----|--------|----|-------|-----------|-----------|--------|
  1   37.953 BB   0.8582 1190.19446   16.44826   50.7760
  2   41.416 BB   0.9578 1153.81384   14.89321   49.2240

Totals :                  2344.00830   31.34147
```
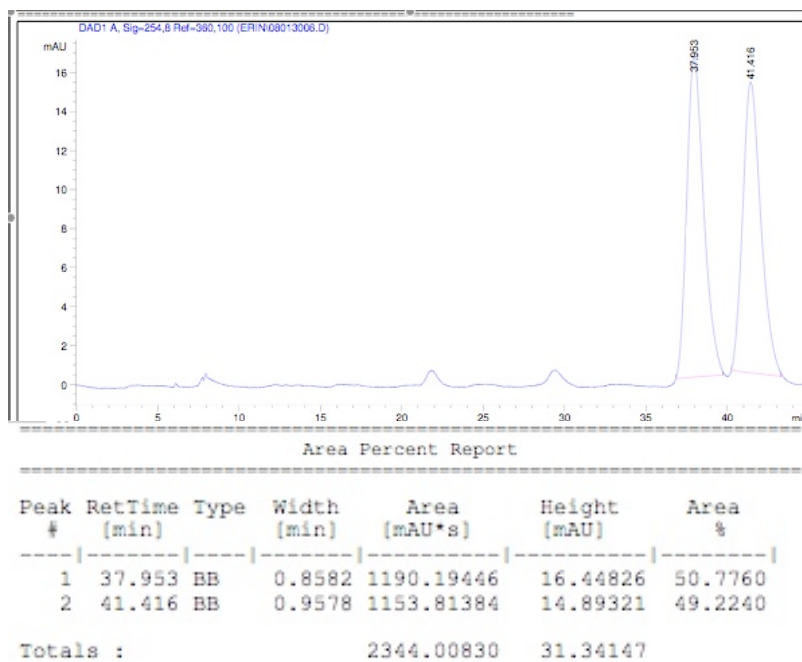
Figure A57. Racemic sample of **2.23**.


```
Area Percent Report
=============================================================================

Peak  RetTime Type  Width     Area       Height     Area
 #     [min]        [min]    [mAU*s]     [mAU]        %
----|--------|----|-------|-----------|-----------|--------|
  1   38.111 BB   1.1354 6571.26172   86.20113   97.6568
  2   41.686 MM   1.2794  157.67551    2.05406    2.3432

Totals :                  6728.93723   88.25519
```
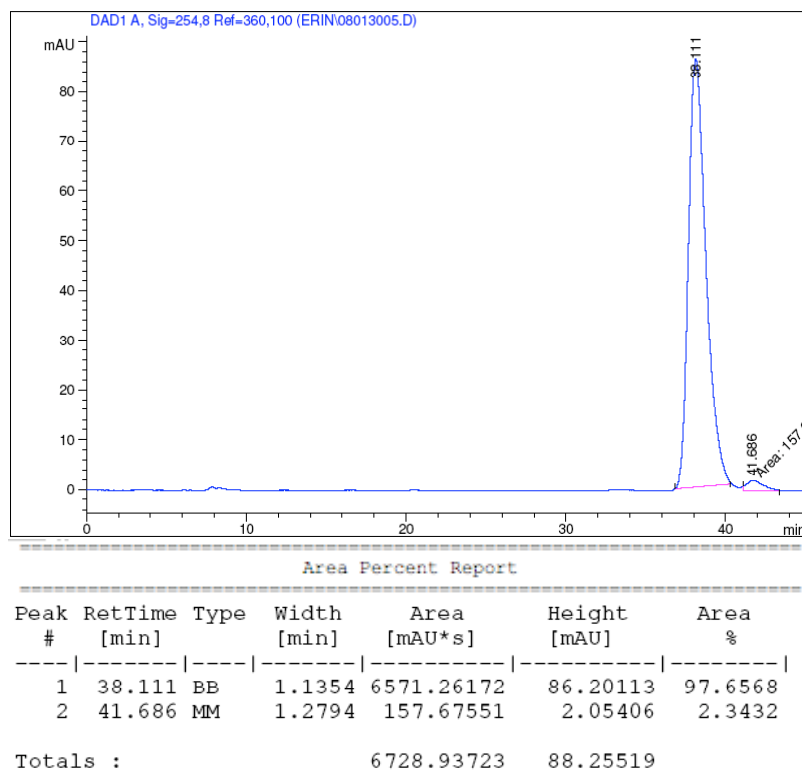
Figure A58. Optically enriched sample of (*S*)-(+)-**2.23** (Table 1, Entry 1).
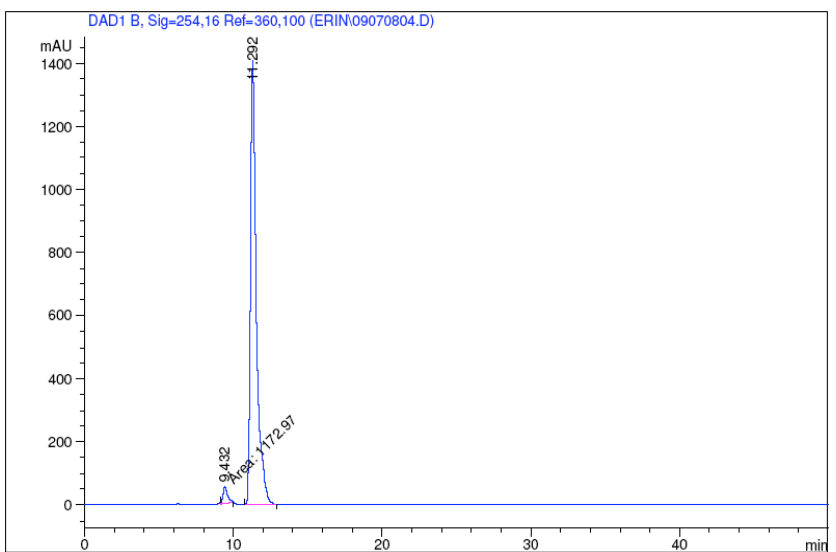
237

```
                          Area Percent Report
===============================================================================
Peak RetTime Type   Width      Area        Height      Area
  #    [min]        [min]    [mAU*s]        [mAU]        %
----|-------|----|-------|----------|----------|--------|
   1   9.432 MM    0.3590 1172.96936   54.45091    2.9146
   2  11.292 BB    0.4089 3.90710e4  1411.55530   97.0854

Totals :                    4.02439e4  1466.00621
```

Figure A59. Optically enriched sample of (*R*)-(–)-**2.23** (Table 1, Entry 2).

Figure A60. Racemic sample of the (*S*)-Mosher ester adduct of **2.24** (^{19}F NMR spectrum, 470 MHz).

Figure A61. Optically enriched sample of (*R*)-Mosher ester adduct of (*S*)-(+)-**2.24**; ^{19}F NMR spectrum, 376 MHz (Table 1, Entry 3).

Figure A62. Optically enriched sample of the (*S*)-Mosher ester adduct of (*S*)-(+)-**2.24**; ^{19}F NMR spectrum, 376 MHz.
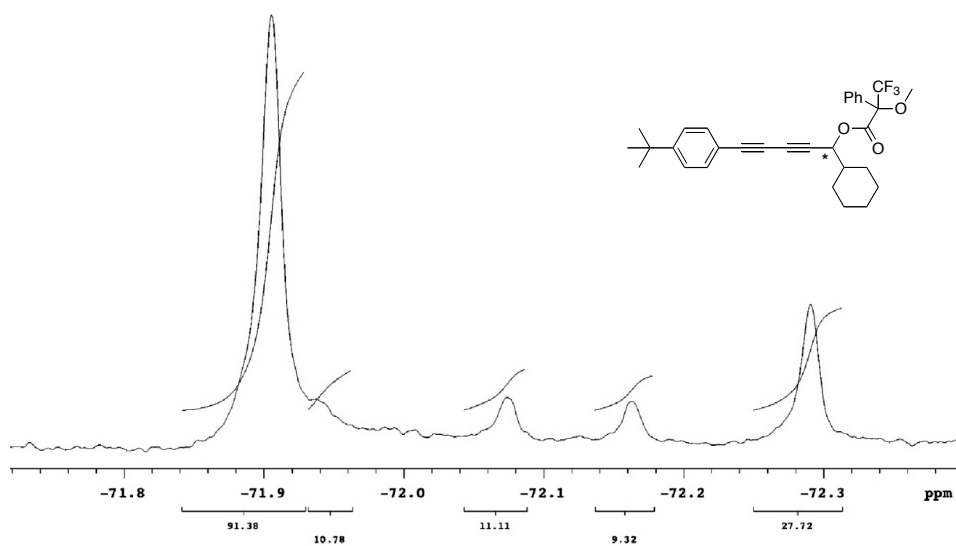
Figure A63. Optically enriched sample of (*S*)-Mosher ester adduct of (*S*)-(+)-**2.24** spiked with racemic **2.24**; ^{19}F NMR spectrum, 376 MHz.

240
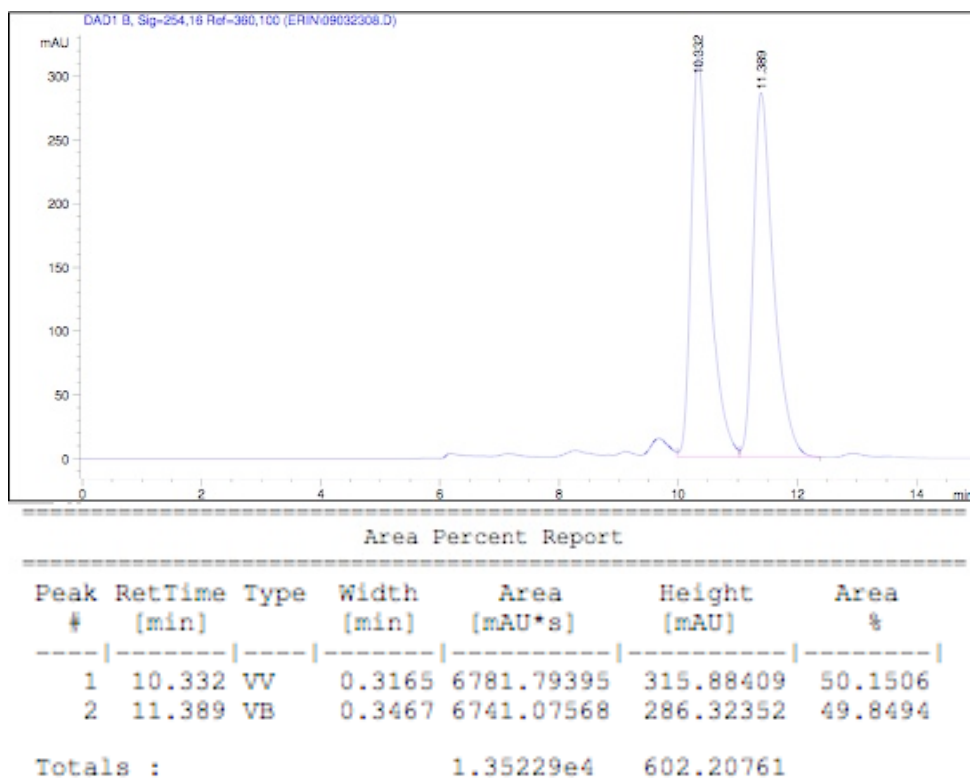
Figure A64. Racemic sample of **2.25**.

Area Percent Report

Peak #	RetTime [min]	Type	Width [min]	Area [mAU*s]	Height [mAU]	Area %
1	10.332	VV	0.3165	6781.79395	315.88409	50.1506
2	11.389	VB	0.3467	6741.07568	286.32352	49.8494

Totals :   1.35229e4   602.20761

Area Percent Report

Peak #	RetTime [min]	Type	Width [min]	Area [mAU*s]	Height [mAU]	Area %
1	10.320	MM	0.2917	600.12207	34.28689	5.2005
2	11.384	VB	0.3482	1.09395e4	465.46857	94.7995
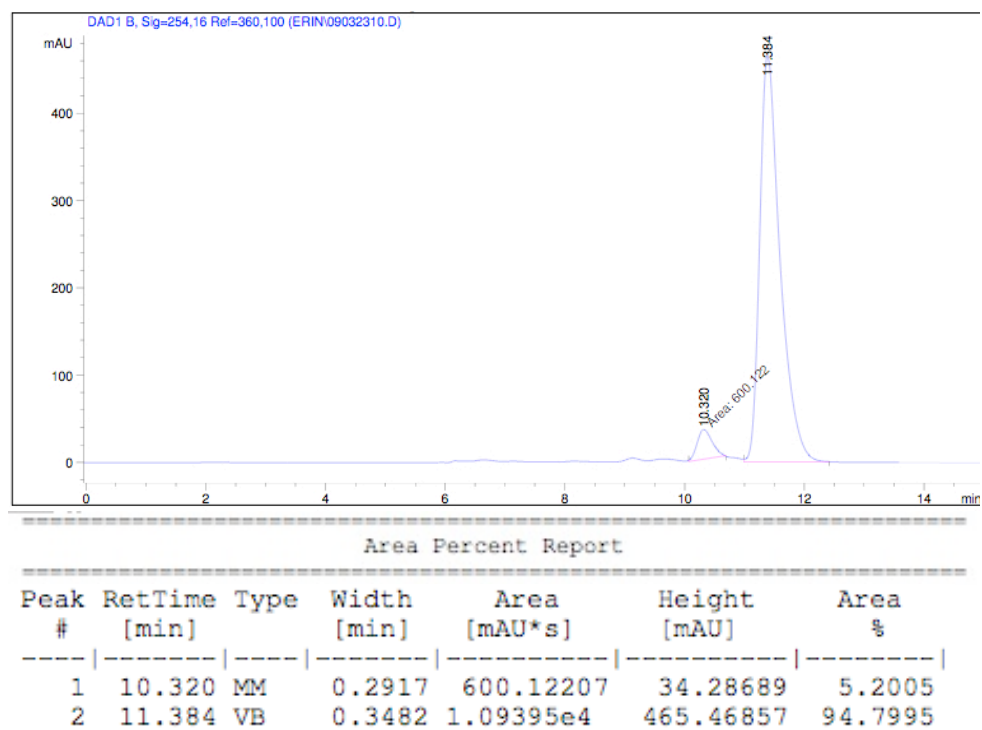
Figure A65. Optically enriched sample of (*R*)-(−)-**2.25** (Table 1, Entry 4).
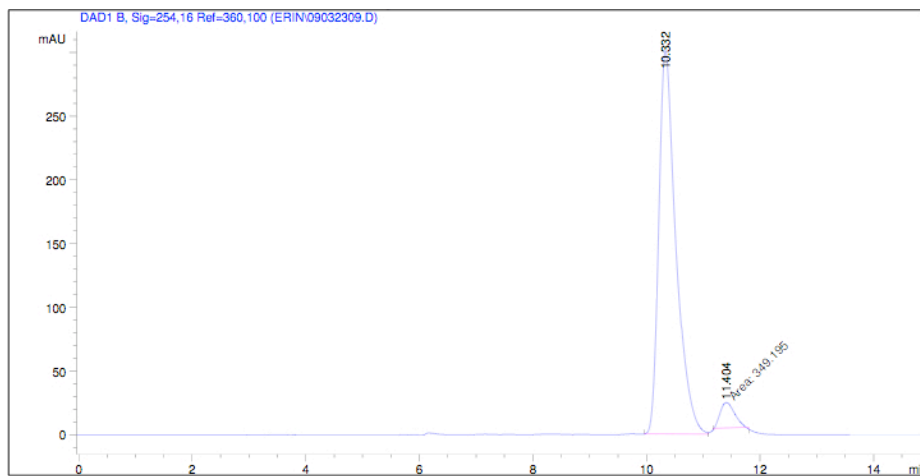
```
                    Area Percent Report
========================================================

Peak RetTime Type  Width     Area        Height     Area
 #    [min]        [min]    [mAU*s]       [mAU]       %
----|-------|----|-------|-----------|-----------|--------|
  1  10.332 PV   0.3115 6332.45850   300.88315   94.7738
  2  11.404 MM   0.2899  349.19525    20.07327    5.2262

Totals :                6681.65375   320.95642
```

Figure A66. Optically enriched sample of (*S*)-(+)-**2.25** (Table 1, Entry 5).

Figure A67. Racemic sample of (*S*)-Mosher ester adduct of **2.26**; ^{19}F NMR spectrum, 376 MHz.
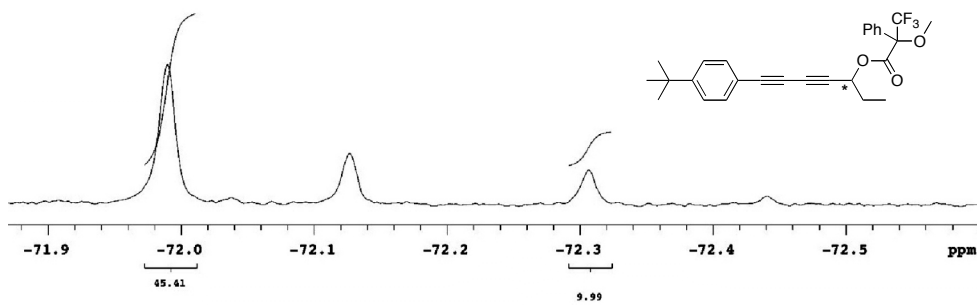
Figure A68. Optically enriched sample of (*S*)-Mosher ester adduct of (*S*)-(−)-**2.26**; ^{19}F NMR spectrum, 376 MHz (Table 1, Entry 6).
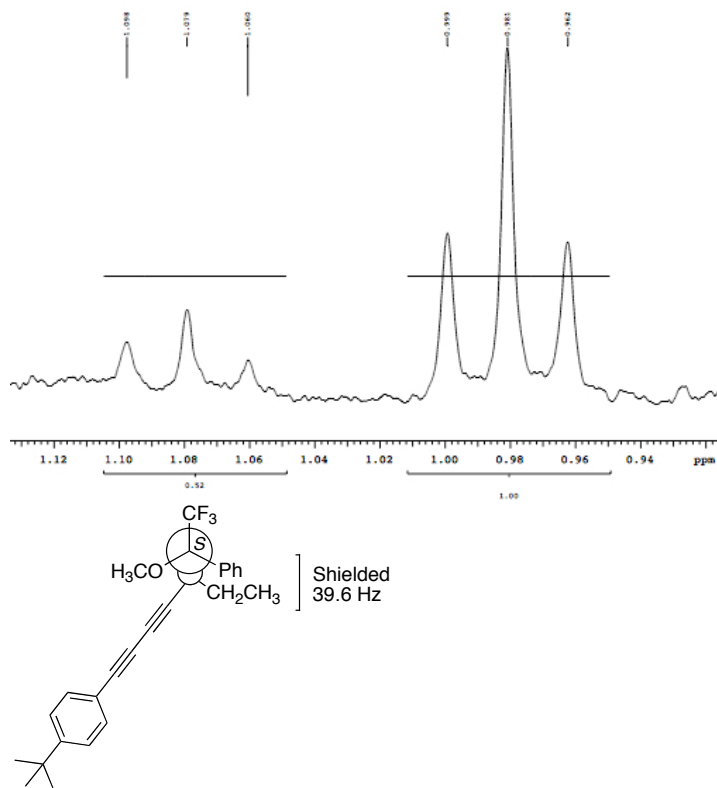
Figure A69. ^{1}H NMR spectrum of the (*S*)-Mosher ester of (*S*)-(−)-**2.26**. Right: Absolute configuration of (−)-**2.26** was determined to be the (*S*)-enantiomer using the modified Mosher method.

```
                DAD1 B, Sig=254,16 Ref=360,100 (ERIN\08062402.D)
  mAU
                                        8.864
                                        9.632
  250

  200

  150

  100

   50

    0

         0          5          10          15          20
```

Area Percent Report
===

```
Peak  RetTime  Type  Width       Area        Height      Area
 #     [min]         [min]    [mAU*s]        [mAU]        %
----|--------|-----|-------|-----------|-----------|--------|
  1   8.864   VV    0.2507  4912.91309  285.59427   48.5306
  2   9.632   VB    0.2903  5210.41357  261.68332   51.4694

Totals :                    1.01233e4   547.27759
```

Figure A70. Racemic sample of **2.29**.


```
                DAD1 B, Sig=254,8 Ref=360,100 (ERIN\09102005.D)
  mAU
                                        8.971
  500

  400

  300

  200

  100
                                              9.843
    0

         0     2.5     5     7.5    10    12.5    15    17.5   min
```

Area Percent Report
===

```
Peak  RetTime  Type  Width       Area        Height      Area
 #     [min]         [min]    [mAU*s]        [mAU]        %
----|--------|-----|-------|-----------|-----------|--------|
  1   8.971   BV    0.2444  9042.27832  537.02722   96.0880
  2   9.843   VB    0.2789   368.13391   19.09340    3.9120

Totals :                    9410.41223  556.12062
```
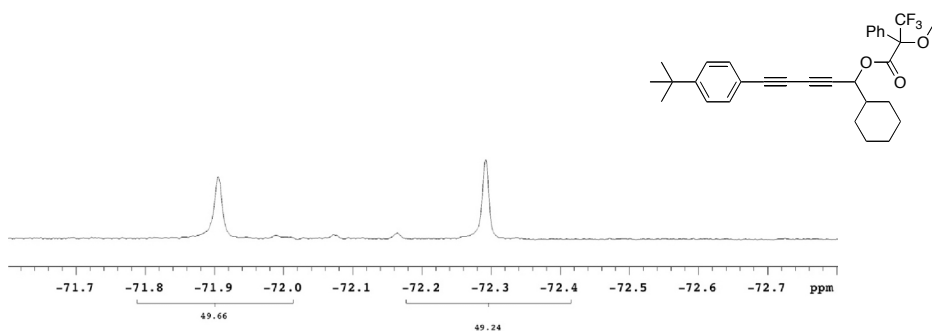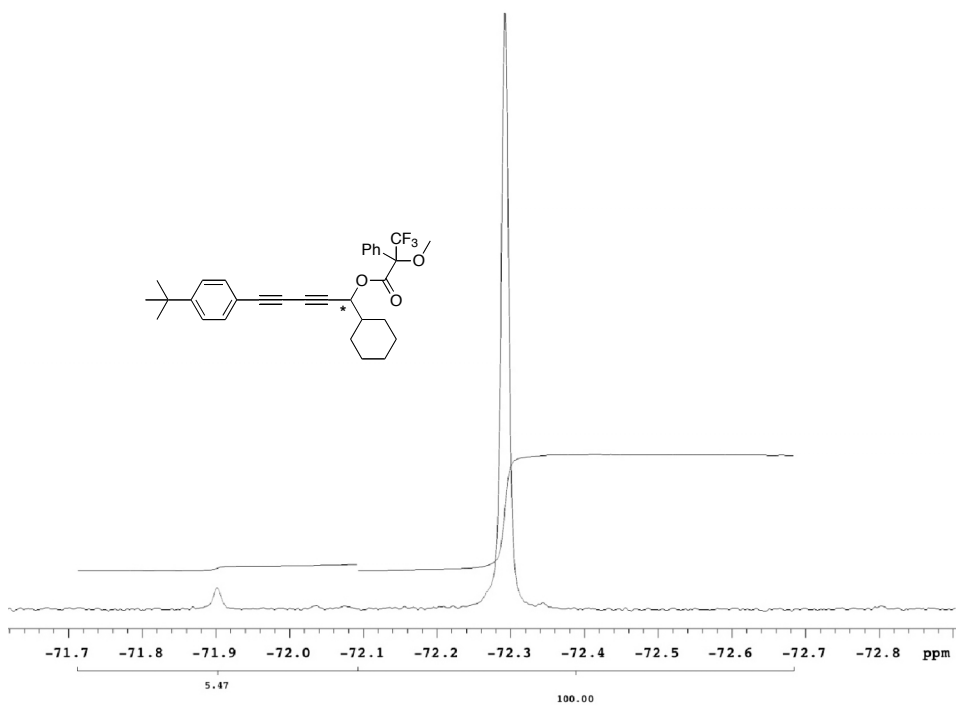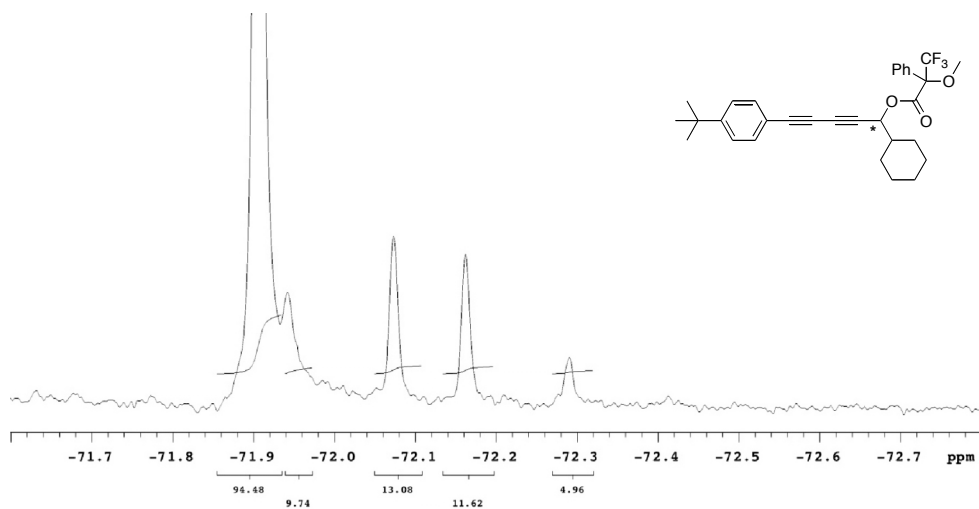
Figure A71. Optically enriched sample of (*R*)-(–)-**2.29**.

Figure A72. Racemic sample of (*S*)-Mosher ester adduct of **2.30**; ^{19}F NMR spectrum, 376 MHz.

Figure A73. Optically enriched sample of (*S*)-Mosher ester adduct of (*S*)-(+)-**2.30**; ^{19}F NMR spectrum, 376 MHz.

Figure A74.Racemic sample of (*S*)-Mosher ester adduct of **2.30**; ^{1}H NMR spectrum, 400 MHz.

Figure A75. Optically enriched sample of the (*S*)-Mosher ester adduct of (*S*)-(+)-**2.30**; ^{1}H NMR spectrum, 400 MHz.

```
DAD1 B, Sig=254,16 Ref=360,100 (ERIN\09091604.D)

=============================================================
                    Area Percent Report
=============================================================

Peak  RetTime Type  Width     Area        Height      Area
 #     [min]        [min]    [mAU*s]       [mAU]        %
----|--------|----|-------|-----------|-----------|--------|
  1  42.071  BB   1.3720  7988.97949   85.66622   50.1293
  2  49.300  BB   1.4048  7947.76367   81.70779   49.8707

Totals :                  1.59367e4   167.37401
```
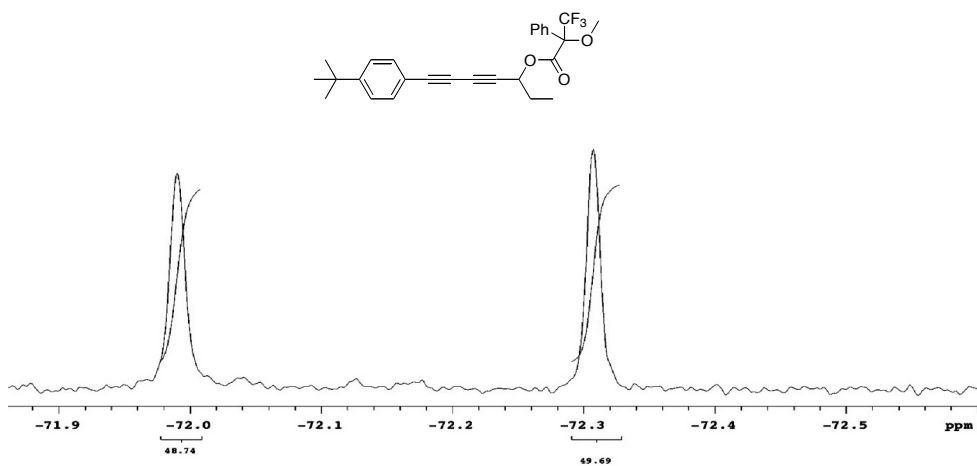
Figure A76. Racemic sample of **2.31**.


```
DAD1 B, Sig=254,16 Ref=360,100 (ERIN\09091605.D)

=============================================================
                    Area Percent Report
=============================================================

Peak  RetTime Type  Width     Area        Height      Area
 #     [min]        [min]    [mAU*s]       [mAU]        %
----|--------|----|-------|-----------|-----------|--------|
  1  42.619  MM   1.3482  1.96623e4   243.06831   98.9398
  2  49.367  MM   1.0224  210.69543     3.43449    1.0602

Totals :                  1.98730e4   246.50280
```

Figure A77. Optically enriched sample of (S)-(+)-**2.31**.

248
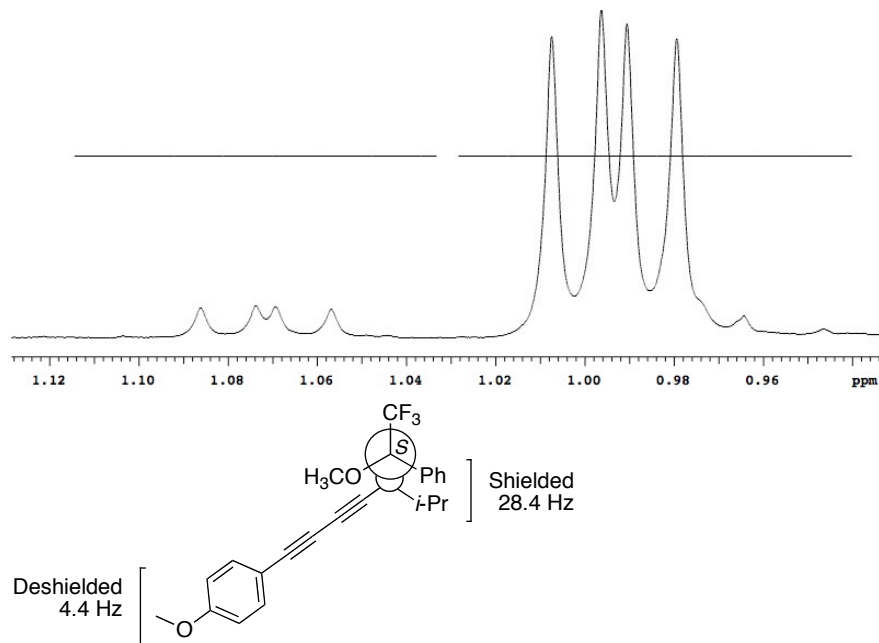
Figure A78. ^{1}H NMR spectrum of the (*S*)-Mosher ester of (+)-**2.31**. Absolute configuration was determined to be (*S*)-enantiomer by the modified Mosher ester method.
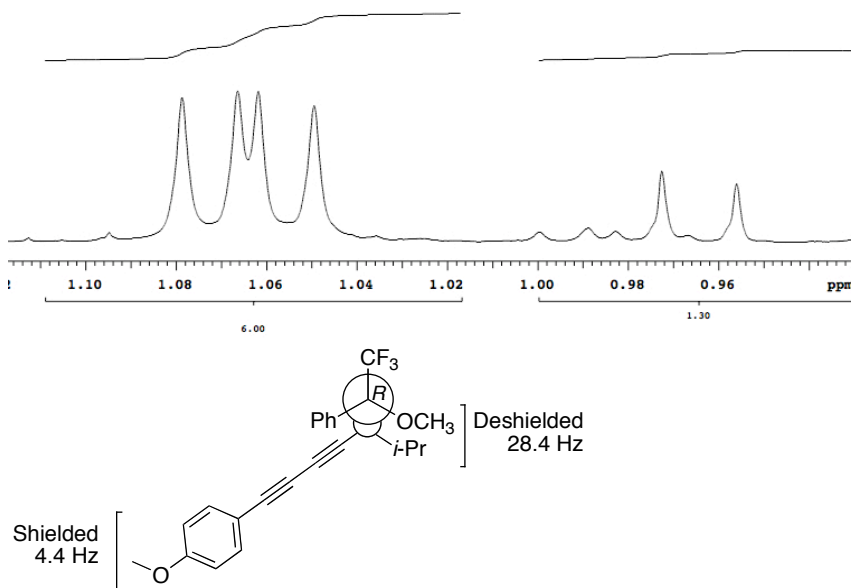
Figure A79. ^{1}H NMR spectrum of the (*R*)-Mosher ester of (+)-**2.31**. Absolute configuration was determined to be the (*S*)-enantiomer by the modified Mosher ester method.

Figure A80. Racemic sample of (*S*)-Mosher ester adduct of **2.32**; ^{19}F NMR spectrum, 376 MHz.

Figure A81. Optically enriched sample of (*S*)-Mosher ester adduct of (*R*)-(−)-**2.32**; ^{19}F NMR spectrum, 376 MHz.
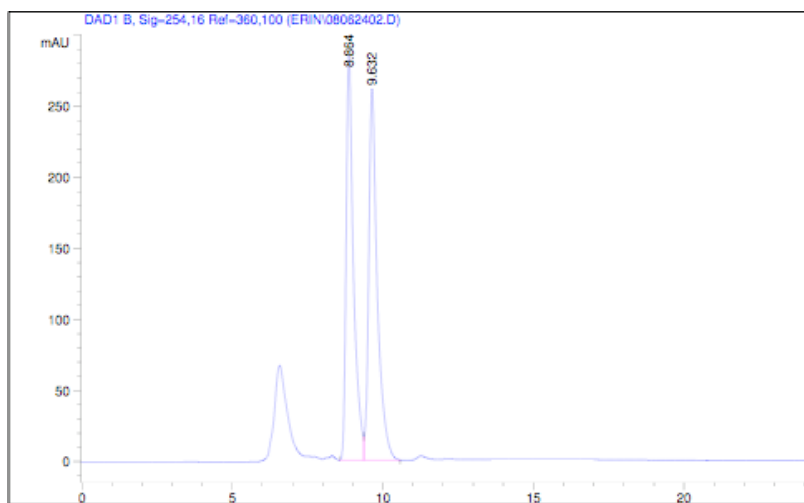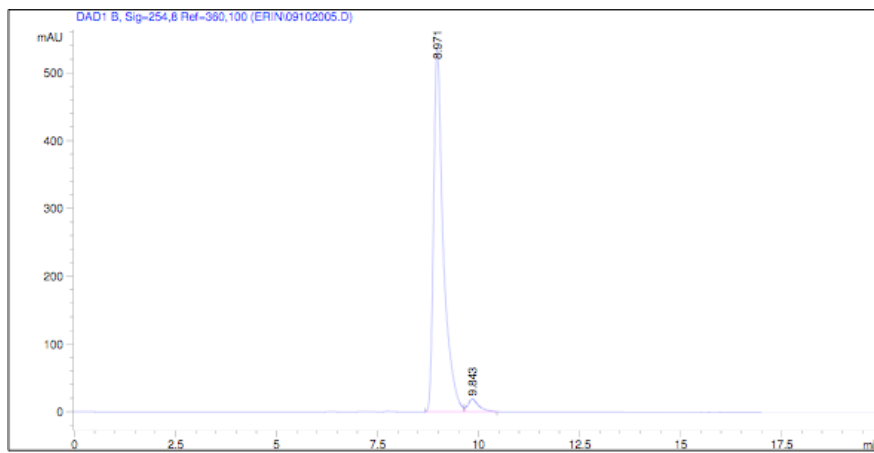
Figure A82. Racemic sample of (*S*)-Mosher ester adduct of **2.32**; ¹H NMR spectrum, 400 MHz.

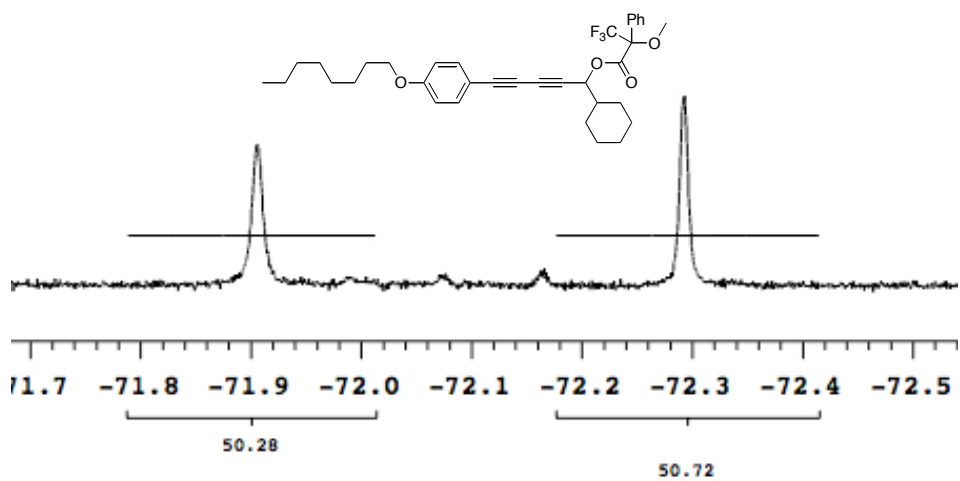Figure A83. Optically enriched sample of (*S*)-Mosher ester adduct of (*R*)-(−)-**2.32**; ¹H NMR spectrum, 500 MHz.

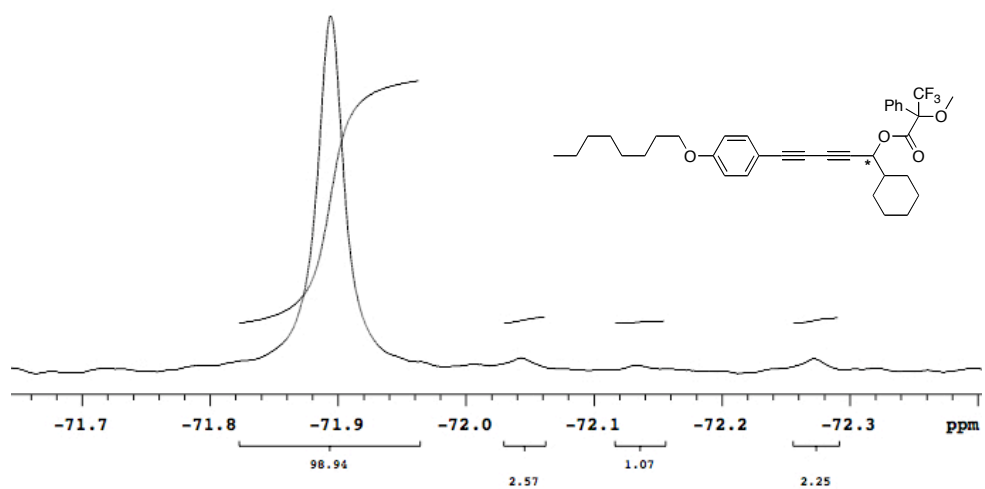Figure A84. Racemic sample of (S)-Mosher ester adduct of **2.33**; ^{9}F NMR spectrum, 376 MHz.

Figure A85. Optically enriched sample of (S)-Mosher ester adduct of (S)-(+)-**2.33**; ^{19}F NMR spectrum, 376 MHz.

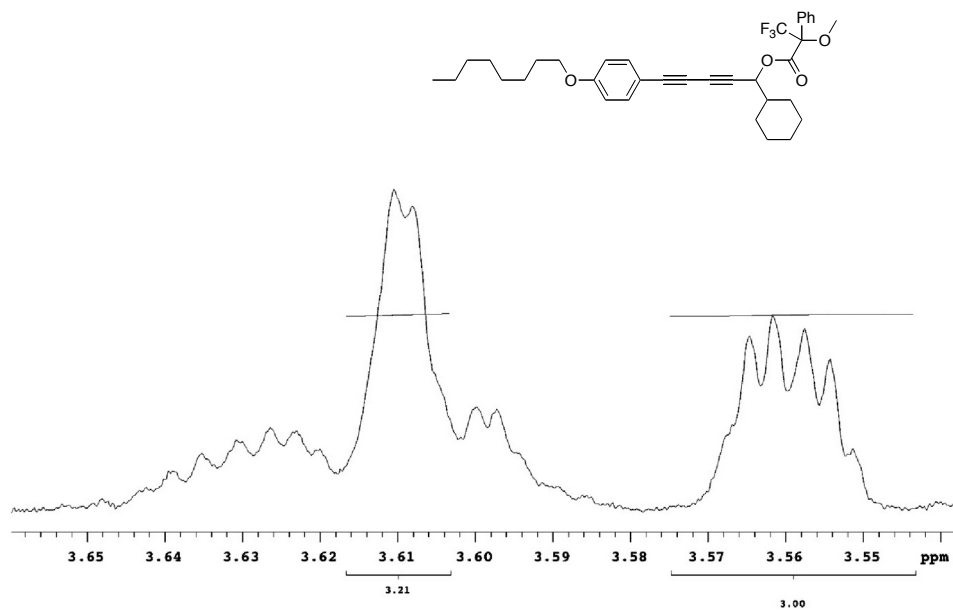Figure A86. Racemic sample of (*S*)-Mosher ester adduct of **2.33**; ^{1}H NMR spectrum, 400 MHz.

Figure A87. Optically enriched sample of (*S*)-Mosher ester adduct of (*S*)-(+)-**2.33**; ^{1}H NMR spectrum, 400 MHz.

Figure A88. Left: Optically enriched sample of (*S*)-Mosher ester adduct of (*S*)-(+)-**2.33** (¹H NMR spectrum, 400 MHz). Right: The absolute configuration of (+)-**2.33** was determined to be the (*S*)-enantiomer by the modified Mosher ester method.
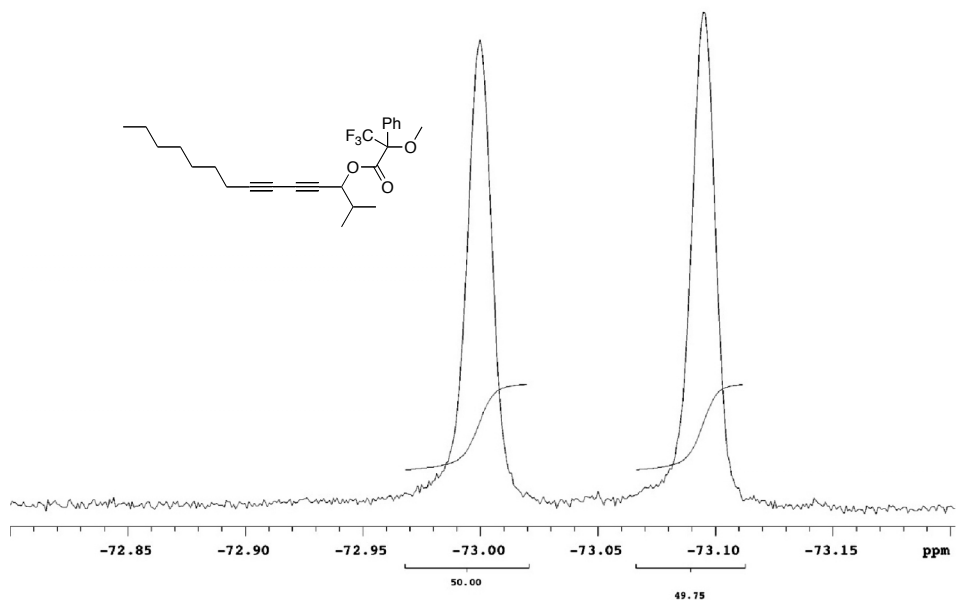
Figure A89. Racemic sample of (*S*)-Mosher ester adduct of **2.34**; ^{19}F NMR spectrum, 376 MHz.
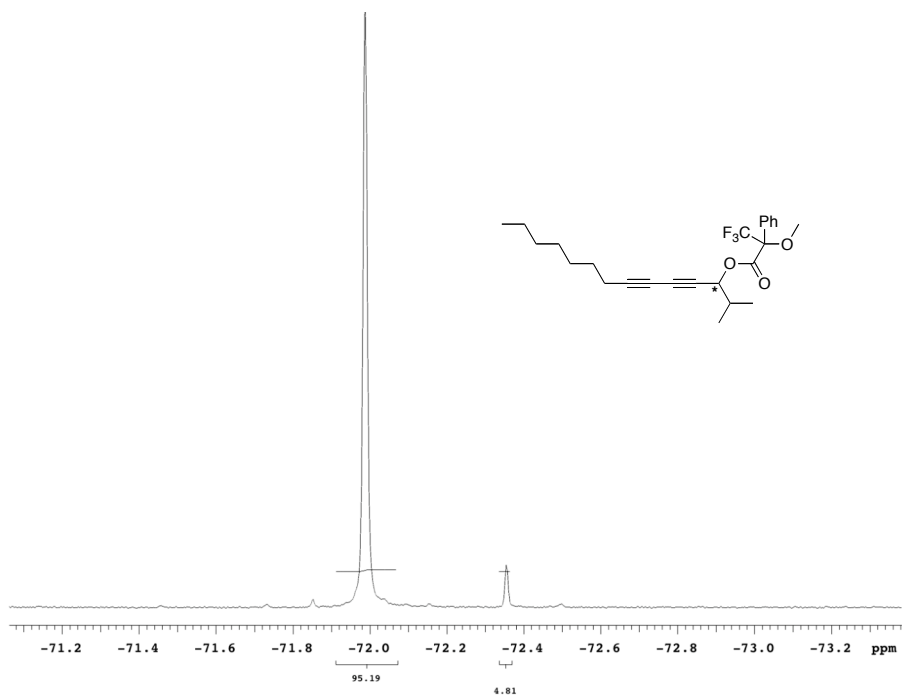
Figure A90. Optically enriched sample of (*S*)-Mosher ester adduct of (*S*)-(+)-**2.34**; ^{19}F NMR spectrum, 376 MHz.
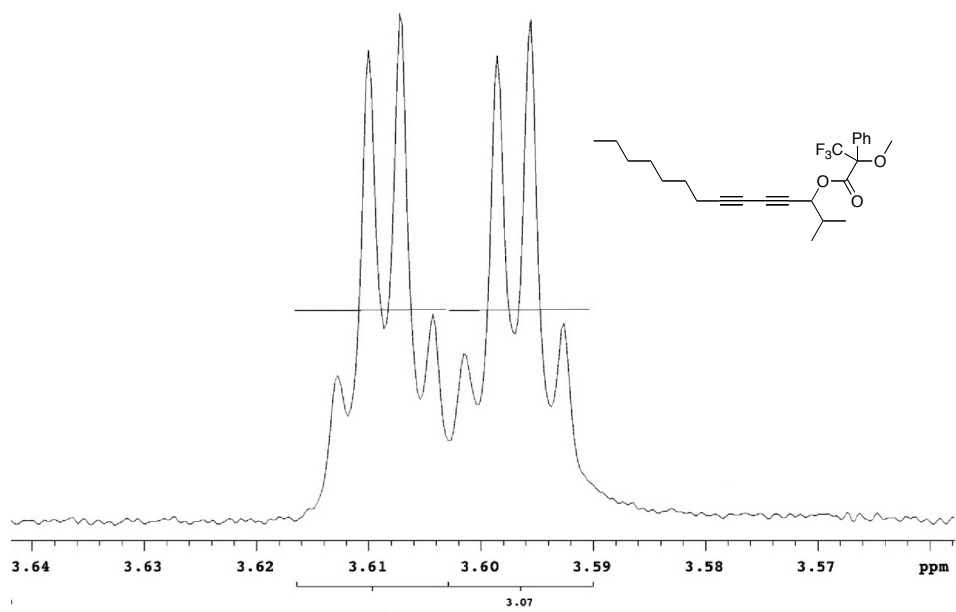
Figure A91. Racemic sample of (*S*)-Mosher ester adduct of (*S*)-(+)-**2.34**; ^{1}H NMR spectrum, 400 MHz.
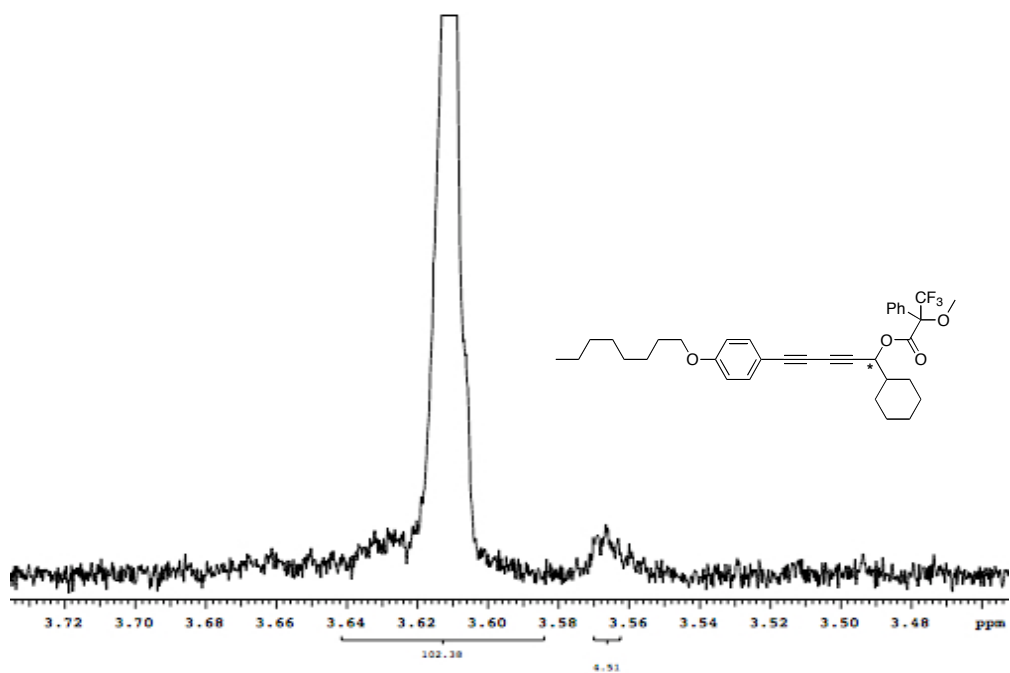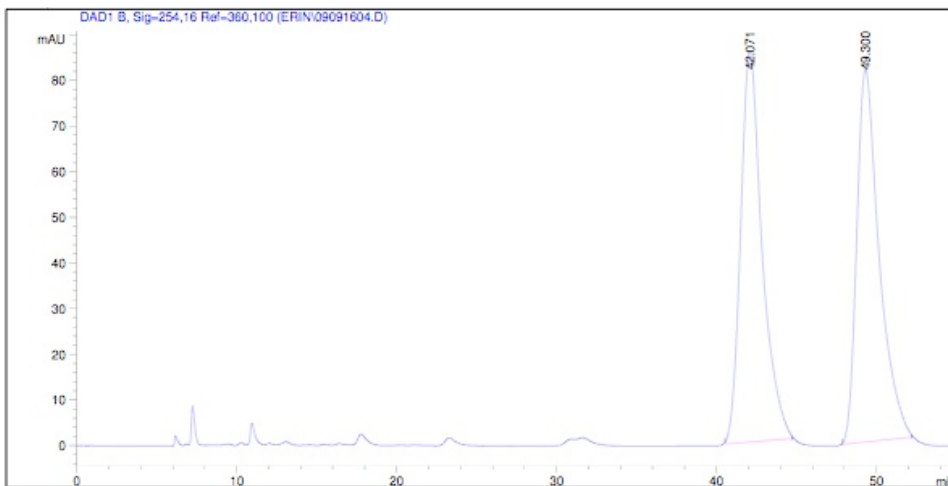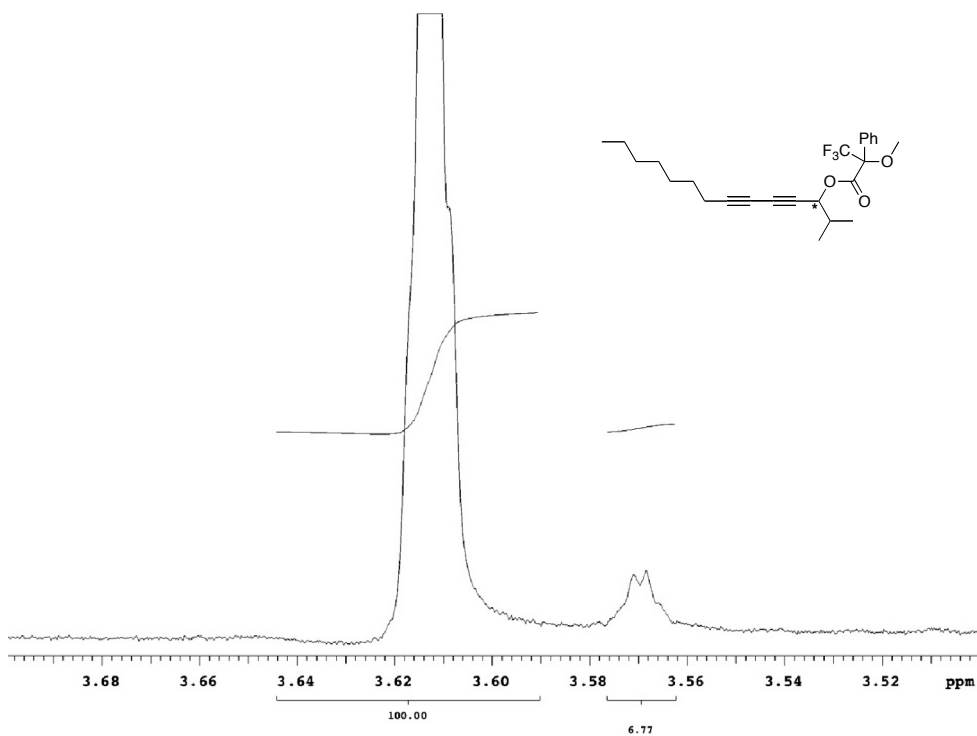

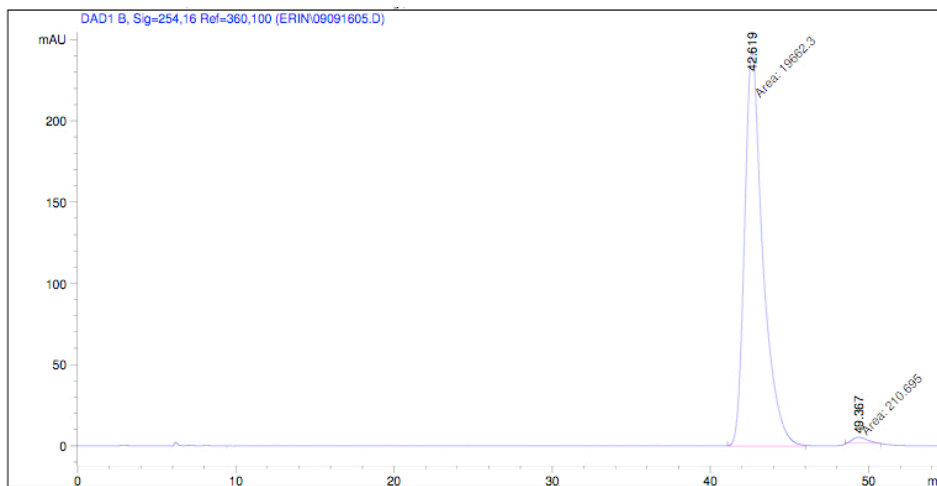Figure A92. Optically enriched sample of (*S*)-Mosher ester adduct of (*S*)-(+)-**2.34**; ^{1}H NMR spectrum, 400 MHz.

256
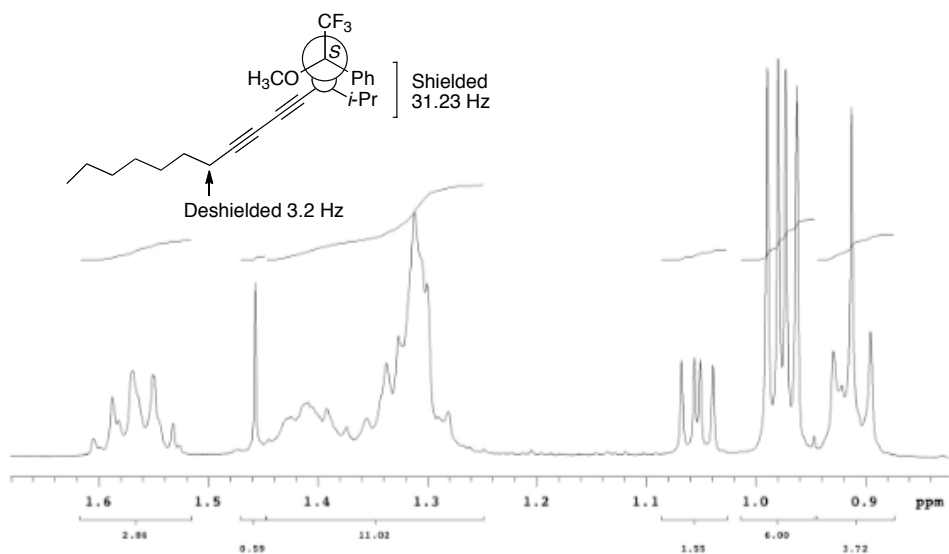
Figure A93. Optically enriched sample of (*S*)-Mosher ester adduct of (*S*)-(+)-**2.34**; ^{1}H NMR spectrum, 400 MHz. The absolute configuration of (+)-**2.34** was determined to be the (*S*)-enantiomer by the modified Mosher ester method.
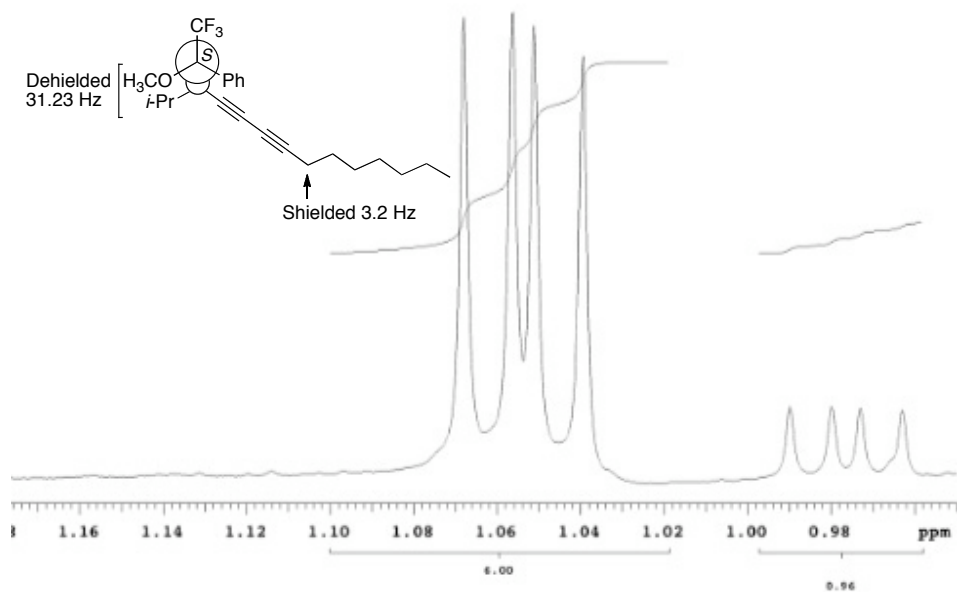
Figure A94. Optically enriched sample of the (*S*)-Mosher ester of (*R*)-(–)-**2.34**; ^{1}H NMR spectrum, 400 MHz. The absolute configuration of (–)-**2.34** was determined to be the (*R*)-enantiomer by the modified Mosher ester method.
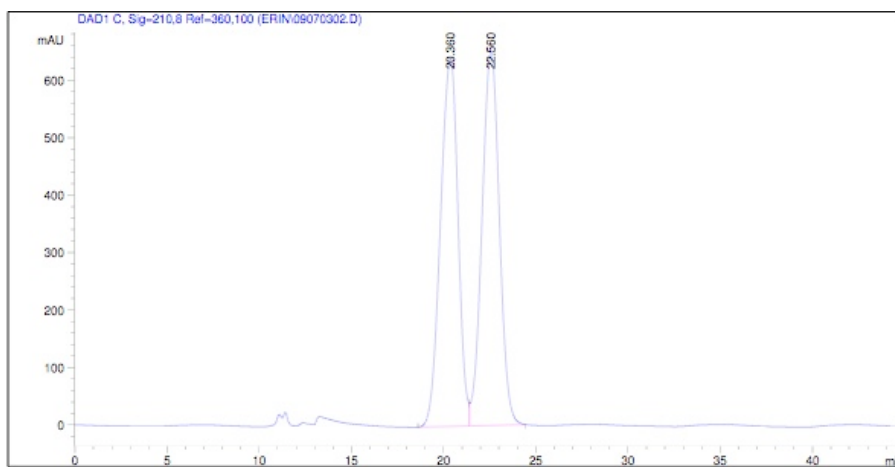
```
Area Percent Report

Peak  RetTime  Type   Width      Area        Height      Area
  #    [min]          [min]    [mAU*s]        [mAU]        %
----|--------|----|--------|------------|-----------|--------|
  1   20.360  BV   1.0044  4.24391e4    641.00330   49.8556
  2   22.560  VB   0.9947  4.26850e4    651.19153   50.1444

Totals :                   8.51241e4   1292.19482
```

Figure A95. Racemic sample of **2.35**.
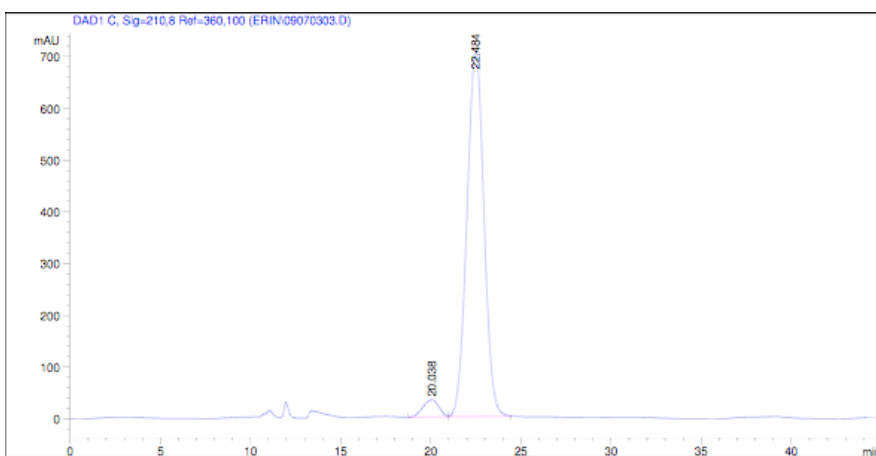

```
Area Percent Report

Peak  RetTime  Type   Width       Area        Height      Area
  #    [min]          [min]     [mAU*s]        [mAU]        %
----|--------|----|--------|------------|-----------|--------|
  1   20.038  BV   0.8985  2081.10986    33.32651    4.2930
  2   22.484  VB   0.9754  4.63960e4    705.35675   95.7070

Totals :                   4.84771e4    738.68326
```

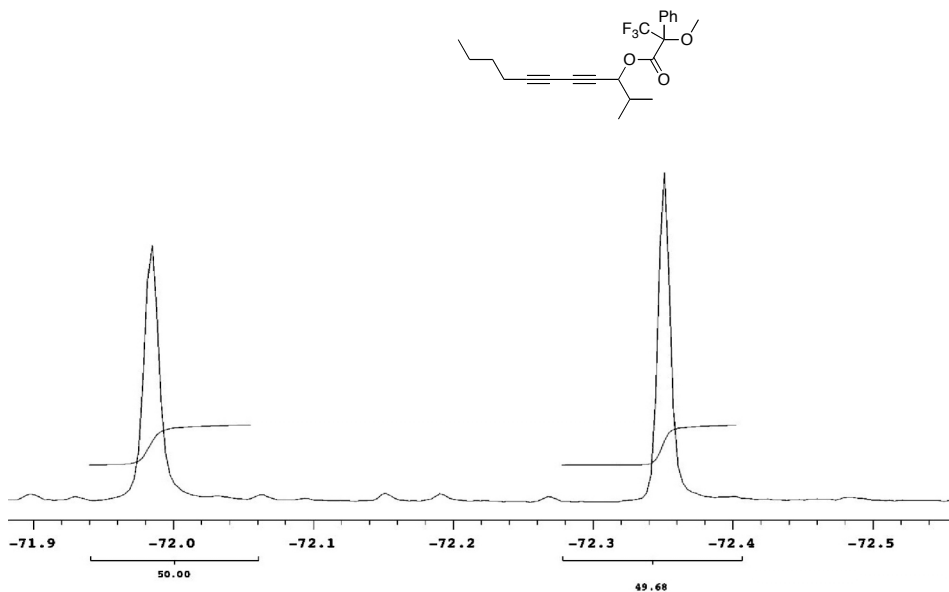Figure A96. Optically enriched sample of (*S*)-(+)-**2.35**.

258
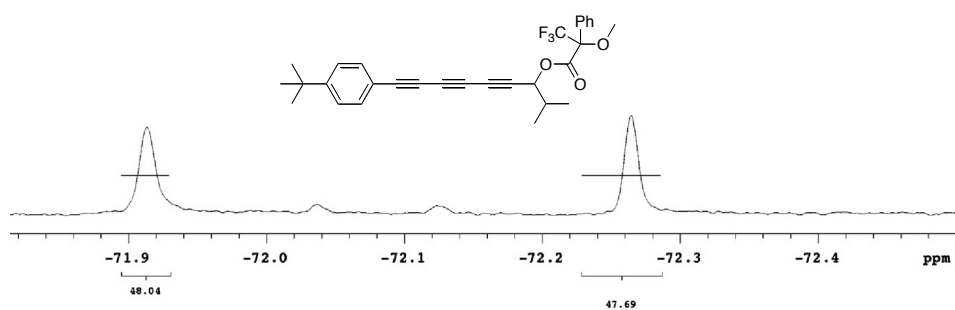
Figure A97. Racemic sample of (*S*)-Mosher ester adduct of **2.38**; ^{19}F NMR spectrum, 376 MHz.
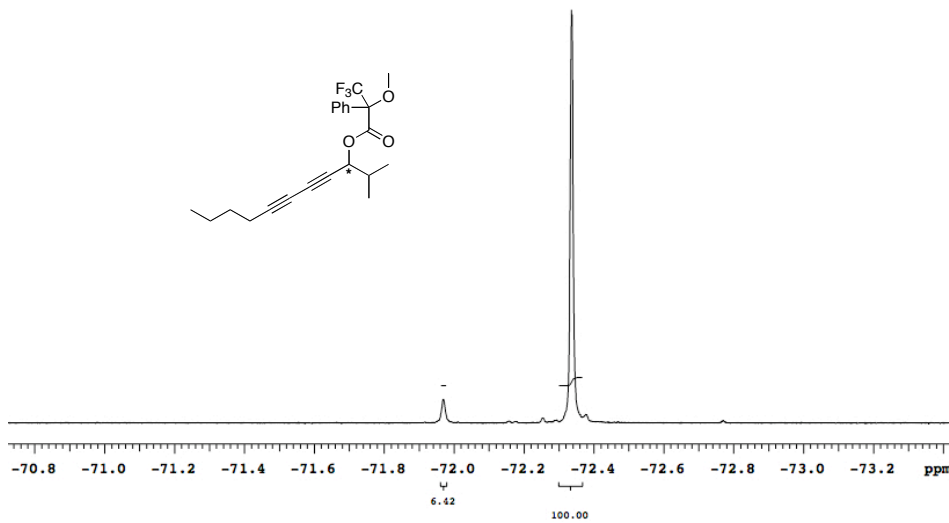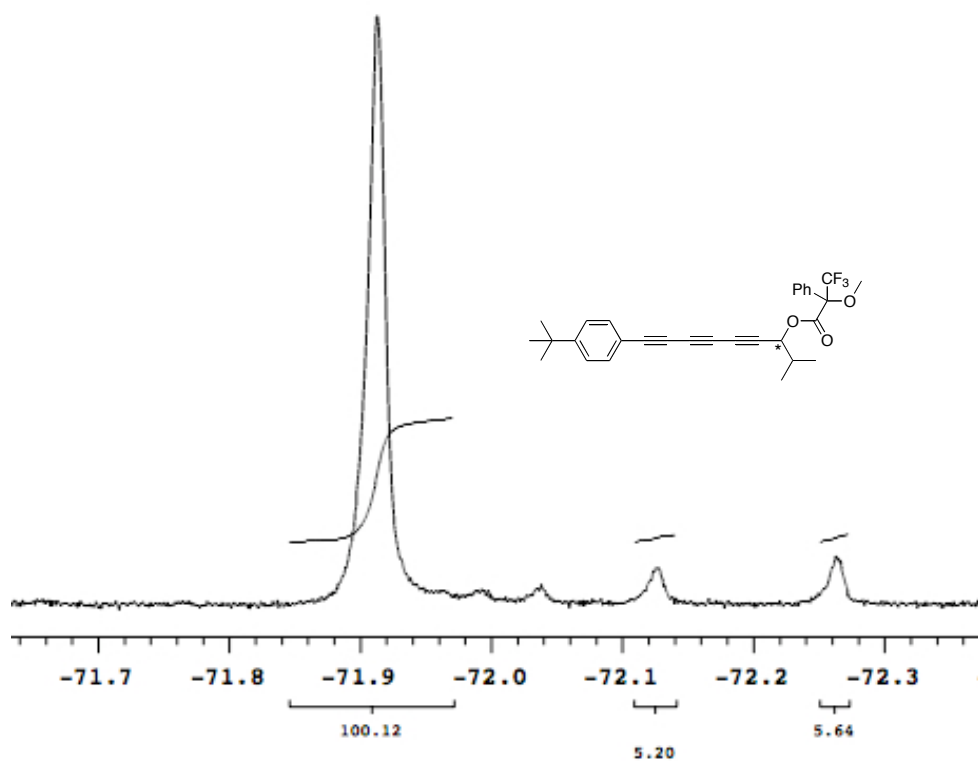

Figure A98. Optically enriched sample of (*S*)-Mosher ester adduct of (*S*)-(+)-**2.38**; ^{19}F NMR spectrum, 376 MHz.
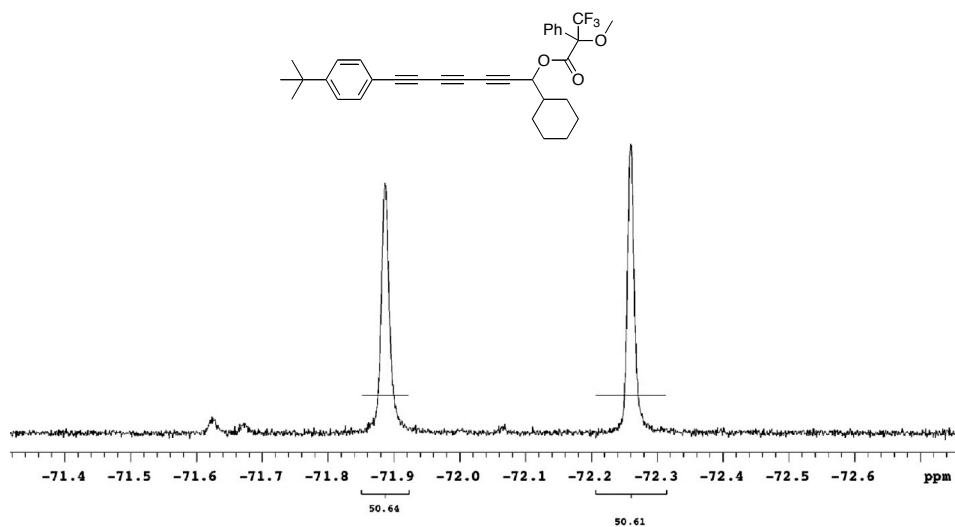
Figure A99. Racemic sample of (*R*)-Mosher ester adduct of **2.39** (^{19}F NMR spectrum, 376 MHz).
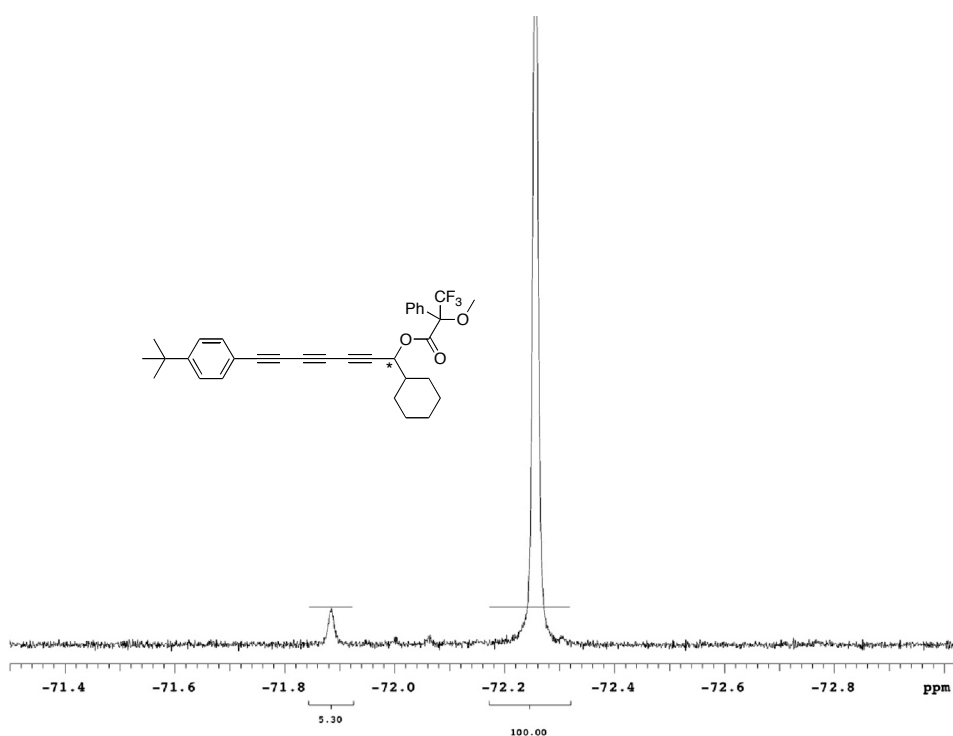
Figure A100. Optically enriched sample of (*R*)-Mosher ester adduct of (S)-(+)-**2.39** (^{19}F NMR spectrum, 376 MHz).
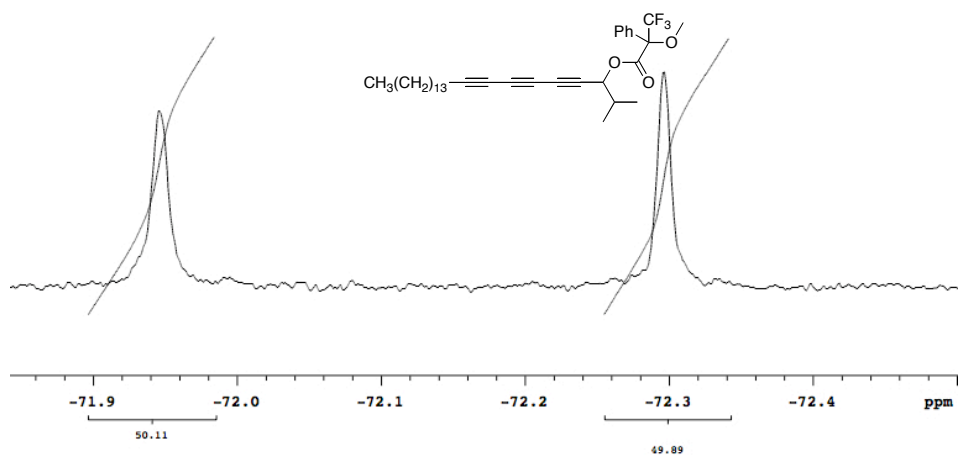
Figure A101. Racemic sample of (*S*)-Mosher ester adduct of **2.40**; ^{19}F NMR spectrum, 376 MHz.
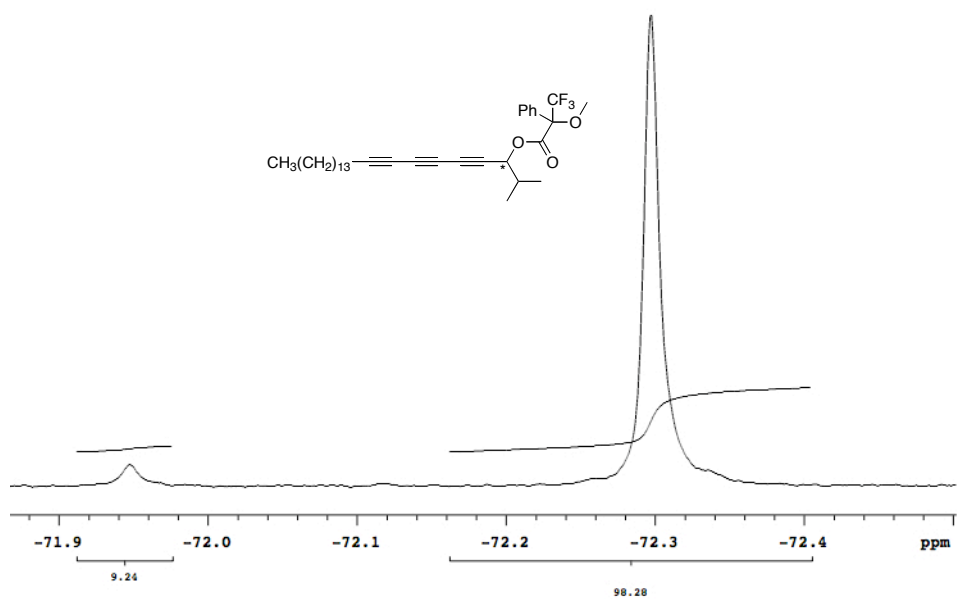
Figure A102. Optically enriched sample of (*S*)-Mosher ester adduct of (*R*)-(–)-**2.40**; ^{19}F NMR spectrum, 376 MHz.
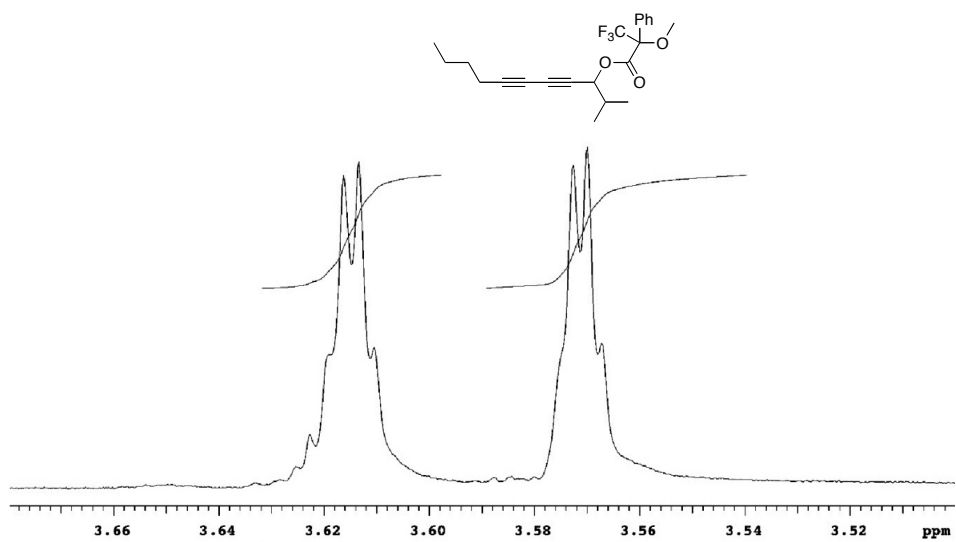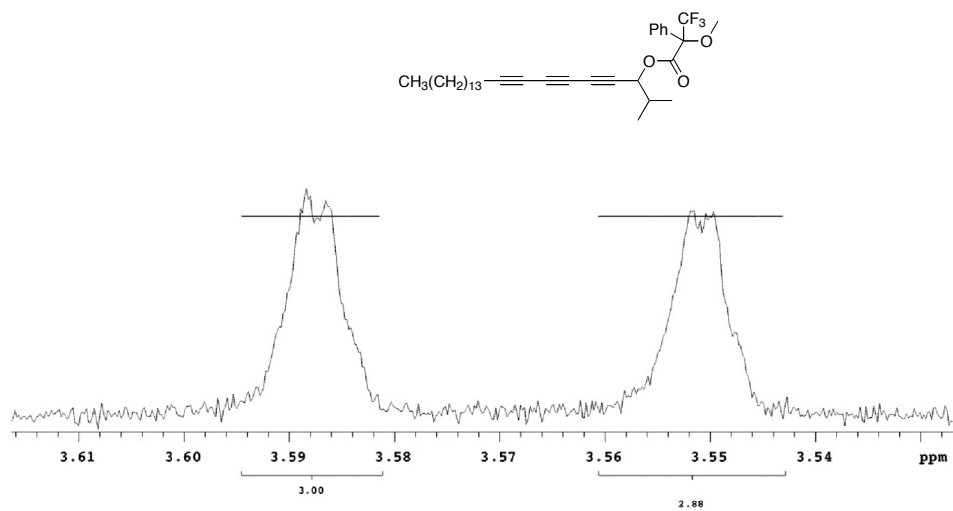
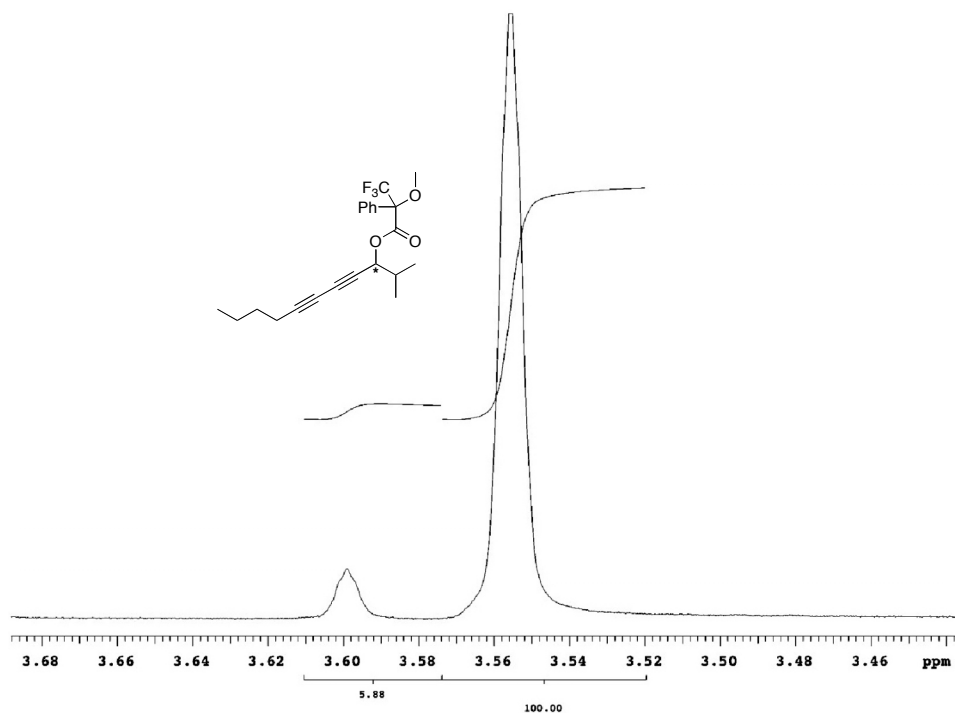Figure A103. Racemic sample of (*S*)-Mosher ester adduct of **2.40**; ^{1}H NMR spectrum, 500 MHz.
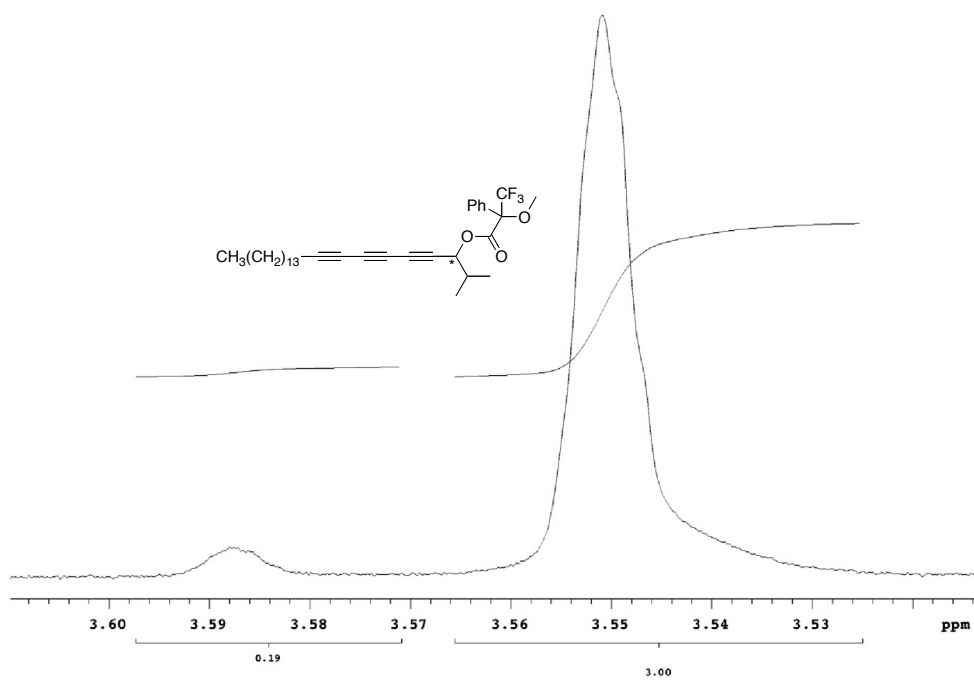
Figure A104. Optically enriched sample of (*S*)-Mosher ester adduct of (*R*)-(−)-**2.40**; ^{1}H NMR spectrum, 500 MHz.
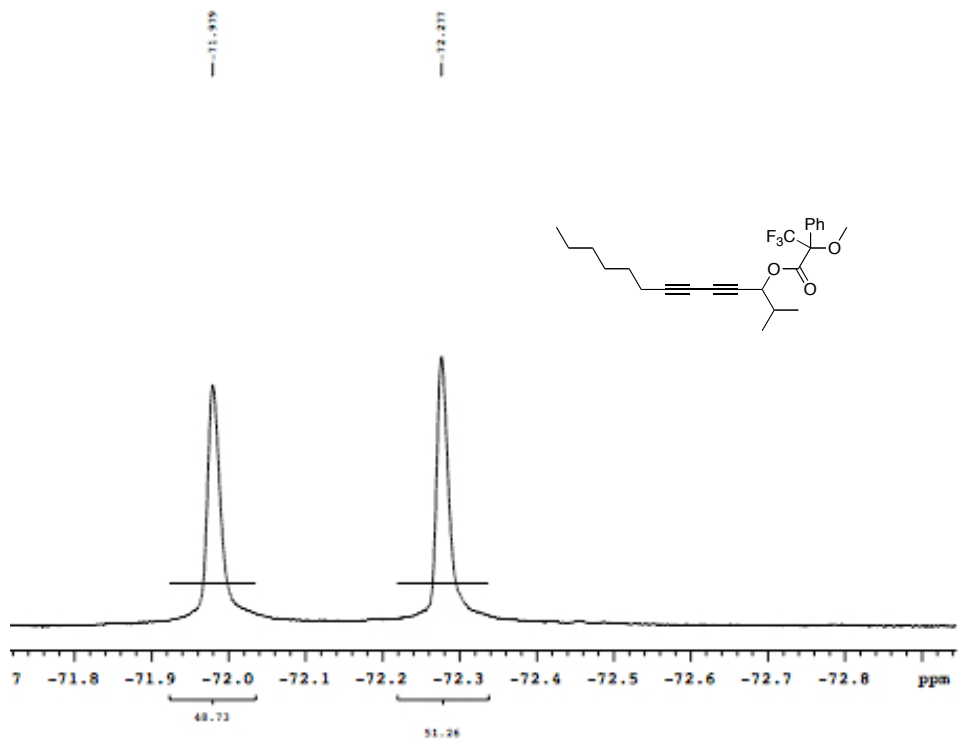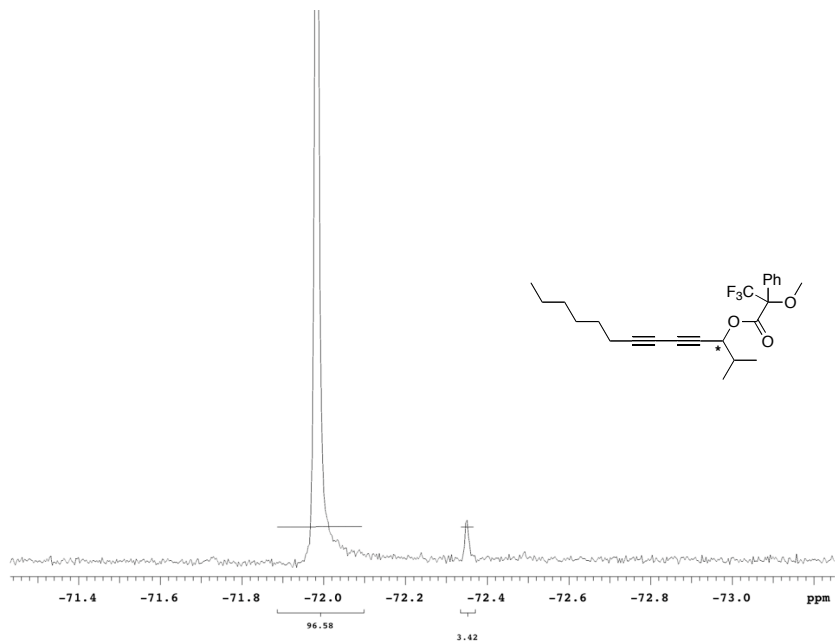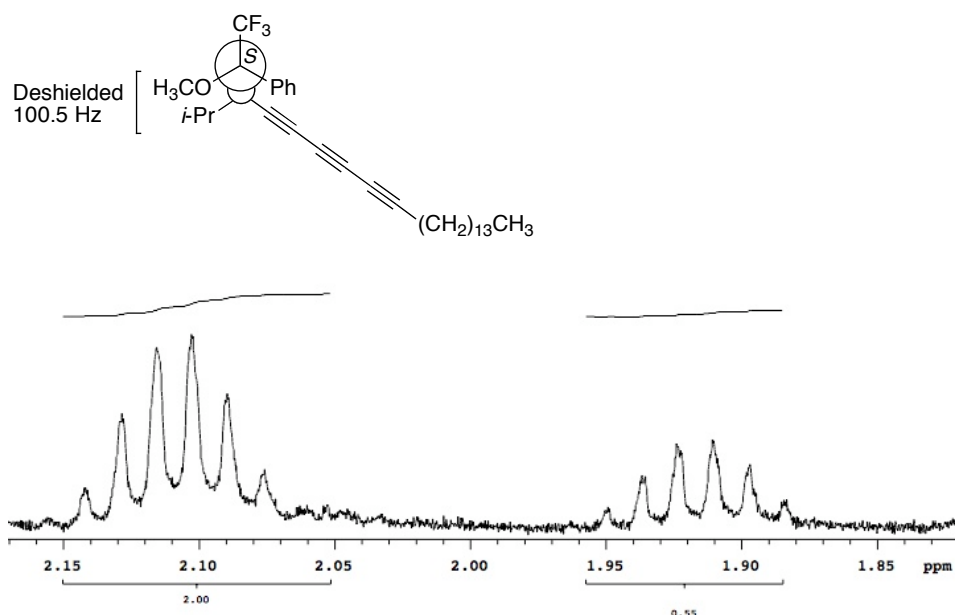
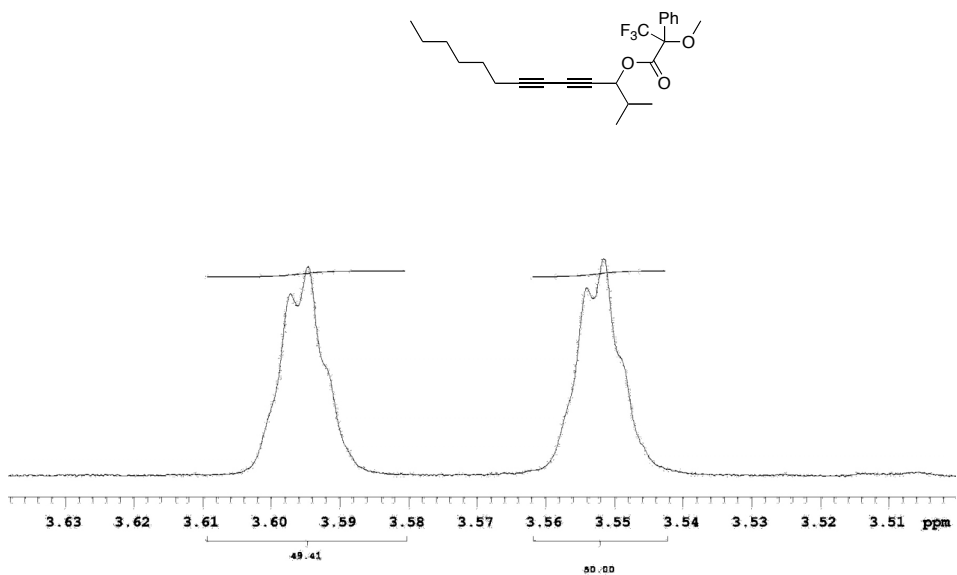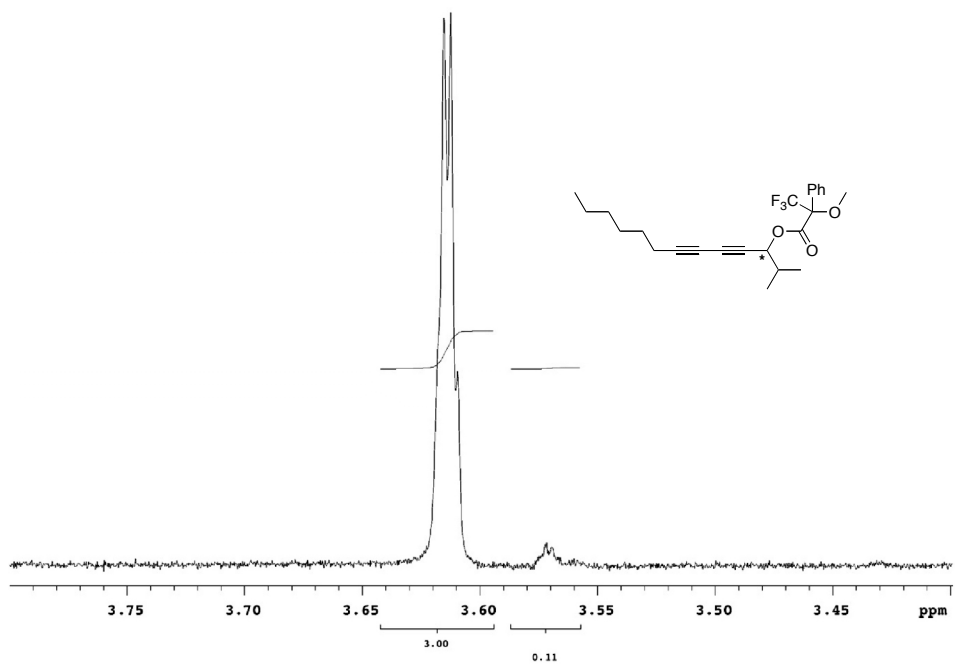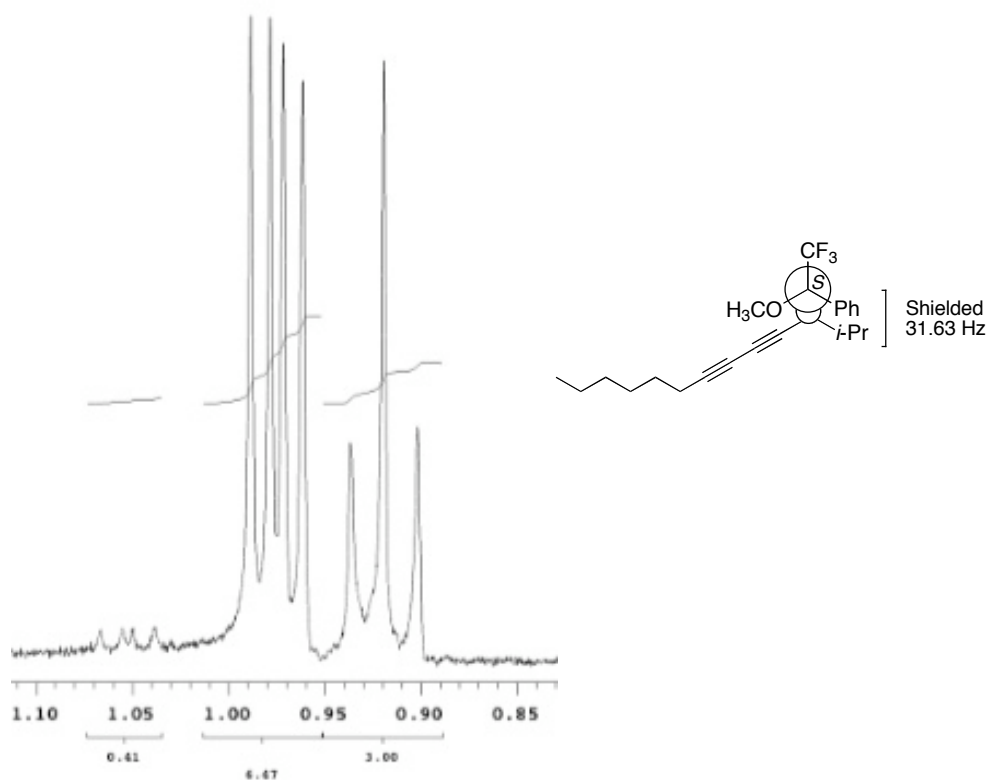Figure A105. Optically enriched sample of (*S*)-Mosher ester adduct of (*R*)-(–)-**2.40**; [^1]H NMR spectrum, 500 MHz. The absolute configuration of (–)-**2.40** was determined to be the (*R*)-enantiomer by the modified Mosher ester method.
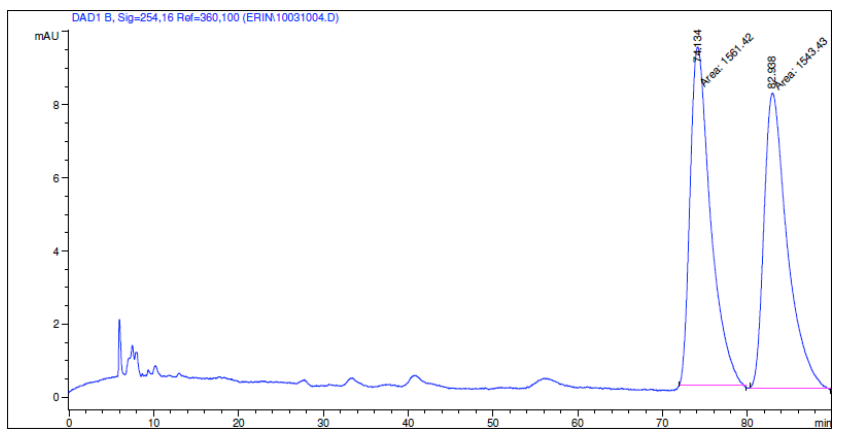
DAD1 B, Sig=254,16 Ref=360,100 (ERIN\10031004.D)

```
                         Area Percent Report

========================================================================
Peak  RetTime  Type   Width      Area       Height      Area
 #     [min]          [min]    [mAU*s]      [mAU]         %
----|--------|------|-------|-----------|-----------|--------|
   1   74.134   MM   2.8074  1561.41504    9.26963   50.2896
   2   82.938   MM   3.1762  1543.42920    8.09900   49.7104

Totals :                     3104.84424   17.36862
```

Figure A106. Racemic sample of **2.42.**
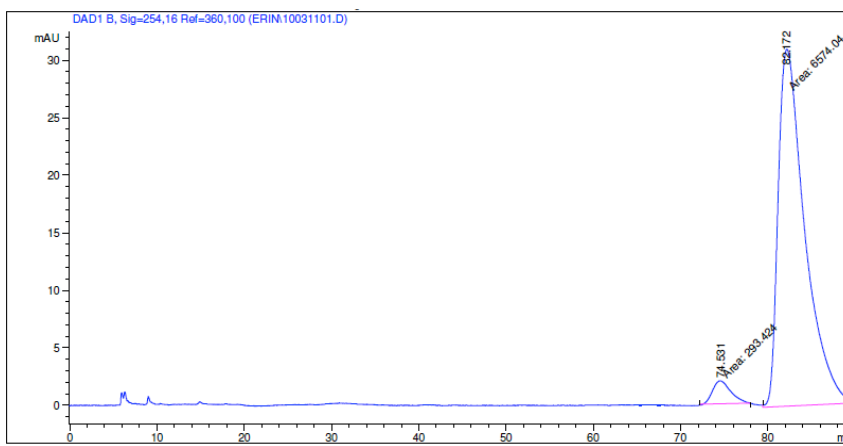
DAD1 B, Sig=254,16 Ref=360,100 (ERIN\10031101.D)

```
                         Area Percent Report

========================================================================
Peak  RetTime  Type   Width      Area       Height      Area
 #     [min]          [min]    [mAU*s]      [mAU]         %
----|--------|------|-------|-----------|-----------|--------|
   1   74.531   MM   2.4310   293.42426    2.01171    4.2727
   2   82.172   MM   3.5237  6574.03760   31.09468   95.7273

Totals :                     6867.46185   33.10639
```

Figure A107. Optically enriched sample of (*S*)-(−)-**2.42.**
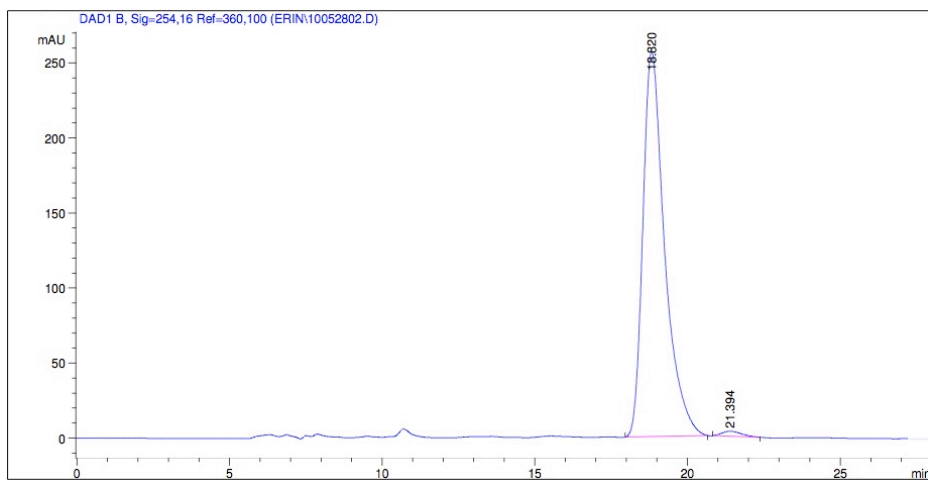
264

```
DAD1 B, Sig=254,16 Ref=360,100 (ERIN\10052802.D)
```

```
Area Percent Report

Peak RetTime Type  Width     Area      Height     Area
  #   [min]        [min]    [mAU*s]     [mAU]       %
----|-------|----|-------|-----------|----------|--------|
  1  18.820 BB   0.7448 1.27334e4   256.68417  98.7943
  2  21.394 BB   0.5481  155.39796    3.41981   1.2057

Totals :                1.28888e4   260.10399
```

Figure A108. Optically enriched sample of (*S*)-(−)-**2.43.**
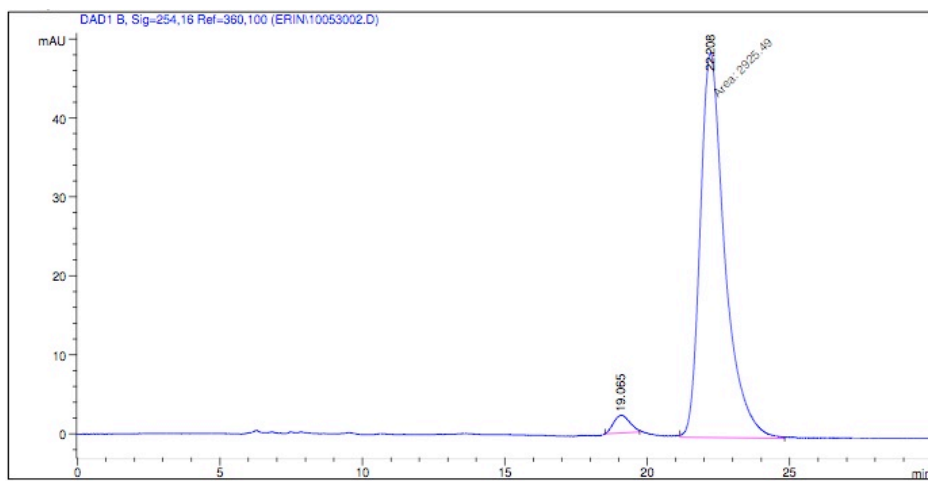

```
DAD1 B, Sig=254,16 Ref=360,100 (ERIN\10053002.D)
```

```
Area Percent Report

Peak RetTime Type  Width     Area      Height     Area
  #   [min]        [min]    [mAU*s]     [mAU]       %
----|-------|----|-------|-----------|----------|--------|
  1  19.065 BB   0.4661   89.41335    2.29712   2.9657
  2  22.208 MM   0.9994 2925.48730   48.78698  97.0343

Totals :                3014.90066   51.08410
```

Figure A109. Optically enriched sample of (*R*)-(+)-**2.43.**
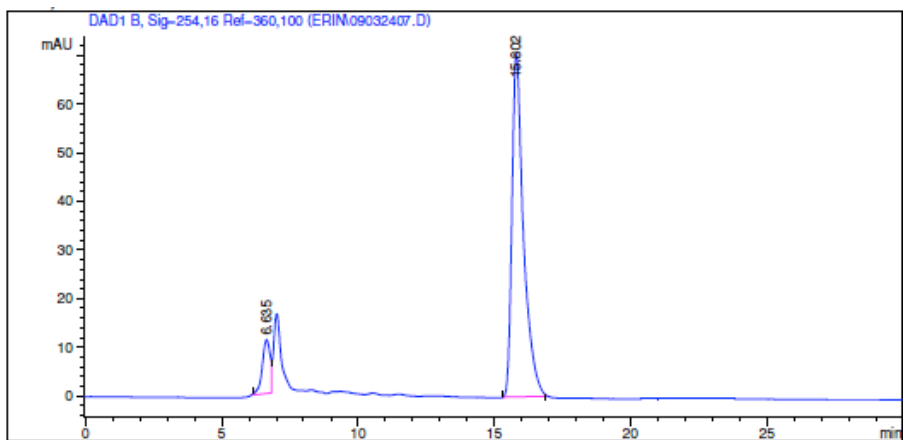
```
Area Percent Report

Peak  RetTime  Type   Width      Area        Height      Area
 #     [min]          [min]     [mAU*s]      [mAU]        %
----|--------|-----|--------|------------|-----------|--------|
 1    6.635   BV    0.3090   224.14343    11.03187    9.6779
 2   15.802   BB    0.4315  2091.90186    70.63273   90.3221

Totals :                    2316.04529    81.66460
```

Figure A110. Optically enriched sample of **2.46**, synthesized with (+)-*N*-methylephedrine.
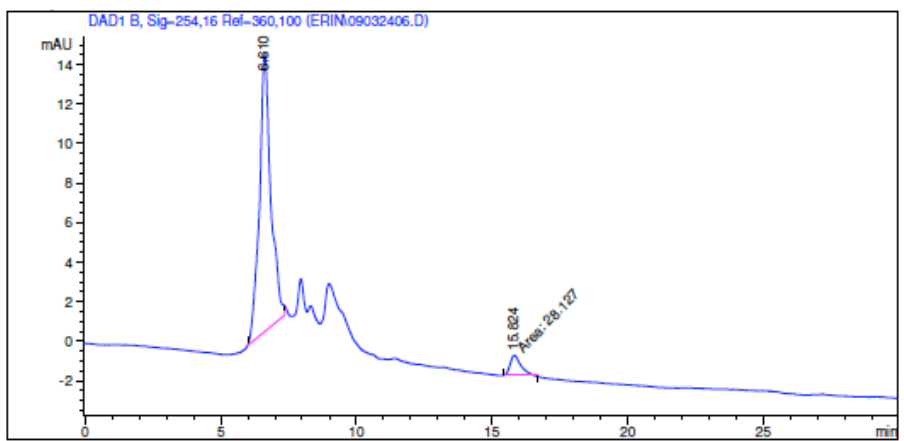

```
Area Percent Report

Peak  RetTime  Type   Width      Area        Height      Area
 #     [min]          [min]     [mAU*s]      [mAU]        %
----|--------|-----|--------|------------|-----------|--------|
 1    6.610   BB    0.4156   415.21799    14.09960   93.6557
 2   15.824   MM    0.4568    28.12696     1.02620    6.3443

Totals :                     443.34495    15.12581
```

Figure A111. Optically enriched sample of **2.46**, synthesized with (−)-*N*-methylephedrine.

A.4. One-pot protocol optimization.


```
      DAD1 B, Sig=254,16 Ref=360,100 (ERIN\08062403.D)
mAU
140
120
100
 80
 60
 40
 20
  0
      0         5        10        15        20        25      min
```
e

```
                       Area Percent Report

Peak RetTime Type  Width      Area        Height      Area
  #    [min]        [min]    [mAU*s]       [mAU]        %
----|--------|----|-------|-----------|-----------|--------|
  1    8.893 BV    0.2499   723.95868    42.24388   18.5139
  2    9.664 VB    0.2890  3186.38794   160.92300   81.4861

Totals :                   3910.34662   203.16689
```
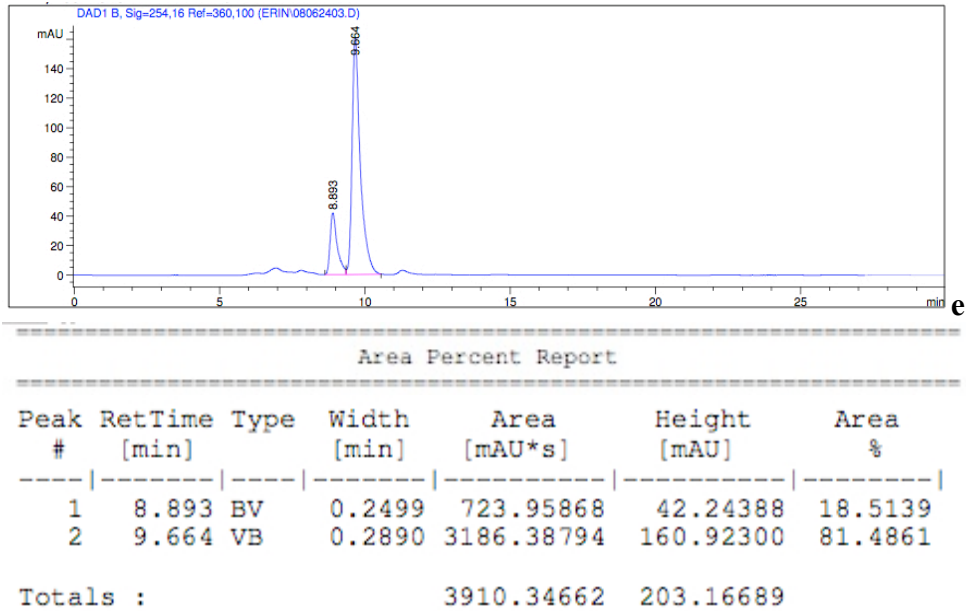
Figure A112. One pot protocol with Procedure 2.


```
      DAD1 B, Sig=254,8 Ref=360,100 (ERIN\09091001.D)
mAU

 80

 60

 40

 20

  0
      0        10        20        30        40        50     min
```

```
                       Area Percent Report

Peak RetTime Type  Width      Area        Height      Area
  #    [min]        [min]    [mAU*s]       [mAU]        %
----|--------|----|-------|-----------|-----------|--------|
  1   38.978 BB    1.2955  8113.62744    92.30463   82.8412
  2   42.558 BB    1.2134  1680.57117    20.01840   17.1588

Totals :                   9794.19861   112.32304
```
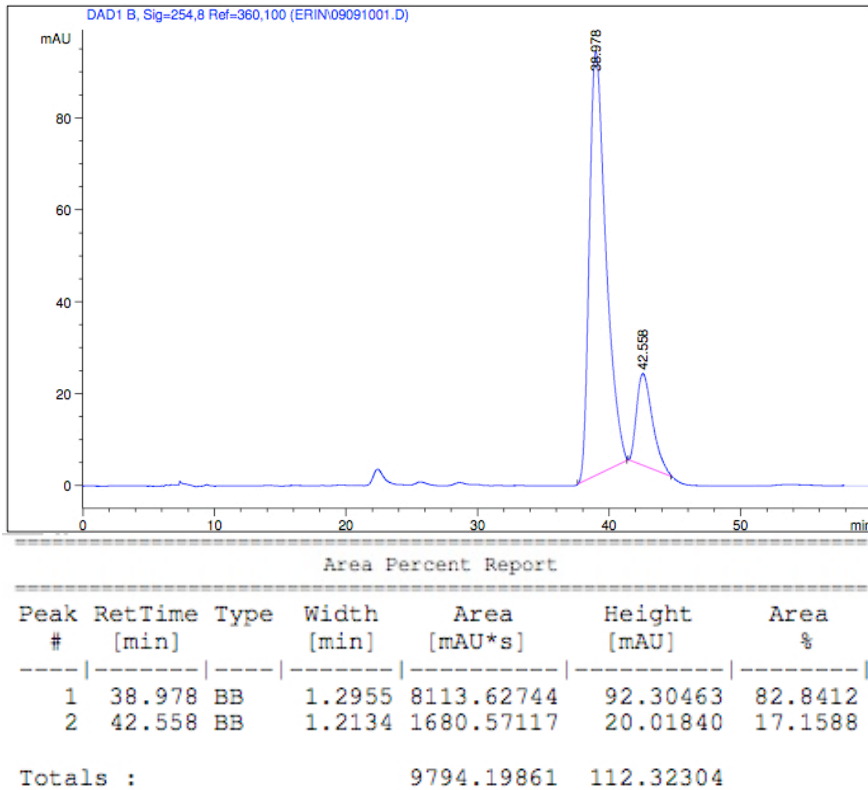
Figure A113. One pot protocol with Procedure 3.
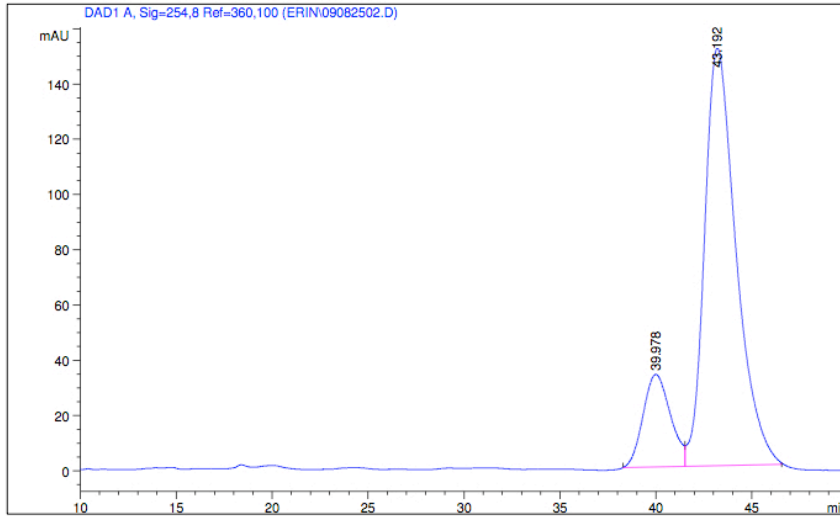
267

Figure A114. One pot protocol from Procedure 4.
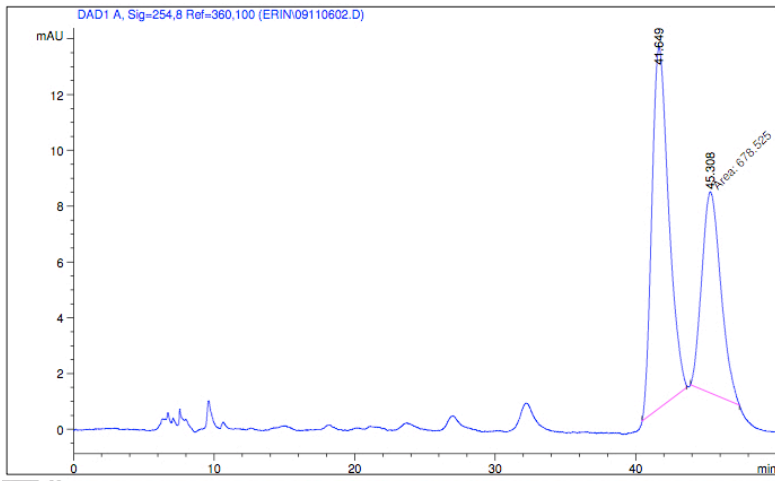
Figure A115. One pot protocol from Procedure 5.
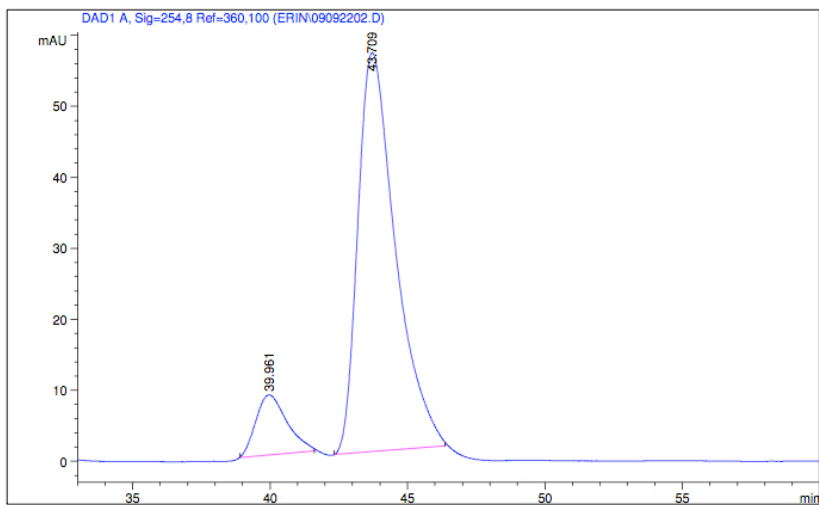
268

```
Area Percent Report

Peak RetTime Type   Width      Area       Height     Area
  #   [min]        [min]    [mAU*s]      [mAU]        %
----|-------|----|-------|----------|-----------|--------|
  1  39.961 BB   0.9558   671.25006    8.49598   11.1422
  2  43.709 BB   1.3989  5353.15088   56.21851   88.8578

Totals :                6024.40094   64.71449
```

Figure A116. One pot protocol from Procedure 6.
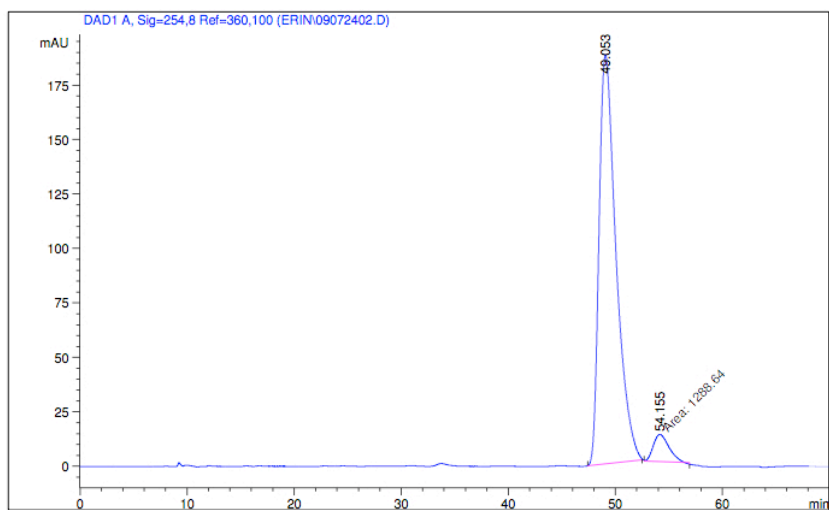

```
Area Percent Report

Peak RetTime Type   Width      Area       Height      Area
  #   [min]        [min]    [mAU*s]       [mAU]         %
----|-------|----|-------|----------|-----------|--------|
  1  49.053 BB   1.6341  2.07279e4   187.74333   94.1470
  2  54.155 MM   1.7094  1288.63696   12.56452    5.8530

Totals :                2.20166e4   200.30785
```

Figure A117. One pot protocol from Procedure 7.

A.5. ^{1}H and ^{13}C NMR spectra for new compounds from Chapter 3.
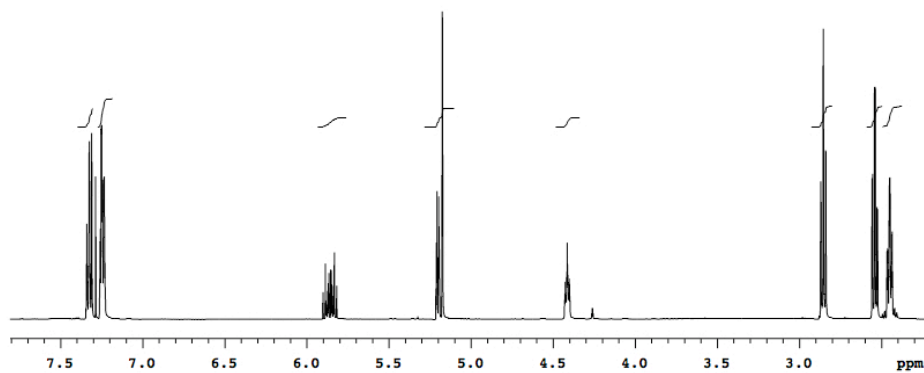
Figure A118. 1H NMR spectrum of **3.64** in CDCl$_3$, 400 MHz.
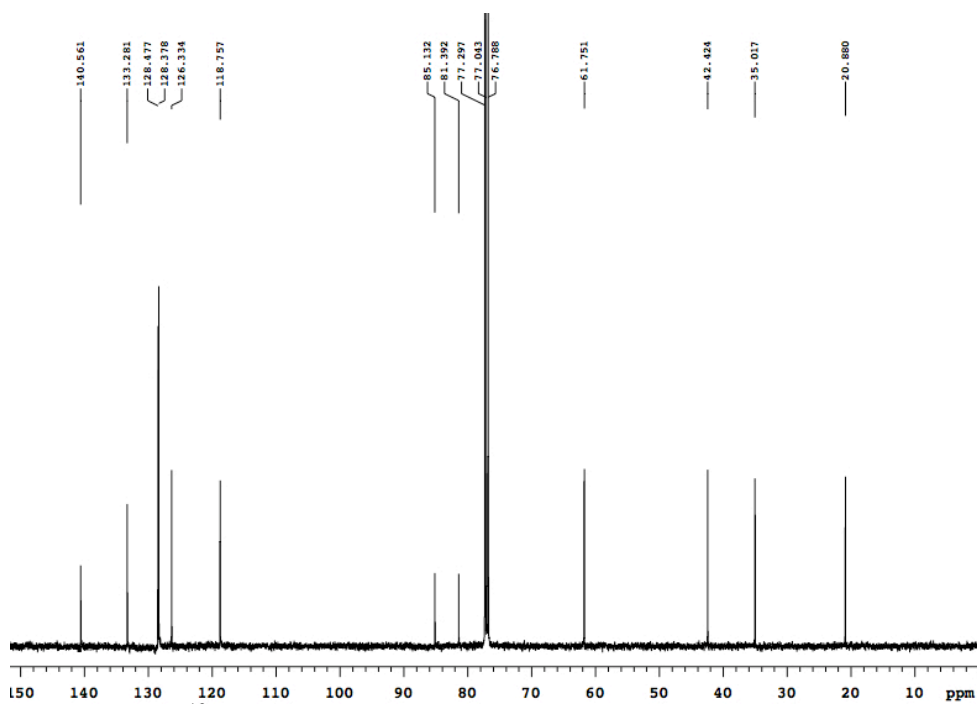
Figure A119. ^{13}C NMR spectrum of **3.64** in CDCl$_3$, 125 MHz.
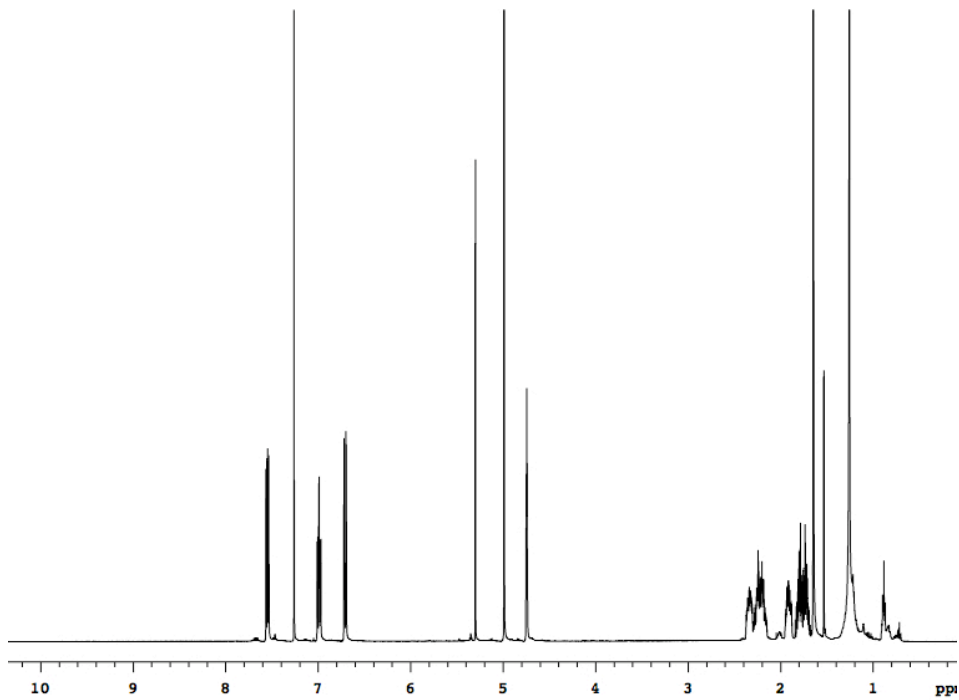
Figure A120. ^{1}H NMR spectrum of **3.75** in CDCl$_3$, 500 MHz.
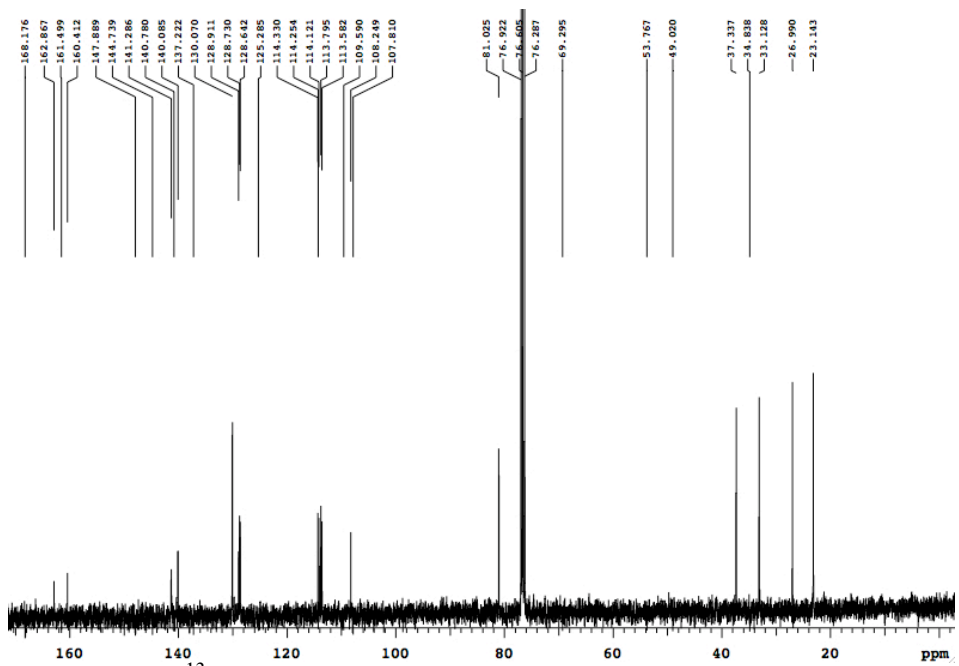
Figure A121. ^{13}C NMR spectrum of **3.75** in CDCl$_3$, 125 MHz.
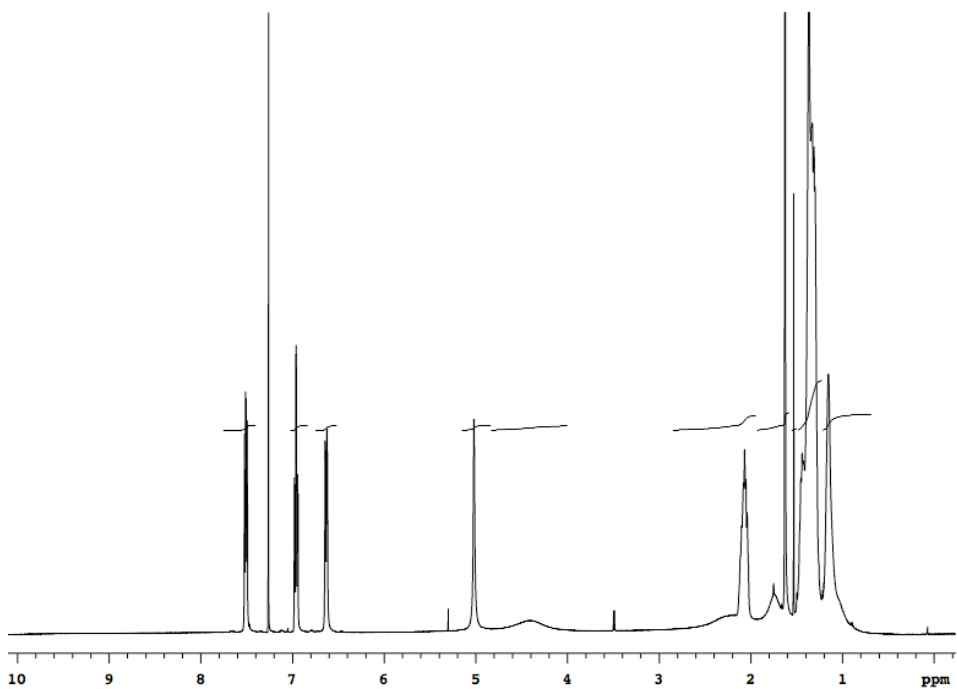
Figure A122. ^{1}H NMR spectrum of **3.77** in CDCl$_3$, 500 MHz.
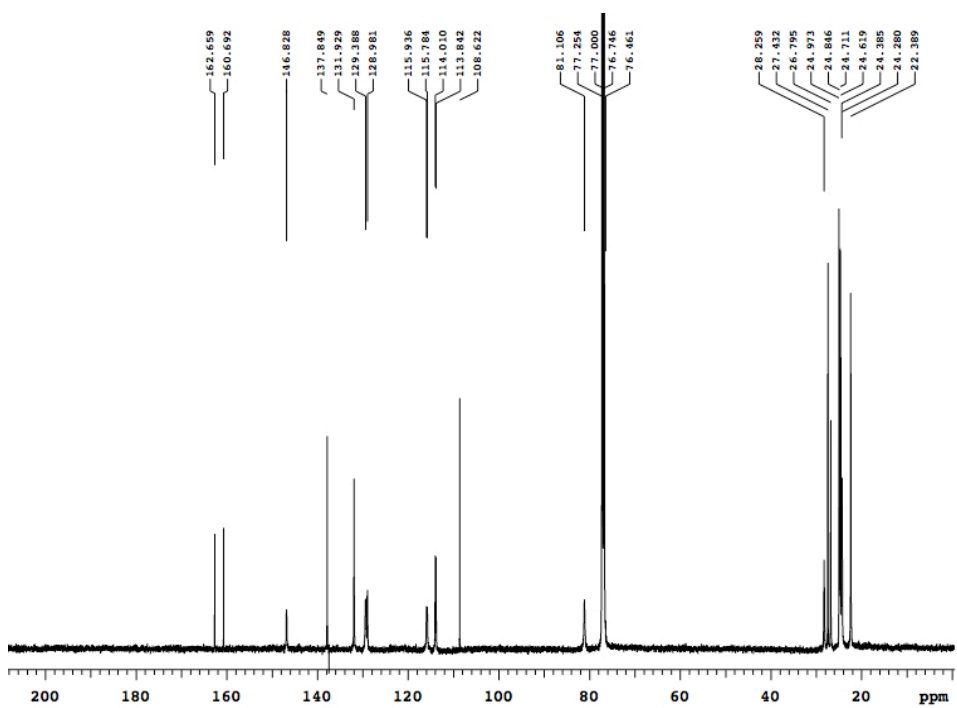
Figure A123. ^{13}C NMR spectrum of **3.77** in CDCl$_3$, 125 MHz.
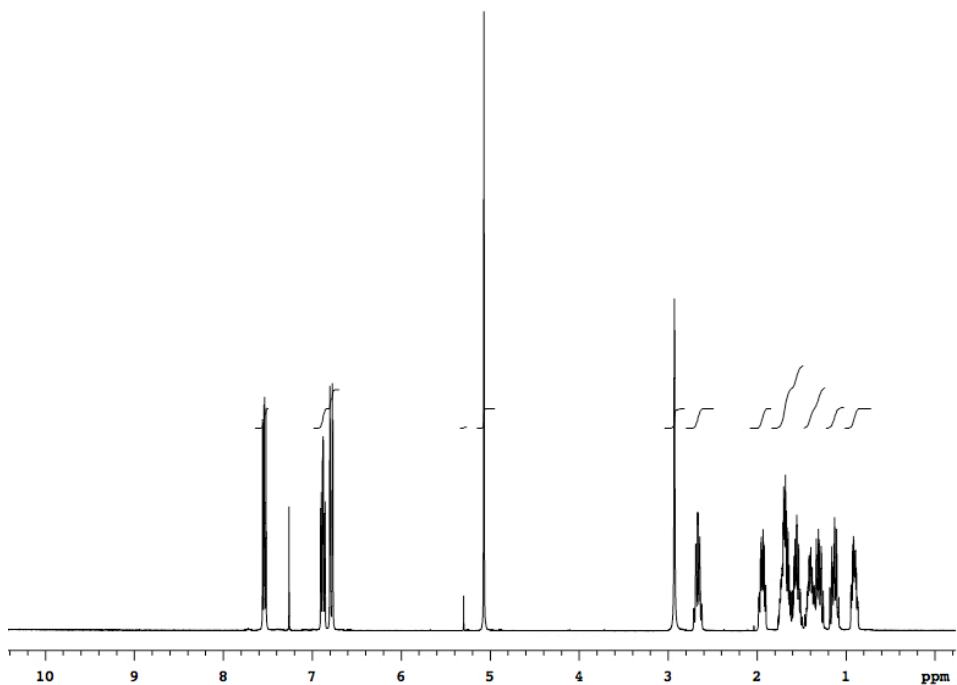
Figure A124. ^{1}H NMR spectrum of **3.79** in CDCl$_3$, 400 MHz.
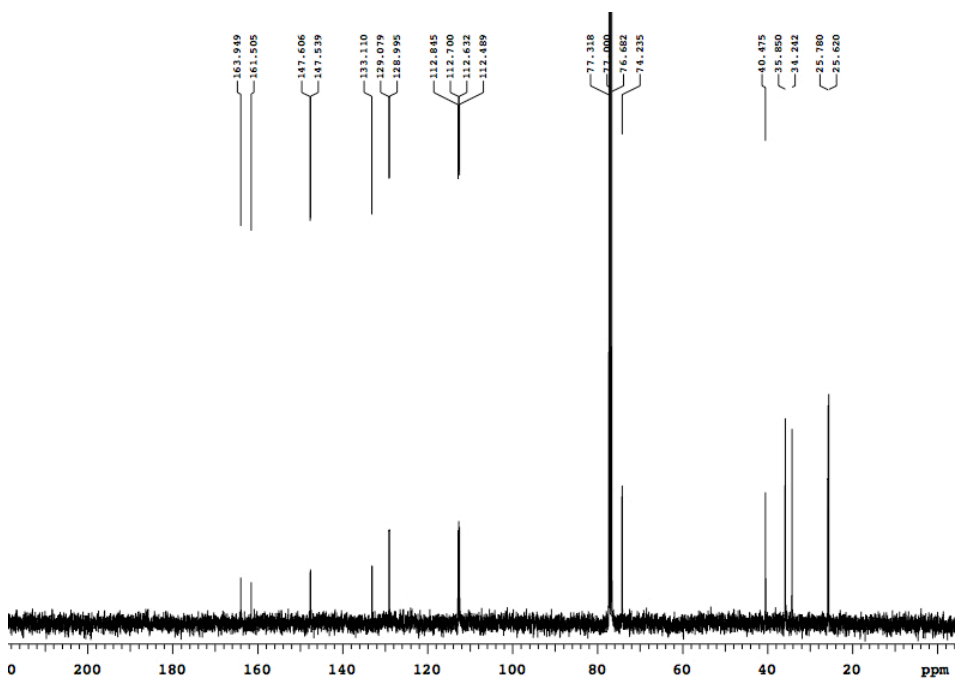
Figure A125. ^{13}C NMR spectrum of 3.79 in CDCl$_3$, 100 MHz.

273

Figure A126. ^{1}H NMR spectrum of **3.76** in CDCl$_3$, 500 MHz.

Figure A127. ^{13}C NMR spectrum of **3.76** in CDCl$_3$, 125 MHz.
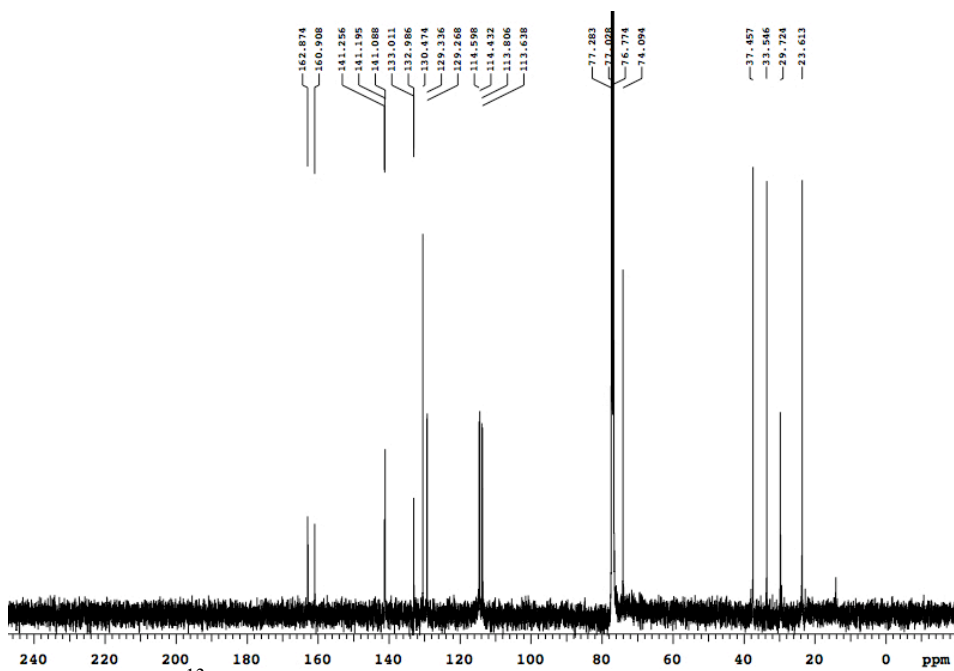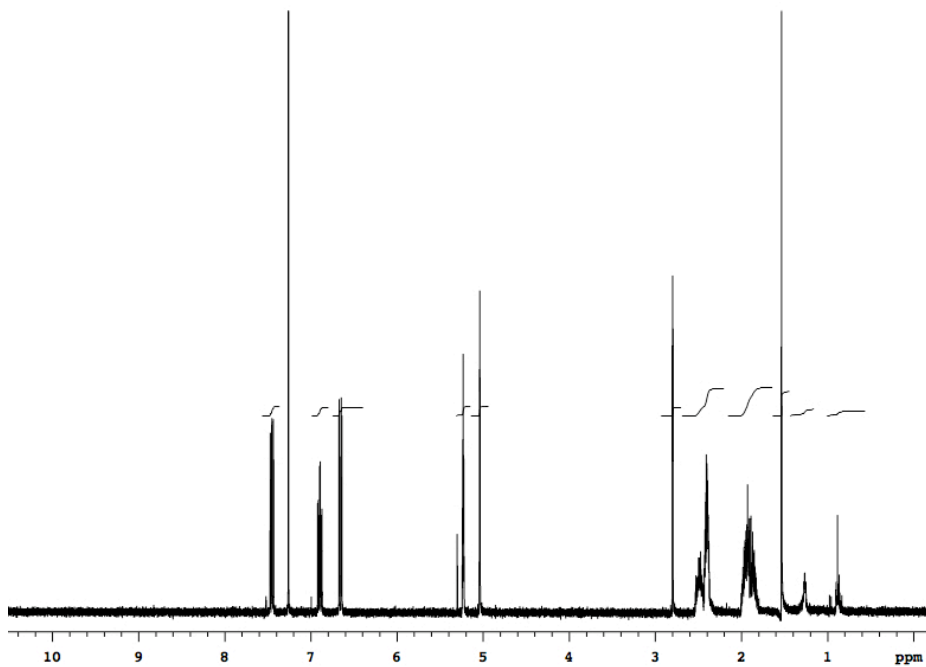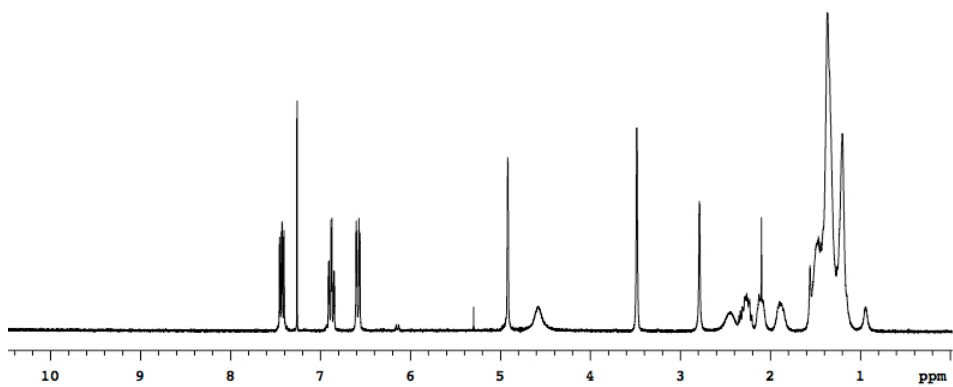
Figure A128. ^{1}H NMR spectrum of **3.78** in CDCl$_3$, 400 MHz.
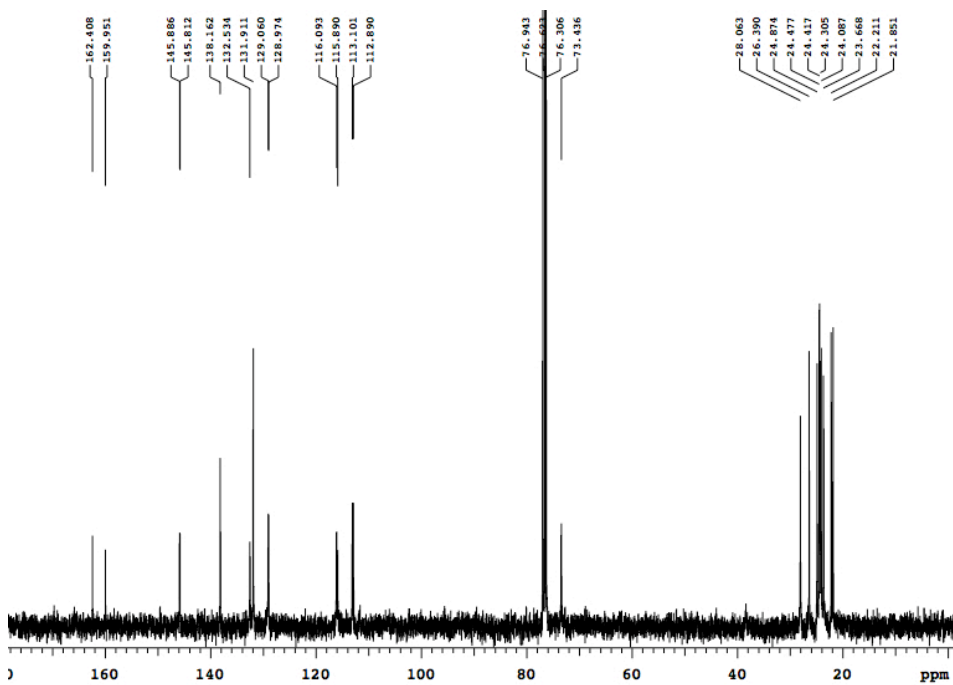
Figure A129. ^{13}C NMR spectrum of **3.78** in CDCl$_3$, 100 MHz.

275
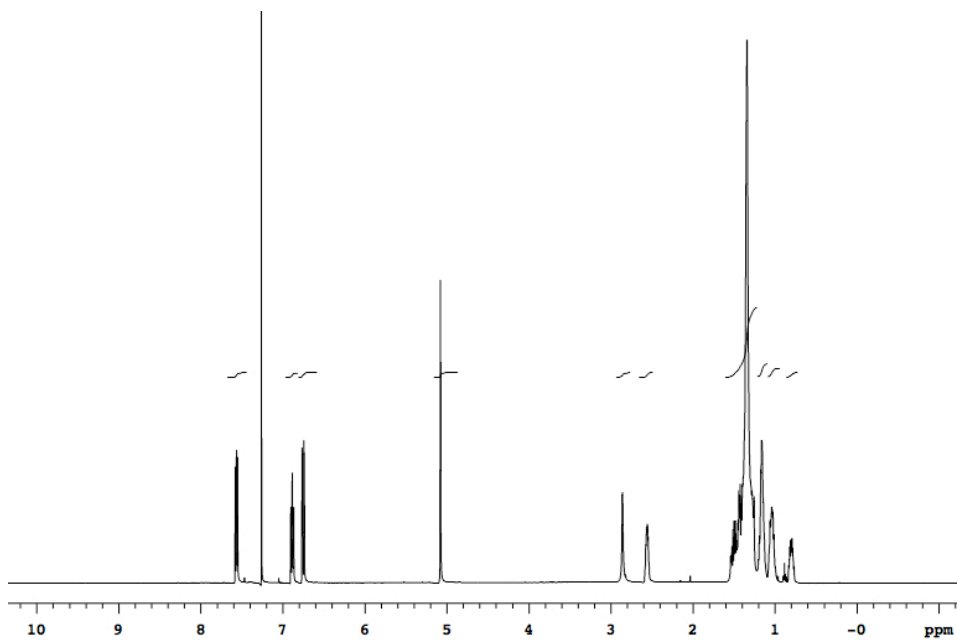
Figure A130. ^{1}H NMR spectrum **3.80** in CDCl$_3$, 500 MHz.
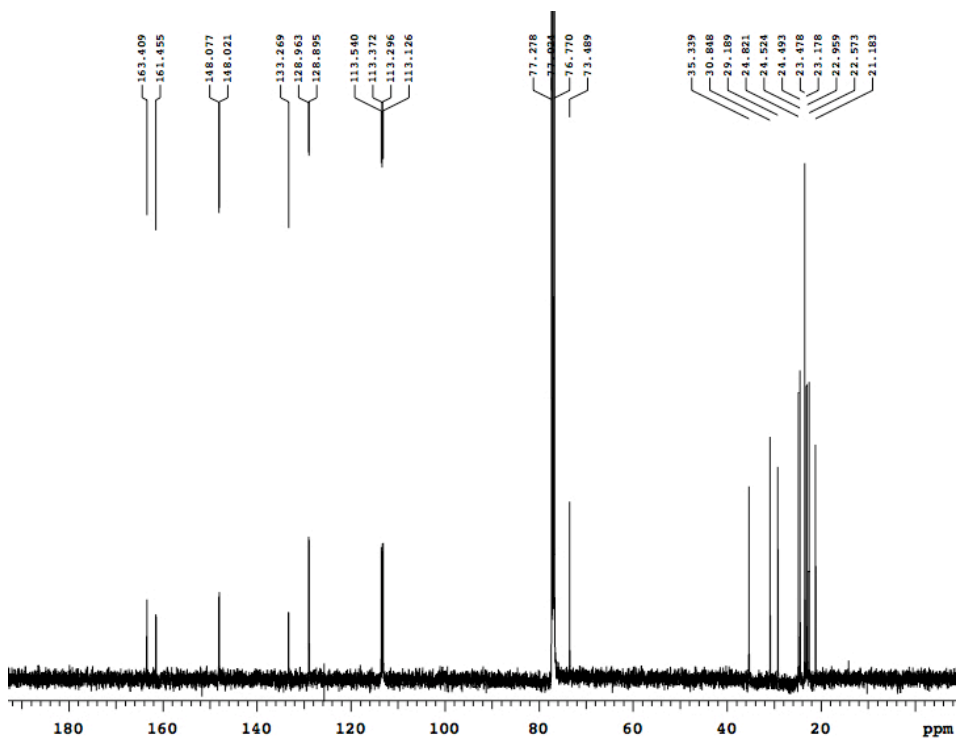
Figure A131. ^{13}C NMR spectrum of **3.80** in CDCl$_3$, 125 MHz.

276
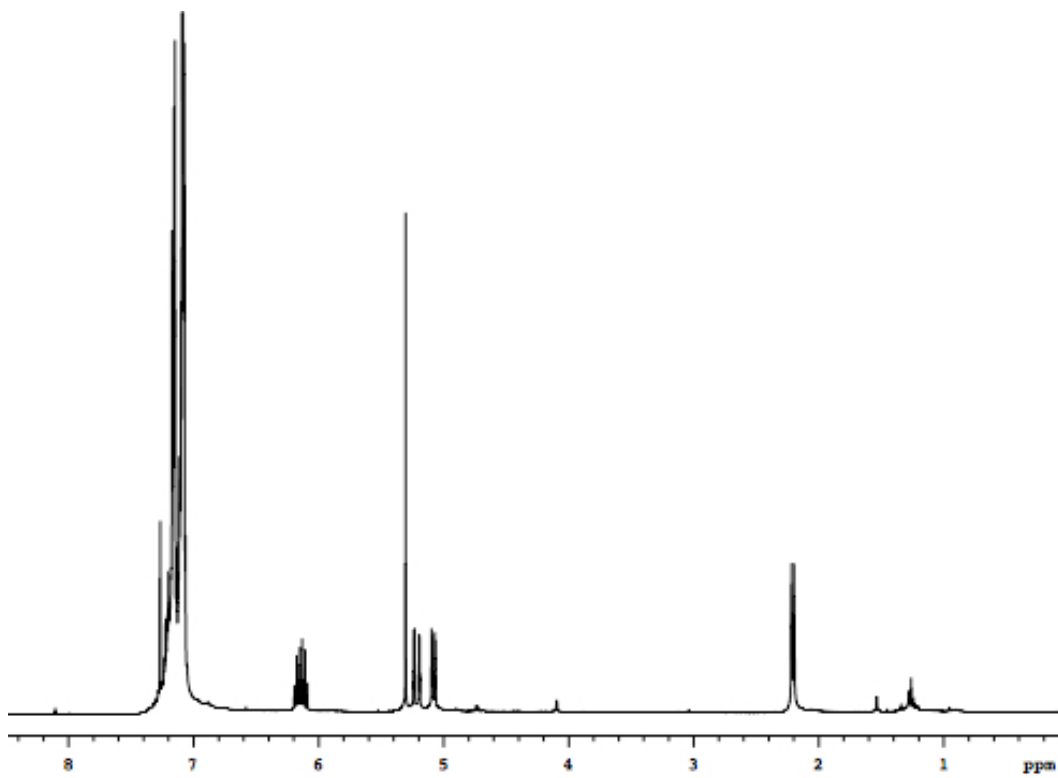
Figure A132. ^{1}H NMR spectrum of **3.83** in CDCl$_3$, 400 MHz.

277
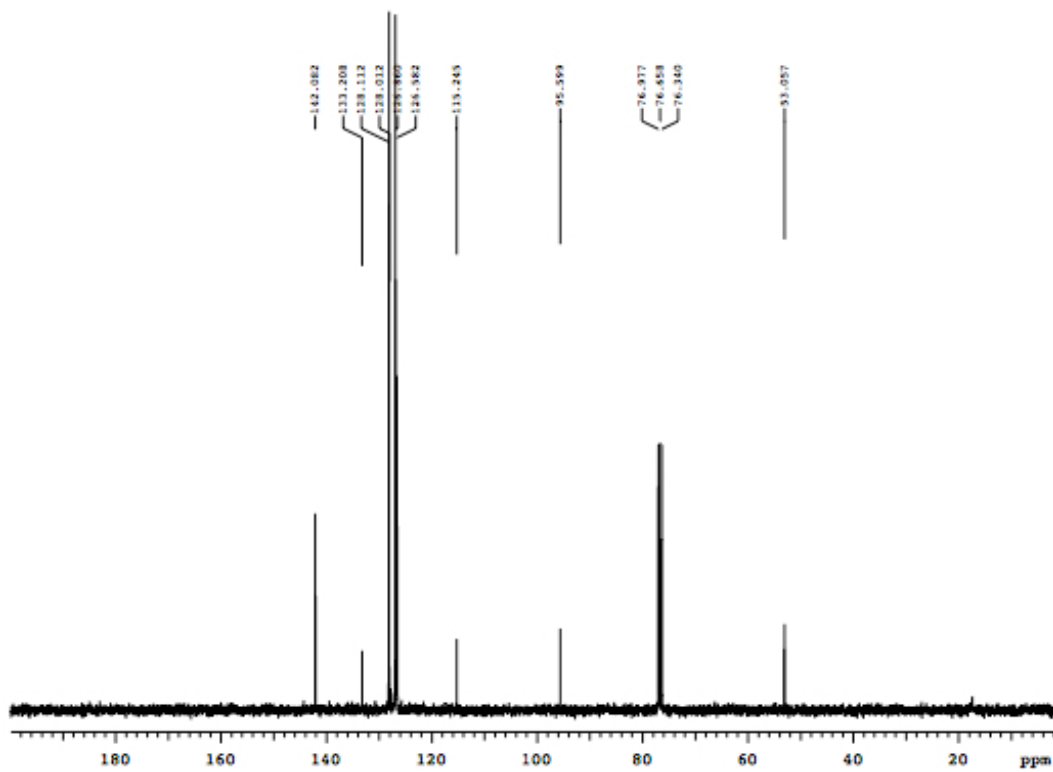
Figure A133. ^{13}C NMR spectrum of **3.83** in CDCl$_3$, 100 MHz.

A.5.1. HPLC traces for new compounds in Chapter 3.


```
                        Area Percent Report
=========================================================================

Peak RetTime Type  Width     Area       Height     Area
  #    [min]       [min]    [mAU*s]      [mAU]       %
----|-------|----|-------|----------|----------|--------|
   1   7.260 BB   0.1909 9888.65820  745.02399  83.8301
   2   9.285 VB   0.2583 1907.41479  106.83940  16.1699

Totals :                  1.17961e4  851.86339
```
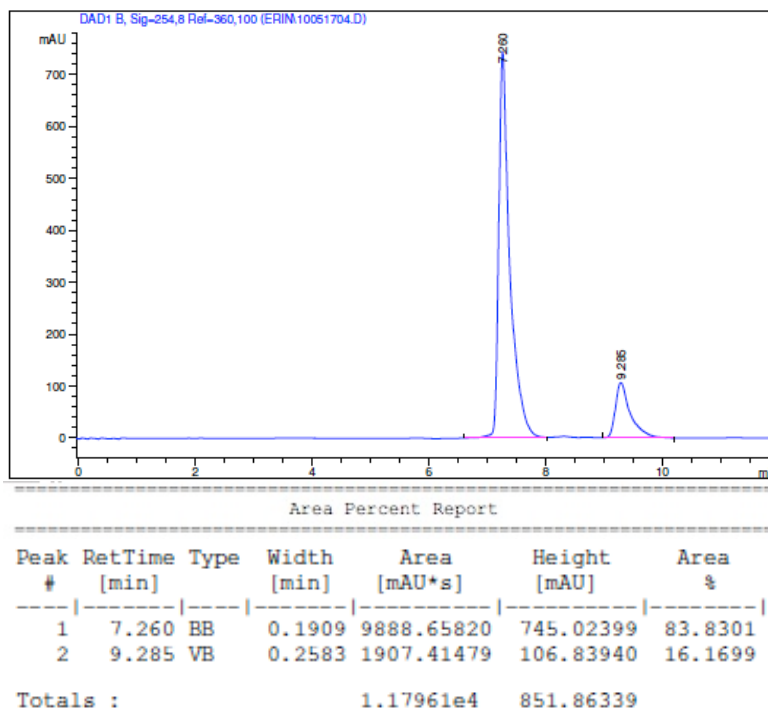
Figure A134. HPLC trace of **3.23**, 68% *ee*.


```
                        Area Percent Report
=========================================================================

Peak RetTime Type  Width     Area       Height     Area
  #    [min]       [min]    [mAU*s]      [mAU]       %
----|-------|----|-------|----------|----------|--------|
   1   8.017 BB   0.2104  417.93048   28.60929  87.3207
   2  11.201 PB   0.3057   60.68486    2.97831  12.6793

Totals :                   478.61534   31.58760
```
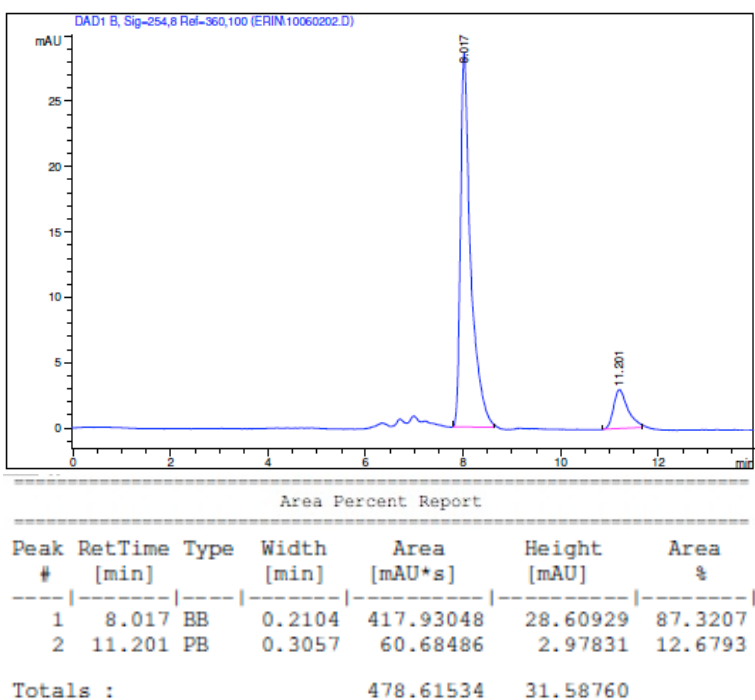
Figure A135. HPLC trace of **3.64**, 75% *ee*.
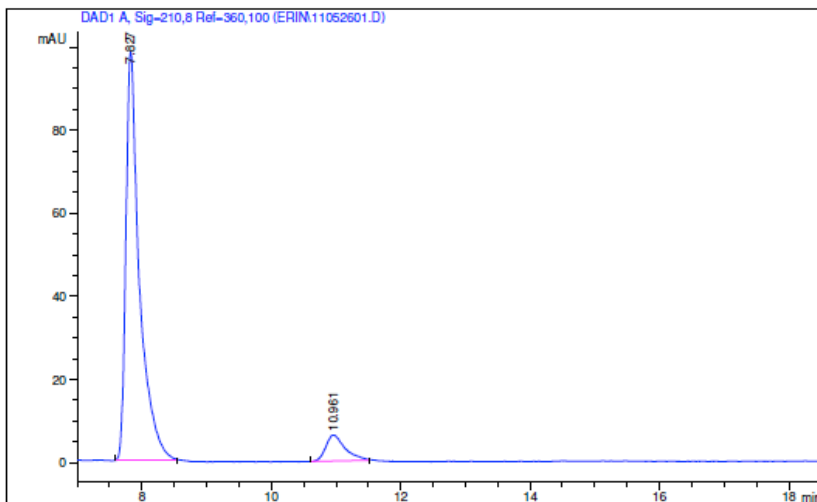
```
DAD1 A, Sig=210,8 Ref=360,100 (ERIN\11052601.D)
```

```
Area Percent Report
```

```
Peak  RetTime Type  Width     Area       Height     Area
 #     [min]        [min]    [mAU*s]     [mAU]       %
----|--------|----|--------|----------|----------|--------|
 1    7.827  BB    0.2100  1431.90686   98.25534  91.5894
 2   10.961  PB    0.3083   131.49088    6.27926   8.4106

Totals :                   1563.39774  104.53460
```

Figure A136. HPLC trace of **3.64**, 83% *ee*.

A.6. Crystallographic data for **3.75**.

Further Crystallographic data for this unpublished compound is available from the X-ray Crystallographic Laboratory, Department of Chemistry, University of Alberta.

XCL Code: DGH1005   **Date:** 13 October 2010

Compound: 4,5-bis{2-(cyclopent-1-en-1-yl)-4-fluorophenyl}-2,2-dimethyl-1,3-dioxolane

Formula: $C_{27}H_{28}F_2O_2$

Supervisor: D. G. Hall   **Crystallographer:** M. J. Ferguson

280
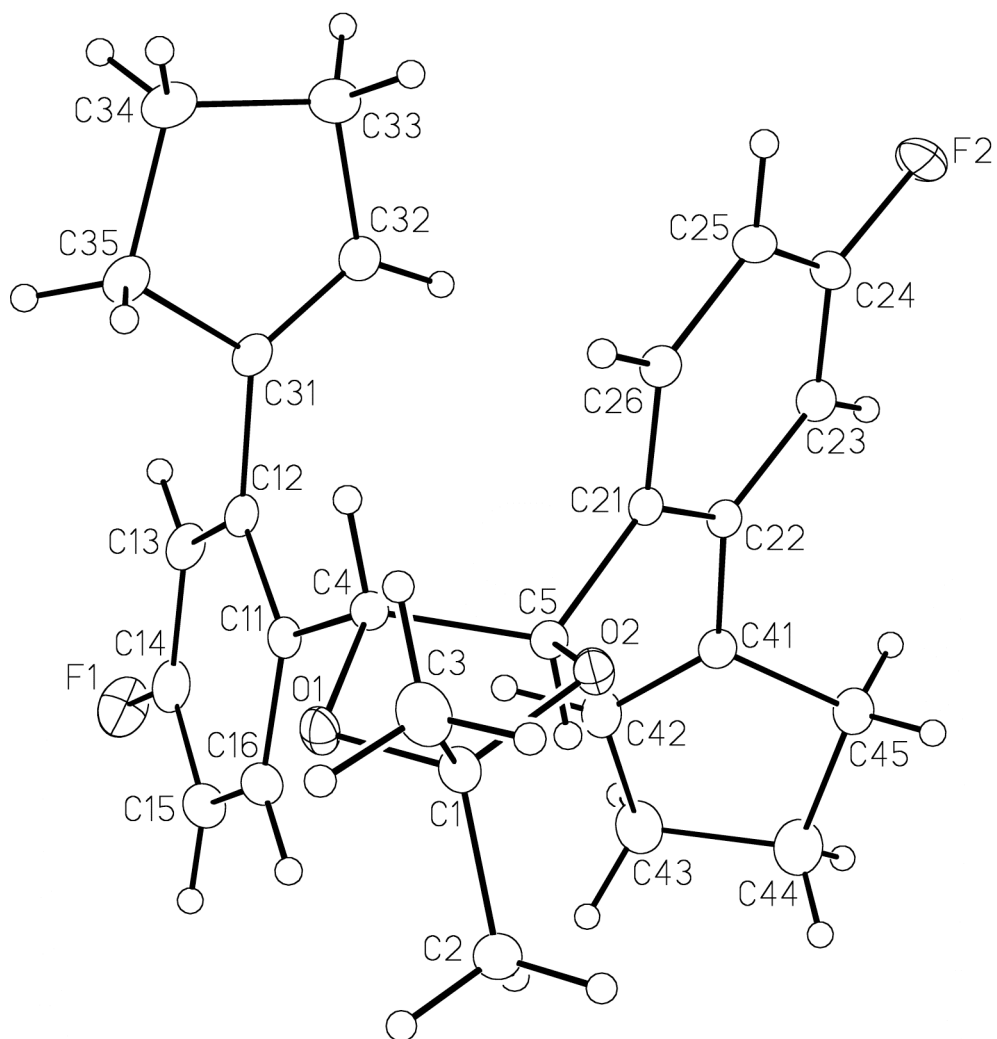
Table 1. Crystallographic Experimental Details for 3.XX.

A. Crystal Data

formula	$C_{27}H_{28}F_2O_2$
formula weight	422.49
crystal dimensions (mm)	$0.49 \times 0.43 \times 0.25$
crystal system	orthorhombic
space group	$P2_12_12_1$ (No. 19)
unit cell parameters[a]	
a (Å)	8.9830 (3)
b (Å)	9.1694 (3)
c (Å)	27.3354 (8)

V (Å^3)	2251.58 (12)
Z	4
ρ_{calcd} (g cm^{-3})	1.246
μ (mm^{-1})	0.088

B. Data Collection and Refinement Conditions

diffractometer	Bruker D8/APEX II CCD[b]
radiation (λ [Å])	graphite-monochromated Mo Kα (0.71073)
temperature (°C)	-100
scan type	ω scans (0.3°) (20 s exposures)
data collection 2θ limit (deg)	55.02
total data collected	19946 ($-11 \le h \le 11$, $-11 \le k \le 11$, $-35 \le l \le 35$)
independent reflections	2960 (R_{int} = 0.0150)
number of observed reflections (*NO*)	2814 [$F_o{}^2 \ge 2\sigma(F_o{}^2)$]
structure solution method	direct methods (*SHELXD*[c])
refinement method (*SHELXL–97*[d])	full-matrix least-squares on F^2
absorption correction method	Gaussian integration (face-indexed)
range of transmission factors	0.9779–0.9583
data/restraints/parameters	2960 / 0 / 280
Flack absolute structure parameter[e]	not calculated
goodness-of-fit (*S*)[f] [all data]	1.043
final *R* indices[g]	
R_1 [$F_o{}^2 \ge 2\sigma(F_o{}^2)$]	0.0302
wR_2 [all data]	0.0799
largest difference peak and hole	0.211 and -0.160 e Å^{-3}

[a]Obtained from least-squares refinement of 9430 reflections with $4.68° < 2\theta < 55.02°$.

[b]Programs for diffractometer operation, data collection, data reduction and absorption correction were those supplied by Bruker.

[c]Schneider, T. R.; Sheldrick, G. M. *Acta Crystallogr.* **2002**, *D58*, 1772-1779.

[d]Sheldrick, G. M. *Acta Crystallogr.* **2008**, *A64*, 112–122.

[e]Flack, H. D. *Acta Crystallogr.* **1983**, *A39*, 876–881; Flack, H. D.; Bernardinelli, G. *Acta Crystallogr.* **1999**, *A55*, 908–915; Flack, H. D.; Bernardinelli, G. *J.*

Appl. Cryst. **2000**, *33*, 1143–1148. The low anomalous scattering power of the atoms in this structure (none heavier than fluorine) implies that the data cannot be used for absolute structure assignment; Friedel pairs were merged prior to final refinement and thus the Flack parameter cannot be calculated.

$^fS = [\Sigma w(F_o^2 - F_c^2)^2/(n - p)]^{1/2}$ (n = number of data; p = number of parameters varied; $w = [\sigma^2(F_o^2) + (0.0399P)^2 + 0.4361P]^{-1}$ where $P = [\text{Max}(F_o^2, 0) + 2F_c^2]/3$).

$^gR_1 = \Sigma||F_o| - |F_c||/\Sigma|F_o|$; $wR_2 = [\Sigma w(F_o^2 - F_c^2)^2/\Sigma w(F_o^4)]^{1/2}$.

Table 2. Atomic Coordinates and Equivalent Isotropic Displacement Parameters

Atom	x	y	z	U_{eq}, Å^2
F1	0.22294(17)	-0.45775(11)	0.30100(5)	0.0604(4)*
F2	0.83811(12)	0.37310(15)	0.33070(4)	0.0556(3)*
O1	0.06533(12)	0.11630(14)	0.41508(4)	0.0337(3)*
O2	0.26182(12)	0.24923(12)	0.44446(4)	0.0312(2)*
C1	0.10986(17)	0.21146(18)	0.45429(5)	0.0311(3)*
C2	0.0977(2)	0.1283(2)	0.50186(6)	0.0394(4)*
C3	0.0173(2)	0.3485(2)	0.45326(8)	0.0459(4)*
C4	0.18572(16)	0.10424(17)	0.38105(5)	0.0274(3)*
C5	0.32081(16)	0.13467(17)	0.41402(5)	0.0265(3)*
C11	0.18410(16)	-0.04479(17)	0.35799(5)	0.0280(3)*
C12	0.22484(17)	-0.06286(17)	0.30876(5)	0.0291(3)*
C13	0.2372(2)	-0.20408(19)	0.29000(6)	0.0372(4)*
C14	0.2082(2)	-0.32115(19)	0.31983(7)	0.0417(4)*
C15	0.1638(2)	-0.3068(2)	0.36754(7)	0.0429(4)*
C16	0.15223(19)	-0.1664(2)	0.38628(6)	0.0377(4)*
C21	0.46040(16)	0.18846(17)	0.38942(5)	0.0267(3)*
C22	0.59532(16)	0.11116(18)	0.39038(5)	0.0283(3)*
C23	0.72284(18)	0.1767(2)	0.37027(6)	0.0357(4)*
C24	0.71231(19)	0.3117(2)	0.34936(6)	0.0379(4)*
C25	0.5812(2)	0.38851(19)	0.34669(6)	0.0369(4)*
C26	0.45606(18)	0.32562(18)	0.36731(5)	0.0321(3)*
C31	0.24945(18)	0.06419(17)	0.27584(5)	0.0304(3)*
C32	0.37782(19)	0.1241(2)	0.26315(6)	0.0352(3)*
C33	0.3580(2)	0.2529(2)	0.22983(7)	0.0445(4)*
C34	0.1939(2)	0.2461(2)	0.21553(7)	0.0519(5)*
C35	0.1192(2)	0.1410(2)	0.25205(6)	0.0410(4)*
C41	0.61463(17)	-0.03482(18)	0.41282(5)	0.0309(3)*

C42	0.5358(2)	-0.15438(19)	0.40480(7)	0.0408(4)*
C43	0.5931(3)	-0.2840(2)	0.43231(9)	0.0537(5)*
C44	0.7040(3)	-0.2160(3)	0.46781(10)	0.0687(7)*
C45	0.7449(2)	-0.0678(2)	0.44643(7)	0.0443(4)*

Anisotropically-refined atoms are marked with an asterisk (*). The form of the anisotropic displacement parameter is: $\exp[-2\pi^2(h^2a^{*2}U_{11} + k^2b^{*2}U_{22} + l^2c^{*2}U_{33} + 2klb^*c^*U_{23} + 2hla^*c^*U_{13} + 2hka^*b^*U_{12})]$.

Table 3. Selected Interatomic Distances (Å)

Atom1	Atom2	Distance
F1	C14	1.3607(19)
F2	C24	1.3616(19)
O1	C1	1.4387(18)
O1	C4	1.4307(17)
O2	C1	1.4337(18)
O2	C5	1.4410(18)
C1	C2	1.511(2)
C1	C3	1.507(2)
C4	C5	1.537(2)
C4	C11	1.505(2)
C5	C21	1.5059(19)
C11	C12	1.404(2)
C11	C16	1.387(2)
C12	C13	1.397(2)
C12	C31	1.489(2)
C13	C14	1.373(3)
C14	C15	1.370(3)
C15	C16	1.389(3)
C21	C22	1.404(2)
C21	C26	1.396(2)
C22	C23	1.405(2)
C22	C41	1.483(2)
C23	C24	1.367(3)
C24	C25	1.374(3)
C25	C26	1.383(2)
C31	C32	1.324(2)

284

C31	C35	1.513(2)
C32	C33	1.502(2)
C33	C34	1.526(3)
C34	C35	1.541(3)
C41	C42	1.323(2)
C41	C45	1.518(2)
C42	C43	1.497(3)
C43	C44	1.524(3)
C44	C45	1.525(3)

Table 4. Selected Interatomic Angles (deg)

Atom1	Atom2	Atom3	Angle
C5	C21	C22	123.02(14)
C5	C21	C26	117.73(14)
C22	C21	C26	119.14(14)
C21	C22	C23	118.72(15)
C21	C22	C41	124.36(14)
C23	C22	C41	116.89(14)
C22	C23	C24	119.62(16)
F2	C24	C23	118.26(16)
F2	C24	C25	118.68(16)
C23	C24	C25	123.06(15)
C24	C25	C26	117.47(15)
C21	C26	C25	121.97(15)
C12	C31	C32	127.78(14)
C12	C31	C35	120.64(14)
C32	C31	C35	111.57(14)
C31	C32	C33	112.45(16)
C32	C33	C34	103.75(16)
C33	C34	C35	106.28(15)
C31	C35	C34	103.48(15)
C22	C41	C42	128.08(15)
C22	C41	C45	121.35(14)
C42	C41	C45	110.36(15)
C41	C42	C43	112.97(16)
C42	C43	C44	102.72(16)
C43	C44	C45	106.12(17)
C41	C45	C44	102.93(16)

Table 5. Torsional Angles (deg)

Atom1	Atom2	Atom3	Atom4	Angle
C1	O1	C4		108.73(11)
C1	O2	C5		106.39(11)
O1	C1	O2		105.76(12)
O1	C1	C2		108.36(13)
O1	C1	C3		109.77(14)
O2	C1	C2		110.61(13)
O2	C1	C3		108.68(13)
C2	C1	C3		113.38(14)
O1	C4	C5		101.63(10)
O1	C4	C11		109.59(13)
C5	C4	C11		114.71(13)
O2	C5	C4		100.40(11)
O2	C5	C21		108.98(12)
C4	C5	C21		117.06(11)
C4	C11	C12		120.40(14)
C4	C11	C16		119.91(13)
C12	C11	C16		119.54(15)
C11	C12	C13		118.80(15)
C11	C12	C31		121.71(14)
C13	C12	C31		119.46(13)
C12	C13	C14		119.45(15)
F1	C14	C13		118.46(17)
F1	C14	C15		118.50(17)
C13	C14	C15		123.04(16)
C14	C15	C16		117.52(17)
C11	C16	C15		121.60(16)
C4	O1	C1	O2	-3.20(16)
C4	O1	C1	C2	-121.82(14)
C4	O1	C1	C3	113.87(15)
C1	O1	C4	C5	26.38(15)
C1	O1	C4	C11	148.13(12)
C5	O2	C1	O1	-23.52(15)
C5	O2	C1	C2	93.59(14)
C5	O2	C1	C3	-141.32(13)
C1	O2	C5	C4	38.68(14)
C1	O2	C5	C21	162.21(11)

O1	C4	C5	O2	-39.25(13)
O1	C4	C5	C21	-156.97(14)
C11	C4	C5	O2	-157.37(12)
C11	C4	C5	C21	84.90(17)
O1	C4	C11	C12	144.24(13)
O1	C4	C11	C16	-40.23(18)
C5	C4	C11	C12	-102.23(16)
C5	C4	C11	C16	73.29(18)
O2	C5	C21	C22	128.85(14)
O2	C5	C21	C26	-47.24(16)
C4	C5	C21	C22	-118.19(15)
C4	C5	C21	C26	65.72(18)
C4	C11	C12	C13	173.35(15)
C4	C11	C12	C31	-9.0(2)
C16	C11	C12	C13	-2.2(2)
C16	C11	C12	C31	175.48(15)
C4	C11	C16	C15	-173.63(17)
C12	C11	C16	C15	1.9(2)
C11	C12	C13	C14	0.5(2)
C31	C12	C13	C14	-177.19(16)
C11	C12	C31	C32	99.2(2)
C11	C12	C31	C35	-81.17(19)
C13	C12	C31	C32	-83.2(2)
C13	C12	C31	C35	96.49(19)
C12	C13	C14	F1	-179.06(16)
C12	C13	C14	C15	1.5(3)
F1	C14	C15	C16	178.78(17)
C13	C14	C15	C16	-1.8(3)
C14	C15	C16	C11	0.0(3)
C5	C21	C22	C23	-174.14(13)
C5	C21	C22	C41	3.8(2)
C26	C21	C22	C23	1.9(2)
C26	C21	C22	C41	179.80(13)
C5	C21	C26	C25	175.59(14)
C22	C21	C26	C25	-0.7(2)
C21	C22	C23	C24	-1.5(2)
C41	C22	C23	C24	-179.54(14)
C21	C22	C41	C42	52.6(2)
C21	C22	C41	C45	-133.29(17)
C23	C22	C41	C42	-129.49(19)

C23	C22	C41	C45	44.7(2)
C22	C23	C24	F2	179.24(14)
C22	C23	C24	C25	-0.2(2)
F2	C24	C25	C26	-177.99(14)
C23	C24	C25	C26	1.5(3)
C24	C25	C26	C21	-1.0(2)
C12	C31	C32	C33	-179.00(14)
C35	C31	C32	C33	1.30(19)
C12	C31	C35	C34	-171.15(14)
C32	C31	C35	C34	8.57(19)
C31	C32	C33	C34	-10.7(2)
C32	C33	C34	C35	15.3(2)
C33	C34	C35	C31	-14.6(2)
C22	C41	C42	C43	176.98(16)
C45	C41	C42	C43	2.3(2)
C22	C41	C45	C44	169.73(17)
C42	C41	C45	C44	-15.2(2)
C41	C42	C43	C44	11.6(3)
C42	C43	C44	C45	-20.4(2)
C43	C44	C45	C41	21.7(2)

Table 6. Anisotropic Displacement Parameters (U_{ij}, Å^2)

Atom	U_{11}	U_{22}	U_{33}	U_{23}	U_{13}	U_{12}
F1	0.0779(9)	0.0309(5)	0.0723(8)	-0.0121(5)	-0.0200(7)	0.0112(6)
F2	0.0385(6)	0.0748(8)	0.0536(6)	0.0196(6)	0.0072(5)	-0.0188(6)
O1	0.0245(5)	0.0458(6)	0.0309(5)	-0.0089(5)	0.0044(4)	-0.0046(5)
O2	0.0270(5)	0.0371(6)	0.0297(5)	-0.0084(5)	0.0038(4)	-0.0038(5)
C1	0.0265(7)	0.0359(8)	0.0308(7)	-0.0045(6)	0.0029(6)	-0.0024(6)
C2	0.0369(8)	0.0504(10)	0.0309(7)	-0.0017(7)	0.0047(6)	-0.0052(8)

C3	0.0365(9)	0.0408(9)	0.0602(11)	-0.0068(9)	0.0032(8)	0.0040(8)
C4	0.0239(6)	0.0334(7)	0.0248(6)	-0.0003(6)	0.0016(5)	-0.0010(6)
C5	0.0261(7)	0.0300(7)	0.0234(6)	-0.0018(6)	0.0009(5)	-0.0015(6)
C11	0.0226(6)	0.0315(7)	0.0301(7)	-0.0017(6)	-0.0034(6)	-0.0020(6)
C12	0.0247(7)	0.0339(7)	0.0289(7)	-0.0028(6)	-0.0054(6)	0.0026(6)
C13	0.0381(8)	0.0386(8)	0.0348(8)	-0.0064(7)	-0.0074(7)	0.0060(7)
C14	0.0422(9)	0.0292(8)	0.0535(10)	-0.0073(7)	-0.0159(8)	0.0034(8)
C15	0.0437(10)	0.0328(8)	0.0520(10)	0.0081(8)	-0.0067(8)	-0.0067(8)
C16	0.0364(8)	0.0388(9)	0.0380(8)	0.0026(7)	-0.0008(7)	-0.0058(7)
C21	0.0256(7)	0.0334(7)	0.0212(6)	-0.0019(6)	-0.0013(5)	-0.0042(6)
C22	0.0267(7)	0.0356(8)	0.0227(6)	-0.0019(6)	-0.0007(5)	-0.0034(6)
C23	0.0258(7)	0.0500(9)	0.0314(7)	0.0013(7)	0.0013(6)	-0.0017(7)
C24	0.0326(8)	0.0520(10)	0.0291(7)	0.0058(7)	0.0025(6)	-0.0134(8)
C25	0.0428(9)	0.0375(8)	0.0303(7)	0.0069(7)	-0.0018(7)	-0.0079(8)
C26	0.0321(7)	0.0355(8)	0.0287(7)	0.0014(6)	-0.0020(6)	-0.0009(7)
C31	0.0329(7)	0.0341(7)	0.0241(6)	-0.0050(6)	-0.0018(6)	0.0056(7)
C32	0.0351(8)	0.0385(8)	0.0321(7)	-0.0041(7)	0.0006(6)	0.0007(7)
C33	0.0539(10)	0.0420(9)	0.0375(8)	0.0006(8)	0.0049(8)	-0.0028(9)
C34	0.0585(12)	0.0516(11)	0.0455(10)	0.0129(9)	-0.0042(9)	0.0044(11)
C35	0.0368(8)	0.0487(10)	0.0375(8)	0.0045(8)	-0.0030(7)	0.0098(8)

C41 0.0265(7) 0.0368(8) 0.0296(7) 0.0000(6) 0.0004(6) 0.0019(7)

C42 0.0376(9) 0.0356(8) 0.0492(9) -0.0007(8) -0.0086(8) 0.0008(7)

C43 0.0542(12) 0.0364(9) 0.0704(13) 0.0041(9) -0.0105(11) 0.0011(9)

C44 0.0713(15) 0.0532(12) 0.0817(16) 0.0243(12) -0.0320(14) -0.0055(12)

C45 0.0363(8) 0.0468(10) 0.0497(10) 0.0083(8) -0.0121(8) -0.0007(8)

The form of the anisotropic displacement parameter is:

$$\exp[-2\pi^2(h^2a^{*2}U_{11} + k^2b^{*2}U_{22} + l^2c^{*2}U_{33} + 2klb^*c^*U_{23} + 2hla^*c^*U_{13} + 2hka^*b^*U_{12})]$$

Table 7. Derived Atomic Coordinates and Displacement Parameters for Hydrogen Atoms

Atom	x	y	z	U_{eq}, Å^2
H2A	0.1585	0.0397	0.5000	0.047
H2B	-0.0065	0.1016	0.5076	0.047
H2C	0.1332	0.1897	0.5288	0.047
H3A	0.0292	0.3968	0.4215	0.055
H3B	0.0503	0.4143	0.4794	0.055
H3C	-0.0877	0.3235	0.4582	0.055
H4	0.1772	0.1812	0.3553	0.033
H5	0.3436	0.0468	0.4344	0.032
H13	0.2654	-0.2190	0.2569	0.045
H15	0.1418	-0.3897	0.3871	0.051
H16	0.1218	-0.1534	0.4193	0.045
H23	0.8158	0.1274	0.3712	0.043
H25	0.5766	0.4812	0.3313	0.044
H26	0.3645	0.3773	0.3664	0.038
H32	0.4720	0.0896	0.2739	0.042
H33A	0.4228	0.2446	0.2007	0.053

H33B	0.3810	0.3452	0.2471	0.053
H34A	0.1829	0.2093	0.1817	0.062
H34B	0.1481	0.3441	0.2176	0.062
H35A	0.0599	0.1952	0.2766	0.049
H35B	0.0537	0.0708	0.2349	0.049
H42	0.4516	-0.1576	0.3838	0.049
H43A	0.6426	-0.3541	0.4101	0.064
H43B	0.5118	-0.3343	0.4500	0.064
H44A	0.7936	-0.2782	0.4709	0.082
H44B	0.6586	-0.2044	0.5006	0.082
H45A	0.7541	0.0069	0.4724	0.053
H45B	0.8395	-0.0728	0.4279	0.053